ANALYSIS OF FGF RECEPTOR SIGNALLING AND TRAFFICKING BY LIVE-CELL IMAGING

by

GIULIO AUCIELLO

A thesis submitted to
The University of Birmingham
for the degree of
DOCTOR OF PHILOSOPHY

School of Biosciences
The University of Birmingham
April 2013

ABSTRACT

Fibroblast growth factor receptors (FGFRs) regulate fundamental cellular processes, including proliferation, differentiation and angiogenesis and have emerged as growth factor receptors central to oncogenesis. This study developed a live-cell assay system for studying FGFR endocytosis and trafficking by employing both confocal and total internal reflection fluorescence (TIRF) microscopy in cells expressing a previously characterised GFP-tagged FGFR2 construct. Data from this work have demonstrated that endocytosis of activated FGFR occurs through clathrin-mediated endocytosis. Interestingly, FGF treatment also significantly increased the number of CCPs as well as the number of clathrin-mediated endocytic events. However, treatment of cells with the Src family inhibitor Dasatinib or depletion of Src kinase target Eps8, prevents the FGF induced increase in plasma membrane clathrin and reduces the internalization of FGFR. This study also shows that both Src and Eps8 are required for receptor to exit from EEA1 positive peripheral compartment into the perinuclear recycling and the lysosomal degradative compartments. Eps8 depletion also inhibits the early phases of ERK activation in response to FGFR activation, placing this signalling event early in the trafficking pathway of the receptor. Thus, these results have identified the endocytic pathway for endocytosis of FGFR2 and described Eps8 and Src as key mediators of the early phases of activated FGFR trafficking and signalling.

TABLE OF CONTENTS

CHAPTER 1: INTRODUCTION 1

1.1 Receptor tyrosine kinases 1

1.2 The FGFR family 6

1.2.1 The fibroblast growth factor family of ligands 7

1.2.2 FGFR structure and alternative splicing 13

1.2.2.1 Extracellular domain 13

1.2.2.2 Transmembrane domain 17

1.2.2.3 Cytoplasmic domain 17

1.2.3 Evolution 21

1.2.4 FGFR in development and human diseases 24

1.2.4.1 Role of FGFR during development 24

1.2.4.2 FGFR genetic alterations in skeletal disorders 25

1.2.4.3 Genetic alterations in FGFR genes in cancer 28

1.2.5 Cell signalling via FGFR 34

1.2.5.1 Receptor trans-phosphorylation 34

1.2.5.2 RAS–mitogen-activated protein kinase pathway 36

1.2.5.3 PI3 kinase-AKT pathway 39

1.2.5.4 PLCγ/PKC pathway 41

1.2.5.5 STAT pathway 41

1.2.5.6 Correlation between FGFR signalling pathways and biological responses 42

1.2.6 Regulation of signalling from FGFR 44

1.2.6.1 Extracellular modulators and autoinhibitory mechanisms 44

1.2.6.2 Intracellular modulators and feedback loops 45

1.3 Endocytosis and endocytic trafficking 50

1.3.1 Pathway of receptor endocytosis 51

1.3.1.1 Clathrin mediated endocytosis 51

1.3.1.2 The early endosomal compartment 55

1.3.1.3 Clathrin-independent endocytosis 57

1.3.2 Endocytosis of FGFRs 60
1.3.3 Crosstalk between endocytosis and RTK signalling 62
1.4 Src family kinase 67
1.4.1 c-Src 68
1.4.2 Src and RTKs 69
1.5 Eps8 72
1.5.1 Eps8 and RTKs 73
1.5.2 Eps8 and cancer 75
1.6 Thesis aims 78

CHAPTER 2: MATERIALS AND METHODS 79

2.1 Buffers and Solutions 79
2.1.1 Bacterial culture 79
2.1.2 Mammalian cell culture 79
2.1.3 Protein manipulation 79
2.1.4 Immunofluorescence 80
2.1.5 Live cell imaging 80
2.2 Reagents and Antibodies 81
2.3 Plasmids 82
2.4 Cell biology techniques 83
2.4.1 Preparation of (heat shock) competent bacterial cells 83
2.4.2 Heat shock transformation of competent bacterial cells 83
2.4.3 Mammalian cell lines and cell culture 84
2.4.4 Transfection 84
2.4.5 Stimulations and inhibitions 85
2.4.6 Immunochemistry 85
2.5 Molecular biology techniques 86
2.5.1 Plasmid DNA purification and isolation 86
2.5.2 Cell lysis and measure of protein concentration 86
2.5.3 Immunoprecipitation, SDS PAGE and immunoblotting 87

2.6 Microscopy techniques 87

2.6.1 Laser Scanning Confocal Microscopy (LSCM), Epi-fluorescence Microscopy (E-FM) and Super-resolution microscopy 87

2.6.2 Total Internal Reflection Fluorescence Microscopy (TIR-FM) 88

2.7 Miscellaneous techniques 88

2.7.1 Receptor trafficking assay 88

2.7.2 Transferrin and cholera toxin B uptake assay 89

2.7.3 Colocalization of FGFR2/EGFR with clathrin and caveolin1 90

2.7.4 Analysis of recruitment of FGFR2 and clathrin 91

2.7.5 Analysis of redistribution of clathrin to cell surface 91

2.7.6 Analysis of endocytic events at plasma membrane 92

2.7.8 Time dependent colocalization of FGFR2 with Eps8 92

2.7.9 Colocalization of FGFR2 with makers for endocytic compartment 92

CHAPTER 3: RESULT 94

3.1 Identification of a model system and expression of functional GFP-tagged FGFR2 94

3.2 Establishment of live-cell imaging assays to study FGFR 99

3.2.1 Confocal live-cell imaging of FGFR trafficking 99

3.2.2 Total internal reflection fluorescence live-cell imaging of FGFR2 dynamics at plasma membrane 104

3.3 Pathway for internalisation of FGFR2 110

3.3.1 FGFR2 is internalised through dynamin-dependent endocytosis 110

3.3.2 FGFR2 is internalised through clathrin-dependent endocytosis 115

3.3.3 Active FGFR2 colocalises with clathrin at the plasma membrane but not with caveolin1 120

3.3.4 Activated FGFR clusters at sites of pre-formed, clathrin-coated pits 123

3.4 FGFR signalling promotes CME through Src and Eps8 128

3.4.1 FGFR2 activation induces recruitment of clathrin at the cell surface and promotes CME 128

3.4.2 FGF-dependent increase in CME is mediated by Src and Eps8 134

3.5 Regulation of FGFR2 trafficking and signalling through Src and Eps8 141

3.5.1 Src kinase activity regulates early endocytic trafficking of FGFR2 141

3.5.2 Role of Eps8 on endocytic trafficking of FGFR2 142
3.5.3 Role of Eps8 in trafficking FGFR2 out of early endocytic system 150
3.5.4 Role of Eps8 in FGFR2 signalling 151

CHAPTER 4: DISCUSSION 157

CHAPTER 5: REFERENCE LIST 169

APPENDIX: PUBLISHED PAPERS 206

LIST OF FIGURES AND TABLES

CHAPTER 1: INTRODUCTION

Figure 1.1 Molecular architecture and mechanism of activation of RTK 3

Figure 1.2 Domain structure of FGFR isoforms 8

Table 1.1 Specificity of FGF/FGFR internaction 10

Figure 1.3 Structure of FGF2 and interaction surface between FGF2 and Heparin . 12

Figure 1.4 View of ligand binding domain and kinase domain structure of FGFR1 and representation of two-end model of FGF:FGFR:heparin complex 15

Figure 1.5 FGFR isoforms generated by alternative splicing of FGFR transcripts 19

Figure 1.6 Phylogenetic tree of FGFR genes 23

Figure 1.7 FGFR mutations associated with skeletal disorders 29

Figure 1.8 Sites of tyrosine phosphorylation in FGFRs 35

Figure 1.9 Intracellular signalling pathways activated by FGFR 43

Figure 1.10 Mechanisms of regulation of FGFR signalling 49

Figure 1.11 Endocytosis and endocytic trafficking of RTKs 59

Table 1.2 Components of endocytic machinery aberrantly expressed in human cancers..... 66

Figure 1.12 Domain organization of Eps8 and its role as coordinator of signals downstream of EGFR 76

CHAPTER 2: MATERIALS AND METHODS

Table 2.1 List of all primary and secondary antibodies used in this study 81

CHAPTER 3: RESULTS

Figure 3.1. Cellular localisation of FGFR2-GFP in HEK-293T and HeLa cells 96

Figure 3.2. Cellular localisation of endogenous FGFR1 in HEK-293T cells 98

Figure 3.3. Advanced optical microscopy techniques used in this study 101

Figure 3.4. Live-cell confocal microscopy analysis of FGFR2 trafficking 103

Figure 3.5. FGFR2 kinase activity is required for receptor internalisation 105

Figure 3.6. Clustering of active FGFR2 at plasma membrane 107

Figure 3.7. Inhibition of GTPase dynamin activity via Dynasore treatment reduces transferrin uptake 113

Figure 3.8. FGFR2 is internalized through dynamin dependent endocytosis 114

Figure 3.9. Silencing α-adaptin subunit of AP2 complex or caveolin1 expression leads to significant reduction of transferrin or cholera toxin B uptake, respectively 116

Figure 3.10. Active FGFR2 enters cells through clathrin-mediated endocytosis 118

Figure 3.11. FGFR2 endocytosis does not occur via caveolae 119

Figure 3.12. Activated EGFR colocalizes with clathrin at the plasma membrane but not with caveolin1 122

Figure 3.13. Activated FGFR2 colocalises with clathrin at the plasma membrane but not with caveolin1..... 124

Figure 3.14. Activated FGFR2 is recruited at sites of pre-existing clathrin-coated pits..... 126

Figure 3.15. Activated FGFR2 signals through Src to promote an increase of CCPs at the plasma membrane 131

Figure 3.16. FGF2 treatment promotes clathrin-mediated endocytosis but does not result in an increase in transferrin uptake 132

Figure 3.17. FGF2-dependent redistribution of CCPs at the cell surface in FGFR2 expressing LNCaP cells 133

Figure 3.18. Activated FGFR2 signals through Eps8 to promote an increase of CCPs at the plasma membrane 136

Figure 3.19. Eps8 interacts with AP2, clathrin and dynamin 137

Figure 3.20. Src kinase activity is required for FGFR2 trafficking 143

Figure 3.21. Silencing of Eps8 impairs FGFR2 trafficking 144

Figure 3.22. Localisation of Eps8 action on FGFR2 trafficking is restricted to the early endosomal system 148

Figure 3.23. Colocalisation between Eps8 and active Src 149

Figure 3.24. Eps8 is required for sorting activated FGFR2 out of peripheral early endosomes and toward degradative and peri-nuclear recycling compartments..... 152

Figure 3.25. Eps8 regulates RAS-MAPK signalling pathway downstream of FGFR2 154

CHAPTER 1

INTRODUCTION

1.1 Receptor tyrosine kinases

Transmission of extracellular signals into the cell is a fundamental process mediated by molecules on the plasma membrane that act as receptors for soluble extracellular ligands, generating specific intracellular physiological events. One of the largest and most important families of membrane-bound receptors involved in signal transduction is the receptor tyrosine kinase (RTK) family, which includes receptors for insulin and for essential growth factors, such as epidermal growth factor receptor (EGFR), fibroblast growth factor receptor (FGFR), platelet-derived growth factor receptor (PDGFR), vascular endothelial growth factor receptor (VEGFR), and nerve growth factor receptor (NGFR) (Lemmon and Schlessinger 2010, Mason I. 2007).

RTKs mediate a wide variety of cellular responses, both during embryonic development and in adult tissue (Mason I. 2007, Ullrich A. and Schlessinger 1990). Cell proliferation, cell differentiation, cell migration, and apoptosis are only a few of the physiological processes regulated by RTKs (Lemmon and Schlessinger 2010). Further, many pathological conditions, including cancer, diabetes, and atherosclerosis, are linked to RTK signalling (Cotton et al. 2008, Jang et al. 2001, Slamon 1987).

RTK signalling is critical for proper functioning of multicellular organisms. Humans have 58 known RTKs, divided into 20 subfamilies (Robinson D. R. et al. 2000), all sharing a

similar molecular architecture (Figure 1.1): an extracellular N-terminal domain containing the ligand and recognition-binding site, a single hydrophobic transmembrane α-helix, and a cytoplasmic C-terminal domain consisting of a juxtamembrane region (just after the transmembrane helix), followed by the tyrosine kinase catalytic domain (TKD) and a carboxy-terminal tail. This molecular architecture, which reflects a shared mechanism of RTK activation, is highly conserved throughout evolution from the nematode *C. elegans* to humans (Popovici et al. 1999). Numerous RTKs have been also identified in the genomes of unicellular organisms (Manning et al. 2008, Suga et al. 2012). The overall architecture of these RTKs possesses similar features as metazoan RTKs in spite of a low sequence homology (Schultheiss et al. 2013).

Most RTKs exist as monomers in the absence of ligand. In this conformation, the tyrosine kinase domain is *cis*-autoinhibited by intramolecular interactions specific to each class of receptor (Lemmon and Schlessinger 2010). Oligomerization induced by ligand binding brings 2 TKDs together in a stable dimer; by promoting allosteric effects, this releases *cis*-autoinhibition and triggers the intrinsic activity of the receptor (Nolen et al. 2004) (Figure 1.1). The originally proposed model for RTK dimerization suggests that a bivalent ligand induces dimerization by simply binding to 2 receptor molecules at the same time, cross-linking them together (Leppanen et al. 2010, Wiesmann et al. 1999). This model, however, is valid only for some receptors, such as NGFR and VEGFR, whose ligands exist as homo-dimeric molecules. In the case of a monomeric ligand, as in the case of EGFR, receptor dimerization seems to be driven mainly by receptor–receptor interaction: ligand binding induces conformational changes that expose a previously occupied dimerization site on the monomeric receptor, resulting in its enhanced affinity for another ligand-

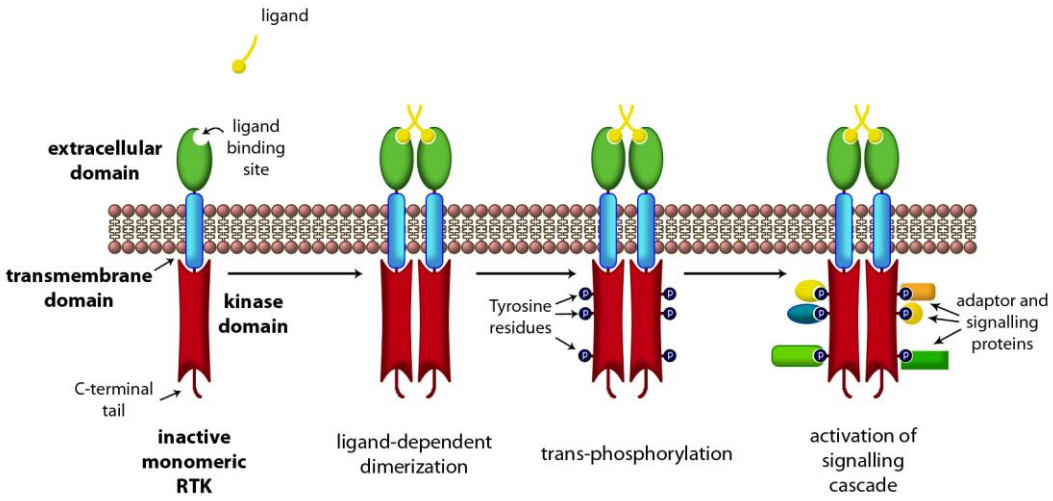

Figure 1.1 Molecular architecture and mechanism of activation of RTKs

All RTKs comprise an N-terminal extracellular domain containing the ligand-binding site, a single hydrophobic transmembrane α helix, and an intracellular domain which includes a region with tyrosine-kinase activity and a carboxy-terminal tail. Ligand binding promotes dimerization of RTKs, resulting in conformational changes in the intracellular domain critical for activation of the kinase domain. In turn, each receptor monomer phosphorylates a number of tyrosine residues in the cytoplasmic domain of its dimer partner (trans-phosphorylation). The resulting phospho-tyrosines function as docking sites for other scaffold and signalling proteins involved in the RTK signalling cascade.

bound monomer (Bouyain et al. 2005). Following ligand binding, a number of tyrosine residues are phosphorylated in a precise order within the activation loop (A-loop) of the TK domain (Favelyukis et al. 2001, Furdui et al. 2006), and the receptor becomes fully activated. Exceptions to catalytic enhancement via dimerization include the insulin receptor (IR), which already exists as a stable disulfide-bonded dimer of α/β pairs. In the case of IR, ligand binding induces conformational rearrangements in the α/β chains, in turn stimulating kinase activity of the receptor (Ward et al. 2007).

Following receptor activation, additional tyrosines are autophosphorylated in other parts of the cytoplasmic region of RTKs, generating docking sites for the recruitment of multiple cytoplasmic molecules containing Src homology-2 (SH2) and phosphotyrosine-binding (PTB) domains (Lemmon and Schlessinger 2010) (Figure 1.1). These molecules are either signalling or scaffold proteins; they can themselves be phosphorylated by RTKs and are responsible for the initiation of various intracellular signal–transduction cascades, including Ras/mitogen activated protein kinase (MAPK) cascade, phosphatidylinositol-3-OH kinase (PI3K)/AKT cascade, and phospholipase-C (PLC)/protein kinase C (PKC) cascade (Lemmon and Schlessinger 2010).

Consistent with the key roles RTKs play in organisms, their activity is subject to very tight temporal and spatial regulation. The first regulation steps occur during the activation process itself, when the receptor goes through several *trans*-autophosphorylation events within the TK domain. These events play a critical regulatory role in most RTKs, and they can increase receptor kinase activity up to 200-fold, as in the case of IR (Cobb et al. 1989). Exceptions to regulation via catalytic-domain phosphorylation include EGFR. Mutation of the only tyrosine residue in the EGFR's TK domain (Tyr845) to phenylalanine, does not

have any effect on the autophosphorylation activity of the receptor (Tice et al. 1999). In the case of EGFR, however, catalytic activity seems to be enhanced by an allosteric mechanism driven by ligand binding (Burgess et al. 2003). RTKs are also regulated by the activity of protein tyrosine phosphatases (PTPs) (Ostman and Bohmer 2001) as well as protein kinases (Ullrich A. and Schlessinger 1990). By modulating the phosphorylation status of RTKs and the downstream signalling and adaptor molecules associated with RTKs, these proteins can modulate the activated signalling response. A further level of regulation is the negative feedback mechanism achieved by the activity of inhibitors of RTK signalling that are transcriptionally induced downstream of the RTK signalling pathway itself (Amit et al. 2007). This is a very robust response mechanism of regulation, by which the cell is able to adjust the final RTK response to an appropriate level, directly sensing the current activated pathway (Avraham and Yarden 2011).

A more complicated mechanism cells employ to finely modulate the activity and level of RTKs is internalization of activated receptors from the cell surface and their subsequent trafficking to intracellular compartments. These 2 processes have long been considered principally mechanisms of signal attenuation: the former by physically removing from the plasma membrane the receptor pool available for activation, the latter by sorting the internalized receptors into the intralumenal vesicles of multivesicular bodies (MVBs), where receptors are degraded and signalling is terminated (Beguinot et al. 1984, Stoscheck and Carpenter 1984). However, a number of RTKs have been found that are able to cycle back to the plasma membrane upon internalization, and this process provides rapid recovery of cellular signalling responsiveness. Further, accumulating evidence suggests that signalling from activated RTKs persists along their endocytic

pathway after internalization (Jiang and Sorkin 2002, Li H. S. et al. 2005, Sorkin and Von Zastrow 2002). In fact, regulated endocytosis and intracellular trafficking compartmentalise RTKs and their associated signalling proteins within specific, spatially localized subcellular domains, thus exerting a powerful influence on the spatial and temporal dynamics of RTK signalling (Di Fiore and De Camilli 2001, Disanza et al. 2009, Polo and Di Fiore 2006, von Zastrow and Sorkin 2007). The interplay between RTK trafficking and signalling is discussed in greater detail in Section 1.3.3, Crosstalk between RTK endocytosis and signalling.

1.2 The FGFR family

FGFRs represent a subfamily of RTKs and play an important role in a wide spectrum of cellular processes, including differentiation, apoptosis, angiogenesis, migration, and survival (Powers et al. 2000, Turner and Grose 2010). The FGFR family consists of 4 distinct gene products (FGFR1, FGFR2, FGFR3, and FGFR4), each composed of an extracellular ligand-binding domain, a transmembrane helix domain, and a cytoplasmic domain that hosts the kinase activity (Figure 1.2). The 4 FGFRs are highly homologous, with some regions, such as the kinase domain, having sequence identity of up to 90% (Johnson D. E. and Williams 1993). A fifth member, FGFR5 or FGFRL1 (fibroblast growth factor receptor-like 1) was recently identified (Wiedemann and Trueb 2000); it is the most distantly related member of the FGFR family, showing approximately 30% amino acid identity to other FGFR proteins. Unlike other members of the FGFR family, FGFR5 lacks the intracellular domain required for signal transduction (Sleeman et al. 2001) (Figure 1.2) and is believed to function as a negative regulator of the activity of the other

FGFRs, by binding and sequestering FGF ligands (Sleeman et al. 2001, Steinberg et al. 2010) or by dimerizing with a conventional FGFR and inhibiting *trans*-phosphorylation events.

1.2.1 The fibroblast growth factor family of ligands

The fibroblast growth factors (FGFs) comprise a large family of developmental and physiological signalling molecules that mediate a wide range of cellular responses, such as cell growth, cell differentiation, cell survival, and cell migration (Beenken and Mohammadi 2009). Over the past 35 years, genes coding for FGFs have been found in both vertebrates and invertebrates, with 3 genes indentified in *Drosophila melanogaster* (*branchless*, *pyramus*, and *thisbe*) and 2 in *Caenorhabditis elegans* (Itoh and Ornitz 2004, Ornitz and Itoh 2001). In humans and mice, the FGF family of ligands includes 23 members, 18 of which exert their function primarily through their high affinity interactions with cell-surface FGFRs; they all contain a conserved 120–amino acid residue core, with 30–60% amino acid identity (Itoh and Ornitz 2004).

Because FGFRs exhibit overlapping recognition and redundant specificity for different FGFs (Table 1.1), the developmental and tissue-specific distribution of FGFs and FGFRs ensures the specificity of cellular response generated in different cell types and in different developmental stages by different FGFs. This cell-specific 'competence' is typified, for instance, by FGF7 which, unlike FGF2, is mitogenic for keratinocytes but not for endothelial cells (Rubin J. S. et al. 1989). In addition to their receptors, FGFs show high affinity for heparin and heparin sulphate-like glycosaminoglycans (HLGAGs) (Klagsbrun 1990), acid polysaccharides containing sulphate groups attached throughout their

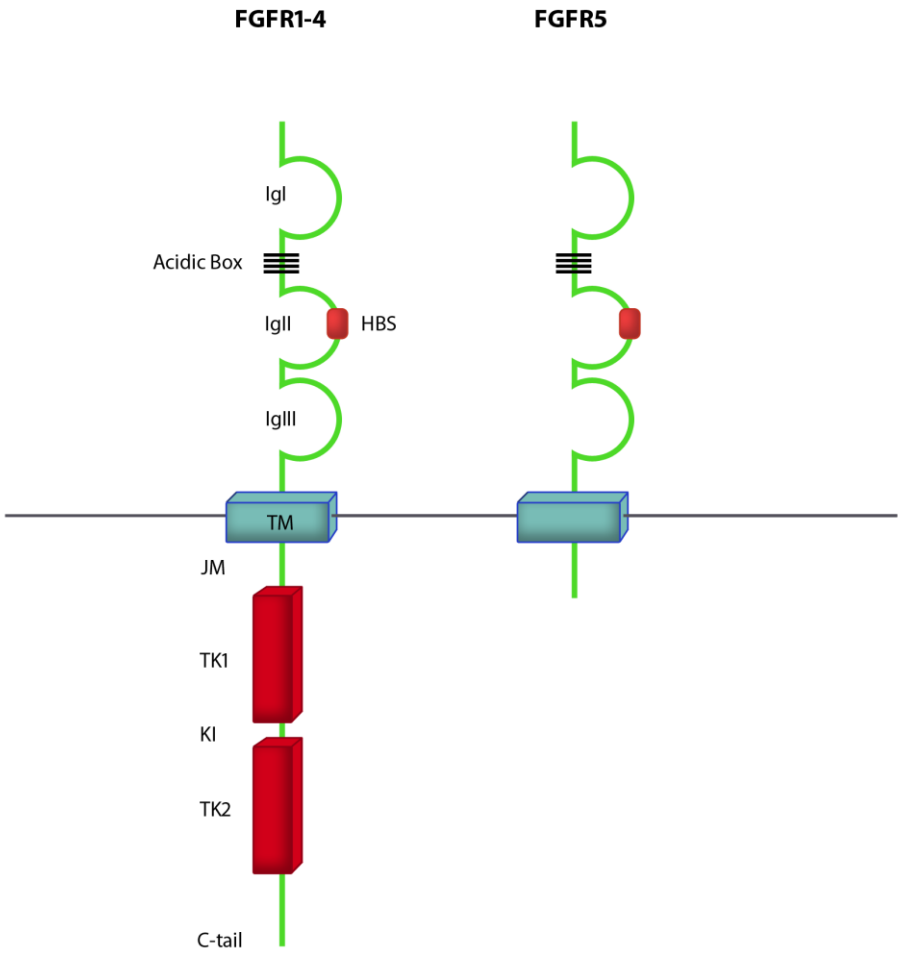

Figure 1.2 Domain structure of FGFR isoforms

Ig: Immunoglobulin-like domain; **HBS**: heparin binding site; **TM**: transmembrane domain; **JM**: juxtamembrane domain; **TK**: tyrosine kinase domain; **KI**: kinase insert

polysaccharide chains, found in the extracellular matrix and on the cell surface. Physiologically, the binding of the FGFs to heparin or HLGAGs has 2 relevant roles:protection of the FGFs from degradation (Damon et al. 1989, Sommer and Rifkin 1989), and creation of a local reservoir of growth factors critical to strict spatial regulation of FGF signalling (Gould et al. 1995). In the context of FGFRs, extensive research defines the role of heparin in receptor activation.

Yayon et al., show that in HLGAG-deficient mutant CHO cells, FGFR1 loses the ability to bind FGF2, and that binding ability is restored by addition of heparin or heparan sulphate (Yayon et al. 1991). Cell surface HLGAGs have also been demonstrated to promote binding of FGFs to FGFR2 (Mansukhani et al. 1992), triggering a consequent mitogenic and angiogenic response (Aviezer et al. 1994, Rapraeger et al. 1991). These and other observations demonstrate that heparin and HLGAGs function as accessory molecules in the regulation of FGF binding and receptor activation (Ornitz and Itoh 2001) through different mechanisms, including promoting FGF oligomerization (Herr et al. 1997, Ornitz et al. 1992, Spivak-Kroizman et al. 1994), regulating the ligand diffusion rate (Dowd et al. 1999, Flaumenhaft et al. 1990) and driving the specificity of FGF–FGFR interaction (Guimond and Turnbull 1999, Kan et al. 1999, Pye and Kumar 1998).

By binding heparan sulphates with high affinity, most FGFs become trapped within the extracellular matrix of tissues and act locally as paracrine or autocrine ligands of FGFRs (Beenken and Mohammadi 2009). However, the 3 members belonging to the FGF19 subfamily (FGF19, FGF21, and FGF23) bind to heparan sulphates with low affinity and can diffuse from the secretion tissue into the circulation and act in an endocrine fashion on distant tissues. Once the target tissues have been reached, the endocrine FGFs bind to a

FGF ligand	Interaction with FGFR						
	FGFR1b	**FGFR1**	**FGFR2b**	**FGFR2c**	**FGFR3b**	**FGFR3c**	**FGFR4**
FGF1	+	+	+	+	+	+	+
FGF2	+	+	-	+	-	+	+
FGF3	+	-	+	-	-	-	-
FGF4	-	+	-	+	-	+	+
FGF5	-	+	-	+	-	-	-
FGF6	-	+	-	+	-	-	+
FGF7	-	-	+	-	-	-	+
FGF8	-	+	-	+	+	+	+
FGF9	-	-	-	+	+	+	-
FGF10	+	-	+	-	-	-	-
FGF11	-	-	-	-	-	-	-
FGF12	-	-	-	-	-	-	-
FGF13	-	-	-	-	-	-	-
FGF14	-	-	-	-	-	-	-
FGF15	-	+	+	+	+	+	+
FGF16	-	-	-	+	-	+	-
FGF17	-	+	-	+	-	+	+
FGF18	-	-	-	+	-	+	+
FGF19	-	+	+	+	+	+	+
FGF20	-	+	-	+	+	+	+
FGF21	+	+	+	+	+	+	+
FGF22	+	-	+	-	-	-	-
FGF23	-	+	+	+	+	+	+

Table 1.1 Specificity of FGF/FGFR interaction

Data were adapted from (Cotton et al. 2008, Mason 2007)

co-receptor, known as klotho (Kurosu et al. 2006). The klotho proteins appear to play a similar function to HLGAGs: by interacting with both the endocrine FGF ligand and their cognate receptor, they increase FGF-FGFR affinity and function as cofactor necessary for FGF signalling activation (Kurosu et al. 2007, Kurosu et al. 2006, Lin B. C. et al. 2007, Urakawa et al. 2006).

Most FGFs contain classic N-terminal signal peptides required for secretion (FGFs 3–8, 10, 17–19, 21, and 23) or use an un-cleavable hydrophobic N-terminal sequence as an unconventional signal for secretion (FGFs 9, 16, and 20) (Ornitz and Itoh 2001). On the contrary, FGF1 and FGF2 lack any signal peptides, thus they cannot be secreted and are instead passively released from damaged cells (Ornitz and Itoh 2001). FGFs 11–14 also lack signal peptides, but they are not even released and remain intracellular, functioning within cells in a receptor-independent manner (Schoorlemmer and Goldfarb 2001).

All FGFs adopt a β-trefoil structure consisting of 12 antiparallel β-strands (β1–β12) arranged in 3 repetitions of 4-stranded β-sheets (Murzin et al. 1992) (Figure 1.3A). The main interaction surface between FGF and heparin utilises a Lysine/Arginine–rich region on FGF, which includes the β1–β2 loop and parts of the region between the β10 and β12 strands, and negatively charged groups on heparin (Faham et al. 1996) (Figure 1.3B).

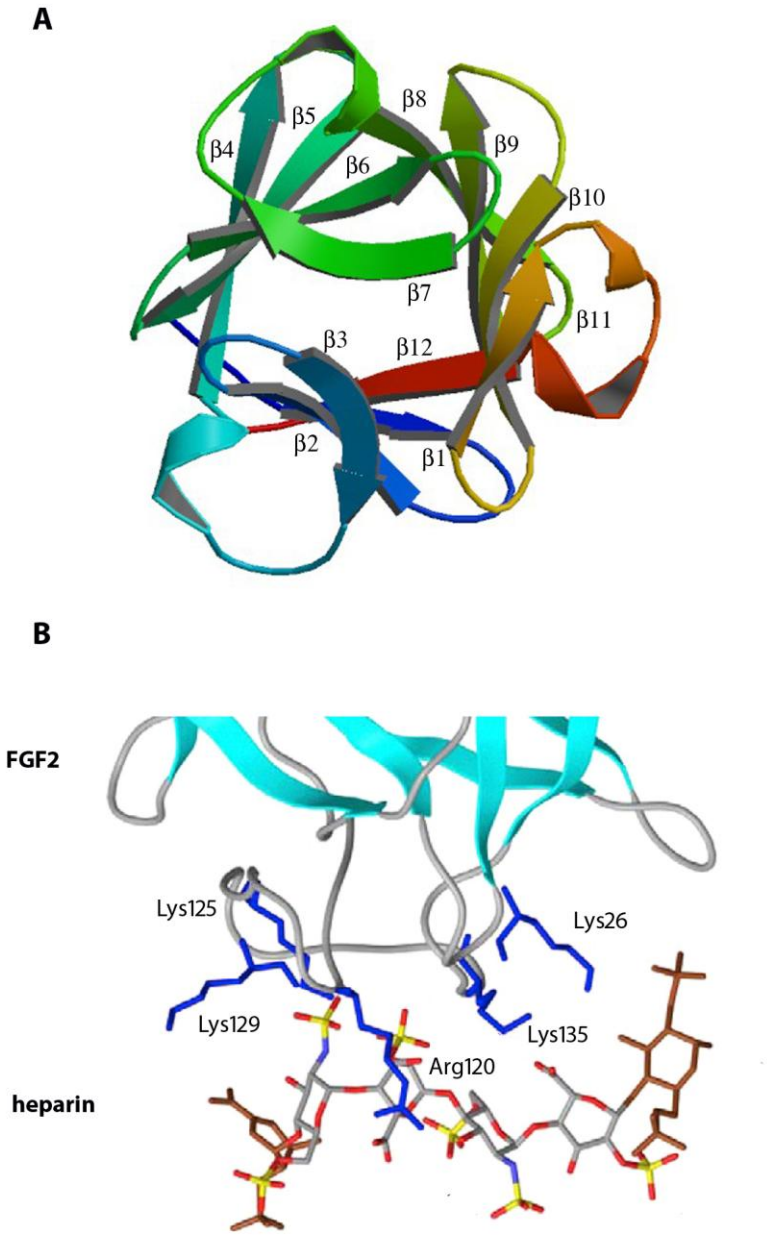

Figure 1.3 Structure of FGF2 and interaction surface between FGF2 and heparin

A. The secondary structure of FGF-2 shows a β-trefoil fold made up of three sets of four anti-parallel β-strands (PDB coordinates: 2FGF). **B**. Stereo view of the binding surface between FGF2 and heparin. The sidechains of the FGF2 residues involved in the interaction are represented by thick blue lines (PDB coordinates: 1BFC). These images were obtained from PDB and labelled using Adobe Photoshop.

1.2.2 FGFR structure and alternative splicing

1.2.2.1 Extracellular domain

All FGFR family members share the same overall architecture in the extracellular portion, consisting of 3 immunoglobulin (Ig)-like domains (D1–D3) connected by flexible linkers (Plotnikov et al. 1999). The region between D1 and D2 consists of an acidic, serine-rich region of 8 amino acids, called “Acidic Box” (AB). The D2 domain contains a highly conserved, negatively charged sequence that has high affinity for heparin, forming the heparin binding site (HBS) (Kan et al. 1993).

The crystal structure of domains D2 and D3 of different FGFRs in complex with the FGFs ligands has been solved and demonstrates that D2 and D3 are necessary and sufficient for specific ligand binding (Plotnikov et al. 2000, Stauber et al. 2000, Yeh et al. 2003). The D2-D3 domain of FGFR1 in complex with FGF2 is shown in Figure 1.4A and consists of 2 FGF2-D2-D3 units in a 2:2 stoichiometry, with the ligands localizing on opposite sides of the dimer. Each ligand interacts extensively with D2-D3 and the intervening linker between them, and the whole dimeric structure is stabilized by direct D2–D2 interactions and interactions that the ligand forms with the domain D2 of the other receptor in the dimer. While the D2–D3 domain is necessary for ligand binding, the D1 domain and the AB are thought to participate in binding regulation. The AB region is highly conserved among FGFR family members and consists of a glutamate, aspartate, and serine-rich sequence that mimics the negative potential surface of heparin, and thus its avidity interacts with the HBS on the D2 domain of the FGFRs (Kalinina et al. 2012). When FGF is present at low concentrations, the AB region intramolecularly binds the HBS, while the D1 domain folds

back and interacts with the D2–D3 region, which represents the ligand-binding site on FGFR. In this conformation, the receptor is in a 'close' state, the interaction with heparin and FGF is sterically inhibited, and the initiation of biological response is suppressed (Kalinina et al. 2012, Olsen et al. 2004, Wang F. et al. 1995a).

The crystal structure of the entire extracellular domain of FGFR in complex with FGF and heparin is shown in Figure 1.4C and is based on the 'two end' model proposed by Schlessinger et al. (Schlessinger et al. 2000). According to this model, heparin plays a dual role in driving the assembly of a 2:2:2 stoichiometry FGF:FGFR:heparin complex: first, it induces formation of a stable 1:1:1 FGF:FGFR:heparin ternary complex, by interacting with both FGF and FGFR via heparin non-reducing ends. This then drives recruitment of a second 1:1:1 FGF:FGFR:heparin ternary complex to the first complex. Contact between the 2 complexes is stabilized by direct FGFR:FGFR interaction, by secondary interactions between the FGF molecule in one ternary complex and the FGFR molecule in the other complex, and by indirect contact between the FGFR monomers mediated by heparin (Schlessinger et al. 2000).

Multiple FGFR isoforms that differ in the extracellular domain are generated by alternative splicing of FGFR transcripts. The main event of alternative splicing in FGFR1–3 involves exon encoding for the D3 domain, and this represents the main mechanism for regulating ligand-binding specificity of FGFRs (Yeh et al. 2003) (Figure 1.5). The exons (7–9) that, combined, codify for the 3 D3 isoforms (designated IgIIIa, IgIIIb and IgIIIc) are contiguous in *fgfr1*, *fgfr2*, and *fgfr3* (Chellaiah et al. 1994, Johnson D. E. et al. 1991). Exon 7 unequivocally encodes for the N-terminal portion of D3 (IgIIIa), while exon 8 and exon 9 are alternatively translated for the second half of D3 (generating IgIIIb or IgIIIc,

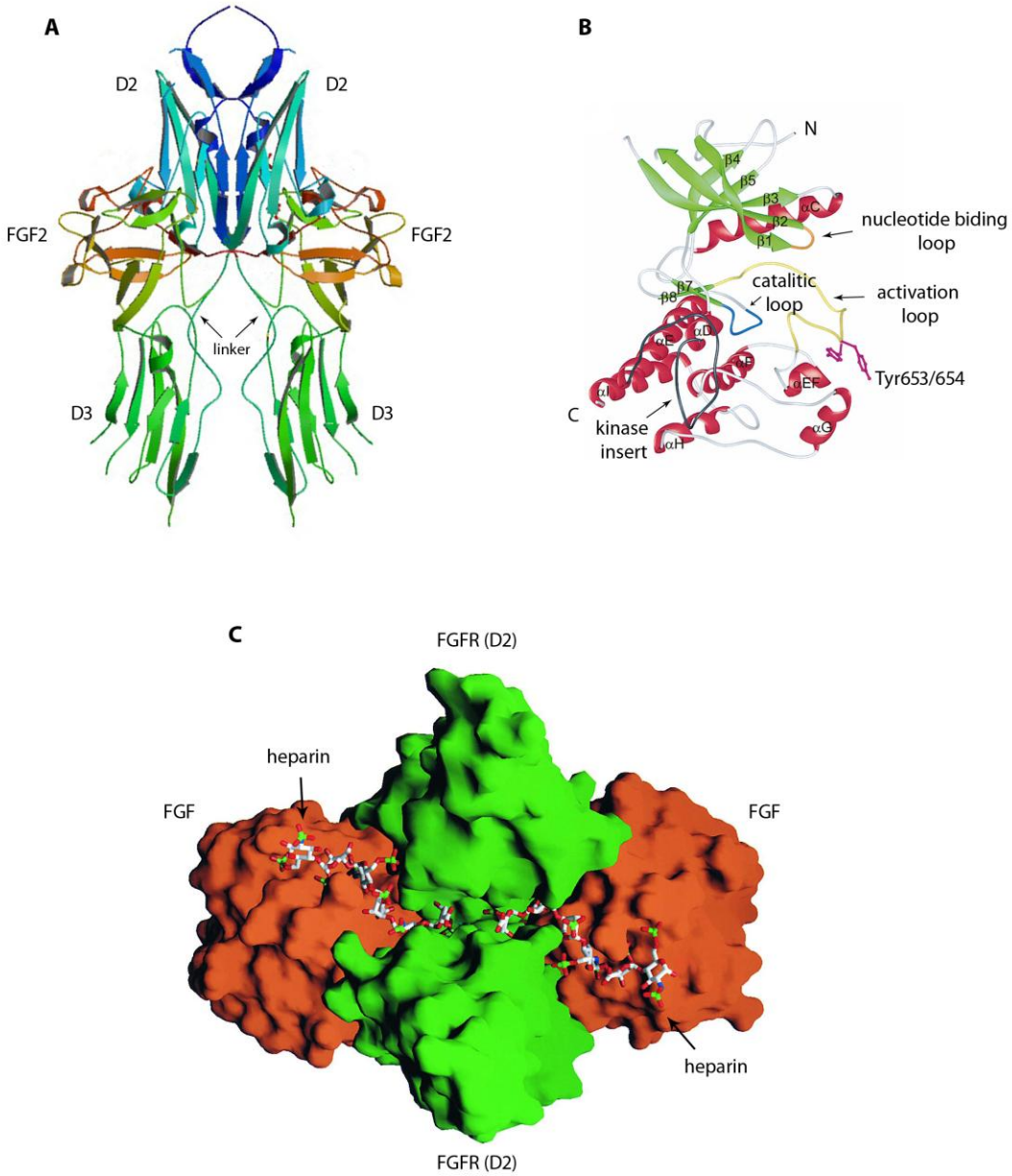

Figure 1.4 View of ligand binding domain and kinase domain structure of FGFR1 and representation of two-end model of FGF:FGFR:heparin complex

A. Ribbon diagram of domains D2 (in blue) and D3 (in green) of FGFR1 in complex with FGF2. Each FGF2 localizes on opposite sides of the dimer and interacts with D2, D3, and with the intervening linker (in grey) between them (PDB coordinates: 1DJS). **B**. Ribbon diagram of the kinase domain of FGFR1, comprising an N-terminal lobe formed by five anti-parallel β strands (β1-β5) and one α helix (αC) and a C-terminal lobe comprising two β strands (β7, β8) and seven α helices (αD, αE, αF, αG, αH, αI) (PDB coordinates: 1FGK). **C**. Molecular surface representation of 2:2:2 stoichiometry FGF:FGFR:heparin complex. The complex is viewed from the top, with the two heparin chains fitting in the heparin binding canyon. The images in (**A**) and (**B**) were obtained from PDB and labelled using Adobe Photoshop. The image from (**C**) was adapted from Schlessinger et al. 2000.

respectively). The IgIIIa splice variant generates a truncated soluble protein which cannot activate any signal transduction, but nevertheless appears to play a specific role in generating biological activity, probably functioning as a negative regulator of the other FGFRs by binding and sequestering FGF ligands (Guillonneau et al. 1998) (Figure 1.5). A truncated soluble FGFR1IIIa, for instance, has been found to be differentially expressed in the adult murine retina compared to full-length FGFR1IIIc, suggesting, for this isoform, a specific role in development of the retina (Guillonneau et al. 1998). On the contrary, differential expression of the IgIIIb and IgIIIc variants results in the epithelial ‘‘b’’ and mesenchymal ‘‘c’’ isoforms of FGFRs, respectively (Jin et al. 2004, Orr-Urtreger et al. 1993), which possess different ligand-binding specificities (Mohammadi et al. 2005, Olsen et al. 2006, Yayon et al. 1992, Yeh et al. 2003). For example, FGFR2IIIb binds FGF7 and FGF10, but not FGF2, whereas the FGFR2IIIc isoform binds FGF2, but not FGF7 and FGF10 (Dell and Williams 1992, Miki et al. 1992). This alternative splicing event occurs in a tissue-specific fashion, guarantying the isoform-specific responses generated in different cell types, which is particularly important for this development. For instance, the FGFR2b isoform is specifically expressed in epithelial cells, whereas the FGFR2c isoform is specifically expressed in mesenchymal cells (Orr-Urtreger et al. 1993).

Consistent with lineage-specific expression of FGFR2 isoforms, a class switch from FGFR2b to FGFR2c has been shown to occur during progression of prostate cancer and bladder cancer from a non-malignant, stromal-dependent, epithelial tumour to an invasive, stromal-independent tumour (Yan et al. 1993). Another major alternative splicing event involves the exons encoding for D1 and the AB-containing region between D1 and D2. FGFR isoforms lacking D1 and the D1–D2 linker region possess higher affinity

for FGF and heparin, with consequent increased signalling capability, further supporting the observation that these extracellular domains are involved in receptor autoinhibition (Olsen et al. 2004, Roghani and Moscatelli 2007, Shi et al. 1993, Shimizu et al. 2001, Wang F. et al. 1995a). Consistent with their altered signalling capacity, FGFR isoforms lacking D1 domain or AB region have been shown to be associated with cancer (Bruno et al. 2004, Onwuazor et al. 2003, Tomlinson and Knowles 2010, Yamaguchi F. et al. 1994a).

1.2.2.2 Transmembrane domain

Similar to other RTKs, the transmembrane region of FGFRs consists of an α-helix of approximately 20 amino acids with a number of hydrophobic residues oriented outside the α-helical core and interacting with the membrane lipid bilayer, therefore conferring stability to the protein (Creighton 1984). The existence of multiple mutations in the TM domain on FGFRs is associated with cancer and skeletal malformations (further discussed in Section 1.2.4.2) as result of increased receptor activation, suggesting that the TM could also be involved in the process of receptor dimerization (Li E. et al. 2006).

A number of soluble FGFR isoforms have been described that include truncated molecules that lack the TM domain or that harbour the N-terminal half of IgIII domain fused to the first 3 aminoacids of the TM domain (Duan et al. 1992, Hanneken 2001). Similarly to the IgIIIa splice variants, these soluble FGFR isoforms have been show to act as negative regulator of FGFR signalling *in vitro* and *in vivo* (Wheldon et al. 2011).

1.2.2.3 Cytoplasmic domain

The cytoplasmic domain of FGFRs comprises a juxtamembrane domain (JM), 2 tyrosine kinase subdomains (TK1 and TK2) interrupted by a short kinase insert (KI), and a C-

terminal tail (CT) (Eswarakumar et al. 2005). The juxtamembrane domain of FGFRs is considerably longer compared to that of other RTKs and contains a very highly conserved sequence of 12 amino acids (aa 419-430 in FGFR1), including a valine and threonine, known as the 'VT site' (Val^{427}-Thr^{428} In FGFR1) (Gillespie et al. 1995). The presence of these 2 residues is very important for initiation of signal transduction from FGFRs, since they serve as binding sites for the PTB domain of the adaptor protein FGF receptor substrate-2 (FRS2), which links FGFRs to the downstream MAPK signalling pathway (Burgar et al. 2002). In FGFR1 and -2, the 3′ end of exon 10, encoding the VT site, is subject to alternative splicing, generating 2 different isoforms of FGFRs, containing or excluding this motif (denominated VT+ and VT−, respectively) (Burgar et al. 2002). The VT- isoforms of FGFRs have been shown to be incapable of generating any mitogenic response, further supporting the key role of the 2 residues in driving the interaction of FRS2 to the receptor. Two members of the FRS2 family have been identified, FRS2α (or FRS2, or SNT1) and FRS2β (or FRS3 or SNT2), which share high homologies in amino acid sequence and structure domains and are expressed with a differential spatial/temporal pattern (Kouhara et al. 1997). Both FRS2α and FRS2β have been shown to be involved in signal transduction from FGFRs by means of direct interaction with the VT site of receptor (Kouhara et al. 1997, Meakin et al. 1999, Xu et al. 1998). This interaction is constitutive and does not depend on receptor activation at basal level (Ong et al. 2000), even though recent studies demonstrate that FGFR1-FRS2α binding, but not FGFR1-FRS2β binding, could be tyrosine-phosphorylation regulated (Zhang et al. 2008).

The only potential site for FGFR-mediated phosphorylation identified thus far in the juxtamembrane region is the residue Y463. When phosphorylated, Y463 has been shown

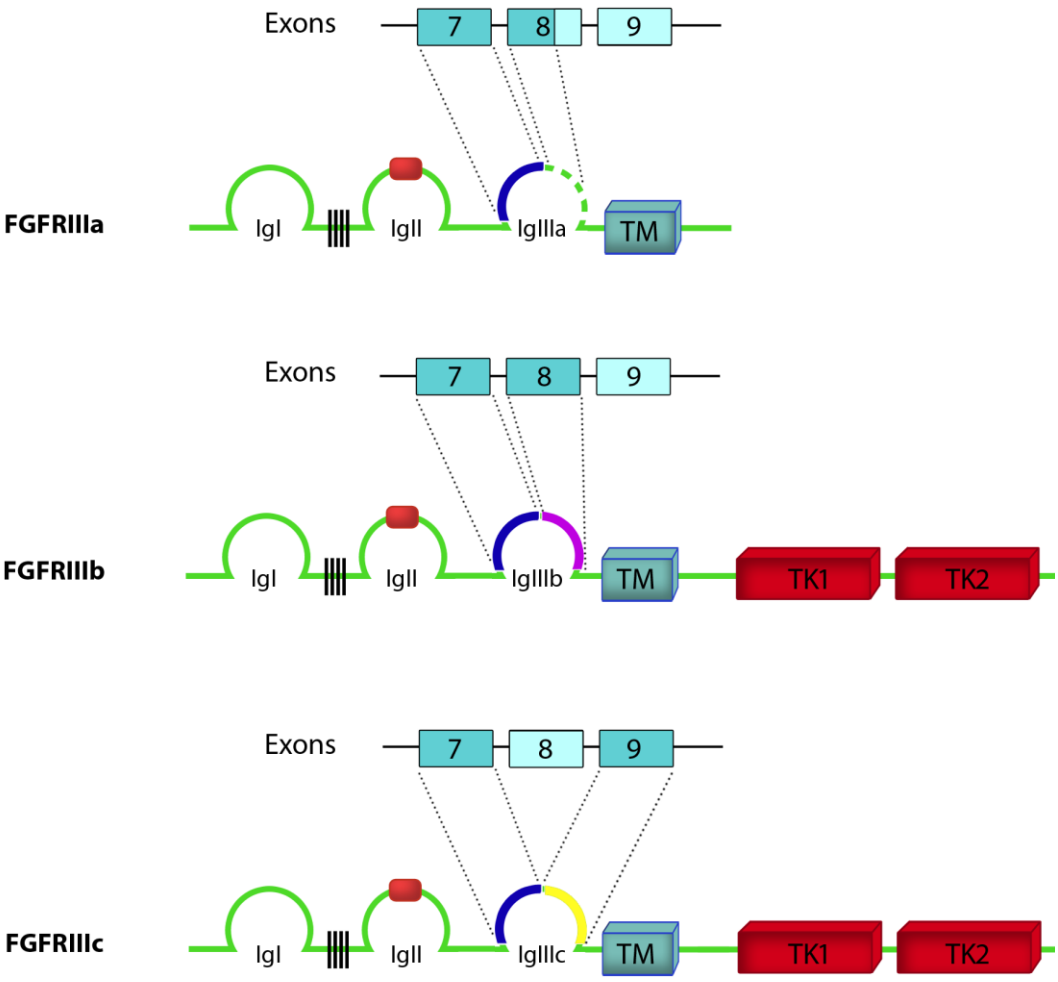

Figure 1.5 FGFR isoforms generated by alternative splicing of FGFR transcripts

The two main isoforms of FGFR are generated by alternative splicing of exons 8 and 9. Exon 7 unequivocally encodes for the N-terminal part of D3 (IgIII), while exons 8 and 9 are alternatively translated in the second half of D3, generating IgIIIb or IgIIIc, respectively. An IgIIIa splice variant is also possible, when only a part of exon 8 is translated. IgIIIa variant generates a truncated inactive soluble protein.

to interact with the SH2 domain of the docking molecule Crk, which mediates Jun N-terminal Kinase (JNK) and ERK1/2 signalling in FGF2-stimulated endothelial cells (Larsson et al. 1999).

The TKD of FGFRs is split in 2 lobes, similarly to that of platelet-derived growth factor (PDGF), with a very short KI region of 14 amino acids. Autophosphorylation of a number of tyrosines throughout the TKD is essential for both the catalytic activity of tyrosine kinase and for subsequent initiation of the signalling cascade (Mohammadi et al. 1996b). The X-ray crystal structure of the TK domain of FGFR1 has been solved (Figure 1.4B) and comprises an N-terminal lobe formed by a curled β sheet of 5 antiparallel β strands (β1-β5) and one α helix (αC) and a C-terminal lobe comprising two β strands (β7, β8) and 7 α helices (αD, αE, αF, αG, αH, αI) (Mohammadi et al. 1996a). The relative orientation of the N- and C-lobes to each other changes between the active and inactive forms of the kinase, and it displays a more open disposition in the unphosphorylated inactive FGFR (Johnson L. N. et al. 1996). The C-terminal lobe allocates the activation loop of the kinase, where 2 conserved tyrosine residues (Y653/Y654) are *trans*-phosphorylated to fully activate the kinase function (Furdui et al. 2006). Autophosphorylation of Tyr653 and Tyr654 of FGFR1 enhances the rate of substrate catalysis up to 500-fold (Furdui et al. 2006). In the absence of ligand, the majority of RTKs are maintained in an inactive state by residues in the activation loop that sterically block substrate access to the active site. In FGFRs, however, the activation loop is disposed so that substrate access to its binding site is not blocked by Y653 and Y654, but by other residues, such as Arg-661 (in FGFR1) (Mohammadi et al. 1996a). A different autoinhibitory mechanism has been described for FGFR2 (Chen H. et al. 2007) and involves a triad of residues (E565, in the kinase hinge

region, N549 in the loop between the αC helix and the β4 strand, and K641 in the β8 strand). By interacting with each other, these 3 residues form a network of hydrogen bonds that inhibits movements of the N-terminal lobe towards the C-terminal lobe, keeping the kinase in an autoinhibited state. Consistent with this, a number of pathogenic mutations within the triad E565/N549/K641 have been identified in FGFR2, which result in ligand-independent activation of receptor (Chen H. et al. 2007).

Several kinase-deficient FGFR variants have been described in cells that express FGFR active forms. Since kinase-deficient and active isoforms of the receptor can hetero-dimerize, generating non-functional receptor dimers and down-regulating FGF signal transduction, the kinase-deficient FGFR isoforms are thought to be involved in a mechanism of regulation of FGFR activity (Shi et al. 1993).

The carboxyl terminal tail of FGFR contains the residue Y766, which is one of the major autophosphorylation sites in all FGFRs. Once phosphorylated, this tyrosine and its flanking sequences act as a high affinity binding site for one of the SH2 domains of Phospholipase-Cγ (PLCγ) (Mohammadi et al. 1991), recruiting this molecule at the plasma membrane, where it can catalyse the hydrolysis of Phopshatidylinositol-4,5 bisphosphate PI(4,5)P2 and generate diacylglycerol (DAG) and inositol 1,4,5-trisphosphate (IP3) (Mohammadi et al. 1992, Peters et al. 1992).

1.2.3 Evolution

Genes encoding for FGFRs have been identified in many multicellular organisms, ranging from human (*Homo sapiens*) to mouse (*Mus musculus*) to nematode (*Caenorhabditis*

elegans), but not in unicellular organisms. The expansion of the FGFR gene family is strictly linked with that of their ligand FGFs and is thought to be achieved from a common ancestral gene by 2 large-scale gene/genome duplications only during early vertebrate evolution (Itoh and Ornitz 2004). Identification of an FGFR gene in the species *Hydra vulgaris* (Sudhop et al. 2004) reveals that signalling by FGFRs arose early in the evolution of metazoans (Figure 1.6). Using a bioinformatic approach, Rebscher et al. were able to trace FGFR back to the placozoan, showing that already in this phylum the predicted level of organization of FGFR shows its full modular structure, with 3 Ig-like domains, a TM region, and a bi-lobed TK domain present (Rebscher et al. 2009). However, protein domain analysis predicted for both the Placozoa and Cnidaria phyla the lack of AB between IgI and IgII, suggesting that the acidic domain evolved in the last common ancestor of triploblasts (Figure 1.6). Further, outside the Deuterostomia, no alternative splicing of IgIII has been found. This is consistent with the fact that alternative splicing in the extracellular Ig-like domains, which determines ligand-binding specificity, significantly increased FGFR functional diversity in more complex phyla, such as that of Deuterostomia (McKeehan et al. 1998). The Rebscher study cited above also revealed the presence of more than 3 Ig-like loops within the insect group, although their function remains unknown (Beermann and Schroder 2008, Klambt et al. 1992). In the *C. elegans* genome, only one FGFR homologue (*egl-15*) was identified (DeVore et al. 1995), while 2 FGFR proteins, DFR1 and DFR2, have been described in *Drosophila melanogaster* (Shishido et al. 1993) (Figure 1.6). All invertebrate FGFRs contain Ig-like domains and they share only 30% and 60% amino acid identity with their vertebrate homologues in the extracellular ligand-binding domain and the intracellular kinase domain, respectively. However,

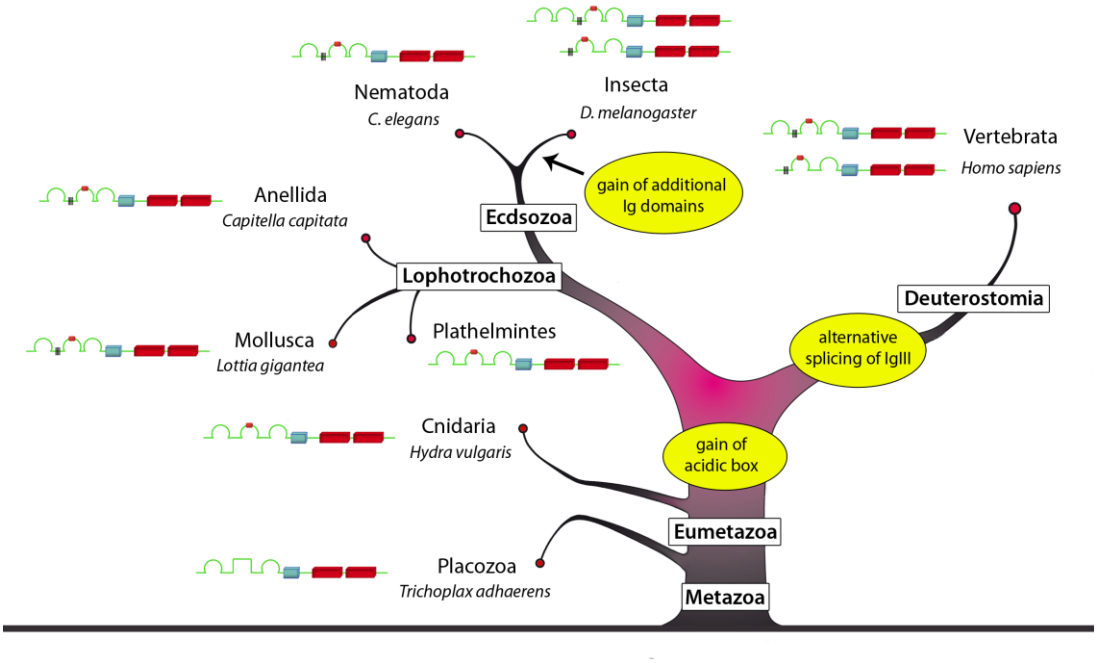

Figure 1.6 Phylogenetic tree of FGFR genes

Representation of the main evolutionary changes on the protein domain structure of FGFR. The legend for the protein domains is given in Figure 1.2.

comparative modelling studies on the sequence of FGFs and their receptors in *C. elegans* and *D.melanogaster* indicate that these two species can assume similar conformations and make equivalent interactions as those observed in corresponding human structures, indicating that the properties driving formation of the ligand-receptor complex are conserved through evolution (Nagendra et al. 2001).

1.2.4 FGFR in development and human diseases

1.2.4.1 Role of FGFR during development

Signalling from FGFs and their receptors plays a significant role both in adult tissue and during development in vertebrates. At early stages of embryogenesis, the FGF/FGFR system regulates key processes during gastrulation, ensuring correct patterning and timing of embryonic differentiation (Dorey and Amaya 2010). Experiments carried out in Xenopus and Zebrafish demonstrated that FGF signalling is essential for the induction/maintenance of both axial and paraxial mesoderm, which form the notochord, and the axial skeleton, skeletal muscles, and dermis, respectively (Amaya et al. 1991, Amaya et al. 1993, Griffin et al. 1995). FGF signalling through FGFRs also plays an essential role in the coordination of cell movements during gastrulation and neurulation: *Fgfr1*-null and *Fgf8*-null mouse embryos, for instance, display severe defects in cell migration during gastrulation (Deng et al. 1994, Sun et al. 1999, Yamaguchi T. P. et al. 1994b) and Xenopus embryos expressing a dominant-negative FGFR result in failure of blastopore closure (Amaya et al. 1991). The role of FGF signalling in regulating embryonic morphogenetic movements is not restricted to vertebrates: in Drosophila, a

mutation in the *fgfr2* gene results in defects in mesodermal cell migration during gastrulation (Beiman et al. 1996, Gisselbrecht et al. 1996).

In addition to its role during early embryonic development, FGF/FGFR signalling plays a fundamental role in skeletogenesis and it is required for the development of several organs in the adult, such as the kidney (Bates 2011), prostate (Cotton et al. 2008), limb (Cohn et al. 1995, Delezoide et al. 1998), skin (Li C. et al. 2001), inner ear (Wright and Mansour 2003), lung (Colvin et al. 2001, Min et al. 1998), brain (Ford-Perriss et al. 2001), heart (Lu et al. 2008, Meyers E. N. et al. 1998), ocular lens (Robinson M. L. 2006) and the gonadotropin-releasing hormone (GnRH) neuronal system (Gill et al. 2004). Transgenic and knockout mouse models for all FGFR isoforms have been generated, covering a wide range of diseases affecting each of the organs mentioned above.

1.2.4.2 FGFR genetic alterations in skeletal disorders

FGFR1, FGFR2, and FGFR3 are highly expressed in bone primordial and show finely regulated spatial and temporal expression patterns throughout bone development, suggesting their key roles during this process (Ornitz and Marie 2002). Consistent with this, a number of germline mutations have been identified for all FGFRs that give rise to a variety of inherited skeletal malformations (Wilkie et al. 1995) (Figure 1.7). All FGFR-related skeletal disorders can be classified in 2 categories: the chondrodysplasias are conditions characterized by defects in long-bone elongation as a result of impaired chondrocyte function during endochondral bone formation and include achondroplasia syndrome, milder disorder of hypochondroplasia, and neonatal lethal thanatophoric dysplasia 2 (TDII) and 1 (TDI); the syndromes belonging to the second class all share a common phenotypic feature, craniosynostosis, manifested by premature ossification and

fusion of the sutures between the developing flat bones of the skull, due to a defect in osteoblast function (Cohen 2006). This class includes syndromes such as Pfeiffer, Crouzon, and Jackson-Weiss syndromes. Endochondral and intramembranous ossification, regulated by chondrocytes and osteoblasts, respectively, are very intricate processes and require involvement of a wide spectrum of molecules, such as growth factors, hormones, transcription factors, etc. Although it is clear that proliferation, differentiation, and apoptosis of osteoblasts and chondrocytes are dependent on the temporal expression and activity of FGFRs (Shimoaka et al. 2002), the precise role of FGF signalling in these processes is not entirely clear.

Summarized below are the most relevant germline mutations identified for all FGFRs that give rise to the above-described skeletal disorders:

Extracellular domain: The majority of the mutations that arise in the ectodomain of FGFR2 and FGFR3 in bone development disorders are located in the domain D3 or in the linker between D2 and D3 and result in a dominant gain-of-function phenotype (Kannan and Givol 2000) (Figure 1.7). A consistent number of these is due to substitution of a conserved cysteine residue in D3 (mainly at positions 278 or 342 in FGFR2). The subsequent presence of unpaired cysteines prevents formation of stabilizing intrachain disulfide bonds within the Ig-like domains and induces the formation of intermolecular disulfide bonds, resulting in covalent dimerization of mutant receptor molecules and therefore in their constitutive, ligand-independent activation (Cornejo-Roldan et al. 1999). A similar effect is caused by mutations that involve residues adjacent to Cys in the D3 domain, such as Y340H or T341P in FGFR2 (Lajeunie et al. 2006, Nagase et al. 1998).

This class of mutation occurs in skeletal disorders classified as 'receptor dimerization syndromes', which include Pfeiffer, Crouzon, and Jackson-Weiss syndromes.

Transmembrane domain: The most common mutation on *fgfr3* results from either a G-to-A transition or a G-to-C transversion, changing the codon for Gly380 to Arg in the transmembrane domain of FGFR3 (Passos-Bueno et al. 1999). The G380R mutation is dominant and causes acondroplasia, the most common form of human genetic dwarfism (Rousseau et al. 1994), characterized by defects in long-bone elongation as a result of impaired chondrocyte function during endochondral bone formation (Ponseti 1970). Interestingly, Monsonego-Ornan et al., showed that G380R substitution results in a specific defect in internalization of FGFR3, leading to accumulation of the mutant receptor at the plasma membrane and subsequent uncontrolled and prolonged ligand-dependent receptor activation in chondrocytes (Monsonego-Ornan et al. 2000). Substitution of an alanine residue (Ala391Glu) in proximity to the site of the principal achondroplasia mutation in *fgfr3* causes a entirely different phenotype, Crouzon syndrome (Meyers G. A. et al. 1995). This mutation is thought to induce hyperactivation of the receptor by stabilizing the dimers through the formation of new hydrogen bonds. A number of mutations associated with skeletal pathologies have been identified at the junction between the extracellular and transmembrane domain of FGFR2 (S372C and Y375C) and FGFR3 (G370C, S371C, Y373C, and G375C) (Adar et al. 2002, Przylepa et al. 1996) (Figure 1.7). Similar to those in the extracellular domain of FGFR, these mutations also result in the creation of Cys residues, forming new intermolecular disulfide bonds, suggesting that these residues are not buried in the lipid bilayer of the cell.

Kinase domain: A significant number of mutations causing craniosynostosis have been identified also in the kinase domain of FGFRs (Figure 1.7). The N549H, N549T, E565G, E565A, and K641R substitutions, for example, which map within the kinase hinge, or the K659N and R678G, which map into the activation loop of FGFR2, all induce ligand-independent FGFR2 activation by preventing receptor autoinhibition (Chen H. et al. 2007). The milder disorder of hypochondroplasia has been shown to be due to the substitution of a residue of asparagine (N540) into the tyrosine kinase region of FGFR3 (Bellus et al. 1996), whereas K650E (Tavormina et al. 1995) and K650M (Tavormina et al. 1999), which has been shown to cause the strongest constitutive activation of the known mutants of FGFR3, cause neonatal lethal thanatophoric dysplasia 2 (TDII) and 1 (TDI), respectively. Mutagenesis studies on position 650 and adjacent positions show that the K650E mutation mimics the conformational changes normally induced by autophosphorylation of Tyr residues within the activation loop (Webster et al. 1996).

An interesting class of point mutations are those located in homologous positions in all 3 FGFRs. The P252R in FGFR1, the P253R in FGFR2, and P250R in FGFR3, for example, all involve a residue of proline highly conserved within the DII–DIII linker (Bellus et al. 1999). The phenotype resulting from each of those mutations, however, is different (Pfeiffer syndrome in FGFR1, Apert syndrome in FGFR2, and Muenke syndrome in FGFR3), and this reflects different temporal and spatial expression of the specific FGFR mutated (Kannan 2000).

1.2.4.3 Genetic alterations in FGFR genes in cancer

All members of the FGFR family have been found to be deregulated in a variety of cancers, ranging from solid tumours to haematological malignancies (Wesche et al. 2011).

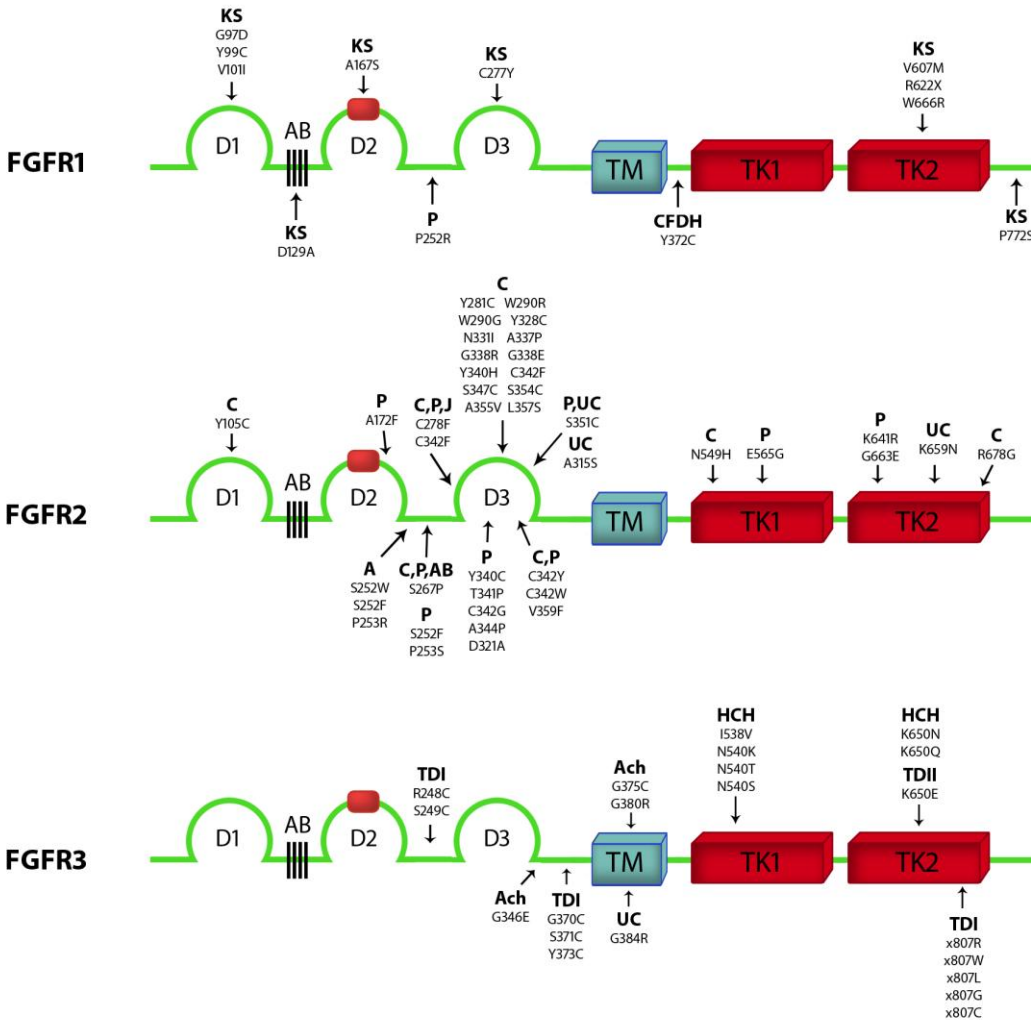

Figure 1.7 FGFR mutations associated with skeletal disorders

Schematic diagram showing FGFR1-3 and major sites of mutations. AB: acidic box, D1-3: Immunoglobulin-like domain 1-3, TM: transmembrane domain, TK: tyrosine kinase domain, A: Apert syndrome, Ach: Achondroplasia, C: Crouzon syndrome, CFDH: Craniofacial dysplasia with hypophosphatemia, HCH: Hypochondroplasia, J: Jackson-Weiss syndrome, KS: Kallmann syndrome, P: Pfeiffer syndrome, TD: Thanatophoric dysplasia (types I and II), UC: unclassified disorders.

Activating mutations or receptor overexpression induce FGFRs to become constitutively active, leading to tumorigenesis and cancer development. However, several other mechanisms can contribute to imbalanced FGFR signalling resulting in cancer, including SNPs on *fgfr* genes, overexpression of ligands, and defects in receptor degradation.

Somatic mutations: Genetic alterations causing sustained activation of FGFRs have been found in human cancers (Wesche et al. 2011). Similarly to those associated with skeletal disorders, these mutations can have various molecular effects on the protein, from enhancing ligand binding to altering ligand specificity, or inducing constitutive dimerization of the receptor. *Fgfr3*, which appears to be one of the most commonly mutated oncogenes in human bladder cancer (Cheng et al. 2009), harbours a variety of cancer-associated point mutations, both in the extracellular domain and in the kinase domain. Interestingly, a number of these mutations are the same as those found to be the cause of many of the skeletal disorders previously described (Pandith et al. 2010). For instance, S249C and Y373C in the ectodomain, and K650Q/M/N/E in the kinase region of FGFR3, are frequently found in bladder cancer and are responsible for the lethal skeletal disorder thanatophoric dysplasia (Pandith et al. 2010). Activating mutations in FGFR2 are present in about 10% of human endometrial carcinomas (Pollock et al. 2007), and similar to those in FGFR3, are frequently identical to those that cause skeletal disorders. These include, for example, S252W and P253R, located in the region between D2 and D3, which alter FGFR ligand-binding specificity, causing Apert syndrome (Yu K. et al. 2000). Missense mutation of *fgfr2* gene also occurs in breast cancer, gastric cancer, lung cancer, and ovarian cancer. Mutations in the kinase domain of FGFR4 have been identified in

childhood sarcoma RMS (Rhabdomyosarcoma) (Taylor J. G. th et al. 2009); most of these mutations appear to promote autophosphorylation of the receptor.

Receptor overexpression: FGFR overexpression resulting in ligand-independent signalling may be caused by either gene amplification or aberrant transcriptional regulation of FGFRs. The most characterised cancer-related FGFR amplification is that occurring at 8p11-12, the chromosomal region where *fgfr1* is located. This amplicon, which results in overexpression of FGFR1, is found in ~10% of human breast cancers and is associated with poor prognosis (Gelsi-Boyer et al. 2005, Letessier et al. 2006). FGFR1 is also frequently overexpressed in human prostate cancer, where it disrupts the interplay between the stroma and epithelium of the prostate (Kwabi-Addo et al. 2004). Gene amplification of the *fgfr2* gene occurs in diffuse-type gastric cancer (Jang et al. 2001), as well as in primary breast cancer (Adnane et al. 1991). In the latter case, the overexpressed receptor is subject to C-terminal deletion due to exclusion of the last exon from the FGFR2 amplicon. This region includes the residue Y769, which upon ligand-dependent phosphorylation functions as binding site for PLCγ (Ceridono et al. 2005). The result of C-terminal truncation on the FGFR2 amplicon is a receptor that signals in a ligand-independent manner (Moffa and Ethier 2007). FGFR3 is overexpressed as a result of chromosomal translocation t(4;14) (Kalff and Spencer 2012), which brings FGFR3 under the influence of a strong transcriptional enhancer. Approximately 15% to 20% of patients with multiple myeloma, a blood cell cancer, harbour this translocation-mediated FGFR3 overexpression, which is associated with poor prognosis (Chang et al. 2005, Chesi et al. 1997).

Ligand availability: Potent aberrant FGF signalling can also result from upregulation of FGF expression, which increases ligand availability. Elevated levels of FGFs have been found in several human cancers. FGF8 expression, for example, has been shown to be upregulated in human breast and prostate cancer (Marsh et al. 1999, Mattila and Harkonen 2007), whereas elevated levels of FGF2 are associated with tumour vascularisation, consistent with the intimate crosstalk between FGF2 and VEGF signalling during angiogenesis (Seghezzi et al. 1998).

Fusion events: Events of chromosomal translocation can result in FGFR fusion proteins with aberrant signalling properties. FGFR fusion proteins are generated by the fusion between the tyrosine kinase domain of the receptor and a dimerization domain, leading to constitutive dimerization and activation of the tyrosine kinase (Jackson et al. 2010). A significant number of FGFR1 fusion proteins have been identified in EMS (8p11 myeloproliferative syndrome), also called SCLL (stem cell leukaemia lymphoma syndrome), a rare myeloproliferative disorder that rapidly progresses into acute leukaemia (Wesche et al. 2011).

Single nuclear polymorphisms: Germline single nuclear polymorphisms (SNPs) have been found in both FGFR2 and FGFR4. The G388R SNP is associated with breast and colorectal cancer (Bange et al. 2002, Spinola et al. 2005) and causes a missense mutation in the transmembrane domain of FGFR4, leading to a defect in receptor lysosomal degradation and a sustained signalling (Wang J. et al. 2008). Furthermore, The SNPs found on FGFR2, however, are likely to alter the binding affinity of the receptor with transcription factors, inducing FGFR overexpression (Easton et al. 2007). FGFR2 SNPs are associated with an increased risk of breast cancer.

Impaired FGFR down-regulation: The activity of FGFRs is finely regulated at different levels (described in greater detail in Section 1.2.6, Regulation of signalling from FGFR), and any defect in the regulatory mechanisms that control FGFR activity can potentially lead to imbalanced signalling and result in the development of a malignant phenotype. The expression level of the protein Sef, for instance, a feedback inhibitor of FGFR signalling (Kovalenko et al. 2003), has been found to be considerably reduced in breast, ovary, thyroid, and prostate tumours (Zisman-Rozen et al. 2007). A defective endocytosis of FGFRs can also lead to oncogenesis by delaying receptor degradation and resulting in prolonged signalling. For instance, the FGFR3, G380R, and K650E mutations found in bladder, prostate, testicular cancer, and multiple myeloma (MM), as well as in achondroplasia, are thought to increase recycling of mutated receptor, resulting in sustained signalling (Cho et al. 2004). A splicing variant of FGFR2 identified in some cancer cell lines results from deletion of a region in the CT containing an endocytic motif (Cha et al. 2009). This deletion results in inefficient down-regulation of the receptor, increased levels of receptor at plasma membrane, and prolonged signalling.

The critical roles that FGFRs play in multiple steps of tumorigenesis make FGFR an attractive target for therapeutic intervention in cancer. A number of therapeutic strategies are currently being employed or developed to interfere with FGFR activity, including antibodies and small molecule tyrosine kinase inhibitors (Knights and Cook 2010).

1.2.5 Cell signalling via FGFR

1.2.5.1 Receptor trans-phosphorylation

Ligand-dependent dimerization leads to a conformational change in receptor structure that activates the intracellular kinase domain, resulting in trans-autophosphorylation of multiple tyrosine residues in the cytoplasmic domain of the receptor (Eswarakumar et al. 2005). Phosphorylated tyrosine residues function as docking sites for various signalling and scaffold proteins, which themselves may also be directly phosphorylated by FGFR, leading to activation of various signal transduction pathways. The combination of structural biology techniques and chemical quench methodology allows mapping in real time the autophosphorylation sites of FGFR, and reveals that this process follows a specific dynamic order that reflects activation of a distinct pattern of downstream effector proteins (Furdui et al. 2006). This phenomenon is not restricted to the FGFR family, but has also been observed for other RTKs, such as the IR (Wei L. et al. 1995) and the insulin-like growth factor 1 (IGF-1) receptor (Favelyukis et al. 2001). In the case of FGFR1, 7 tyrosine residues distributed throughout the intracellular domain (Y463, Y583, Y585, Y653, Y654, Y730, and Y766) have been shown to be subject to autophosphorylation following receptor activation (Mohammadi et al. 1996b) (Figure 1.8). Y653 in the activation loop of the kinase domain is the first residue to be phosphorylated (Furdui et al. 2006, Lew et al. 2009). This event has 2 effects: first, it enhances 50-to-100 fold the intrinsic catalytic activity of the receptor, resulting in autophosphorylation of the other tyrosine residues; second, it triggers recruitment of signalling molecules on the intracellular tail of the receptor.

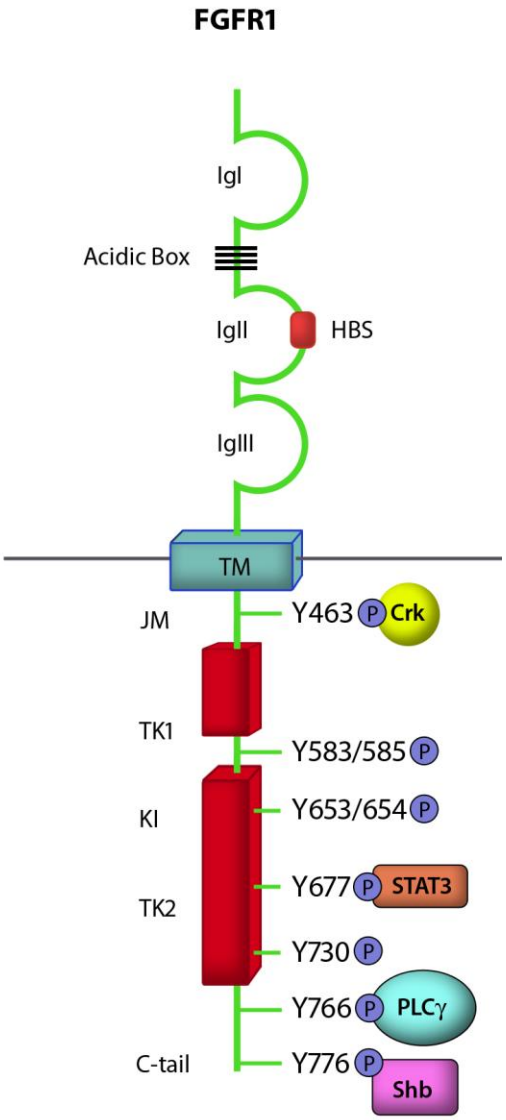

FGFR1	FGFR2	FGFR3	FGFR4
Y463	Y466	-	-
Y583/585	Y686/588	Y577	-
Y653/654	Y656/657	Y647/648	Y624/643
Y677	-	-	-
Y730	Y733	Y724	Y719
Y766	Y724	Y760	Y754
Y776	Y719	Y754	Y764

Figure 1.8 Sites of tyrosine phosphorylation in FGFRs

The major sites of tyrosine phosphorylation in FGFR1 are shown in the figure. The table on the right shows the corresponding tyrosine residues in FGFR2, FGFR3 and FGFR4.

Subsequently, the residues Y583, Y463, Y766, and then Y585 are phosphorylated. Phosphorylation of these residues does not affect the activation state of the receptor, but it has been shown to be necessary for the FGFR-mediated mitogenic response (Mohammadi et al. 1996b). Y463, for instance, which is the only residue identified thus far in the juxtamembrane region of the kinase domain of FGFR1, acts as a binding site for the docking molecule Crk, which mediates JNK and ERK1/2 signalling in FGF2-stimulated endothelial cells (Larsson et al. 1999) (Figure 1.8). Y766 is instead located in the carboxy terminal tail and mediates the binding of PLCγ (Mohammadi et al. 1991), whereas Y583 and Y585 are situated within the insert region of the kinase subdomains (Figure 1.8). The succeeding phosphorylation events occur on Y654, in the activation loop. This further enhances receptor catalytic activity and induces tyrosine phosphorylation of the recruited signalling proteins (Furdui et al. 2006, Lew et al. 2009). Further, in a recent study, Dudka A. et al. identified an additional tyrosine residue (Y677) in the kinase domain of FGFR1 subject to phosphorylation following receptor activation (Dudka et al. 2010). Phosphorylation of Y677 has been shown to be required for recruitment and activation of the signal transducers and activators of transcription 3 (STAT3) (Figure 1.8), a transcription factor that mediates signalling via the cytokine family of signalling receptors (Lim and Cao 2006).

1.2.5.2 RAS–mitogen-activated protein kinase pathway

The MAPK pathway is the best characterized pathway downstream of FGFRs and includes ERK 1/2, p38 and JNK kinases (Figure 1.9). Each kinase of the MAPK family phosphorylates specific serines or threonines of target substrates, promoting downstream critical cellular responses, such as cell differentiation and cell proliferation (Turner and Grose 2010).

Initiation of the cascade involves the lipid-anchored adaptor protein FGF receptor substrate 2 (FRS2) which, through its PTB domain, associates with the juxtamembrane region of the inactive receptor in a constitutive, phosphotyrosine-independent manner (Gotoh et al. 2004, Ong et al. 2000). In addition to the PTB-mediated binding, FRS2 constitutively associates to the plasma membrane via a myristoylation modification in its N-terminus, which drives the protein in proximity of the receptor (Kouhara et al. 1997). Upon activation, FGFR1 can phosphorylate FRS2 on 6 different tyrosines (Ong et al. 2000). Once phosphorylated, these tyrosines serve for recognition and assembly of a number of signalling and scaffold proteins. Through FRS2, the activated receptor becomes a platform for the recognition and recruitment of a specific signalling complex (Ong et al. 2000). One of the molecules recruited by phosphorylated FRS2 is the SH2-containing protein tyrosine phosphatase Shp2 (Gotoh et al. 2004), which is in turn tyrosine phosphorylated by the receptor, resulting in the recruitment of the adaptor molecule growth factor receptor-bound 2 molecule (GRB2) via its SH2 domain. Additionally, FRS2 itself contains 4 binding sites for GRB2, which can therefore also be directly recruited by FRS2. GRB2 is constitutively associated, via its SH3 domain, with the guanine nucleotide exchange factor (GEF) son of sevenless (SOS) (Lowenstein et al. 1992). Translocation of the FRS2/GRB2/SOS signalling complex to the proximity of the plasma membrane allows SOS to activate H-Ras by GTP exchange, resulting in activation of the downstream RAF and MAPK pathways (Eswarakumar et al. 2005) (Figure 1.9).

The Ras sarcoma (Ras) oncoproteins are members of the family of small guanosine triphosphatases (GTPases) and function as GDP/GTP-regulated molecular switches cycling between a GDP-bound inactive state and a GTP-bound active state (Vetter and

Wittinghofer 2001). The Ras family comprises 3 different groups of highly homologous proteins, Harvey-Ras (H-Ras), Kirsten-Ras (K-Ras), and Neuroblastoma-Ras (N-Ras), that differ significantly only in their C-terminal 40 amino acids (Hancock 2003). Here, a different post-translational modification in each class dictates specific subcellular locations to different plasma membrane microdomains. H-Ras, is anchored to the cytoplasmic face of the plasma membrane via 2 palmitoylated cysteine residues, Cys181 and Cys184, and a C-terminal *S*-farnesyl cysteine carboxymethylester (Roy et al. 2005). This localization brings H-Ras in close proximity to the signalling complex, where the protein SOS drives the exchange of GDP bound to H-Ras with GTP from the cytosol (Schmidt and Hall 2002).

When in its GTP-bound state, H-RAS can bind to and promote translocation of the Raf Murine Sarcoma Viral Oncogene Homolog (Raf) kinase to the plasma membrane (Terai 2005), where it is fully activated upon additional phosphorylation events (Avruch et al. 2001). Raf is a serine/threonine kinase and phosphorylates the MAPK/ERK Kinase1 and 2 (MEK1/2) at 2 serine residues at positions 217 and 221 in the activation loop, resulting in activation of MEK1/2 kinase activity (Alessi et al. 1994). Mammals possess 3 Raf proteins, Raf-1, A-Raf, and B-Raf, which present different tissue-specific expression patterns (Storm et al. 1990) and target specificity: B-Raf activates predominantly MEK1 and Raf-1 activates both MEK1 and MEK2, whereas A-Raf is a weak activator (Kolch 2000). The direct targets of MEK1/2 phosphorylation are the MAP kinases ERK1 and ERK2. To be fully activated, ERK1/2 must be phosphorylated at both a threonine and a tyrosine residue (Thr202/Tyr204 for human ERK1 and Thr185/Tyr187 for human ERK2) with the tyrosine phosphorylation preceding the threonine phosphorylation (Ferrell and Bhatt 1997).

ERK1/2 are proline-neighbouring serine/threonine kinases. Once active, ERK1/2 can phosphorylate a number of different cytoplasmic proteins, such as the Ribosomal Protein S6 Kinases (RSKs), which upon translocation into the nucleus play a role as transcriptional regulators (Chen R. H. et al. 1993), or SOS, initiating negative and positive feedback loops acting on the MAPK pathway itself (Kamioka et al. 2010). Alternatively, active ERK1/2 can translocate into the nucleus, where they promote phosphorylation of chromatin remodelling enzymes as well as transcription factors, such as c-myc, AP1, and the Ets-like gene 1 protein (Elk-1), ultimately inducing cellular responses such as cell differentiation or proliferation (Marais et al. 1993) (Figure 1.9).

A parallel cascade is initiated by the recruitment of the docking molecule Crk to the phosphor-tyrosine Y463 on FGFR1 (Larsson et al. 1999). Endothelial cells expressing a mutant of FGFR1 in the binding site for Crk (Y463F) show no change in the catalytic activity of the receptor, but fail to proliferate due to defective activity of the kinases Jun and ERK, demonstrating that Crk is responsible for further propagating mitogenic signals by FGF (Larsson et al. 1999).

1.2.5.3 PI3 kinase-AKT pathway

Activation of the PI3 kinase/AKT pathway by FGFRs can occur through 3 mechanisms (Figure 1.9). First, GRB2, recruited by phosphorylated FRS2, can bind the proline-rich region of GRB2-associated binding protein 1 (GAB1) via its C-terminal Sh3 domain (Ong et al. 2001). Assembly of the trimeric complex FRS2/GBR2/GAB1 leads to activation of phosphatidylinositol-3-kinase kinase (PI3K) via its kinase-regulatory subunit p85, resulting in production of phosphatidylinositol 3,4,5-trisphosphate [PI(3,4,5)P3]. This product specifically binds the Pleckstrin homology (PH) domain of the serine/threonine protein

kinase B (PKB), also known as AKT, regulating its cellular localization and activity (Ong et al. 2001). Full activation of AKT is reached when the serine/threonine kinase Phosphoinositide-dependent kinase 1 (PKD1) and 2 (PKD2) are also recruited to the plasma membrane and phosphorylate the threonine residue-308 in its kinase domain (T-loop) and the serine residue-473 within the hydrophobic motif (HM) in the CT, respectively (Franke 2008). In addition to being controlled by interaction of its regulatory p85 subunit with GAB1, the PI3 kinase can also be activated by directly binding to a phosphorylated tyrosine residue on FGFR via the p85 subunit (Ryan et al. 1998). Finally, activated Ras can also induce translocation of the PI3 kinase catalytic subunit p110 to the membrane, consequently promoting its activation (Rodriguez-Viciana et al. 1994).

Cellular responses activated by the PI3 kinase/AKT pathway range from primarily metabolic functions such as glucose transport and glycolysis to cell-cycle progression, apoptosis, and cell survival (Franke 2008). The wide range of biological responses reflects the ability of AKT to phosphorylate a wide variety of target proteins, both in the cytoplasm and in the nucleus (Figure 1.9). Among the best characterized targets of AKT with direct implications on cell survival is the pro-apoptotic BCL2-antagonist of death (BAD) protein. Once phosphorylated, BAD is retained in the cytosol, where its pro-apoptotic activity is effectively neutralized (Zha et al. 1996). Other targets include caspase-9 (Cardone et al. 1998) and the X-linked inhibitor of apoptotic proteins (XIAP) (Dan et al. 2004), which mediate the AKT-dependent maintenance of mitochondrial integrity by keeping cytochrome *c* and other apoptogenic factors in the mitochondria (Kennedy et al. 1999). Key regulators of metabolic functions controlled by AKT include the glycogen synthase kinase-3 (GSK-3), which mediates an insulin-mediated increase in

glycogen synthesis and suppression of glycogenolysis, (Cross et al. 1995), whereas $p21^{Cip1/WAF1}$ and $p27^{Kip1}$ are 2 cell-cycle regulator proteins controlled by AKT (Liang et al. 2002, Rossig et al. 2002, Rossig et al. 2001).

1.2.5.4 PLCγ/PKC pathway

The PLCγ pathway involves binding of phospholipase C-gamma (PLCγ) to specific phosphotyrosines on activated FGFR1-4 (Ceridono et al. 2005, Mohammadi et al. 1991, Vainikka et al. 1994). Recruitment of PLCγ to the membrane is further promoted by binding of the PH domain of PLCγ to PI(3,4,5)P3 molecules generated by FGF-dependent PI3 kinase activity (Falasca et al. 1998). Following activation, PLCγ induces hydrolysis of phosphatidylinositol-4,5-biphosphate [PI(4,5)P2], generating 2 second messengers, inositol-1,4,5-triphosphate [I(1,4,5)P3], which promotes the release of intracellular $Ca2^{+}$, and diacylglycerol (DAG). The resulting increase in DAG levels triggers recruitment of protein kinases C (PKCs) to the membrane domains, where they undergo conformational changes that result in exposure of binding sites to substrates and scaffolding proteins (Griner and Kazanietz 2007). In parallel, the increased levels of $Ca2^{+}$ in the cytoplasm further promote the activity of PKCs. Once activated, PKCs can phosphorylate several cytoplasmic targets, promoting cellular processes such as cytoskeletal organization, cell motility, or cell differentiation (Figure 1.9).

1.2.5.5 STAT pathway

A recent study suggested the existence of a novel signalling pathway activated by FGFR which involves the activity of the transcription factor STAT3 (Dudka et al. 2010). Although generally associated with cytokine signalling, a role for STAT3 has already been described

in the signalling cascade activated by EGFR (Alvarez et al. 2006). Similarly, Dudka et al. recently showed that STAT3 binds to phosphorylated Tyrosine677 of activated FGFR1, resulting in Src-dependent phosphorylation of STAT3 itself on tyrosine residues (Dudka et al. 2010). However, the biological effects resulting from FGFR-dependent STAT activation remain to be elucidated.

1.2.5.6 Correlation between FGFR signalling pathways and biological responses

In the last several years, a considerable effort has been undertaken to define a correlation between FGFR-dependent signalling pathways and specific cellular response activation. However, analysis of the role of each signalling cascade in a given biological outcome reveals that the situation is more complex and no simple correlation can be drawn. Some studies, for instance, showed that the FGF-induced ERK1/2 pathways mediate cell cycle arrest in chondrocytes (Raucci et al. 2004), while in PC12 cells this is required for cell differentiation (Maher 1999), suggesting that activation of differential FGF signalling pathways is cell-type specific. In addition, a number of studies consistently suggest that differences in the duration of signalling could dictate the specific cellular outcome. Traverse et al., for instance, showed that in PC12 cells, sustained ERK1/2 activation causes growth arrest and differentiation, while a shorter stimulus induces proliferation (Traverse et al. 1992). These and many other observations demonstrate the complexity of the FGF response, which is the result of a multidimensional network of communication between the large number of components, crosstalk between different pathways, and the synergic action of the many mechanisms of regulation and feedback loops.

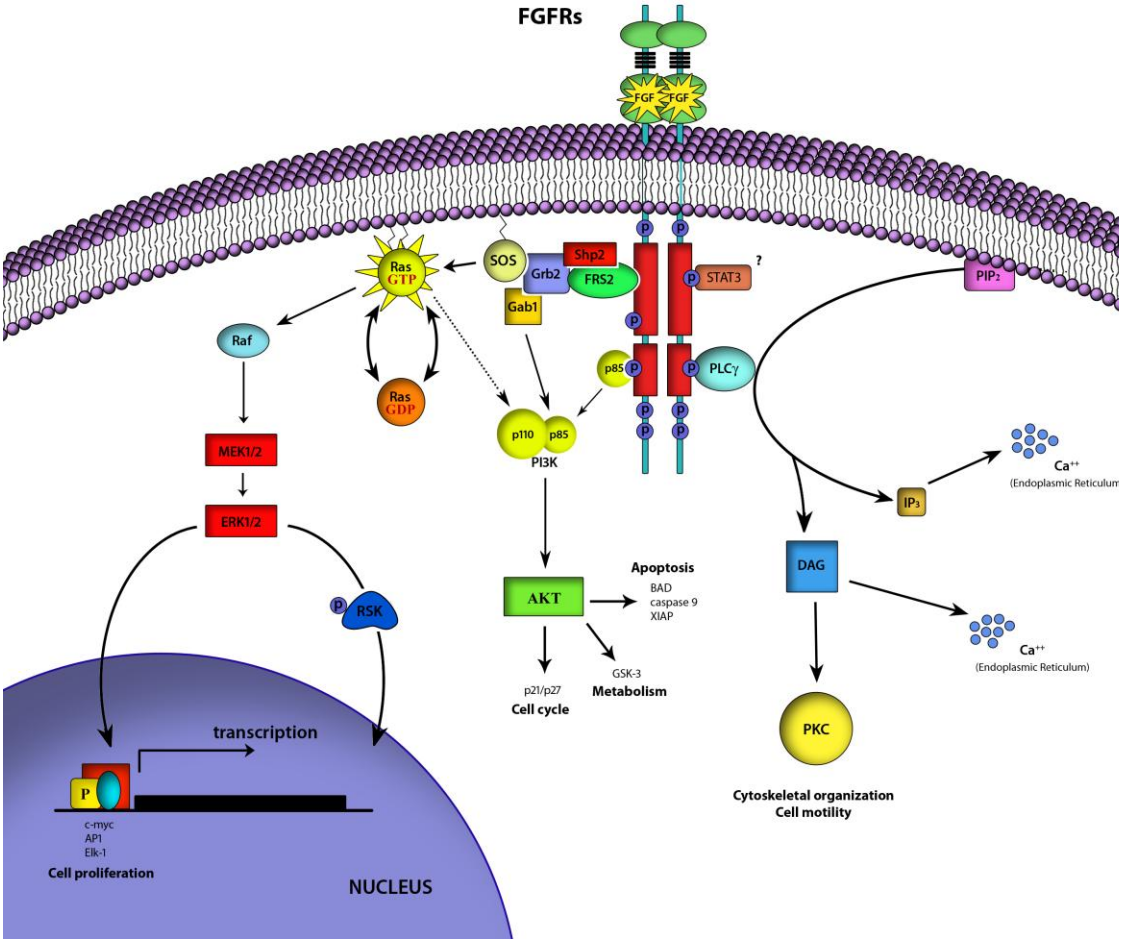

Figure 1.9 Intracellular signalling pathways activated by FGFR

Following ligand binding and receptor dimerization, the intracellular kinase domains trans-phosphorylate each other, leading to recruitment of multiple signalling and scaffold proteins and activation of several signal transduction pathways. The Ras/MAPK pathway involves docking protein FRS2, which constitutively binds to FGFR and becomes phosphorylated after FGFR activation. Phosphorylated FRS2 recruits a multiprotein complex in the proximity of the plasma membrane, comprising Grb2 and SOS, resulting in activation of the Ras/MAPK signalling cascade. The PI3 kinase/AKT pathway can be initiated by multiple mechanisms, all resulting in activation of the PI3 kinase. Initiation of the PLCγ/PKC pathway occurs via recruitment of PLCγ to a phosphotyrosine residue of FGFR. PLCγ activity results in release of intracellular calcium and activation of PKC.

1.2.6 Regulation of signalling from FGFR

Considering the critical biological responses regulated by FGFRs, it is not surprising that their activity is finely regulated in cells. A number of regulatory mechanisms have been described that operate at many levels. These include intrinsic capabilities of the receptor to auto-inhibit its own catalytic activity, as well as the action of a number of proteins modulating FGF-mediated signalling both in the extracellular space and within the cell.

1.2.6.1 Extracellular modulators and autoinhibitory mechanisms

Heparin or HLGAGs are responsible for one of the first mechanisms of modulation of FGFR activity. By bridging 2 FGFR monomers together, HLGAGs drive the assembly of an active 2:2:2 FGF:FGFR:heparin complex (Schlessinger et al. 2000). In addition, HLGAGs have been shown to be important in determining the specificity of FGF/FGFR interaction (Guimond and Turnbull 1999, Kan et al. 1999, Pye and Kumar 1998). Finally, by binding and retaining FGFs in the extracellular matrix, HLGAGs limit FGF diffusion into interstitial spaces, thereby contributing to creating a local reservoir of FGFs, which is necessary for generating the strict spatial regulation of FGFR activation within a tissue (Flaumenhaft et al. 1990, Gould et al. 1995). Allen et al. investigated how spatio-temporal changes in heparan sulphate can promote formation of a ternary complex with FGF and FGFR; they found that synthesis of HS is tightly regulated throughout development (Allen and Rapraeger 2003). Similar to other RTKs, FGFR activation is intrinsically controlled by autoinhibitory mechanisms that keep the receptor in inactive structural conformations. As described in Section 1.2.2 (FGFR structure and alternative splicing) a first autoinhibitory mechanism is mediated by the D1 domain and the AB in the extracellular portion, which at low concentration of ligand intramolecularly interact with the ligand-

binding site (D2-3) and the HBS on FGFR, respectively (Figure 1.10A). In this state, any interaction with ligand and a cofactor is prevented and the receptor is maintained in an inactive state (Kalinina et al. 2012, Olsen et al. 2004, Wang F. et al. 1995b). A second auto-inhibitory mechanism occurs within the kinase domain of FGFR, which directly affects the phosphotyrosine catalytic activity of the receptor. FGFR1, for example, has been shown to assume an inactive state when, in the absence of ligand, Arg-661 and Pro-663 sterically block access of the substrate (Mohammadi et al. 1996a). In contrast, the FGFR2 autoinhibitory mechanism is mediated by a network of hydrogen bonds formed by the residues E565, N549, and K641, which inhibit the movements of the N-terminal lobe towards the C-terminal necessary for kinase activation (Chen H. et al. 2007).

1.2.6.2 Intracellular modulators and feedback loops

Multiple mechanisms of regulation are activated by the components of the FGFR signalling cascade itself, generating negative and positive feedback loops that shape the level of signalling output. A well characterised example of negative feedback loop acting in the FGFR pathway is mediated by ERK1/2. This occurs through direct phosphorylation of threonine residues on FRS2 by ERK1/2, which result in preventing FRS2 itself from being further tyrosine phosphorylated by FGFR (Gotoh 2008).

Because MAPKs require serine/threonine and tyrosine phosphorylation for full activity, a number of dual specificity phosphatases (DSPs) also act as positive or negative regulators downstream in the FGFR cascade (Figure 1.10B). MAPK phosphatase-3 (MKP3), also known as DSP6, is a well established negative regulator of FGF signalling during vertebrate development (Dickinson et al. 2002, Eblaghie et al. 2003). This regulator is expressed in response to FGFR activation, as shown in a recent mouse knockout

experiment, in which *MKP-3*-null embryos displayed elevated levels of phospho-ERK in limb and several FGFR-associated skeletal dysfunctions (Li C. et al. 2007). This and other observations demonstrate that MPK3 is part of a feedback loop which works to set the levels of phospho-ERK downstream of the FGFR signalling pathway. In contrast, tyrosine phosphatase Shp-2, in addition to its role in the assembly of the complex GRB2/SOS following FGFR activation, also functions as a positive regulator of FGF cascade, acting upstream of MAPK (Tang et al. 1995). However, the precise molecular mechanism of Shp2 action has not yet been described.

Finally, an important negative feedback loop in the FGF signalling cascade is mediated by Sprouty proteins (Figure 1.10B). The regulatory mechanism controlled by Sprouty was initially identified in Drosophila (dSpry) for its inhibitory effect on FGF-dependent development of thacheal branches (Hacohen et al. 1998). In mammals, 4 Sprouty proteins (Sprouty 1–4) have been identified, with Sprouty2 acting similarly to *dSpry*, regulating branching of the mammalian lung (Tefft et al. 1999). Spread1 and Spread2, two members of the Sprouty family, have been shown to inhibit FGFR-dependent Ras/MAP-kinase activation (Gross et al. 2001, Yusoff et al. 2002). A number of studies also demonstrate an inhibitory effect of Spread4 on the FGFR signalling pathway (Sasaki et al. 2001). The mode of action of Sprouty proteins in FGF signalling remains elusive, and it appears to strongly depend on the cellular context. What is certain is that following FGF stimulation, Sprouty1 and 2 undergo tyrosine phosphorylation via a Src-dependent process (Hanafusa et al. 2002, Li X. et al. 2004, Mason J. M. et al. 2004, Rubin C. et al. 2003). The phosphorylated tyrosine serves as a binding site for SH2 domain-containing proteins, such as the adaptor GRB2 and the E3 ubiquitin-protein ligase Cbl. Binding of GRB2 to

Sprouty upon FGFR activation has been shown to be sufficient to disengage the docking protein from the FRS2/GRB2/SOS signalling complex, resulting in inhibition of the signalling (Hanafusa et al. 2002). The role of Cbl in the negative feedback loop mediated by Sprouty is not clear. Binding to Cbl in fact has been shown to drive Sprouty ubiquitination and subsequent proteasomal degradation (Hall et al. 2003, Mason J. M. et al. 2004). One possible explanation is that Sproutys serve as docking proteins rather than being a direct substrate for Cbl-mediated ubiquitination. This would bring Cbl in proximity to potential targets of ubiquitination and degradation, resulting in a negative effect on the signalling cascade (Guy et al. 2009).

Another mechanism of regulation of FGFR activity is mediated by the transmembrane modulator Sef. In mouse and zebrafish, *Sef* genes together with *fgf8* and the *sprouty* genes form a synexpression group, genetic modules in which the expression of different genes codifying members of a common pathway is co-regulated (Lin W. et al. 2002, Niehrs and Pollet 1999). Sef proteins function as negative modulators of FGFR signalling (Furthauer et al. 2002), exerting their inhibitory effects at multiple levels (Figure 1.10B), although the precise molecular mechanism of Sef action is still controversial. Some studies, for example, show that overexpressing Sef inhibits FGFR1 and FRS2 phosphorylation (Kovalenko et al. 2003). Other reports, in contrast, demonstrate that Sef localizes to the Golgi, where, by binding activated MEK, it inhibits dissociation of the MEK/ERK complex, blocking translocation of active ERK into the nucleus (Torii et al. 2004). Interestingly, ERK can also signal from the Golgi apparatus, where it is responsible, for instance, for the mechanism of selection of positive thymocyte, suggesting that the

activity of Sec as an FGF signalling inhibitor can be functionally relevant (Daniels et al. 2006).

In addition to negative regulators, several molecules that positively modulate signalling from FGFR have also been described. Among them, the best characterized are the fibronectin- and leucine-rich transmembrane (FLRT) proteins, that mediate cell adhesion functions. For all the 3 members (FLRT 1–3) thus far identified in higher vertebrates (Lacy et al. 1999), the capability to interact with FGFR1 has been demonstrated (Bottcher et al. 2004, Haines et al. 2006), while only recently has FLRT2 also been shown to interact with FGFR2 (Wei K. et al. 2011). The tissue-specific expression pattern of all FLRTs appears to highly correlate with regions of FGFR expression, further supporting the requirement for interaction between FGFR and FLRT (Haines et al. 2006). The role of positive modulator of FGF-mediated ERK1/2 signalling has been described for both FLRT1 and FLRT3 (Bottcher et al. 2004, Wheldon et al. 2010) (Figure 1.10B). However, the precise mechanism of action of FLRT remains unclear.

In addition to FLRT proteins, FGFR signalling can also be modulated by the neural cell adhesion molecule (NCAM) (Cavallaro and Christofori 2004) a cell surface glycoprotein that mediates important processes in the central nervous system such as intercellular adhesion, axonal growth, and cell migration (Hinsby et al. 2004). NCAM-derived peptides have been reported to interact with both FGFR1 and FGFR2 (Christensen et al. 2006, Kiselyov et al. 2003) and induce specific responses. In the case of FGFR1 for instance, NCAM stimulation was reported to induce sustained recycling of receptor to the cell surface in a Rab11 and Src-dependent manner and to promote cell migration (Francavilla et al. 2009).

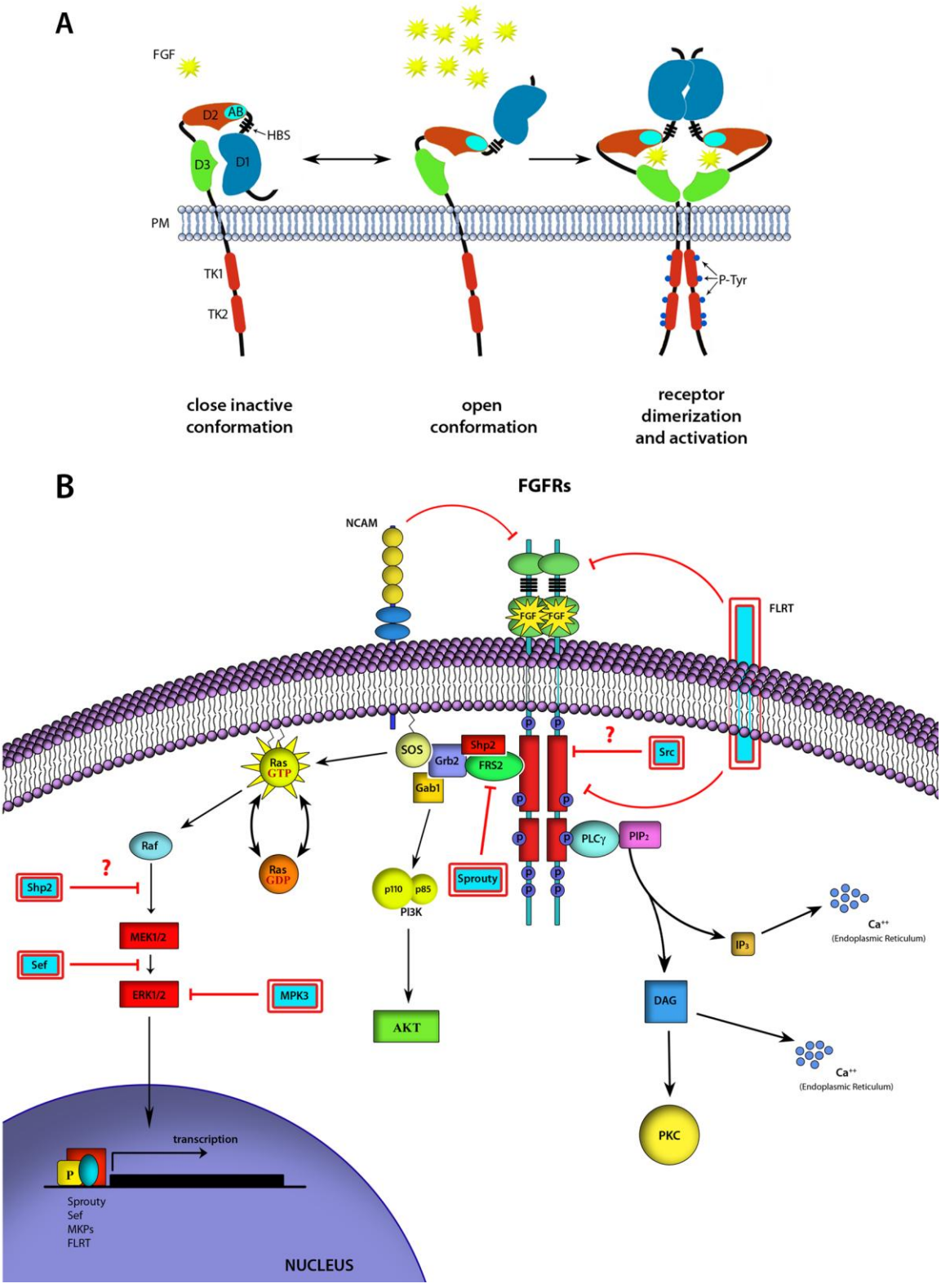

Figure 1.10 Mechanisms of regulation of FGFR signalling

A. Conformational opening and activation of FGFR induced by high concentration of ligand. Autoinhibitory conformation is held by intramolecular interaction between the D1 domain and the D2-D3 region, and between the Acidic box (AB) and the heparin binding site (HBS). **B**. Diagram depicting the main intracellular factors (double red border objects), which either positively or negatively interfere with FGFR signalling cascade.

Finally, Src proto-oncogene protein tyrosine kinase, which is a key component of the signalling pathway by FGFR, has also been implicated as a regulatory factor. Src activity and involvement in FGFR cascade is discussed in more detail in Section 1.4, Src family kinase.

1.3 Endocytosis and endocytic trafficking

Endocytosis represents an important mechanism of signal regulation for a wide variety of membrane-bound receptors, including all members of the RTKs. Through endocytosis, activated receptors undergo regulated internalization and are transferred into the cytosol from the cell surface. Thus, by controlling the number of receptors available for activation on the plasma membrane, endocytosis actively modulates the desensitization state of cells to extracellular signals.

Once internalized, receptors follow different endocytic routes inside the cells, by which they are sorted through predetermined specific cellular compartments up to their final destination. Traditionally, endocytic trafficking of RTKs was considered merely a cellular strategy to attenuate receptor signalling by sorting the internalized ligand-activated receptors into acidic compartments where ligands dissociate and signalling is terminated (Beguinot et al. 1984, Stoscheck and Carpenter 1984). However, increasing evidence suggests that endocytosis and signal transduction by RTKs are tightly coupled, and that trafficking of receptors along the endocytic pathway contributes to spatio-temporal regulation of signal transduction (Di Fiore and De Camilli 2001, von Zastrow and Sorkin 2007).

Section 1.3.1 below describes the main endocytic routes for internalization of RTKs, with particular emphasis on FGFRs, and it illustrates supporting evidence for crosstalk between RTKs endocytosis and signalling.

1.3.1 Pathway of receptor endocytosis

Generally speaking, endocytosis is the process by which plasma membrane lipids and macromolecules embedded within them, as well as extracellular fluids and dissolved solutes, are fully internalized into the cell. This is mediated by formation of an endocytic vesicle, which is generated by the invagination and subsequent budding of plasma membrane. An endocytic vesicle therefore can include not only effector molecules such as growth factors and hormones or nutrients, but also toxins and pathogens. Thus, the physiological roles of endocytosis vary widely: from removal of membrane-bound proteins from the cell surface (as in the case of transmembrane receptors) to the life cycle of a number of pathogens, which use endocytosis as mechanism to enter host cells (Thorley et al. 2010), to the maintenance of membrane homeostasis within the cell (Coupin et al. 1999). In the context of RTKs, a number of endocytic pathways have been described; these are defined and classified on the basis of the molecules that mediate internalization of cargo proteins.

1.3.1.1 Clathrin mediated endocytosis

Clathrin mediated endocytosis (CME) was the first endocytic pathway discovered (Roth and Porter 1964), and it remains the best characterized route of entry for RTKs. Through CME, receptors are enclosed and transported into vesicles coated with an organized network of trimers of clathrin (Figure 1.11A), also known as triskelia. A clathrin triskelion

is composed of 3 legs, each comprising one heavy chain and one light chain (Ungewickell and Branton 1981). Under specific conditions (Kirchhausen and Harrison 1981), clathrin assembles in a network of hexagons and pentagons and forms a 'cage' that surrounds the vesicle budding from the membrane (Crowther et al. 1976). The protein coat around a clathrin-coated vesicle (CCV) is a highly complex structure and, in addition to the clathrin triskelion, includes a number of adaptor proteins. These proteins can directly bind to the lipid bilayer of the vesicle on one side, whereas on the other, they interact with the clathrin cage (McMahon and Boucrot 2011). The entire protein coat, therefore, not only provides mechanical strength to the budding vesicle, but also assembles other specific molecules necessary for the endocytosis process to occur properly.

The molecular mechanisms driving the very first steps in the formation of a membrane invagination, also called pit, remain unclear. However recent studies have reported that the endocytic 'hot-spots' on the plasma membrane, enriched in PI(4,5)P2 and where clathrin is very likely to be recruited and vesicles to bud, are always marked by the presence of a network of 3 interacting proteins: the F-BAR domain-containing protein (FCHO), and the scaffold proteins EGFR pathway substrate 15 (Eps15) and Intersectin (Henne et al. 2010). Blocking the formation of this network, by depleting the cells of any of the 3 components, results in inhibition of clathrin coat recruitment, suggesting that these proteins constitute an early module necessary for nascent CCP assembly (Henne et al. 2010, Stimpson et al. 2009). Once a membrane invagination has formed, it may either become abortive or proceed in the budding process by selecting the specific cargo proteins to enclose. Cargo selection is mediated by accessory protein AP2, which is the most abundant component of CME machinery after clathrin (Blondeau et al. 2004) (figure

1.11A). AP2 is recruited to the nucleation module at the plasma membrane via its binding sites for PI(4,5)P2. In this respect, AP2 differs from other AP adaptors, such as AP1, AP3, or AP4, which have different requirements for membrane binding, and are rather found to play a role in CCV formation in secretory or endosomal/lysosomal sorting pathways (Nakatsu and Ohno 2003). Recruitment of cargo molecules is then achieved by direct interaction between the μ2-subunit and the σ-subunit on AP2 and specific motifs on transmembrane receptors (Collins et al. 2002, Kelly et al. 2008, Sorkin 2004). The μ2-subunit recognizes tyrosine-based motifs of the form YXXΦ (where Φ is an amino acid with a bulky, hydrophobic side chain and X is any amino acid), whereas the σ2-subunit, with an additional contribution from the α-subunit, engages the [DE]XXXL[LI] dileucine signals on cargo proteins (Bonifacino and Traub 2003). The binding site on the μ2-subunit is occluded in steady-state conditions, and phosphorylation of residue Thr156 by adaptor-associated kinase 1 (AAK1) is required to 'open' the cargo binding site and induce full binding capacity of AP2 to the cargo molecule (Ricotta et al. 2002). AP2 also interacts with several other accessory proteins via its α and β appendages. These proteins can either interact with specific cargoes and mediate indirect binding of cargos with AP2 (Traub 2009) or function as membrane curvature effectors, as in the case of Epsin (Ford et al. 2002, Ford et al. 2001). Upon cargo selection, clathrin triskelia are recruited to the plasma membrane via interactions with both AP2 and other adaptor proteins. The β2-subunit of AP2 interacts with clathrin via a LΦXΦ[DE] motif (also called 'clathrin box') (Dell'Angelica et al. 1998), inducing clathrin polymerization at the plasma membrane and assembly of the 'cage' around the forming vesicle (Brodsky et al. 2001). In addition, clathrin polymerisation also seems to stabilize a curvature of the membrane, as the coated pit invaginates (Hinrichsen et al. 2006). A number of BAR-domain containing

proteins, such as amphiphysin or endophilin, are then recruited to the area where the curvature of the vesicle neck is forming. Through their BAR domains, these proteins are thought to deform the plasma membrane and to help form the neck (Mim and Unger 2012). Additionally, through an SH3 domain, they bind to the proline-rich region of the GTPase Dynamin, recruiting the enzyme around the vesicle neck (Ferguson et al. 2009). Although the precise mechanism is not clear, Dynamin oligomerization around the vesicle neck appears to induce GTP hydrolysis (Figure 1.11A), ultimately resulting in membrane fission and release of the vesicle into the cytoplasm (Bashkirov et al. 2008). Once the vesicle is formed, the clathrin coat and the adaptor protein layer are removed. Disassembling of the clathrin lattice back to single triskelions is mediated by ATPase heat shock cognate 70 (HSC70) and its cofactor auxilin/GAK (Barouch et al. 1997, Ungewickell et al. 1995). This uncoating allows the formed vesicle to fuse with the target endosome, where the cargo is delivered, and the coating components are released and reused for the next event of vesicle formation (Figure 1.11A). Among the receptors internalized through CME, some are endocytosed constitutively regardless of ligand binding. The best studied of these is Transferrin receptor (TfR), whose trafficking mostly occurs through CME (Jing et al. 1990). On the contrary, many receptors enter cells through CME in a stimulation-dependent manner, including RTKs, such as EGFR or FGFR, and G protein-coupled receptors (GPCRs).

Once internalised, newly formed vesicles fuse with one another or with pre-existing organelles; this is known as sorting/early endosome (SE or EE) (Hsu and Prekeris 2010) (Figure 1.11B). The reduced pH of this compartment induces dissociation of many ligand-receptor complexes, followed by recycling of the receptor component back to the plasma

membrane. Receptor recycling can occur either directly (rapid recycling) (Deneka, M., 2003) or indirectly (slow recycling) via recycling endosomes (REs) (Grant and Donaldson 2009), generally located in proximity to the nucleus, and referred to as the perinuclear recycling compartment (Figure 1.11B). Many cargoes are not recycled, but instead are sorted to late endosomes (LE) and ultimately to lysosomes for degradation. Others are delivered to the trans-Golgi network (TGN) via a retrograde transport (Bonifacino and Hurley 2008) (Figure 1.11B).

Endosomal sorting and vesicular trafficking are regulated by several proteins and lipids. Rab proteins, for instance, are a family of small GTPases that coordinate membrane trafficking by mediating vesicle fusion (Chavrier and Goud 1999), motility (Hammer and Wu 2002), and by recruiting the cargoes (Elizabeth Smythe 2002), as well as specific tethering factors. The functional specificity of each Rab member is conferred by its specific subcellular localization. For this reason different populations of endosomes have been identified according to the presence of a specific Rab member. Protein Rab5 for example is localized to the early endosomal compartments, where it mediates both EE fusion and motility (Gorvel et al. 1991, Nielsen et al. 1999), whereas Rab4 and Rab11 associate with both the rapid and slower recycling compartments, respectively (Ullrich O. et al. 1996, Van Der Sluijs et al. 1991).

1.3.1.2 The early endosomal compartment

The EEs appear as a pleomorphic compartment composed of morphologically, chemically and functionally distinct sub-domains, including thin tubular structures and large vesicles (Gruenberg 2001). As mentioned earlier, the main function of EEs is the sorting of endocytic cargoes to their specific intracellular destination. This is accomplished through

the action of an elaborate machinery comprising several endocytic regulatory and effector proteins. The GTPase Rab5 lies at the centre of this machinery and is the most extensively studied Rab member of the early endosomal compartment (Barbieri et al. 1996, Gorvel et al. 1991). Rab5 regulates a wide range of endocytic processes: it is involved in the formation of clathrin-coated vesicles (McLauchlan et al. 1998), in subsequent fusion of these vesicles with EEs, in the homotypic endosome-endosome fusion (Gorvel et al. 1991) and in the motility of EEs on microtubule tracks (Nielsen et al. 1999). In order to regulate all these processes, Rab5 interacts with several effector proteins on specific domains of the early endosomal compartment where they carry out their specialized endocytic function (Christoforidis et al. 1999, Grosshans et al. 2006). One such effector protein, EEA1, was identified as a key component of the endocytic machinery for docking and fusion of EEs (Christoforidis et al. 1999), and is a widely used marker for EE due to its specific localization to this compartment. Interestingly, while Rab5 is equally distributed between CCVs and early endosomes, the localization of EEA1 is only restricted to the membranes of the EE (Rubino et al. 2000). This observation suggested that the Rab5 effector EEA1 specifies the target compartment in the process of fusion between CCV and EE, thus providing directionality to the vesicular transport from the plasma membrane towards the EE (Rubino et al. 2000).

APPL1 and APPL2 (Adaptor protein containing PH domain, PTB domain and Leucine zipper motif) are other two Rab5 effectors that specifically associate with a distinct subpopulation of Rab5-positive EEs (Miaczynska et al. 2004). Rather than having a role in endosomal transport, APPL proteins have been shown to be important in signalling (Miaczynska et al. 2004, Rashid et al. 2009). This observation suggests that the EE is not

only a transitional compartment, but it can actively play a role in signal transduction. The role of endocytic organelles in signal propagation is discussed in greater detail in Section 1.3.3, Crosstalk between RTK endocytosis and signalling.

1.3.1.3 Clathrin-independent endocytosis

A number of RTKs, as well as other cargo molecules, can also be internalized by endocytic pathways independent of clathrin. Thus far, a relatively high number of clathrin-independent endocytosis (CIE) pathways have been identified. However, less is known about these, and more importantly, the studies that have focused on these alternative routes of entry rely primarily on inhibition of CME as their study methodology, and therefore could not exclude all the indirect effects that inhibition of one pathway can have on another pathway. One of the best-defined alternative pathways is endocytosis via caveolae. Caveolae appear at the electron microscope as plasma membrane invaginations of 50±80 nm in diameter.

Caveolae composition is cell-type dependent (Parton et al. 1997, Rothberg et al. 1992, Stan et al. 1997), but they are always enriched in cholesterol, sphingolipids (Simons and Toomre 2000) and caveolin1 (Rothberg et al. 1992). Each one of these components is essential for the formation and the stability of caveolae: in their absence caveolae formation is prevented (Fra et al. 1995, Rothberg et al. 1992). Caveolin1 constitutes the protein coat, with 100–200 molecules per caveola in HeLa cells (Pelkmans 2005) (Figure 1.11A).

In addition to caveolin1, caveolae have been shown to contain dynamin (Henley et al. 1998, Oh et al. 1998), which, similar to its role in CME, is recruited to the neck of caveolar

invaginations, where it mediates scission of the vesicle from the plasma membrane (De Camilli et al. 1995) (Figure 1.11A). Many other aspects of caveolar endocytosis remain to be established, such as the exact role of caveolin1 in the endocytic process, or the involvement of other accessory proteins. Once internalized, caveolar vesicles fuse and transfer their cargo to larger tubular membrane organelles. These organelles, once thought to be independent compartments distinct from endosomes and known as caveosomes (Pelkmans et al. 2001), have recently been shown to correspond to late endosomal compartments (Hayer et al. 2010). From here, the internalized cargoes are sorted either to the ER, the Golgi complex, or to other compartments (Figure 1.11B).

Cargoes that can be internalized through caveolae include cholera toxin (Montesano et al. 1982), folic acid (Rothberg et al. 1990), serum albumin (Schnitzer and Oh 1994), glycosphingolipid Lactosyl Ceramide (LacCer) (Puri et al. 2001), and Simian Virus 40 (Pelkmans et al. 2002).

The observation that inhibiting both CME and endocytosis via caveolae does not block internalization of several cargoes suggests that other ways of entry that are both clathrin- and caveolin1-independent exist. However, their functional roles and the molecules involved in these pathways remain elusive. In the context of RTKs, mechanisms of internalization involving large volumes of membrane, such as the circular dorsal ruffles (CDRs) or the large protrusions formed during macropinocytosis, have been proposed to mediate ligand-induced endocytosis (Abella et al. 2010, Schmees et al. 2012) (Figure 1.11A).

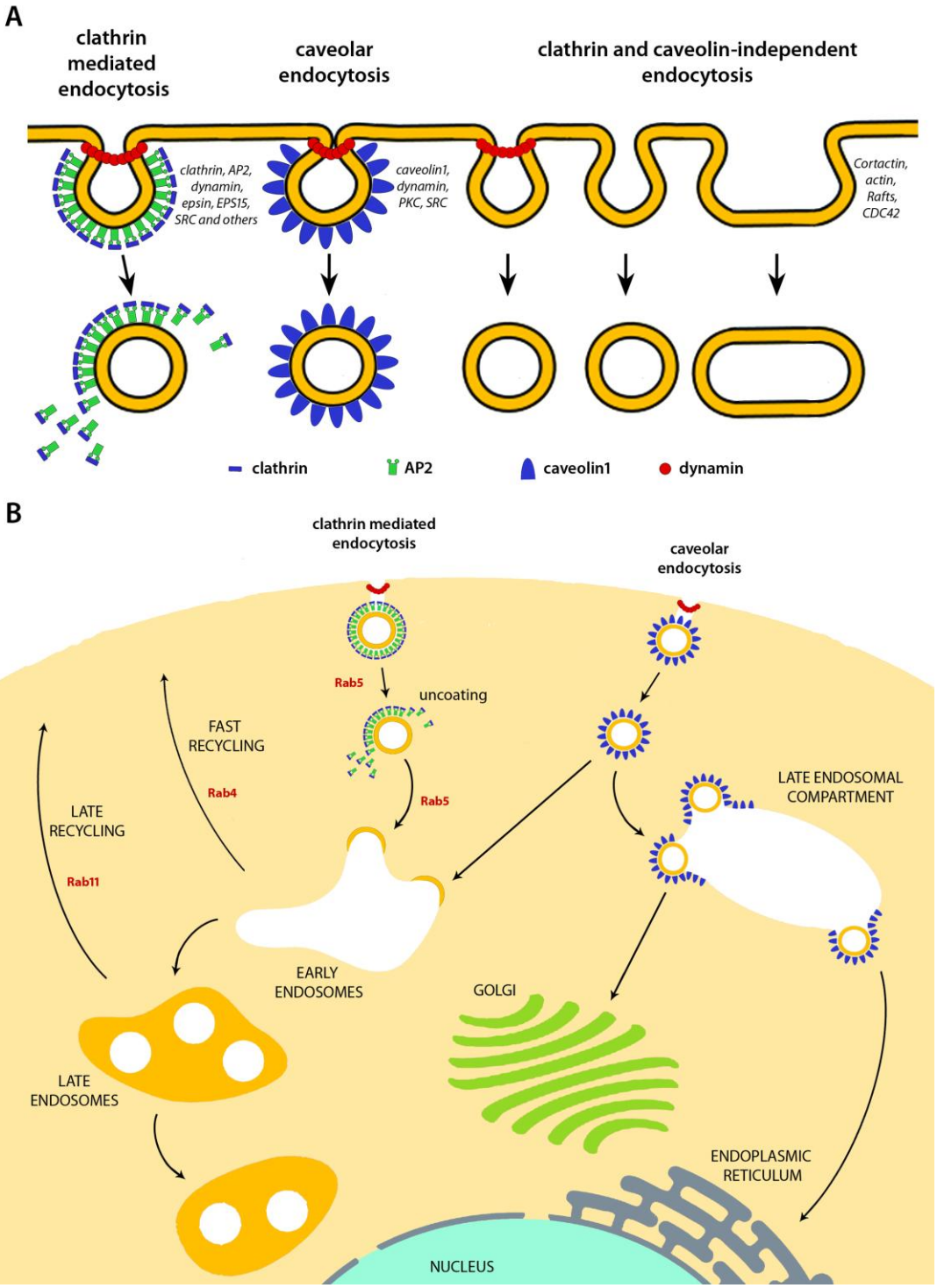

Figure 1.11 Endocytosis and endocytic trafficking of RTKs

A. Major endocytic routes for the entry of RTKs into cells. The diagram shows the main functional attributes known for each pathway. **B**. RTKs internalized through CME are trafficked into the early endosomes and then sorted to late endocytic compartments for degradation (lysosomes). Alternatively, cargoes can be recycled back to the cell surface via either a fast or a slow recycling pathway. Cargoes internalized through caveolar endocytosis are trafficked into an intermediate compartment, where they are sorted either to Golgi or to the endoplasmic reticulum. Alternatively, caveolin1-coated vesicles can deliver their content into early endosomes, sorting cargoes to the canonical endocytic pathway.

1.3.2 Endocytosis of FGFRs

Although the signalling pathways activated by FGFRs have been extensively studied, little is known about the endocytic route mediating their internalization, and the studies to date that have focused on this issue have reached rather controversial conclusions. The first study on FGFR endocytosis dates back on 1996, when Glaizes et al. found that basic FGF, or FGF2, localizes in caveolae structures in BHK cells (Gleizes et al. 1996). This first observation was further supported by the presence of a putative caveolin-binding motif in the cytoplasmic domain of all members of the FGFR family (Couet et al. 1997). Several years later, Marchese et al. examined the effect of stimulation of epithelial cells with keratinocyte growth factor (KGF) or FGF7 (Marchese et al. 1998). KGF specifically binds and activates KGF receptor (KGFR) or FGFR2-IIIb, one of the two alternative splicing products from FGFR2 mRNA specifically expressed in epithelial tissues (Miki et al. 1991, Miki et al. 1992). By using immunogold electron microscopy on NIH 3T3 cells, Marchese et al. observed localization of KGF inside endocytic pits, which these authors speculate to be clathrin-coated structures. A clathrin and caveolae-independent pathway was also proposed for endocytosis of FGFRs. Upon inhibition of endocytosis from both coated pits and caveolae through the endocytic uptake of FGF1 was still occurring, indicative of an alternative route for the internalization of FGFR (Citores et al. 2001). Similarly, Reilly et al. show that uptake of FGFR1 was independent of both caveolae and coated pits (Reilly et al. 2004). Finally, a recent study extensively investigated the mechanism of internalization of both FGFR1 and FGFR3, and demonstrated that after depletion of cells for clathrin, or by expressing a dominant-negative mutant of dynamin, FGFR3 uptake was only partially inhibited, whereas endocytosis of FGFR1 was almost completely blocked (Haugsten et al.

2011). Thus, previous reports about FGFR endocytosis appear to be quite controversial, and it appears that no firm conclusion can be drawn. However, it is possible that the discrepancy is the result of employment by each of the groups mentioned above of different combinations of FGF ligands/FGFR isoforms, or the use of a different cellular platform for analysis of FGFR endocytosis. As a matter of fact, each FGF ligand, as well as each FGFR and the specific combination of the two, has been shown to activate specific intracellular pathways, to physiologically target specific cell types, and to promote its own specific cellular response. It would not be surprising, therefore, that different FGFRs employ different endocytic routes, or that 2 cell lines use different endocytic pathways to internalize the same FGFR.

Following internalization, FGFR appears to follow the canonical intracellular route, being mainly targeted to lysosomes for degradation (Haugsten et al. 2005). However, several reports showed that this process is more complex, and that similar to the internalization pathway, the intracellular fate of FGFR can be receptor/ligand-isoform specific. Supporting evidence emerges from Belleudi et al., who showed that both FGF7 and FGF10 bind to FGFR2-IIIb in epithelial cells, but while FGF7 mainly targets the receptor to lysosomal compartments where the receptor is degraded, FGF10 mostly promotes receptor recycling (Belleudi et al. 2007). FGFR4 also seems to follow either the degradation or the recycling pathway, and the deciding factor between the 2 fates depends on the presence of targeting signals in the cytoplasmic domain of the receptor (Citores et al. 2001). Finally, a comparative study between the 4 members of FGFR family stimulated with the same FGF1 ligand revealed that each of them is targeted to lysosomes or to recycling compartments to different extents, and that the molecular

event that controls this sorting is receptor ubiquitination (Haugsten et al. 2005). In fact, while FGFR1-3 are efficiently ubiquitinated and targeted to lysosomes for degradation, FGFR4 is poorly ubiquitinated and found mostly in the recycling route. A study also described a role for Src kinase and RhoB in the activation and transport of FGFR from the plasma membrane (Sandilands et al. 2007). The role of Src in FGFR signalling and endocytosis is described in more detail in Section 1.4, Src family kinase.

1.3.3 Crosstalk between endocytosis and RTK signalling

As mentioned above, it is increasingly clear that signal transduction by RTKs can be sustained and modulated by endocytosis and that, conversely, receptor signalling can regulate the endocytic machinery. The first regulatory effect that endocytosis might have on receptor signalling is through control of the pool of receptors on the cell surface available for interaction with plasma membrane effector/docking molecules. Most of the molecules forming the signalling platforms during the initial events of RTK activation are required to be targeted to the proximity of the plasma membrane. Thus, physically removing receptors from these compartments could have profound effects on the magnitude of signalling. Despite this, many receptors have been demonstrated to remain active and continue to signal along the endocytic pathway (Jiang and Sorkin 2002, Li H. S. et al. 2005, Sorkin and Von Zastrow 2002). A well known example is that of EGFR, which has been demonstrated to remain associated with the signalling complex GRB2/Shc/SOS in endosomes and to signal from this location through H-Ras (Jiang and Sorkin 2002). Endosomes, therefore, that traditionally were considered as mere transitional compartments, are now thought to function as important signalling platforms where

receptor signalling originated from the plasma membrane is sustained and where new, unique signals are generated (Miaczynska and Zerial 2002, Miaczynska and Bar-Sagi 2010). Two of the most well characterised examples of specific endosomal signal propagation are those mediated by MP1/p14/p18 and APPLs. MP1/p14/p18 is a scaffold protein complex that specifically localizes to the membranes of the late endosomes via the myristoyl and palmitoyl groups of the component p18 (Magee and Cygler 2011). By binding and targeting MEK1 and ERK1 to the late endosomal membranes, the MP1/p14/p18 complex enhances MEK1-dependent activation of ERK1 in response to EFG (Schaeffer et al. 1998). Notably, this ERK1 signal propagation depends strictly on localisation of the MP1/p14/p18 complex on late endosomes, as a mislocalised plasma membrane resident complex does not enhance ERK1 activation (Teis et al. 2002). Similarly, the adaptor proteins APPL, which specifically localizes to a subpopulation of Rab5-positive endosomes (Miaczynska et al. 2004), have been shown to play a role in signal transduction events initiated at the plasma membrane. In response to extracellular stimuli, such as EGF stimulation, APPL proteins translocate from the EE to the nucleus, where they regulate the expression of different genes (Miaczynska et al. 2004). Similarly, APPLs have been shown to interact with and regulate the activity of the kinase Akt upon growth factor stimulation (Schenck et al. 2008). Importantly, APPLs function in regulating both Akt activity and the mitogenic response has been demonstrated to be dependent on their endosomal localization (Schenck et al. 2008) and their binding to Rab5 (Miaczynska et al. 2004).

If receptors are still able to signal from endosomes, the localization of internalized receptors in specific endocytic compartments can be critical to their ability to interact

with membrane-associated signalling/adaptor molecules. In this context, trafficking of activated receptors can also spatially modulate the signalling response by placing the receptor in the appropriate cellular district, where it interacts with the resident molecules.

Finally, endocytosis plays a role in receptor signalling by sorting the internalized receptor to different cellular destinations, resulting in different effects on signalling: targeting the receptor to lysosomal compartments results in attenuation of signalling, by means of protein degradation; on the contrary, sorting the receptor to the recycling routes leads to a 're-sensitization' of the cell to external ligands, by replenishing the cell surface with ligand-free receptor available for activation (Scita and Di Fiore 2010). In this context, it has been proposed that the route of entry for some receptors might be critical to determining a different endocytic pathway and, consequently, a different signalling output (Scita and Di Fiore 2010). EGFR, for example, has been found to be mainly targeted to degradation when it internalizes through CIE, whereas it significantly recycles back to cell surface when it enters through CME. The ultimate signalling output from EGFR appears to be determined by the integration of these 2 pathways (Sigismund et al. 2008).

Ubiquitination plays a particularly important role in regulating RTK trafficking. A number of RTKs have been shown to be ubiquitinated upon activation at the plasma membrane, resulting in targeting the receptor into internal vesicles of the MVB and their degradation in lysosomes (Levkowitz et al. 1998). Mutations that uncouple RTKs from ubiquitination have oncogenic properties, resulting in a sustained mitogenic signal as a result of reduced receptor degradation (Abella and Park 2009). Interestingly, ubiquitination has also been

suggested to regulate other steps of receptor endocytosis. c-Cbl, for instance, the E3 ubiquitin-conjugating enzyme required for ligand-dependent ubiquitination of EGFR (Levkowitz et al. 1998, Waterman and Yarden 2001), has been proposed to control EGFR internalisation into CCVs by interacting with CIN85 (Cbl-interacting protein) and the BAR-containing protein endophilins (Soubeyran et al. 2002), which induces membrane curvature during pit formation. Further, in *Drosophila melanogaster*, c-Cbl appears to be important in concentrating the RTKs in specific subcellular compartments during border cell migration (Jekely et al. 2005).

The role of endocytosis as temporal and spatial regulator of RTK signalling is further supported by the identification of a wide variety of diseases, including cancer, associated with defects in endocytic machinery (Bache et al. 2004, Parachoniak and Park 2012) (Table 1.2). As described above, a significant number of these defects prevent RTKs from being efficiently ubiquitinated and downregulated. Up to 20% of breast cancers, for example, overexpress the EGFR/HER2 hetorodimer, which contrary to the homodimer EGFR/EGFR, is unable to be targeted by c-Cbl, resulting in impaired lysosomal degradation of EGFR, sustained recycling, and enhanced signalling (Muthuswamy et al. 1999). Although involvement of Cbl in endocytosis of FGFR has not been clearly elucidated (Wong et al. 2002), defects in FGFR ubiquitination have been implicated in some forms of skeletal disease. Mutations that prevent FGFR3 Cbl-mediated ubiquitination, resulting in inhibition of lysosomal degradation and amplification of receptor signalling, have been identified in patients with Achondroplasia (ACH) and related Chondrodysplasias (Cho et al. 2004). Other examples of components of the endocytic machinery implicated in cell tumorigenesis are the proteins Eps15 and

Protein	Function in receptor endocytosis	Human cancer	Reference
c-Cbl	Ubiquitilation of ligand-activated RTKs	Point mutations, insertions and deletions in *acute myeloid leukaemia*	(Abbas et al. 2008, Dikic and Giordano 2003, Peschard and Park 2003, Shtiegman and Yarden 2003)
Eps15	Scaffolding protein for clathrin and receptor recruitment.	fusion in *acute myeloid leukaemia*	(Floyd and De Camilli 1998, So et al. 2003)
Endophilin-2	membrane curvature inducing protein during vesicle formation	fusion in *acute myeloid leukaemia*	(Floyd and De Camilli 1998, Habermann 2004, Liu H. et al. 2004)
Sprouty	Competes with RTKs for Cbl binding	Downregulation in *breast* and *prostate cancers*.	(Lo et al. 2006)
Hip1	Interacts with AP-2, clathrin and phosphoinositides	fusion in *Chronic Myelomonocytic Leukemia*	(Ross et al. 1998)
Clathrin heavy chain	Coat protein	fusion in *inflammatory myofibroblastic tumour* and *large B-cell lymphoma*	(Bridge et al. 2001)
Caveolin1	Coat protein	Deregulated in multiple cancer types; Amplification in aggressive *breast carcinomas*	(Shatz and Liscovitch 2008)
Rabaptin-5	Effector of Rab5 required for endosomal fusion	*Myelomonocytic leukaemia*	(Magnusson et al. 2001)
Tsg101	Part of ESCRT1 machinery, sorts ubiquitinated proteins from endosomes to lysosomes	Aberrant transcripts found in different cancers	(Babst et al. 2000, Gruenberg and Stenmark 2004, Li L. and Cohen 1996)
Cortactin	Drives actin polimerization and binds dynamin	Amplification and overexpression in *breast carcinoma* and in *head* and *neck squamous cell carcinoma*	(Buday and Downward 2007)

Table 1.2 Components of endocytic machinery aberrantly expressed in human cancers

Data adapted from (Bache et al. 2004, Mosesson et al. 2008).

Endophilin-2. In some forms of human myeloid leukaemia, chromosomal translocations on chromosome 11q23 often result in fusion proteins comprising the N-terminal domain of ALL1/HRX and either Eps15 or Endophilin-2 (Floyd and De Camilli 1998). Finally, isoforms of FGFR2-IIIb with deletions in the cytoplasmic domain have been found in some human cancers and have been demonstrated to have impaired ligand-induced internalisation, reduced degradation, and sustained receptor activation (Cha et al. 2009).

1.4 Src family kinase

The Src family of protein tyrosine kinases (SFKs) is a family of non-RTKs that play an important role in regulating signals from a multitude of cell surface receptors. By coupling intracellular signalling machinery with membrane-bound receptors, SFKs control cellular processes, including cell adhesion, migration, cell cycle, survival, and differentiation. The SFK family includes 9 members, divided into 2 groups according to their tissue expression patterns: Src, Fyn, and Yes are expressed in a broad range of tissues, while Fgr, Lyn, Hck, Lck, Blk, and Yrc elicit a limited expression range (Courtneidge 2002). All members of the SFK family share a conserved molecular architecture, consisting of 6 distinct domains: an Src homology domain 4 (SH4), which is always myristoylated and under specific conditions palmitoylated (Koegl et al. 1994, Resh 1999) and drives the kinase association with membranes (Pellman et al. 1985); a unique domain, specific for each Src family protein; an SH3 and an SH2 domain, which control the range of Src binding partners; a kinase domain (SH1); and a C-terminal autoinhibitory region (Cooper and King 1986). Dissection of the molecular organization of Src kinases has revealed that they switch between close inactive and open active conformations. This process is driven by

phosphorylation events on 2 tyrosine residues, Tyr416 and Tyr530 in human c-Src, located within the activation loop and the C-terminal regulatory region, respectively. C-terminal Src kinase (CSK)-mediated phosphorylation of Tyr 530 induces Src to be locked in a close auto-inhibited conformation held by interaction between the SH2 domain and the phosphotyrosine residue (Yamaguchi H. and Hendrickson 1996). Disruption of this interaction either by dephosphorylation of Tyr530 or binding of the SH3 and SH2 domains to Src protein partners, converts Src to an open conformation, which results in autophosphorylation of Tyr416 and in full kinase activity (Tatosyan and Mizenina 2000).

1.4.1 c-Src

The c-Src (cellular-Src) oncogene encodes for a 60-kDa cellular protein with tyrosine kinase activity originally identified (Stehelin et al. 1977) for its similarity with the transforming oncoprotein (v-Scr) of the tumour-inducing retrovirus RSV (Rous sarcoma virus) (Brugge and Erikson 1977, Purchio et al. 1978). The main difference between c-Src and v-Src, is that the latter harbours a truncation of the carboxy-terminal tail (Takeya and Hanafusa 1983), which results in high kinase activity and transforming potential (Iba et al. 1984, Tanaka and Fujita 1986). This, in fact, is the region that contains autoinhibitory Tyr530, whose absence in v-Src constitutively locks the kinase in the active conformation.

Subcellular localization of c-Src is a crucial determinant for its activation. c-Src has been found to associate to cellular membranes, including plasma membrane (Willingham et al. 1979), nuclear membrane (David-Pfeuty and Nouvian-Dooghe 1990) and endosomal membrane (Kaplan K. B. et al. 1992). As mentioned above, c-Src targeting to cellular membranes is mediated by the N-terminal domain, where post-translational myristilation (Kaplan J. M. et al. 1988) plus a 6 basic amino acid region are required for c-Src binding to

lipid bilayers (Sigal et al. 1994). In addition to the bound-membrane component, a pool of c-Src has also been detected in the cytoplasm (Willingham et al. 1979). However, while plasma-membrane-associated c-Src is thought to participate in signal transduction events via growth factor receptors or to mediate cell adhesion in the focal adhesion complexes, the role of c-Src at the other cellular locations has not yet been clarified. The pleotropic role that c-Src plays in cells explains the well documented role of the kinase in the development and progression of tumours. The kinase activity of c-Src is often found to be elevated in human colon (Cartwright et al. 1989) and breast cancers (Verbeek et al. 1996), as an effect of various molecular mechanisms, such as mutations and dephosphorylation of Tyr530. In highly metastatic colon carcinoma, for instance, a c-Src mutation has been identified (Irby et al. 1999) that results in truncation of the C-terminal region responsible for the autoinhibitory mechanism. This mutated form of c-Src still contains (and ends with) the Tyr530 residue, but it lacks the adjacent amino acids necessary for intramolecular binding to the SH2 domain, causing the kinase to be constitutively active and resulting in elevated kinase activity (Cantley and Songyang 1994).

1.4.2 Src and RTKs

Involvement of Src kinases in the signalling of RTKs has been extensively demonstrated. The first evidence came from a study on PDGF-stimulated NIH3T3 fibroblasts which revealed that PDGFR is able to directly interact with Src, Yes, and Fyn, consequently inducing their phosphorylation and activation (Kypta et al. 1990, Mori et al. 1993). Similarly, a number of studies also described the implication of Src in signalling activated by EGFR. Src has been shown to potentiate EGF-induced cell proliferation (Luttrell et al.

1988) and tumorigenesis (Maa et al. 1995) by binding to EGFR and inducing receptor autophosphorylation. The direct interaction between the 2 kinases appears to be mediated by 3 auto-phosphorylated tyrosine residues on EGFR which serve as binding sites for Src SH2 domain (Lombardo C. R. et al. 1995). Interestingly, a crosstalk between Src and EGFR has also been implicated in EGFR endocytosis and trafficking. Fibroblasts overexpressing Src elicit an increased rate of internalization of EGFR when compared to endogenously Src expressing control cells, while no effect can be detected on receptor recycling rate (Ware et al. 1997). The molecular mechanism underlying the Src effect on EGFR endocytosis is thought to involve events of phosphorylation on clathrin heavy chain (CHC) (Wilde et al. 1999). According to the model proposed, activated EGFR causes activation of Src, which in turn phosphorylates CHC, inducing clathrin redistribution at the cell surface. Recruitment of new clathrin would result in enhanced uptake of activated EGFR from the plasma membrane (Wilde et al. 1999). Other groups have implicated dynamin in Src-dependent regulation of EGFR endocytosis. Ahn et al., for instance, showed that Src-mediated phosphorylation of dynamin at Tyr597 promotes its GTPase activity, and can consequently result in enhanced endocytosis of EGFR (Ahn et al. 2002).

Src is also one of the key downstream effectors in the signalling cascade from FGFR, and it has been implicated as a crucial FGFR regulatory factor. Evidence for the involvement of Src in FGFR signalling began to emerge in 1994 from the work from Zhan et al., who described direct interaction between FGFR1 and the kinase *in vitro* (Zhan et al. 1994). The interplay between FGFR and Src was further confirmed by a number of other studies which implicated Src in different FGFR-induced cellular responses, such as neurite outgrowth (Kremer et al. 1991), cell migration or cell shape change (Liu J. et al. 1999), and

mesoderm induction during Xenopus development (Weinstein et al. 1998). To date, the exact role of Src in the signalling cascade of FGFR has not been entirely elucidated, but several recent reports describe potential physiological substrates for FGFR-mediated Src activity. Li et al. showed that Src is recruited to active FGFR via the adaptor protein FRS2, and that upon recruitment and activation, Src phosphorylates the signalling negative regulator Sprouty2, which in turn attenuates FGFR signalling via the ERK1/2 pathway (Li et al. 2004). This is the first clear evidence that Src plays a role in a mechanism of regulation of FGFR signalling. In addition to this negative effect, Src has also been proposed to positively regulate the signalling from FGFR. Sandilands et al., found that in FGF2-stimulated fibroblasts, active Src colocalises with activated FGFR at the plasma membrane and that, in the absence of the kinase, only a small pool of active FGFR is targeted at the cell surface (Sandilands et al. 2007). Further, Src inhibition was also shown to affect FGFR downstream signalling output, including both the Akt and the ERK1/2 pathways. These observations suggest that Src may regulate the transport of activated FGFR to and from the plasma membrane, consequently affecting the downstream signalling cascade induced by the receptor. Recently, a study employed ultrahigh resolution mass spectrometry techniques to identify Src kinase substrates involved in the signalling pathway from FGFR. By combining stable isotope labelling by amino acids in cell culture (SILAC) assay with chemical inhibition of Src activity, this study identified a consistent number of new kinases and adaptor proteins phosphorylated by Src in response to FGFR activation (Cunningham et al. 2010). One of the Src targets identified in this work is the scaffold protein Eps8, already implicated in the trafficking of EGFR (Di Fiore and Scita 2002). The physiological function and role of Eps8 in the context of RTKs is described in more detail in Section 1.5, Eps8.

Consistent with the key role that Src plays in the FGFR signalling cascade, it is not surprising that Src is increasingly emerging as a very attractive target for therapy against FGFR-associated malignant disorders, such as stem cell leukaemia-lymphoma syndrome (SCLL) (Ren et al. 2011). In this context, multiple classes of inhibitors selectively affecting Src activity have been developed, such as the combined src/abl inhibitor dasatinib, which however, did not yield significant effects in a phase II trial (Herold et al. 2011), or the inhibitor bosutinib, which, on the contrary, showed evidence of activity in a phase II trial (Campone et al. 2012).

1.5 Eps8

EGFR pathway substrate 8 (Eps8) is a ubiquitously expressed protein of 97 KDa originally discovered in a screening for targets of EGFR-mediated phosphorylation (Fazioli et al. 1993). The structural organization of Eps8, as predicted by analysis of the primary sequence, comprises a phosphotyrosine binding protein (PTB) domain at the N-terminus, followed by an SH3 domain and a sterile α motive-pointed (SAM-PNT) domain (Di Fiore and Scita 2002) (Figure 1.12A). The PTB domain is thought to mediate interaction of Eps8 with signalling/scaffolding proteins, even though no binding partner for this domain of Eps8 has yet been identified. Similarly, the SAM-PNT domain has been proposed to be involved in protein-protein interaction and in the formation of Eps8 homo- and hetero-oligomers (Di Fiore and Scita 2002). A region of 27 residues within this domain, known as the ‘effector region’, has been shown to mediate Eps8 binding to SOS-1, resulting in activation of the signalling complex Eps8/Abi1/SOS1, and to mediate direct interaction of Eps8 with F-actin, driving Eps8 localization to sites of actin remodelling (Scita et al. 2001).

The SH3 domain of Eps8 has been studied extensively and the resolved crystal structure revealed that Eps8-SH3 may represent the prototype of a novel family of SH3 modules. While a canonical SH3 domain, in fact, structurally adopts a well-characterized monomeric β-barrel conformation (Yu H. et al. 1992), Eps8-SH3 appears to assume a dimeric configuration, in which the 2 interacting β-barrels share some polypeptide chains (Kishan et al. 1997). Interestingly, further analysis of SH3 binding affinity revealed that, even if Eps8-SH3 exists in dimeric and monomeric configuration in equilibrium (Kishan et al. 1997), only the monomeric form is available to protein interaction (Mongiovi et al. 1999). Thus, it has been proposed that the dimer may represent a temporary inactive state that prevents Eps8 from interacting with signalling binding partners (Di Fiore and Scita 2002). Another peculiarity of the SH3 domain of Eps8 is its ability to interact with a PXXDY consensus sequence, instead of the canonical XPXXP (Mongiovi et al. 1999). A number of Eps8 interaction partners have been identified which display the PXXDY consensus.

1.5.1 Eps8 and RTKs

As mentioned in Section 1.5, Eps8 was originally identified as a substrate of the kinase activity of active EGFR. Its involvement in signalling from RTKs was further confirmed by the observation that Eps8 overexpression in different cell lines enhances EGF-mediated mitogenic responsiveness (Fazioli et al. 1993) and that alteration of eps8 activity could result in EGFR-associated malignant phenotypes (Matoskova et al. 1995). Clear elucidation of the role of Eps8 and its physiological substrates in the EGFR signalling pathway was described in Scita et al., in which Eps8 was described as coordination of EGFR-mediated signals along the Ras/PI3K/Rac cascade (Scita et al. 1999). In the model

proposed by Scita and illustrated in Figure 1.12B, Eps8 is part of a signalling complex together with the Rac-specific GEF SOS-1 and the scaffold protein E3b1/Abi1, which forms upon EGFR-mediated Ras activation at the plasma membrane. The Eps8/Abi1/SOS-1 ternary complex is targeted via the effector region of the SAM-PNT domain of Eps8 to F-actin sites (Innocenti et al. 2002, Scita et al. 2001), where SOS-1 serves as an activating GEF for the GTPase Rac, ultimately resulting in actin polymerization. The signalling complex requires the presence of each of the 3 components to be functional, and Eps8 depleted cells show no Rac-mediated actin remodelling response (Scita et al. 1999).

A role for Eps8 in endocytosis of EGFR has also been described (Figure 1.12B). Eps8 has been shown to bind to the GAP protein RN-tre, resulting in a negative effect on EGFR internalisation (Lanzetti et al. 2000). Although the exact molecular mechanisms are not yet known, the inhibitory effect on EGFR endocytosis seems to involve the GTPase Rab5, already implicated in the process of receptor internalisation (Bucci et al. 1992). According to the model proposed, when it is sequestered in the complex with Eps8, RN-tre is not able to function as activating GAP for Rab5, resulting in inhibition of receptor endocytosis and sustained receptor signalling at the plasma membrane (Lanzetti et al. 2000). Interestingly, Eps8 has been found to associate with internalised EGFR, while no interaction has been detected with the plasma-membrane pool of the receptor (Burke et al. 2001), further implicating Eps8 in EGFR trafficking regulation.

The fact that Eps8 participates in both Rac and Rab5 signalling depending on the complex it associates with (Eps8/Abi1 and Eps8/RN-tre, respectively), suggests that it can function as coordinator of the 2 alternative pathways. This consideration is further supported by the observation that Abi1 and RN-tre compete for the interaction with Eps8, diverting

Eps8 function from actin to endocytosis regulation, and vice-versa (Figure 1.12B). Further supporting evidence for involvement of Eps8 in receptor endocytosis is from the recent Taylor et al. By using a live-cell total internal reflection fluorescence (TIRF) microscopy based assay, this group examined the recruitment dynamics of a list of endocytic proteins in the process of CCV scission (Taylor M. J. et al. 2011). Eps8 was identified among the proteins recruited during the scission events and showed a pattern of recruitment similar to that of dynamin (Taylor M. J. et al. 2011).

Evidence of a role for Eps8 in the signalling pathway from FGFR is also beginning to emerge. As already mentioned, Cunningham et al. recently showed that Eps8 is phosphorylated at different tyrosine residues in a Src-dependent manner upon FGF stimulation (Cunningham et al. 2010). These phosphorylated tyrosine residues on Eps8 may be important for mediating the recruitment and activation of key signalling effectors in the FGFR pathway, suggesting that the role of Eps8 as coordinator of signalling events could be conserved across different RTKs.

1.5.2 Eps8 and cancer

The first observation of a mitogenic effect for eps8 came from studies on fibroblast and hematopoietic cells which showed increased mitogenic response to EGF upon eps8 overexpression (Fazioli et al. 1993). To date, eps8 has been found to be upregulated in a variety of tumours, including colon and oral tumours (Chu et al. 2012, Maa et al. 2007), and it correlates with migration and invasiveness of different cancer cell lines such as cervical cancer- or oral squamous cell carcinoma (OSCC)-derived cell lines (Chen Y. J. et al. 2008, Yap et al. 2009). Additionally, tyrosine phosphorylation of eps8 has been observed

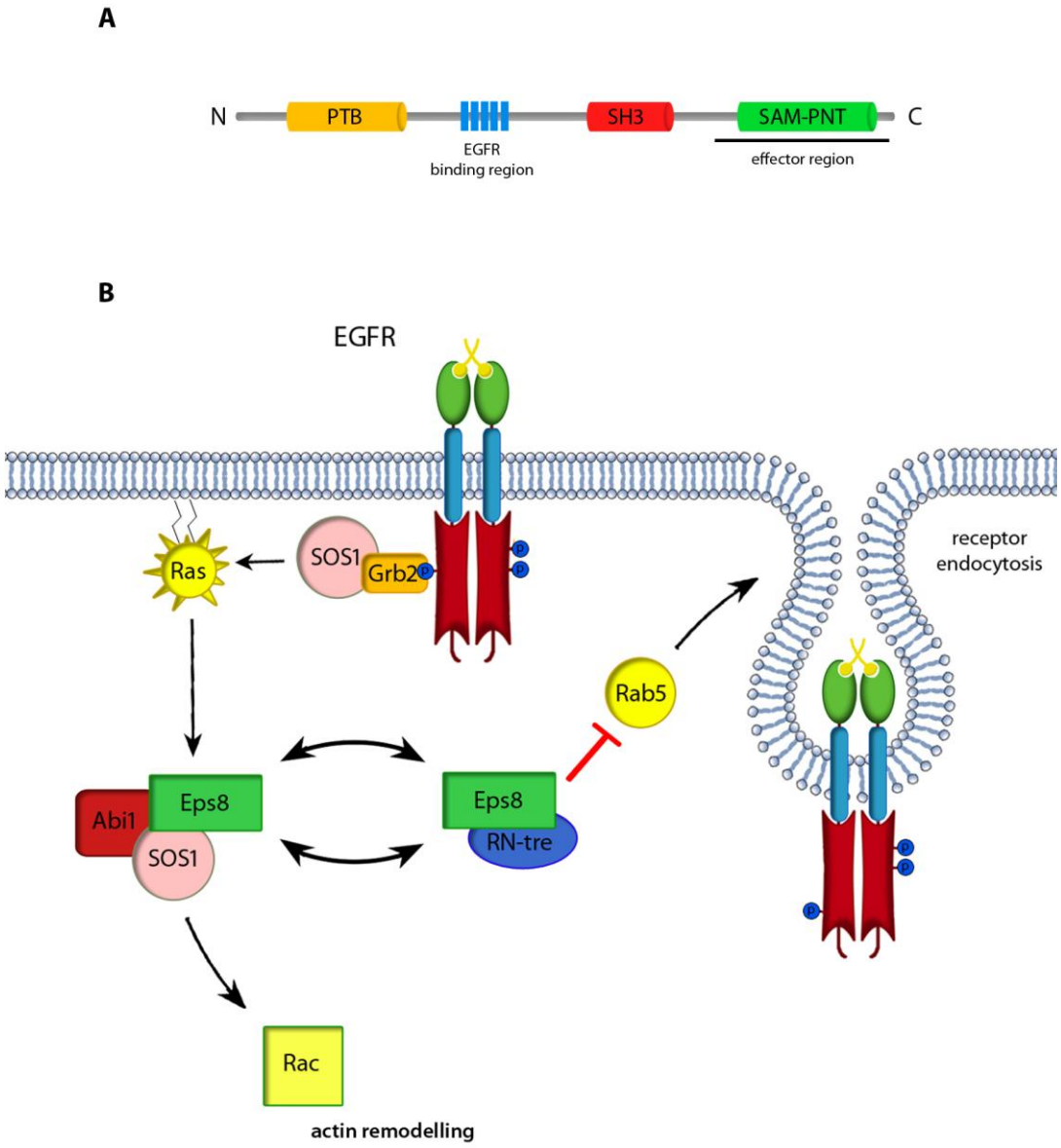

Figure 1.12 Domain organization of Eps8 and its role as coordinator of signals downstream of EGFR

A. Structural organization of Eps8 comprises a PTB domain, followed by an SH3 domain, and a SAM-PNT domain. The latter contains the binding site for the interaction with Sos1, whereas the EGFR binding region is located upstream and is indicated with blue bars. **B**. Eps8 can associate with two signalling complexes (Eps8/Abi1 or Eps8/RN-tre) and participate in either Rac or Rab5 signalling, regulating actin remodelling or EGFR endocytosis, respectively.

to occur constitutively in some human tumours, suggesting that pTyr-eps8 may represent a useful marker for detecting tumour cell lines (Matoskova et al. 1995).

1.6 Thesis aims

FGFRs regulate fundamental processes in the cell, including proliferation, differentiation and angiogenesis, and their activity must be accurately regulated to prevent uncontrolled sustained signalling. Endocytosis and trafficking of FGFRs can modulate initiation and propagation of signals and defects in these 2 processes, which are implicated in a variety of skeletal disorders as well as malignancies. Thus, it is extremely important to understand the mechanisms of FGFR endocytosis and trafficking and the impact they have on the receptor signalling response. Recent proteomic studies have identified Eps8 as a potential coordinator of the interplay between FGFR signalling and trafficking. However, the exact role of eps8 in the context of FGFR remains unknown.

This thesis aims to:

- examine the dynamics of receptor recruitment and clustering at the cell surface prior to internalization
- identify the endocytic pathway for endocytosis of FGFR2
- investigate trafficking of FGFR through the endocytic system
- establish the role of Src and eps8 in regulation of FGFR trafficking and signalling

CHAPTER 2

MATERIALS AND METHODS

2.1 Buffers and Solutions

2.1.1 Bacterial culture

- Luria Bertani broth (LB): 10 g/l bacto-tryptone, 5 g/l yeast extract, 10 mM NaCl, pH 7.4
- Ampicillin plates: LB + 15 g/l bacto-agar, 100 μg/ml ampicilin
- Kanamycin plates: LB + 15 g/l bacto-agar, 50 μg/ml kanamycin

2.1.2 Mammalian cell culture

- Dulbecco's Modified Eagle Medium: pre-made (Invitrogen) and supplemented with 4.5 g/l L-glutamine (Invitrogen)
- Roswell Park Memorial Institute Medium*:* pre-made (Invitrogen)
- Foetal Bovine Serum: purchased as frozen (Labtech International)
- Penicillin-Streptomycin solution (100x): pre-made (Invitrogen)
- 0.05% Trypsin-EDTA solution: pre-made (Invitrogen)

2.1.3 Protein manipulation

- Triton X-100 lysis buffer: 50 mM Tris-HCl pH 7.4, 150 mM NaCl, 1% Triton X-100 (w/v), 1 mM Na_3VO_4, 50 mM NaF, 25 mM β-glycerophosphate supplemented with 1 tablet of complete mini protease inhibitors cocktail (Roche) per 10 ml of buffer

- SDS sample buffer (5x): 250 mM TrisHCl pH 6.8, 10% SDS (w/v), 30% Glycerol (w/v), 5% β-mercaptoethanol (w/v), 0.02% bromophenol blue (w/v)
- Tris-Glycine running buffer: 25 mM Tris, 0.2 M glycine, 0.2% SDS (w/v)
- MOPS running buffer (20X): pre-made (Invitrogen)
- Western blot transfer buffer: 25 mM Tris, 0.2 M glycine, 10% methanol (v/v)
- Phosphate Buffered Saline Tween (PBST): PBS, 0.05% Tween 20 (v/v)
- Immunoblot blocking buffer: pre-made buffer (LI-COR Biosciences) in PBST

2.1.4 Immunofluorescence

- Fixation solution: 4% paraformaldehyde (w/v) in Tris Buffered Saline (TBS) pH 7.4
- Washing buffer: Phosphate Buffered Saline (PBS)
- Glycine wash solution: 100 mM glycine in TBS
- Permeabilization solution: 20 mM glycine and 0.1% saponin (w/v) in TBS
- Blocking solution: 10% FCS and 0.1% saponin (w/v) in TBS

2.1.5 Live cell imaging

- Cell Imaging Media (CIM): Hanks Balanced Salt Solution (HBSS) (SIGMA) and 10 mM Hepes, pH 7.4

2.2 Reagents and Antibodies

All primary and secondary antibodies used are listed in Table 2.1.

Antibody	Species	Manufacturer	Working dilution
Rab11	RP	Invitrogen	1:200 (IF)
EEA1 (clone 1G11)	MM	Abcam	1:200 (IF)
Caveolin1	RP	BD Biosciences	1:1000 (IB)
α-adaptin 1/2 (clone M-300)	RP	Santa Cruz	1:1000 (IB)
α-tubulin	MM	SIGMA	1:10000 (IB)
Clathrin heavy chain (TD.1)	MM	Santa Cruz	1:1000 (IB)
Dynamin2 (C-18)	GP	Santa Cruz	1:1000 (IB)
ERK1 (clone K-23)	RP	Santa Cruz	1:1000 (IB)
pERK 1/2 (clone E-4)	MM	Santa Cruz	1:1000 (IB)
AKT (clone 40D4)	MM	Cell Signalling	1:1000 (IB)
pAKT (Thr 308)	RP	Cell Signalling	1:1000 (IB)
Eps8 (clone M-238)	RP	Santa Cruz	1:1000 (IB)
myc (clone 9E10)	MM	Roche	1:500 (IP) 1:1000 (IB)
Mouse IgG IRDye800CW	GP	LI-COR	1:5000 (IB)
Rabbit IgG IRDye680CW	GP	LI-COR	1:5000 (IB)
Mouse IgG IRDye800CW	GP	LI-COR	1:15000 (IB)
Rabbit IgG IRDye680CW	GP	LI-COR	1:15000 (IB)

Table 2.1 List of all primary and secondary antibodies used in this study, including their working dilutions, species and manufacturer. RP: Rabbit Polyclonal. MM: Mouse Monoclonal. GP: Goat Policlonal. IF: Immunofluorescence. IB: Immunoblotting.

FGF2 was in-house prepared (by Susan Brewer). EGF was purchased from Sigma. Heparin and Dynasore were purchased from Sigma. SU5402 was purchased from Calbiochem. Dasatinib was purchased from Sellek Chemicals. 4-12% NuPAGE Novex Bis-Tris gels used for SDS-PAGE were purchased from Invitrogen.

siRNA oligos targeting α-adaptin (sequence AAGAGCAUGUGCACGCUGGCCA), caveolin1 (SmartPool l-003467) and Eps8 (SmartPool L-017905) and Non-silencing control (NSC) oligoes, were purchased from Dharmacon. All siRNAs were resuspended in RNase-free water (Thermo Scientific) to 20 μM and stored at -20°C.

2.3 Plasmids

The construct encoding C-terminally GFP-tagged FGFR2IIIc (FGFR2-GFP) was a gift from J. Ladbury (The University of Texas, Houston, TX). EGFP-tagged EGFR was a gift from A. Sorkin (University of Pittsburgh, Pittsburgh, PA). N-terminal myc-tagged full-length mNbr1 was made by Gateway cloning (Invitrogen) according to manufacturer's instructions. EGFP-tagged BAIAPL2L-GFP, IRSp53 and IRTKS were gifts from R. Insall (Beatson Institute for Cancer Research, Glasgow, UK). Constitutively active Src was provided by Margaret Frame (Edinburgh Cancer Research UK Centre). DsRed tagged clathrin light chain A (clathrin-dsRed) was a gift from T. Kirchhausen (Harvard Medical School, Boston, MA). Caveolin 1-mRFP was a gift from A. Helenius (ETH Institut of Biochemistry, Zurich, Switzerland). Eps8-mCherry was a gift from Giorgio Scita (IFOM

University of Milan, Milan, Italy).

2.4 Cell biology techniques

2.4.1 Preparation of (heat shock) competent bacterial cells

E. coli DH5α strain was used to propagate plasmids. A single colony was inoculated in 2 ml of LB-medium and grown over night at 37°C while shaking at 250 rpm. The following morning 500 ml of LB-medium were inoculated with 1 ml of saturated overnight culture, and grown to an OD600 nm = 0.5. Cells were transferred in 2 pre-chilled sterile 250 ml centrifuge tubes and cooled on ice for 20 min, before being pelleted by centrifugation at 5000 rpm for 10 min at 4°C. The supernatant was removed and the pellet resuspended in 10 ml ice-cold $MgCl_2$-$CaCl_2$ solution by gentle vortexing. Cells were centrifuged at 2500 rpm for 5 min at 4°C, the supernatant was discarded and the pellet resuspended in 10 ml of ice-cold 0.1 M $CaCl_2$ by gentle vortexing. Cells were then directly used for transformation or dispensed into 50 µl aliquots and stored at -80°C until use.

2.4.2 Heat shock transformation of competent bacterial cells

~1µg of pre-purified plasmid was added directly to 50 µl of DH5α *E.coli* thawed, competent cells. After incubation on ice for 30 min, cells were heat-shocked in a 42°C water bath for 45 seconds and then transferred back to ice for a further 2 min. Cells were resuspended in 1 ml of LB-medium (without antibiotic) and incubated for 1 hr at 37°C in order to assist cell recovery. 100-150 µl of the resulting culture was spread on LB plates (with appropriate antibiotic added) and grown overnight at 37°C. About 12-16 hr later

two colonies per plasmid were picked and processed for the purification and isolation steps.

2.4.3 Mammalian cell lines and cell culture

Eps8 shRNA and control shRNA HeLa cells were a gift from Giorgio Scita (IFOM University of Milan, Milan, Italy). LNCap cells were a gift from Hing Leung (Beatson Institute, Glasgow, UK). HeLa cells were propagated in Dulbecco's Modified Eagle Medium (DMEM) supplemented with 10% foetal bovine serum (FBS), penicillin and streptavidin (100X) and 4.5 g/l L-glutamine in a 5% CO2 atmosphere at 37°C. Cells were split into fresh media at a dilution of 1:16 when they reached ~90% confluency. LNCaP cells were propagated in Roswell Park Memorial Institute (RPMI) medium supplemented with 10% foetal bovine serum (FBS), penicillin and streptavidin (100X) in a 5% CO2 atmosphere at 37°C. Cells were split into fresh media at a dilution of 1:8 when they reached ~80% confluency.

2.4.4 Transfection

All DNA and siRNA transfections were performed by using Lipofectamine2000 transfection reagent (Invitrogen) according to the manufacturer's protocol. DNA transfection was performed when cells had reached 90% confluency. After transfection, cells were incubated for 24 hr, then split 1:2 and incubated for further 24 hr to allow efficient expression of recombinant proteins. Before each experiment, cells were starved for 30 min in serum-free DMEM (unless otherwise stated). For siRNA transfection, cell were allowed to reach 50% confluency. At this stage a first round of transfection was performed, following the manufacturer's protocol, and a second one after 24 hr, when cells had reached a high confluency. After 3-4 hr cells were split 1:2 and incubated for further 24 hr to allow efficient gene silencing.

2.4.5 Stimulations and inhibitions

For the FGFR2 studies, cells were stimulated with 20 μg/ml heparin and 50 ng/ml FGF2 for the indicated amounts of time. In preliminary experiments using different concentrations of FGF2 (1 to 100 ng/ml) 50ng/ml was shown to be the optimal concentration to be used in further experiments. For the inhibition assays cells were either treated with 25 μM SU5402 for 5 min, 80 μM Dynasore for 30 min or 50 nM Dasatinib for 30 min or treated as above in the absence of drug (control) before FGF2 stimulation. To block the stimulation and receptor internalization, cells were rinsed twice with cold PBS and kept on ice before the fixation/lysis. For the EGFR studies, cells were stimulated with 50 ng/ml EGF for 30 min.

2.4.6 Immunochemistry

Cells grown on coverslips were fixed in 4% paraformaldehyde in TBS for 10 min, washed in TBS/100mM glycine and permeabilized with TBS/0.1% saponin/20mM glycine. After blocking with TBS/0.1% saponin/10% FCS, cells were incubated with primary antibodies, then washed and incubated with secondary antibodies. After staining, the coverslips were mounted in Hydromount (National Diagnostic) and imaged in confocal microscopy by using either the Nikon A1R or the Zeiss LSM710 system (see section 2.6). Each experiment was repeated a minimum of 3 times and an image that represented the phenotype of most of the cells was selected and prepared by using NIS-Elements Imaging Software version 3.2 (Nikon).

2.5 Molecular biology techniques

2.5.1 Plasmid DNA purification and isolation

5 ml LB media supplemented with appropriate selection antibiotics were inoculated with a single bacterial colony and grown overnight at 37°C on a shaker. Cells were centrifuged at 6,000 rpm for 15 min. Plasmid DNA was isolated using the QIAGEN Plasmid Maxi Kit, which is based on a modified alkaline lysis procedure, followed by binding of plasmid DNA to anion-exchange resins at low-salt and pH conditions. The DNA pellet was washed once with Isopropanol and once with 70% ethanol and dissolved in 300 µl of autoclaved H_20.

2.5.2 Cell lysis and measure of protein concentration

Confluent cultures of HeLa cells were rinsed twice in cold PBS and lysed in Triton X-100 lysis buffer supplemented with complete mini protease inhibitors cocktail (Roche). Cell lysates were removed from the bottom of the flasks/plates by using a scraper and centrifuged (14,000 g for 20 min at 4°C) to clear the protein phase from the rest of the cellular components. The whole procedure was performed at 4°C. For protein concentration measurement, bovine serum albumin (BSA) standards were prepared at concentration of 2.5, 5, 10, 15, 20 and 25 µg/ml in dH_2O in order to obtain a standard curve for measurements. The concentration of protein samples was determined by Coomassie (Bradford) protein assay (Thermo Scientific) on a range of dilutions from the cleared protein lysates. For the analysis of the whole cell lysates, SDS sample buffer was added to the lysates and the sample boiled for 10 min at 95°C. If not immediately used for SDS PAGE analysis, boiled lysates were stored at -20°C.

2.5.3 Immunoprecipitation, SDS PAGE and immunoblotting

Immunoprecipitation was carried out by incubating the cleared lysates with dynabeads (Invitrogen) crosslinked with anti-myc antibody at 4°C overnight. Beads were then collected by short centrifugation (2.500 g for 3 min at 4°C), washed 5 times in lysis buffer, resuspended in SDS sample buffer and boiled for 10 min at 95°C. Boiled extracts were resolved by a 4-12% NuPAGE Bis-Tris SDS gel in MOPS buffer and transferred to Immobilon PVDF-FL membrane (Millipore) at 4°C using Immunoblot transfer buffer at 100 V for 1:15 hr. The membrane was blocked in methanol and then incubated overnight at 4°C with primary antibody diluted in blocking buffer. After washing in PBST, the membrane was incubated with secondary antibody for 1 hr at room temperature followed by washing and detected using an Odyssey infrared imaging system (LI-COR). Quantification by densitometric scanning of Western blots was performed using Odyssey Application Software version 3.0 (Li-COR). Since the primary antibodies used in this analysis detected both the 42 kDa and 44 kDa form of ERK/pERK, two bands were visualized and captured. The p44 phosphoERK levels were calculated by normalizing, for each point of the timecourse, the relative optical density value of the p44 phosphoERKs band to the corresponding total p44 ERK value.

2.6 Microscopy techniques

2.6.1 Laser Scanning Confocal Microscopy (LSCM), Epi-fluorescence Microscopy (E-FM) and Super-resolution microscopy

Confocal laser and Epifluorescence microscopy were performed with an inverted microscope (Eclipse Ti, Nikon A1R) at 37°C using a 60X 1.45NA oil-immersion objective and Andor iXon 885 EMCCD camera. GFP constructs were excited with an Argon-Ion 457-514 nm laser, mRFP and dsRed constructs with a Green Diode 561 nm laser. Confocal microscopy was also performed with a Zeiss LSM 710 confocal microscope with a 40X 1.3NA oil-immersion objective and a Transmission-Photomultiplier LSM T-PMT. Epifluorescence microscopy was also performed by using a Nikon TE300 Inverted Epi-fluorescence microscope using an 60X 1.40NA oil-immersion objective and a cooled CCD camera (Hamamatsu C4742-98-12WRB). All images were prepared with NIS-Elements Imaging Software version 3.2 (Nikon). Super-resolution imaging was performed on a gSTED system (Leica) and image stacks were deconvolved using Huygens linked within the Leica software.

2.6.2 Total Internal Reflection Fluorescence Microscopy (TIR-FM)

TIRF microscopy was performed with the system described above as well as with an inverted microscope (IX81, Olympus) using a 60X 1.49NA oil-immersion objective and a 12-bit CCD camera (ORCA-R^2 C10600, Hamamatsu). GFP constructs were excited with a 491-50 Diode type laser, dsRed constructs with a 561-50 DPSS type laser. Images were analyzed and prepared with Xcellence Advanced Live Cell Imaging System version 1.1 (Olympus).

2.7 Miscellaneous techniques

2.7.1 Receptor trafficking assay

Cells were transfected with FGFR2-GFP or EGFR-GFP and 24 hr before the experiment were plated into 35-mm glass-bottomed dishes (MatTek Corporation). On the day of the experiment, cells were starved for 30 min and, where indicated, treated with trafficking inhibitors. Media was then removed and cells were washed twice with phosphate-buffered saline (PBS), and incubated in prewarmed (37°C) cell imaging media (CIM). Cells were placed on the microscope stage, inside a temperature control chamber (37°C), and stimulated by addition of ligand. Real-time analysis of receptor trafficking was performed by imaging cells once every 5 min, immediately following stimulation. For the quantification analysis, FGFR2-GFP intensity in the plasma membrane associated region of the cells was calculated for each frame of the time-lapses (1 frame/5 min). From each time point, a background value was subtracted, corresponding to the cytosolic fluorescence intensity before the stimulation with FGF2 (time = 0 min). In order to define the plasma membrane associated region, cells were treated with a red membrane stain (DiI, Invitrogen) for 5 min before the analysis. For the EGFR trafficking assays, the total cellular EGFR-GFP intensity was measured at each time point to quantify receptor degradation, whereas the number of intracellular endosomes positive for EGFR was analyzed at each time point to quantify receptor endocytosis. Data analysis was performed using NIS-Elements Imaging Software version 3.2 (Nikon).

2.7.2 Transferrin and cholera toxin B uptake assay

For siRNA studies, cells were transfected with FGFR2-GFP and either α-adaptin siRNA or caveolin1 siRNA and plated into 35-mm glass-bottomed dishes (MatTek Corporation). Following starvation for 30 min, cells were incubated for 30 min either with Alexa-Fluor-546–transferrin (Invitrogen) or with Alexa-Fluor-555-cholera toxin B (Invitrogen) at 37°C

and 5% CO_2. For the Dynasore studies, cells transfected with FGFR2-GFP and plated into 35-mm glass-bottomed dishes were treated with Dynasore following 30 min starvation. Cells were then incubated for 30 min in Alexa-Fluor-546–transferrin at 37°C and 5% CO_2. For the FGF2-dependent uptake assay, cells were incubated for 30 min with ligand and Alexa-Fluor-546–transferrin at 37°C and 5% CO_2.

Following treatments, cells were acid washed twice to remove transferrin/cholera toxin B still bound at the cell surface, then fixed in 4% paraformaldehyde (PFA) and analyzed. All images were acquired by using a Nikon TE300 Inverted Epi-fluorescence microscope using an 60X 1.40NA oil-immersion objective and a cooled CCD camera (Hamamatsu C4742-98-12WRB).

For quantification of transferrin and cholera toxin uptake, cells randomly located on the coverslips were scanned at fixed intensity settings below pixel-saturation, and the total cellular intensity was determined. Data analysis was performed using ImageJ (National Institutes of Health, NIH). For the triple colocalization, HeLa cells were incubated with Alexa-Fluor-633-transferrin (Invitrogen) for 5 min, in order to mark the early endosomes. Cells were then rinsed, fixed and analyzed via confocal microscopy.

2.7.3 Colocalization of FGFR2/EGFR with clathrin and caveolin1

HeLa cells cotransfected with GFP tagged receptors (FGFR2 or EGFR) and either clathrin-dsRed or caveolin1-mRFP were plated into 35-mm glass-bottomed dishes. On the day of the experiment, cells were starved for 30 min in serum-free media, stimulated with the corresponding ligand for 30 min, then rinsed twice in PBS, fixed in 4% PFA and analyzed in TIRFM. For the quantitative analysis, each spot of FGFR2, EGFR, clathrin and caveolin1

was identified and a circle was drawn around it. Spots were identified as colocalizing when the majority of the fluorescence intensity of the pixels within the circular regions fitted in both the channels. To exclude the possibility that the colocalization was the result of random alignment of receptor spots with clathrin/caveolin spots, a negative control was also included for each experiment. As a control for random colocalization 100 regions that did not contain receptor clusters were analyzed for the presence of clathrin/caveolin. Data analysis was performed using NIS-Elements Imaging Software version 3.2 (Nikon).

2.7.4 Analysis of recruitment of FGFR2 and clathrin

HeLa cells co-expressing FGFR2-GFP and clathrin-dsRed and plated into 35-mm glass-bottomed dishes, were starved for 30 min in serum-free media and then imaged in simultaneous two-colour TIRF microscopy at 37°C (1 frame/30 sec) following receptor stimulation. For the quantification, each timelapse was analyzed backward for the appearance of FGFR2 and Clathrin at colocalizing spot and the percentage of clathrin clusters forming at pre-existing FGFR2 spots, of FGFR2 spots recruited at pre-formed Clathrin clusters or FGFR2 and Clathrin clustering simultaneously at the plasma membrane were normalized for cell surface area. Data analysis was performed using Xcellence Advanced Live Cell Imaging System version 1.1 (Olympus).

2.7.5 Analysis of redistribution of clathrin to cell surface

LNCaP cells expressing clathrin-dsRed and HeLa cells coexpressing FGFR2-GFP and clathrin-dsRed were plated into 35-mm glass-bottomed dishes. 30 min before the experiment, cells were starved in serum-free media and treated, where indicated, with

the trafficking inhibitors or with Eps8 siRNA. Cells were then rinsed in PBS, incubated in prewarmed (37°C) cell imaging media and analyzed in TIRF microscopy before and 30 min after stimulation with ligand. The number of clathrin spots was calculated for each condition and normalized for cell surface area. Data analysis was performed using Xcellence Advanced Live Cell Imaging System version 1.1 (Olympus).

2.7.6 Analysis of endocytic events at plasma membrane

HeLa cells cotransfected with FGFR2-GFP and clathrin-dsRed were starved in serum free media for 30 min, then rinsed in PBS, incubated in prewarmed (37°C) cell imaging media and imaged in live-cell TIRF microscopy at 37 °C for 2 min (1frame/200msec) before and 30 min after ligand addition. The number of clathrin spots disappearing from the TIRF field was calculated and normalized for cell surface area. Data analysis was performed using Xcellence Advanced Live Cell Imaging System version 1.1 (Olympus).

2.7.8 Time dependent colocalization of FGFR2 with Eps8

HeLa cells transiently transfected with FGFR2-GFP and Eps8-mCherry and plated into 35-mm glass-bottomed dishes were starved for 30 min in serum-free media, then rinsed twice in PBS and fixed in 4% PFA, or treated as above upon incubation with ligand for either 10 or 30 min. After fixation, cells were imaged in confocal microscopy using the Nikon A1R system (see section 2.6). Colocalization between FGFR and Eps8 was assessed by identifying every spot and drawing a circle around it. Two spots were identified as colocalizing when the majority of the fluorescence intensity of the pixels within a circle fitted in both the green and red channels. Data analysis was performed using NIS-Elements Imaging Software version 3.2 (Nikon).

2.7.9 Colocalization of FGFR2 with makers for endocytic compartment

Eps8 shRNA and control shRNA HeLa cells transiently transfected with FGFR2-GFP were stimulated with FGF2 for 30 min following 30 min of serum-free media starvation. Cell were then immunostained with anti-EEA1 and anti-Rab11 antibodies (in order to mark the early endosomal and the perinuclear recycling compartment, respectively) and imaged in confocal microscopy. For lysosomal staining, cells were incubated with 75 nM LysoTracker Red (Molecular Probes) for 30 min and immediately imaged in imaging media at room temperature. Data analysis was performed using NIS-Elements Imaging Software version 3.2 (Nikon).

CHAPTER 3

RESULTS

3.1 Identification of a model system and expression of functional GFP-tagged FGFR2

The transcripts of three out of the five fibroblast growth factor receptors (FGFR1-3) are subjected to an alternative splicing event that uses either exon 8 or exon 9 to encode the second half of the D3 domain (Figure 1.5). The two splice variants generated by this event (IgIIIb and IgIIIc) display different ligand-binding specificities and a specific cell-lineage pattern of expression. This study uses FGFR2IIIc as a model for analysis of FGFR endocytosis and trafficking. This splice variant of FGFR2 is specifically expressed in mesenchymal cells, both during early organogenesis and in adulthood (Orr-Urtreger et al. 1993). To investigate in real-time the endocytic dynamics of receptors in mammalian cells, an ectopically overexpressed C-terminal GFP-tagged form of FGFR2IIIc (herein referred to as FGFR2-GFP) was employed. The functionality of this fusion protein was previously validated in a published report from John Ladbury's group (Schuller et al. 2008), which showed that the GFP-fused receptor is kinase active and that tagging does not interfere with receptor functionality.

In living cells, to follow the dynamics of transiently overexpressed FGFR2-GFP, identification of an adequate cell model was a critical step. Two different cell lines were screened as potential cellular platforms for the cell imaging studies, HEK-293T cells

(epithelial cells from embryonic kidney) and HeLa cells (human cervical cancer cells). Both these cell lines have been shown to express very low levels of endogenous FGFR2 (Ahmed et al. 2008), an important criterion to follow to avoid any interference that the endogenous FGFR2 could have with the ectopically transfected counterpart. Preliminary analysis of FGFR2-GFP expression level in HEK-293 and HeLa cells (Figure 3.1) revealed that both cell lines express a sufficient quantity of transfected proteins, allowing for high-quality microscopy analysis. Further, both HEK-293T and HeLa cells expressing FGFR2-GFP and imaged in confocal microscopy in the absence of ligand show plasma membrane localisation of the fusion protein (Figure 3.1, left panels), confirming the correct targeting of FGFR2-GFP.

The b isoform of FGFR2 has the ability to bind multiple ligands of the FGFs family (see Table 1.1). Among these ligands, FGF1 and FGF2 have been shown to interact with very high affinity with FGFR2IIIc (Miki et al. 1992) and to efficiently induce receptor-mediated signalling and biological responses (Mehta et al. 2001, Singh et al. 2012). Consistent with these observations, FGFR2-GFP expressing HEK-293T and HeLa cells were incubated with FGF2 ligand and imaged in confocal microscopy. As shown in Figure 3.1 (right panels), ligand stimulation for 15 minutes induces receptor internalisation from the plasma membrane and redistribution into intracellular endocytic compartments. Notably, in ligand-stimulated HeLa cells (lower right panel), the receptor specifically appears to be targeted to perinuclear regions, suggesting that FGFR2 might be trafficked through a canonical endosomal route by which it is sorted either to degradative or late recycling perinuclear compartments. These observations demonstrate that FGFR2 efficiently

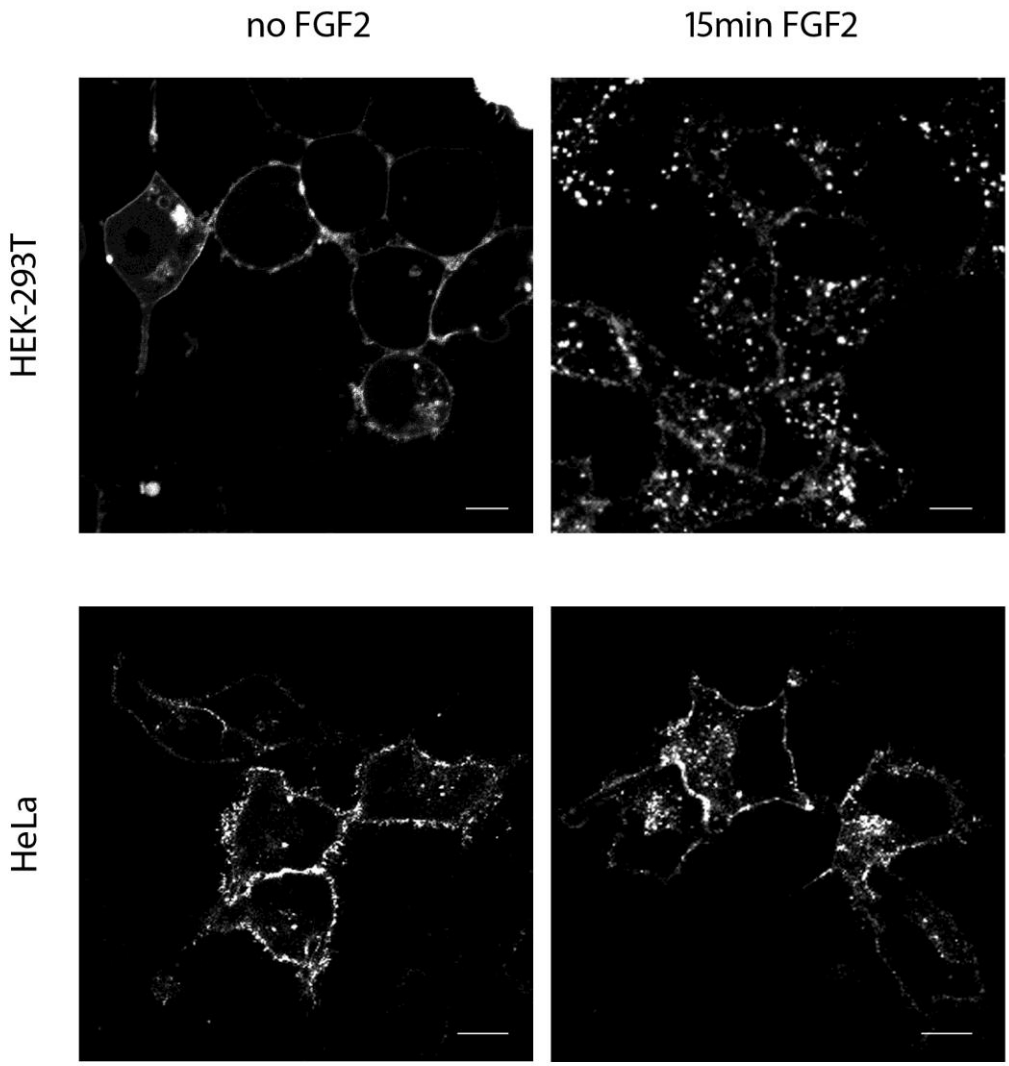

Figure 3.1. Cellular localisation of FGFR2-GFP in HEK-293T and HeLa cells

HEK-293T and HeLa cells transfected with FGFR2-GFP fusion protein were incubated for 15 minutes in the absence (left panels) or presence (right panels) of FGF2 ligand, fixed and imaged in confocal microscopy. In non-stimulation conditions, both cell lines show a predominant membrane localisation of FGFR2. On the contrary, upon ligand stimulation, receptor redistributes from the plasma to intracellular peri-nuclear compartments. Scale bars = 10 µm.

responds to FGF2 stimulation and provide further confirmation of the functionality of the FGFR2-GFP fusion protein.

Finally, to assess whether the cellular localisation and behaviour of FGFR2-GFP reflects that of an endogenous receptor, this study examined the dynamic of internalisation of endogenous FGFR1 in HEK293 cells. As shown in Figure 3.2, localisation of the endogenous receptor is comparable to that of ectopically transfected FGFR2-GFP, both before and after FGF2 stimulation, further validating this system for use in live-cell imaging studies.

3.1.1 Conclusion

Preliminary characterisation of a model system suitable for studying FGFR2 trafficking by live-cell imaging resulted in identification of two cell lines, HeLa and HEK-293T. Both these cell lines express very low levels of endogenously expressed FGFR2 (Ahmed at al. 2008), which makes them a suitable cell platform for studying, in real-time, the endocytic dynamics of an ectopically transfected C-terminal GFP-fused FGFR2. Expression level analysis of the fusion protein in both cell lines showed a level of receptor sufficient to allow live-cell imaging studies and revealed that the GFP tag does not affect either ligand binding or receptor activation and its subsequent internalisation. In conclusion, GFP-tagged FGFR2 has been successfully validated, and both HeLa and HEK293T cells appear to be suitable model systems for studying trafficking of the receptor in living cells.

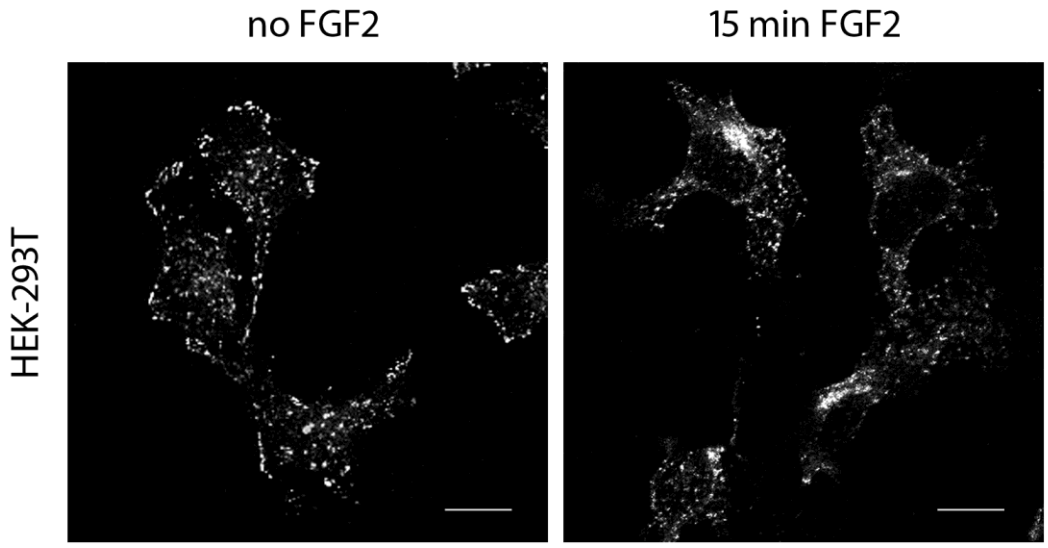

Figure 3.2. Cellular localisation of endogenous FGFR1 in HEK-293T cells

HEK-293T cells were incubated for 15 minutes in the absence (left panels) or presence (right panels) of FGF2 ligand, fixed and immunostained for FGFR1. Confocal microscopy analysis of the cells shows that, similar to overexpressed FGFR2-GFP fusion protein, endogenous receptor localises at the cell surface in absence of ligand, whereas it is targeted to peri-nuclear endocytic compartments upon FGF2 stimulation. Scale bars = 10 µm.

3.2 Establishment of live-cell imaging assays to study FGFR

Having identified an appropriate cell model for studying the endocytic dynamics of FGFR2, the next step was to establish living-cell–based assay systems to investigate, in real time, the basic aspects of receptor trafficking, including receptor dynamics at the cell surface, internalisation, and endocytic trafficking.

As extensively described in the Introduction, ligand-mediated FGFR activation promotes regulated receptor endocytosis from the cell surface and subsequent trafficking into the cell. Several aspects of FGFR endocytosis and trafficking have been studied by several groups, but the conclusions reached appear to be quite contradictory. Further, all previous reports regarding endocytosis and the trafficking route of FGFR employed fixed, cell-based techniques and limited their analysis to antibody-labelling methods. In the present study, practical and efficient tools were developed to visualize in real-time the entire sequence of stages of trafficking of FGFR2, by combining advanced optical microscopy technique with fluorescent tagged proteins expressing cells. The live-cell imaging assays used in this study are described in the next section; their contribution lies in allowing visualization of spatial and temporal endocytic dynamics of the receptor within a live biological context.

3.2.1 Confocal live-cell imaging of FGFR trafficking

Confocal microscopy is an optical imaging technique that allows visualization deep within living cells or tissues and, more importantly, the collection of high-resolution optical slices of the object, from which three-dimensional representation of the sample can be created. The principle of a confocal microscope, as well as its major advantage over a

conventional microscope, is the use of a spatial filtering strategy to remove out-of-focus light from the image (Figure 3.3A). The presence of suitably positioned pinholes allows only the light from the focal plane to reach the detector, resulting in sharply defined images. Other key advantages of confocal over conventional microscopes include: higher level of sensitivity, due to the ability to capture images over time via highly sensitive light detectors; reduced invasiveness, due to reduction of light-scattering artefacts; employment of high-power laser illumination; and digital 3-D reconstructions of the sample.

Confocal microscopy is extensively used in cell biology and, in combination with development of fluorescent fusion proteins, it has become a very effective tool in the study of dynamic processes in living cells, such as actin remodelling and receptor trafficking. To monitor in real-time the dynamics of activated FGFR2 trafficking, time-lapse confocal imaging of FGFR2-GFP expressing HeLa cells, was performed (Figure 3.4A). The flat morphology, wide cytoplasmic area, and ease of culture make HeLas a preferred cell line for live-cell imaging experiments over HEK-293T cells. To create a biological system that retains physiological conditions, cells were kept at 37°C while on the stage of the microscope and imaged repeatedly at defined time points (1 frame/minute) immediately upon addition of FGF2 ligand. Figure 3.4A shows still frames captured from a confocal time-lapse of live FGFR2-GFP expressing HeLa cells stimulated with FGF2. In the absence of ligand stimulation (time 0), FGFR2 exclusively localises at the cell surface and no vesicle is detectable within the cell. A few small FGFR2-containing vesicles begin to appear from the inner surface of the plasma membrane at a very early time point, typically beginning 5 minutes after FGF2 addition (magnification), demonstrating that the

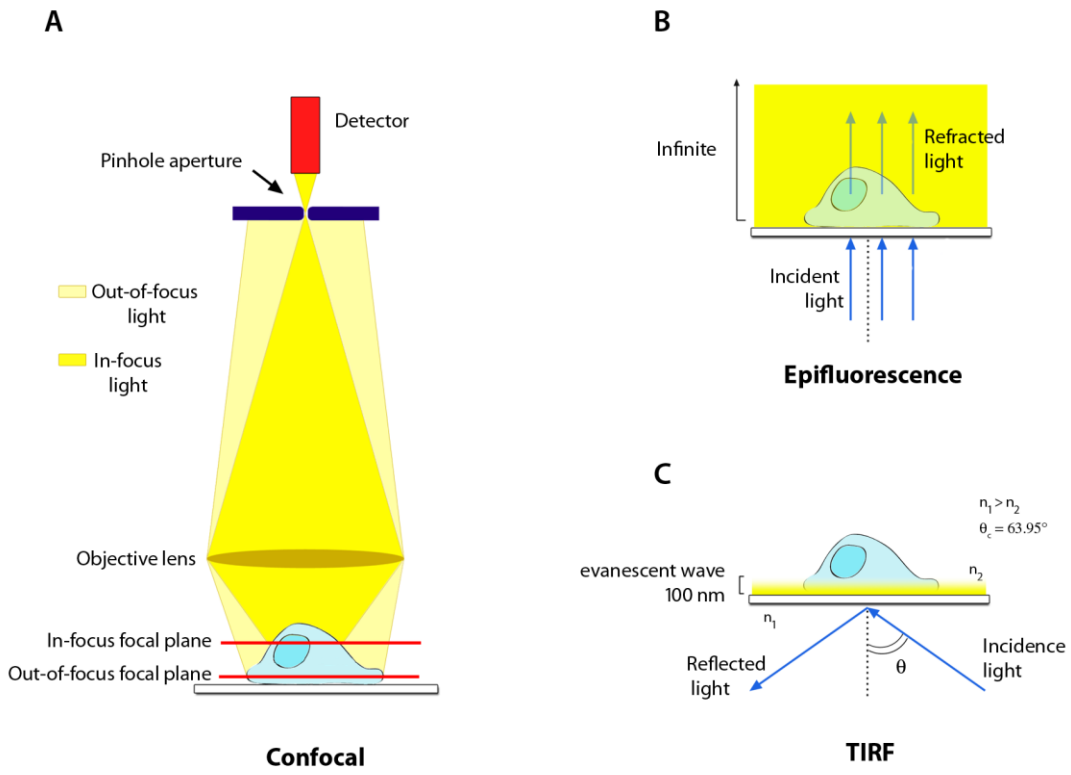

Figure 3.3. Advanced optical microscopy techniques used in this study

A. By employing spatial filtering techniques (pinholes), a confocal microscope allows only the light from the "in-focus" focal plane to reach the detector, removing any out-of-focus light emitted by the sample. This results in collection of high-resolution optical slices of the specimen. **B**. In epifluorescence microscopy, the incident light hits the coverslip/sample interface with a zero degree angle against the vertical axis (dashed line) and is entirely refracted into the medium, resulting in excitement of all parts of the specimen simultaneously. **C**. When the refractive index of the sample (n_2) is less than that of the coverslip (n_1) and the angle of incidence of light (θ) is wider than the critical angle ($\theta_c = 63.95°$ in the case of glass/water interface), the excitation beam is entirely reflected. Complete internal reflection generates an evanescent wave into the sample that extends only a few hundred nanometres, exciting fluorophores within a restricted specimen region immediately adjacent to the coverslip/sample interface.

process of ligand-mediated receptor activation occurs rapidly, within few minutes. This is consistent with similar studies on the kinetics of internalisation of EGFR, another important member of the RTK family, which is observed to undergo internalisation already at 5 minutes following ligand incubation (Schmidt-Glenewinkel et al. 2009). As FGF2 stimulation time increases, vesicles pinch off from the plasma membrane and are released into peripheral cytoplasmic regions, which correspond to early endosomal compartments (as clearly demonstrated later in this chapter). Finally, at late time points following ligand stimulation, FGFR2 is nearly undetectable at the cell surface, as its localisation shifts toward perinuclear compartments. The dynamic of internalisation of FGFR2 was subsequently quantified from the imaging data (Figure 3.4B). The sum of the pixel intensity value of FGFR2-GFP within the plasma membrane associated region of the cells was calculated for each frame of the time-lapses and plotted against time of incubation with FGF (quantification procedures are explained in more detail in the Methods, Section 2.7.1 Receptor trafficking assay). Consistent with the imaging data, the resulting plot reveals an initial latent phase of 5–7 minutes, in which the FGFR2-GFP fluorescent signal remains associated with the plasma membrane region. This corresponds to the phase during which the receptor recognizes and associates with the ligand and vesicles begin to form. With time, fluorescence signals decrease due to receptor internalisation, and reaches minimum value at 30 minutes, when the entire pool of surface-bound receptors is internalised and redistributed within intracellular compartments.

The kinase activity of FGFR seems to play a key role in receptor internalisation. This is demonstrated, for example, by the observation that mutant receptors with inactive

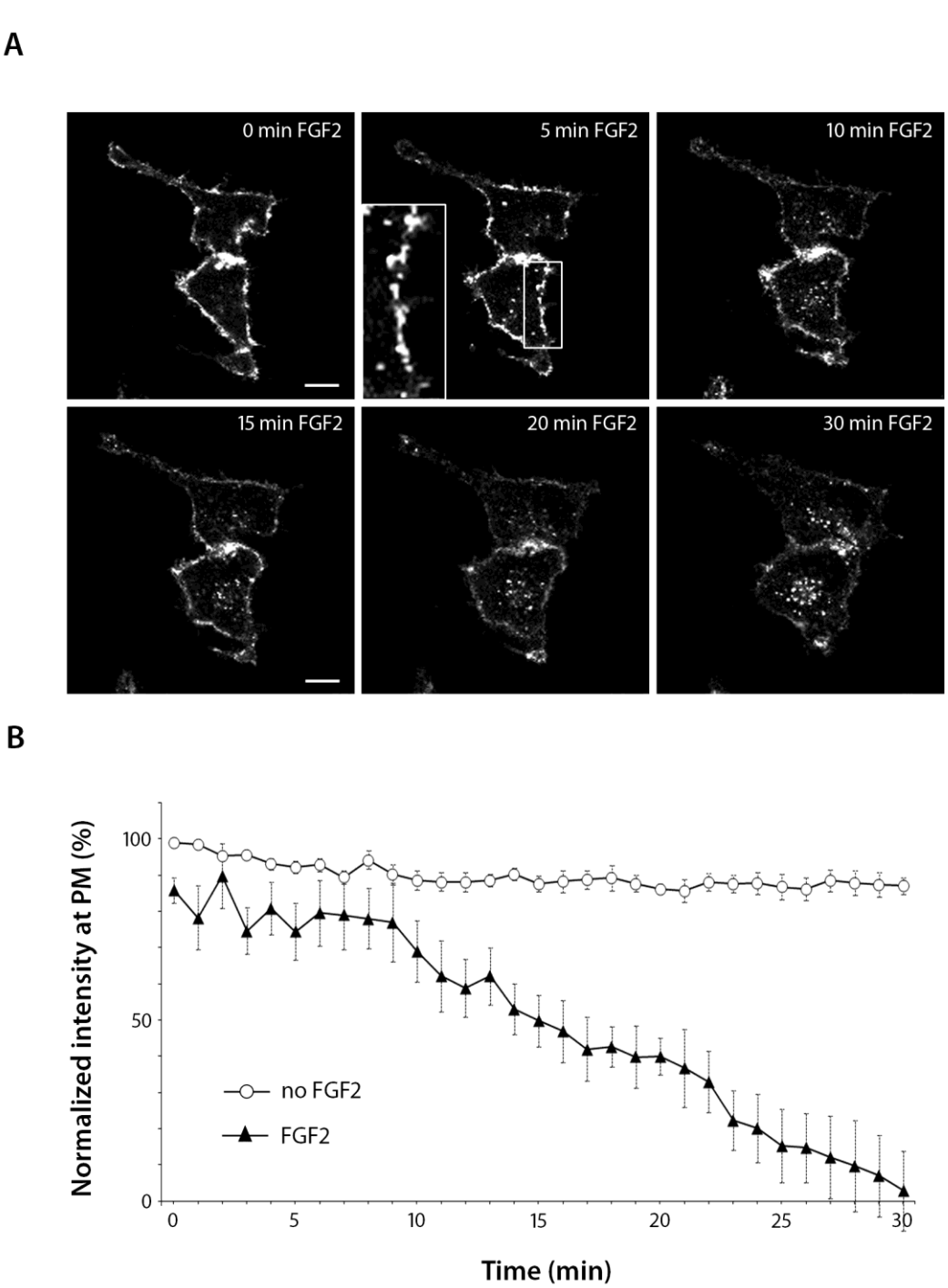

Figure 3.4. Live-cell confocal microscopy analysis of FGFR2 trafficking

A. Selected frames from a confocal time-lapse of live HeLa cells expressing FGFR2-GFP and stimulated with FGF2. Prior to ligand stimulation (0 min FGF2), FGFR2 predominantly localises at the cell surface. Following FGF2 addition, the first receptor-containing vesicles begin to form and to invaginate from the plasma membrane (5 minutes, magnification). At late time points after ligand stimulation, FGFR2 is redistributed away from the cell periphery and targeted to peri-nuclear compartments. Scale bars = 10 µm. **B**. The time-lapse experiment shown in (A) was performed in 14 cells and the FGFR2-GFP pixel intensity within the plasma membrane (PM) region was calculated (as described in Methods) for each time point and plotted as a function of time. A photo-bleaching control curve was obtained from cells expressing FGFR2-GFP and imaged without FGF2 stimulation (mean ± SEM).

kinase, such as the FGFR1 K514A mutant, are unable to internalise properly (Sorokin et al. 1994). To confirm that the kinase activity of FGFR2 is required for receptor internalisation to occur, FGFR2-GFP expressing HeLa cells were treated with the SU5402 compound and receptor trafficking was assessed using the above-described live-cell imaging assay. SU5402 is a potent inhibitor of FGFR kinase activity, with an IC_{50} value of 0.03 µM for FGFR1, and exerts its function by occupying the adenine binding site of ATP with the indolin-2-one core (Mohammadi et al. 1997). As shown in Figure 3.5, following treatment with SU5402 inhibitor, the presence of ligand does not alter localisation of FGFR2, which remains associated with the plasma membrane even after 30 minutes of stimulation, demonstrating that kinase activity of FGFR2 is necessary for receptor internalisation.

3.2.2 Total internal reflection fluorescence live-cell imaging of FGFR2 dynamics at plasma membrane

Total internal reflection fluorescence (TIRF) microscopy is a widely used mode of fluorescence light microscopy. Developed by Daniel Axelrod at the University of Michigan in the early 1980s, TIRF is a powerful method for visualizing processes within membranes of living cells. TIRF employs an evanescent wave generated at the interface between two transparent media with different refractive indices, when the incident light travels at an angle greater than the critical angle and undergoes total reflection (Figure 3.3C). The evanescent wave exponentially decays with distance to the interface, extending only a few hundred nanometres into the sample, resulting in excitation of fluorophores in proximity to the coverslip. This generates images both with high signal-to-noise ratio, as fluorophores in the rest of the cell are not excited, and high axial resolution (on the order

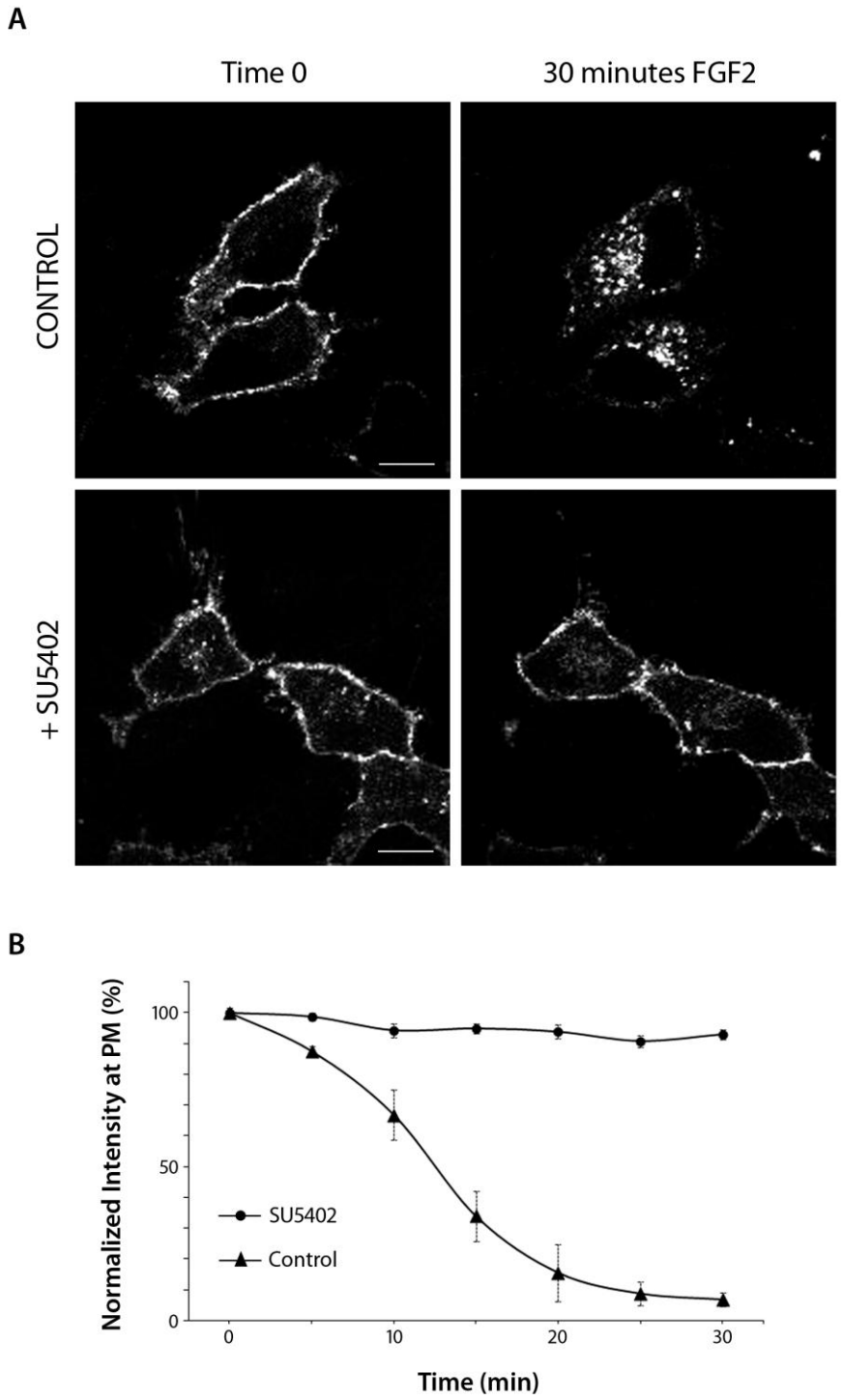

Figure 3.5. FGFR2 kinase activity is required for receptor internalisation

A. HeLa cells transiently transfected with FGFR2-GFP and incubated for 5 minutes in the presence (lower panels) or absence (control, upper panels) of SU5402 and imaged in confocal microscopy for 30 minutes. The first (left panels) and the last frame (right panels) of the time-lapse are shown, corresponding to the situations before and after FGF2 treatment, respectively. While in control cells activated FGFR2 undergoes efficient internalisation from the plasma membrane, treatment with the inhibitor of FGFR kinase activity entirely prevents receptor internalisation. Scale bars = 10 µm. **B**. The experiment in A was performed in 8 cells and the FGFR2-GFP intensity in the PM region of the cells was quantified (as described in Methods) for each frame of the time-lapses and plotted as a function of time (mean ± SEM).

of 100 nanometres), allowing direct, time-resolved visualization of membrane-associated processes such as endocytosis, cytoskeletal dynamics, and cell adhesion. In this study, TIRF microscopy was employed to monitor dynamic processes involving FGFR2 at the plasma membrane, such as clustering of activated receptor or colocalisation with plasma membrane endocytic markers, as well as to visualize individual endocytic events occurring at the cell surface.

A preliminary analysis of the dynamics of activated FGFR at the plasma membrane was performed by imaging in TIRF microscopy FGFR2-GFP expressing HeLa cells before and after stimulation with FGF2. As depicted in Figure 3.6 (lower panels), in the absence of ligand, FGFR2-associated fluorescence appears uniformly diffuse over the cell surface, whereas upon stimulation for 15 minutes, the receptor appears to be redistributed into spots. This suggests that ligand-mediated activation of FGFR2 induces receptor clustering at the cell surface, a phenomenon already described for many other membrane-bound receptors and thought to correlate with the activation state of the receptor itself (Care and Soula 2011, Nagy et al. 1999).

The same cells were also simultaneously imaged in epifluorescence microscopy. This is the most conventional and common fluorescence set-up, so called because it employs an episcopic light to illuminate the sample and because it excites all parts of the specimen simultaneously (Figure 3.3B). Consistent with the TIRF data, cells imaged in epifluorescence prior to stimulation showed diffuse FGFR-associated fluorescence at the plasma membrane, which after FGF addition assumed a heterogeneous punctuate distribution (Figure 3.6, upper panels).

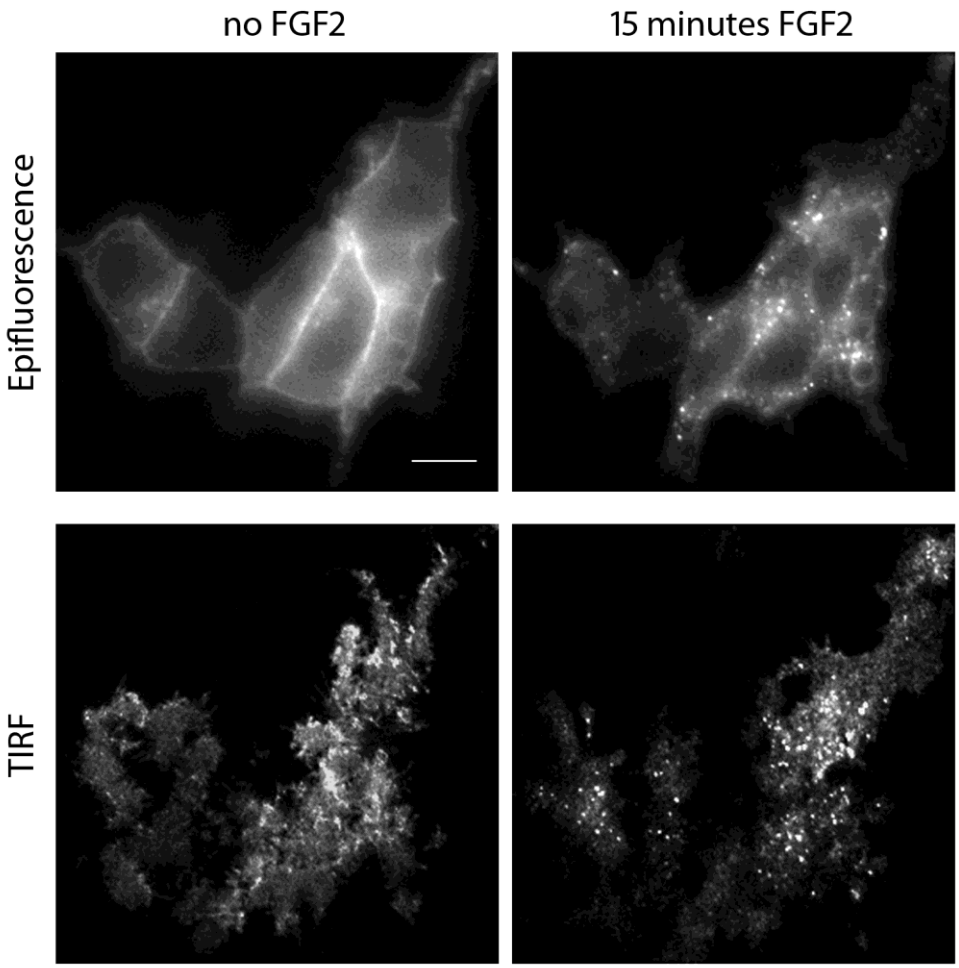

Figure 3.6. Clustering of active FGFR2 at plasma membrane

Live-cell epifluorescence (upper panels) and TIRF (lower panels) imaging of FGFR2-GFP expressing HeLa cells before and after FGF2 stimulation. In absence of ligand, FGFR2 localises at the cell surface, where it appears uniformly distributed. The presence of FGF2 induces heterogeneous redistribution of receptor into punctuate spots on the plasma membrane, suggesting that multiple active FGFR2 form clusters in response to ligand stimulation. Scale bars = 10 µm.

3.2.3 Conclusion

The combination of advanced optical microscopy techniques with the use of fluorescent fusion proteins has proven to be a powerful tool for the study in real-time the dynamics of FGFR2 endocytosis and trafficking within a live biological context. Ligand-dependent internalisation and intracellular trafficking of FGFR2 were investigated using confocal microscopy, allowing high-resolution, time-resolved optical imaging. Ligand stimulation was shown to induce rapid internalisation of FGFR2, preceded by a latency period of 7 minutes, at which time the receptor recognises and associates with ligand, and endocytosis begins. The first receptor-containing vesicles form at 5 minutes after FGF2 addition, and at 15–20 minutes FGFR2-GFP fluorescence is homogeneously distributed between plasma membrane and intracellular compartments. At late time points after ligand stimulation, the entire pool of surface-bound receptor is internalised and targeted to perinuclear compartments.

The first key step in the pathway initiated by FGFR includes trans-phosphorylation events mediated by the kinase domain of the receptor. Here, kinase activity of FGFR2 was demonstrated to play a critical role in receptor internalisation, since SU5402, a potent inhibitor of FGFR kinase activity, completely prevented FGF2-dependent internalisation. Finally, live-cell TIRF microscopy was employed to investigate the dynamics of activated receptor at the plasma membrane. Ligand stimulation was shown to induce redistribution of FGFR2-GFP into heterogeneous punctuate spots, suggesting that, similar to other members of the RTK family (Abulrob et al. 2010), FGFR2 clusters at the plasma membrane in response to ligand stimulation.

By altering receptor density at the cell surface, this process may have profound effects on the activation state of FGFR2. For example, it may contribute to initiation of the intracellular signalling cascade by concentrating active receptors within specific membrane domains enriched in signalling molecules. Or it could strengthen receptor activation by physically recruiting multiple receptors together and enabling them to trans-phosphorylate and activate each other.

3.3 Pathway for internalisation of FGFR2

Similar to other members of RTK family, following ligand binding and receptor activation, FGFRs undergo regulated endocytosis from the plasma membrane. Multiple pathways have been implicated in the internalisation of FGFRs, including both clathrin-mediated and caveolar endocytosis. Additionally, few investigators have observed involvement of pathways that proceed independently of clathrin and caveolins. Thus, identification of the route of entry for FGFRs into the cell remains controversial. One aim of this study is to document the endocytic pathway(s) by which FGFR2 is internalised and trafficked during the early phases of receptor activation.

3.3.1 FGFR2 is internalised through dynamin-dependent endocytosis

The literature has described an increasing variety of pathways that mediate the uptake of transmembrane receptors; they differ in the protein machinery involved, the cargo protein selected, and the intracellular route chosen. The best characterised route of entry for RTKs is clathrin-mediated endocytosis (CME). Through CME, several receptors (including epidermal growth factor receptor and transferrin receptor), along with their ligands, are packaged and transported into clathrin-coated vesicles (CCVs). A network of specific adaptor and accessory proteins coordinates formation of this class of vesicles, including the GTPase dynamin, which mediates the scission of the vesicles from the plasma membrane and their release into the cytoplasm. A number of pathways that proceed independently of clathrin have also been described. Among these, endocytosis via caveolae seem to impart a major contribution to the internalisation process for several RTKs. Even though most aspects of endocytosis via caveolae remain poorly understood, dynamin has also been implicated as a membrane scission protein in

caveolar endocytosis (Henley et al. 1998). The observation that not all receptor endocytosis is blocked by overexpressing a GTPase-inactive form of dynamin2 or by using a small-molecule inhibitor of dynamin GTPases, revealed the existence of other pathways implicated in RTK endocytosis that are dynamin- (and therefore clathrin- and caveolin-) independent. These include processes such as micropinocytosis or the Arf6 and GEEC/CLIC-dependent pathways (Mayor and Pagano 2007).

Both the size of the vesicles and the dynamic of formation from the plasma membrane observed in the FGFR2 trafficking assays (Figures 3.4-3.6), suggest that FGFR2 can be trafficked via a canonical pathway of endocytosis. To unequivocally identify the path of entry for FGFR2, first the involvement of dynamin activity in this process was assessed. A recently developed small-molecule inhibitor of dynamin GTPases (Dynasore) (Macia et al. 2006) was used to block any dynamin-dependent mechanism of endocytosis in HeLa cells, and the effect on FGFR2 trafficking was then investigated. To pre-emptively verify the activity of Dynasore in the cell system, its effect on the uptake of transferrin was examined. Transferrin, along with its receptor, enters cells constitutively by clathrin-mediated endocytosis, a process which is, therefore, entirely dependent on dynamin activity. Fluorescently labelled (red) transferrin was incubated with HeLa cells at 37°C and allowed to internalise for 15 minutes in the presence or absence (control) of Dynasore. Cells were then acid-washed twice to remove transferrin still bound at the cell surface, and transferrin uptake was measured. While in control cells transferrin undergoes efficient endocytosis and traffics to perinuclear compartments, incubation with Dynasore completely blocks uptake and subsequent intracellular accumulation of the ligand (Figure 3.7A). By measuring the integrated intensity of internalised transferrin inside 25–30 cells,

the inhibitory effect of Dynasore on transferrin was quantified, revealing a significant reduction (ca 50%) of internalisation (Figure 3.7B).

After validating its efficacy in HeLa cells, Dynasore treatment was used in combination with the previously described trafficking assay to investigate the role of dynamin in internalisation of FGFR2. HeLa cells transiently expressing FGFR2-GFP were incubated in the presence or absence (control) of Dynasore for 30 minutes, then imaged in live-cell confocal microscopy for an additional 30 minutes upon FGF2 stimulation. The first and the last frames from a selected time-lapse are shown in Figure 3.8A. In control cells, FGFR2 efficiently undergoes ligand-dependent endocytosis from the plasma membrane (upper panels). However, when dynamin activity is inhibited, FGFR2 internalisation is entirely blocked and receptor redistribution away from the cell surface does not occur (lower panels). Interestingly, the endocytosis process seems to initiate properly upon ligand addition, as shown by formation of FGFR2-containing vesicles that invaginate from the plasma membrane (high-magnification images). Although closer analysis is necessary for confirmation, the forming vesicles seem to fail to leave the plasma membrane and, even upon longer stimulation times (30 minutes FGF2), they still appear localised at the cell periphery, consistent with a defect in the vesicle scission event due to inhibition of GTPase dynamin activity. Quantification analysis confirms that impairment of dynamin activity significantly reduces FGFR2 endocytosis, as clearly shown by the flat kinetic curve observed in the Dynasore treatment condition (Figure 3.8B). Thus, these results demonstrate that active FGFR2 enters cells via a dynamin-dependent pathway.

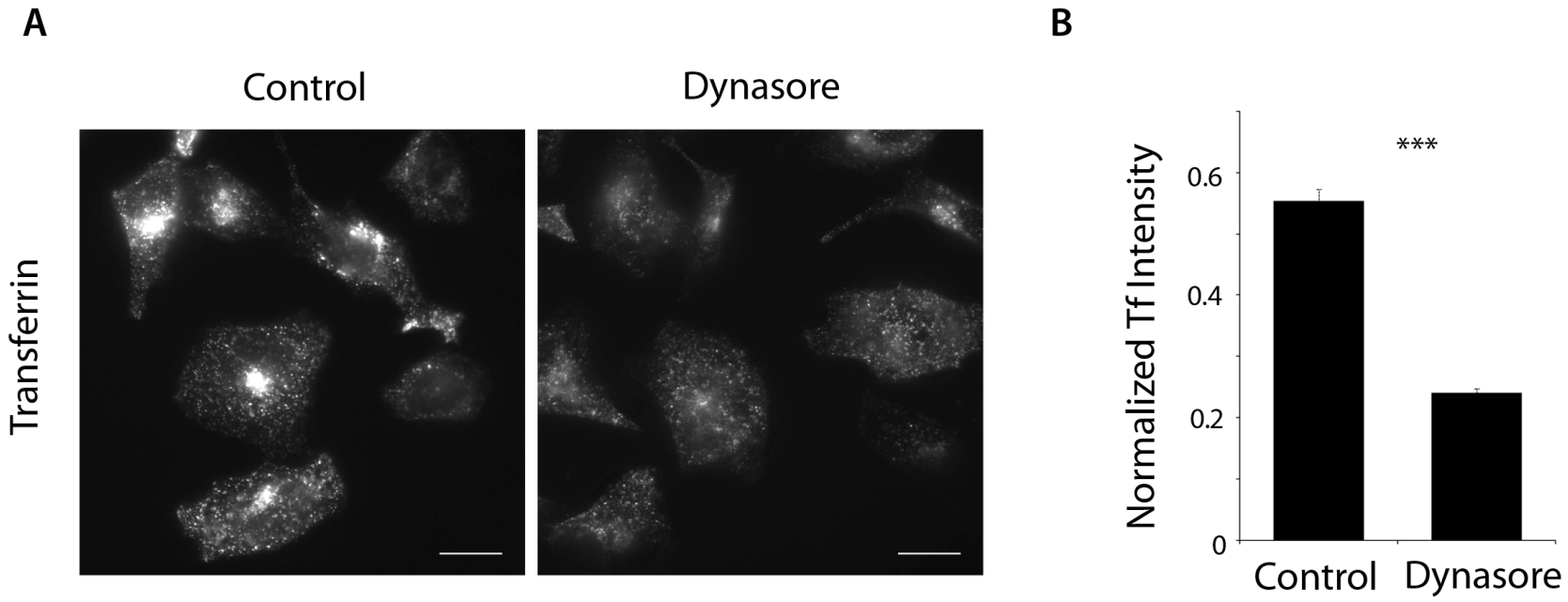

Figure 3.7. Inhibition of GTPase dynamin activity via Dynasore treatment reduces transferrin uptake

A. HeLa cells incubated for 30 minutes in the presence or absence (control) of Dynasore were assessed for capability to uptake extracellular fluorescent-tagged transferrin. Upon incubation with transferrin for 15 minutes, cells were fixed and analysed in epifluorescence microscopy. Pre-treatment of cells with Dynasore clearly prevents transferrin uptake and redistribution to intracellular peri-nuclear compartments. Scale bars = 10 µm. **B**. The experiment in A was performed in 26 cells and transferrin fluorescence intensity was quantified (as described in Methods), confirming that Dynasore activity significantly reduced transferrin entry (mean ± SEM) (*, $p < 0.05$; **, $p < 0.01$; ***, $p < 0.001$)

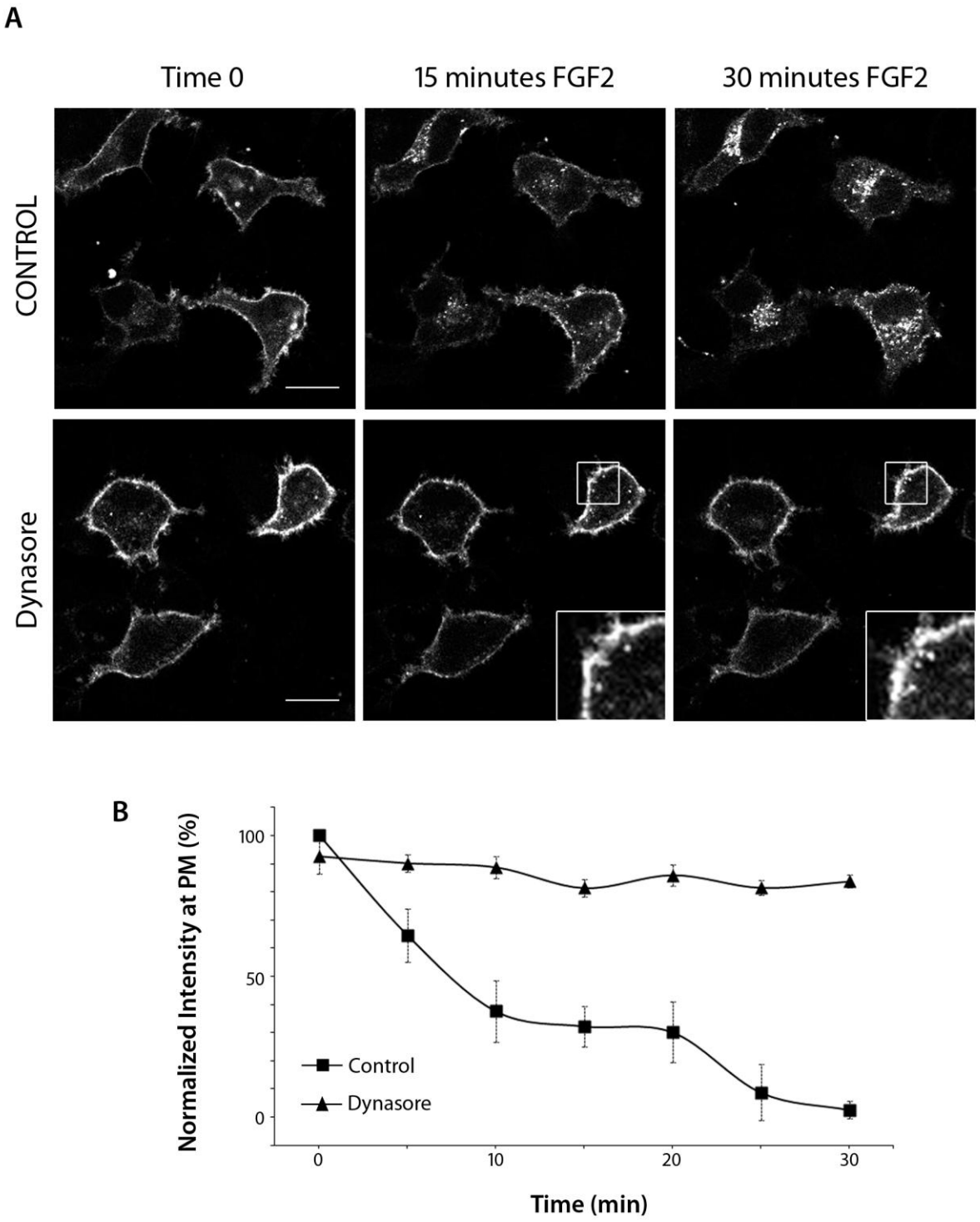

Figure 3.8. FGFR2 is internalized through dynamin dependent endocytosis

A. HeLa cells transiently transfected with FGFR2-GFP and incubated for 30 minutes in the presence (lower panels) or absence (control, upper panels) of Dynasore and imaged in confocal microscopy for 30 minutes. Three frames of a selected time-lapse are shown, corresponding to conditions before, and 15 and 30 minutes after FGF2 treatment. While in control cells activated FGFR2 undergoes efficient internalisation from the plasma membrane, treatment with the dynamin inhibitor entirely blocks receptor endocytosis. Scale bars = 10 µm. **B**. The experiment in A was performed in 14 cells and the FGFR2-GFP intensity in the PM region of the cells was quantified (as described in Methods) for each frame of the time-lapses and plotted as a function of time (mean ± SEM).

3.3.2 FGFR2 is internalised through clathrin-dependent endocytosis

Having established the involvement of dynamin in the internalisation of FGFR2, the next step was to further focus the analysis and identify the specific pathway that mediates endocytosis of FGFR2. As mentioned above, GTPase dynamin has been implicated as a mediator of vesicle scission events in multiple endocytosis pathways. Among these, the best-characterised are CME and entry via caveolae. To assess whether activated FGFR2 enters cells through clathrin or caveolae (or both), each of the endocytosis pathways was selectively inhibited via a small interference RNA (siRNA)-based strategy, and the effect on FGFR2 internalisation was examined. Selective blocking of CME was obtained by employing a synthetic siRNA sequence specific to α-adaptin (Motley et al. 2003), a key component of the clathrin-mediated endocytosis machinery. To demonstrate the effectiveness of α-adaptin siRNA treatment in inhibiting the CME process, the effect on uptake of transferrin, which is a specific marker of clathrin-mediated endocytosis (Hanover et al. 1984), was evaluated. As depicted in Figure 3.9A, HeLa cells with down-regulated α-adaptin expression show low levels of intracellular transferrin when compared to scrambled siRNA (control) treated cells, confirming that α-adaptin siRNA treatment results in potent inhibition of CME. Quantification analysis of transferrin fluorescence intensity reveals a statistically significant reduction (88%) of transferrin internalisation in α-adaptin siRNA treated cells (Figure 3.9B). Selective inhibition of caveolar endocytosis was instead obtained by using a siRNA against caveolin1 (Li W. et al. 2012), which has been shown to be essential for caveolae formation (Rothberg et al. 1992). Similar to the effect observed in α-adaptin siRNA treated cells, HeLa cells transfected with caveolin1 siRNA showed a significantly reduced uptake of cholera toxin

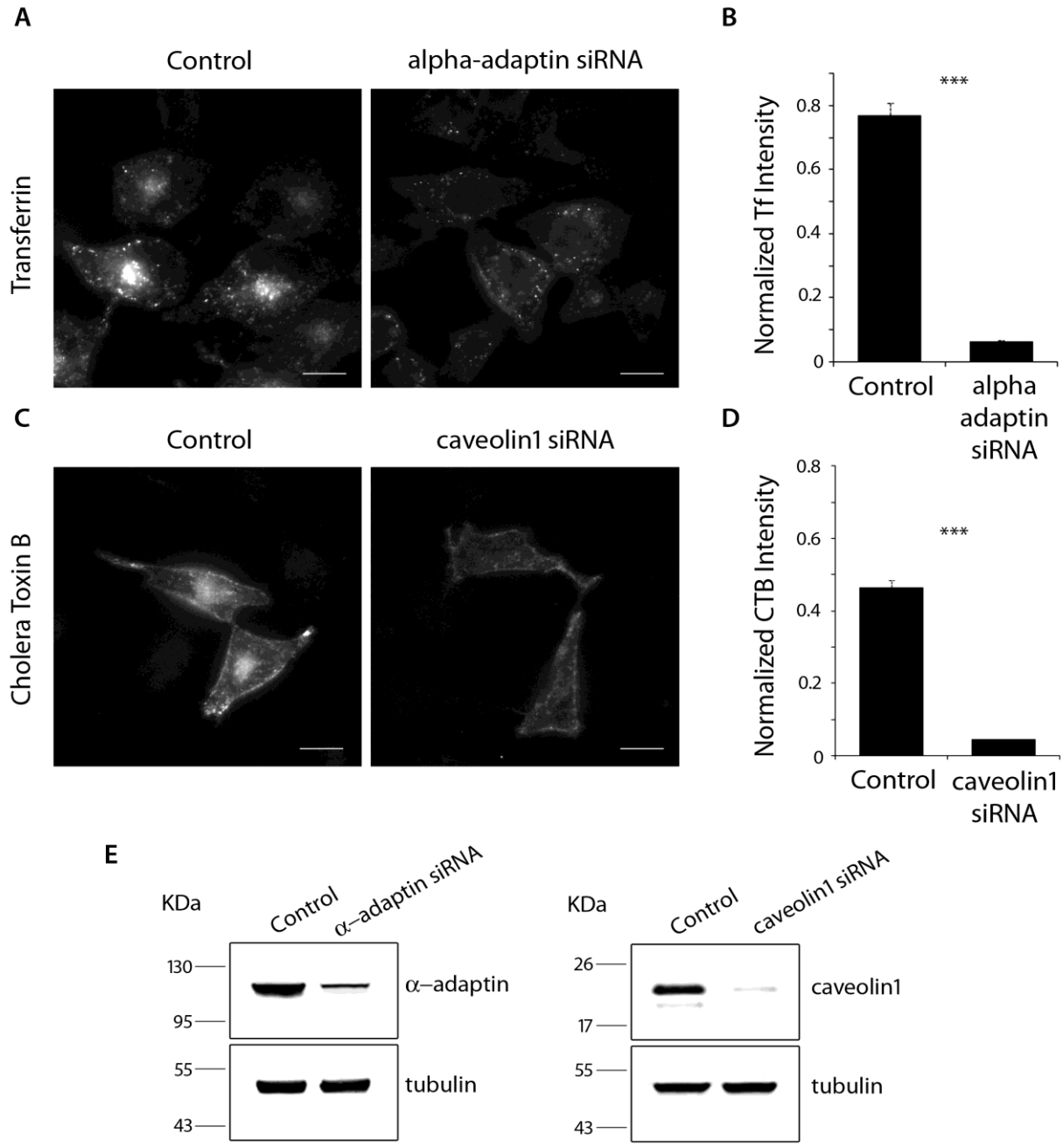

Figure 3.9. Silencing α-adaptin subunit of AP2 complex or caveolin1 expression leads to significant reduction of transferrin or cholera toxin B uptake, respectively

A, **C**. HeLa cells treated with either alpha-adaptin or caveolin1 siRNA were incubated respectively with fluorescent-tagged transferrin or cholera toxin B, then fixed and analyzed in epifluorescence microscopy. siRNA-mediated downregulation of alpha-adaptin expression clearly prevents transferrin uptake and redistribution to intracellular peri-nuclear compartments (A). Similarly, silencing of caveolin1 gene results in inhibition of cholera toxin B internalization (C). Scale bars = 10 µm. **B**, **D**. The experiments in A and C were performed in 24 and 14 cells, respectively, and transferrin/cholera toxin B fluorescence intensity was quantified (mean ± SEM) (*, $p < 0.05$; **, $p < 0.01$; ***, $p < 0.001$). **E**. Western blot analysis of lysates from HeLa cells treated with either alpha-adaptin or caveolin1 siRNA and probed with anti alpha-adaptin or anti-caveolin1 antibody.

B sub-unit (CTxB), a conventional marker of caveolar endocytosis (Pelkmans et al. 2001), demonstrating that downregulation of caveolin1 is an effective strategy to inhibit caveolar endocytosis (Figures 3.9C and 3.9D). Finally, although both siRNA sequences employed in this work have been validated in published studies (Li W. et al. 2012, Motley et al. 2003, Rappoport and Simon 2008), western blot analysis confirmed potent and selective silencing of both α-adaptin and caveolin1 expression by the respective siRNAs, with no effect on negative control proteins (Figure 3.9E).

These inhibitory strategies were used in live-cell imaging studies to identify the endocytosis pathway for FGFR2. HeLa cells expressing FGFR2-GFP and treated either with α-adaptin or caveolin1 siRNA were imaged in confocal microscopy for 30 minutes upon stimulation with FGF2. In addition, a scrambled siRNA, targeting a nonsense sequence, was used as negative control, to discount any indirect effects on FGFR2 trafficking that may result from the siRNA delivery method. As shown in Figure 3.10A, in control condition, the receptor undergoes internalisation from the plasma membrane and eventually traffics to perinuclear compartments (upper panels), demonstrating that scrambled siRNA exhibited no suppressive effect on receptor trafficking. Conversely, α-adaptin siRNA treatment entirely prevented receptor endocytosis, and active FGFR2 remained associated with the cell surface even 30 minutes following FGF2 treatment (lower panels). This is further confirmed by quantification analysis of receptor internalisation (Figure 3.10B), which shows that approximately 80% of the total pool of FGFR2 is still localised at the plasma membrane 30 minutes after ligand stimulation, and by the flat kinetic for FGFR2 uptake in α-adaptin siRNA treated cells in comparison with scrambled siRNA (control) treatment cells. In contrast, downregulation of caveolin1

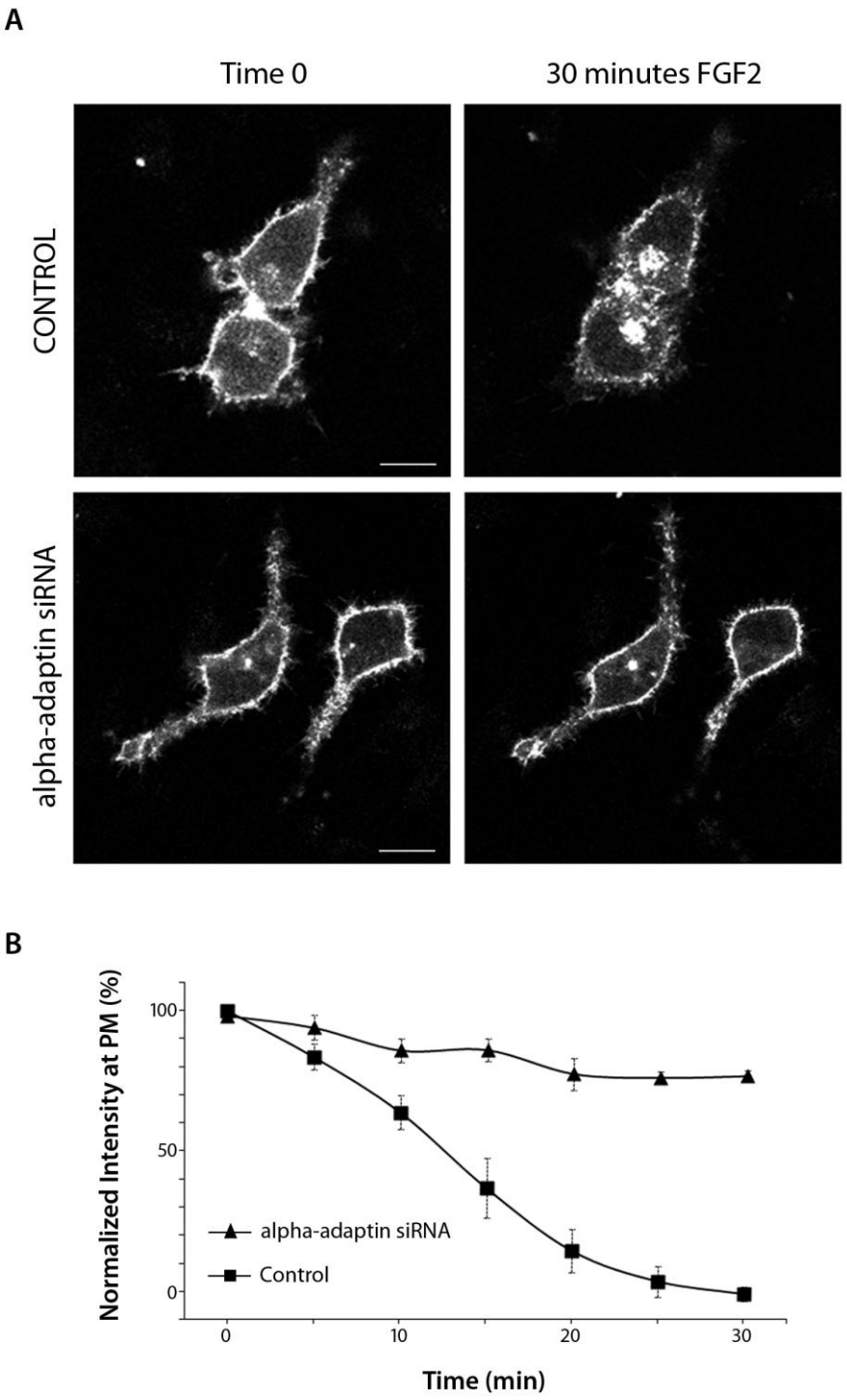

Figure 3.10. Active FGFR2 enters cells through clathrin-mediated endocytosis

A. HeLa cells co-transfected with FGFR2-GFP and alpha-adaptin siRNA (or scrambled siRNA as control) were imaged in confocal microscopy for 30 minutes following stimulation with FGF2. The first (left panels) and the last frame (right panels) of selected time-lapses are shown, corresponding to conditions before and after FGF2 treatment. Silencing alpha-adaptin expression potently blocks FGFR2 endocytosis and consequent redistribution of receptor away from the cell periphery. Scale bars = 10 µm. **B**. The experiment in A was performed in 13 cells and FGFR2-GFP intensity in the PM region of the cells was quantified (as described in Methods) for each frame of the time-lapses and plotted as a function of time (mean ± SEM).

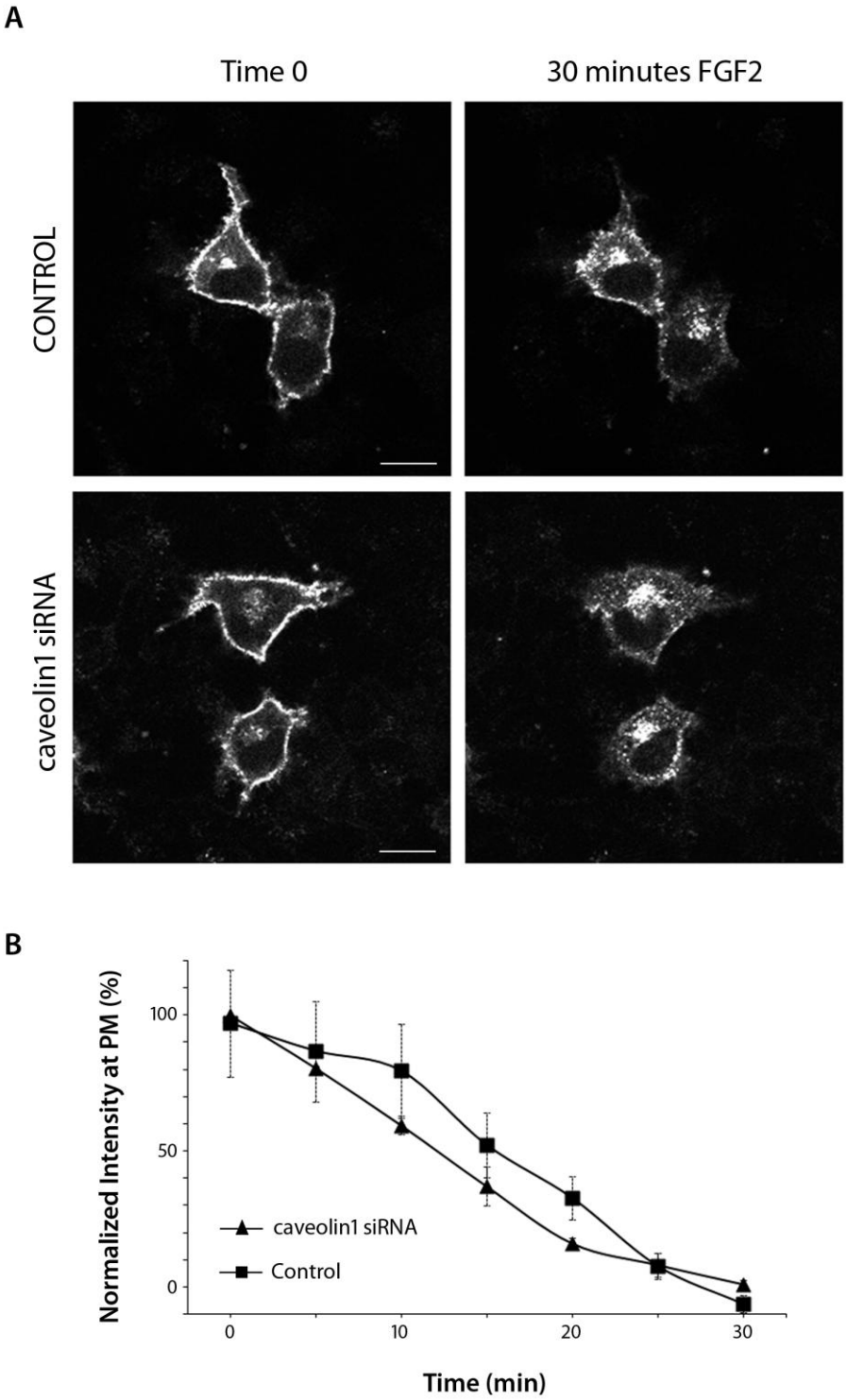

Figure 3.11. FGFR2 endocytosis does not occur via caveolae

A. HeLa cells co-transfected with FGFR2-GFP and caveolin1 siRNA (or scrambled siRNA as control) were imaged in confocal microscopy for 30 minutes following stimulation with FGF2. The first (left panels) and the last frame (right panels) of selected time-lapses are shown, corresponding to conditions before and after FGF2 treatment. Downregulating of caveolin1 expression has no effect on FGFR2 endocytosis, even at longer stimulation times, demonstrating that FGFR2 is not internalised through caveolae. Scale bars = 10 µm. **B**. The experiment in A was performed in 11 cells and FGFR2-GFP intensity in the PM region of the cells was quantified (as described in Methods) for each frame of the time-lapses and plotted as a function of time (mean ± SEM).

expression had no effect on FGFR2 endocytosis (Figure 3.11A) and the kinetic curves for FGFR2 internalisation were similar in absence (control) or presence of caveolin1 (Figure 3.11B). Taken together, these results show that activated FGFR2 enters cells via CME, but not through caveolae.

3.3.3 Active FGFR2 colocalises with clathrin at the plasma membrane but not with caveolin1

In Section 3.2.2, TIRF live-cell imaging to examine FGFR2 dynamics at the plasma membrane showed FGFR2 to form clusters at the plasma membrane in response to ligand stimulation just prior to internalisation. This process is conserved across many different RTKs and ensures that multiple ligand-receptor complexes are concentrated in the same coated pits at the cell surface, and ultimately enclosed and transported into the same coated vesicle. Having demonstrated that endocytosis of FGFR2 proceeds via clathrin, it can be speculated that receptor clustering on the cell surface specifically occurs at sites of CME (and conversely not at caveolae membrane domains). To verify this, colocalisation of activated FGFR2 with known markers for each of these two endocytic pathways was studied. Clathrin and caveolin1, which constitute the vesicle coat proteins, respectively, in clathrin-mediated and caveolar endocytosis (Pearse 1976, Rothberg et al. 1992), have been extensively employed as specific markers for these two internalisation pathways (Damm et al. 2005, Engqvist-Goldstein et al. 2001). To further validate use of the two proteins as markers for CME and entry via caveolae, their distribution at the plasma membrane, along with activated EGFR was investigated by employing dual-colour TIRF microscopy. The uptake of EGFR has been widely studied and it often provides a model for the analysis of receptor-mediated endocytosis. Despite controversial findings about

the specific route of entry, recent works performed in live-cell systems confirmed that EGFR enters cells via clathrin-coated pits, whereas caveolae seem not to be involved in this process (Kazazic et al. 2006, Rappoport and Simon 2009). Consistent with these observations, when HeLa cells co-expressing EGFR-GFP and either clathrin-dsRed or caveolin1-mRFP fusion proteins were stimulated with 100 ng/ml EGF for 15 minutes, striking colocalisation of activated receptor with clathrin was observed, while no colocalisation with caveolin1 was found (Figure 3.12). This result confirms that activated EGFR clusters at the plasma membrane only at sites of clathrin-mediated endocytosis (marked by the presence of clathrin), and not at sites of caveolar endocytosis (marked by caveolin1), further validating the use of these two proteins as markers for the respective endocytosis pathways.

Similar to the EGFR studies, a series of colocalisation analyses were performed between active FGFR2 and either clathrin or caveolin1 to investigate the distribution of FGFR2 at the plasma membrane at sites of clathrin-mediated and caveolar endocytosis, respectively. HeLa cells co-transfected with FGFR2-GFP and clathrin-dsRed or caveolin1-mRFP fusion proteins were stimulated with FGF2 for 15 minutes at 37°C to allow ligand binding and receptor clustering. Cells were then fixed and imaged in TIRF microscopy. An image that represents the phenotype of most of the cells was selected and is represented in Figure 3.13. A high degree of colocalisation (yellow) is detectable between active FGFR2 and clathrin (Figure 3.13A, upper panels), further confirming the potential for clathrin-mediated endocytosis of FGFR2. Despite the significant overlap, a fraction of clathrin can be detected that does not colocalise with FGFR2, consistent with the involvement of clathrin in endocytosis of a variety of other surface receptors. Conversely,

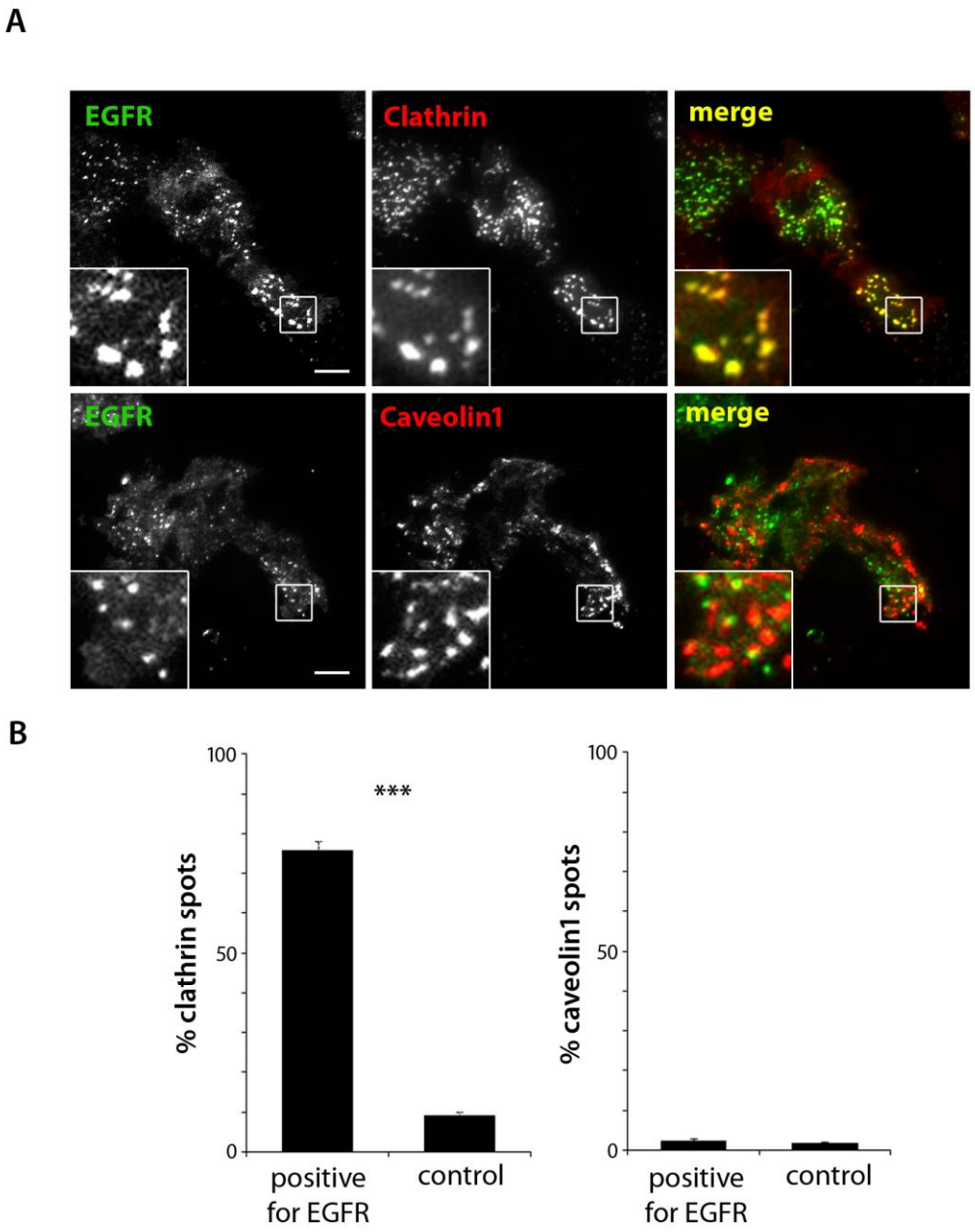

Figure 3.12. Activated EGFR colocalizes with clathrin at the plasma membrane but not with caveolin1

A. HeLa cells co-expressing EGFR-GFP and either clathrin-dsRed (upper panels) or caveolin1-mRFP (lower panels), were incubated with EGF for 30 minutes at 37°C, then fixed and analysed in dual-colour TIRF microscopy. Overlap of EGFR and clathrin/caveolin1 appears in yellow (merge). High-magnification of selected regions from the cells shows clear colocalisation of EGFR with clathrin but not with caveolin1. Scale bars = 5 µm. **B**. Quantification of colocalisation was performed by analyzing the overlapping of clathrin/cavolin1 and EGFR spots. A control of random colocalisation is also shown (mean ± SEM, n = 12 cells) (*, $p < 0.05$; **, $p < 0.01$; ***, $p < 0.001$).

every single FGFR2 spot seems to overlap with clathrin, further suggesting that CME is the only route of entry for FGFR2. This conclusion is confirmed by the absence of any overlap between active FGFR2 and caveolin1 at the plasma membrane (lower panels), demonstrating that caveolae are not involved in internalisation of FGFR2.

Quantitative analysis of colocalisation was also performed. Each FGFR, clathrin and caveolin1 spot was identified and a circle drawn around it. Two spots were identified as colocalising when most of the fluorescence intensity within the circular regions fit in both the red and green channels. Analysis of 25 cells revealed that there was 55% colocalisation of FGFR2 with clathrin, whereas colocalization with caveolin1 resulted in less than 11%. For each experiment, a control of random colocalization was also determined by analyzing a number of circular regions that did not contain FGFR2. As depicted in the graph in Figure 3.13B, this value was statistically indistinguishable from the colocalisation value calculated between FGFR2 and caveolin1. Taken together, these data demonstrate that, upon ligand-mediated activation, FGFR2 colocalises with clathrin at the plasma membrane but not with caveolin1, further confirming that FGFR2 is internalised through clathrin-mediated endocytosis.

3.3.4 Activated FGFR clusters at sites of pre-formed, clathrin-coated pits

CME machinery concentrates receptors, together with other adaptor and accessory proteins, at specific domains of the plasma membrane. These are sites where clathrin polymerises and where membrane invaginates, eventually generating a vesicle. Even

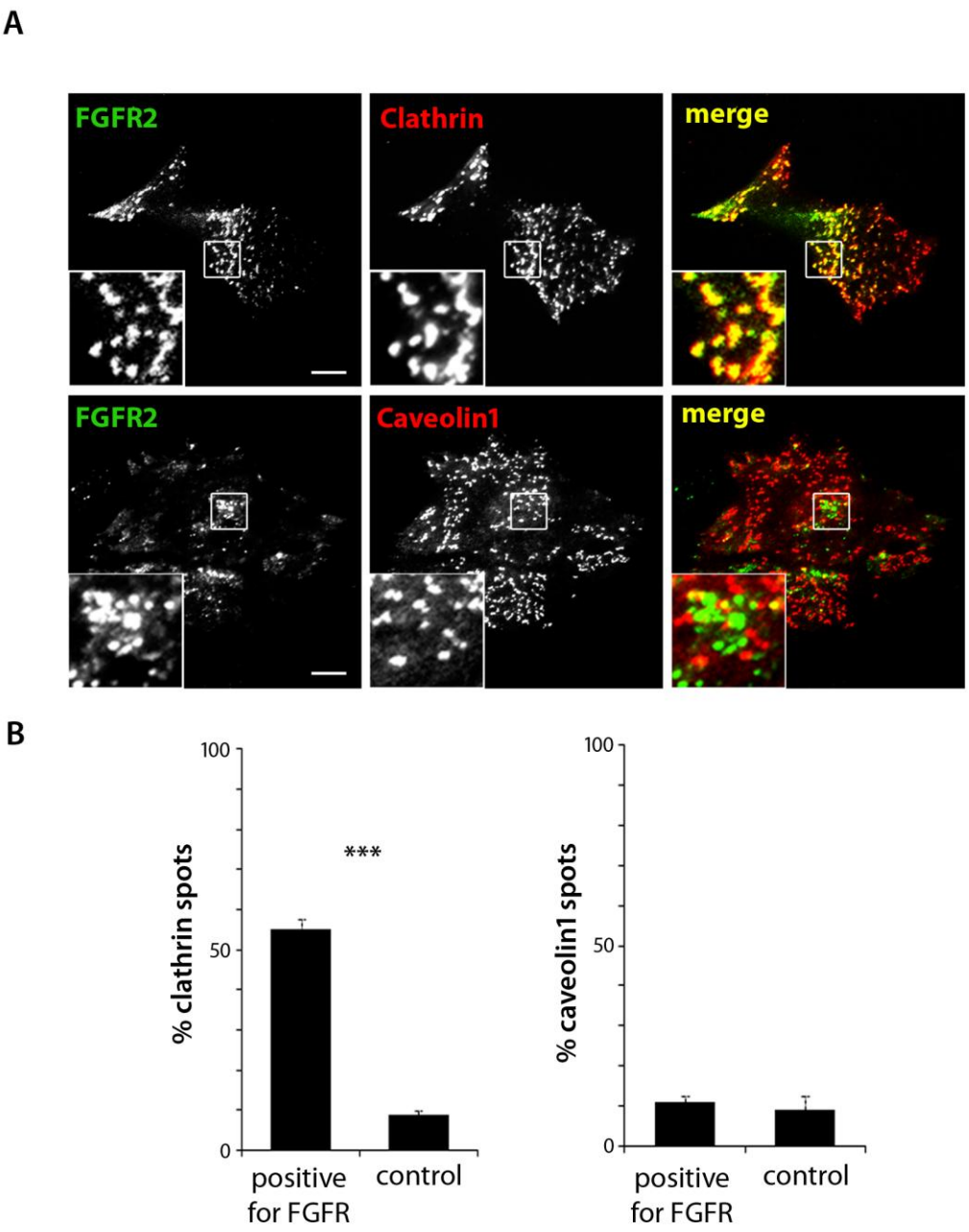

Figure 3.13. Activated FGFR2 colocalises with clathrin at the plasma membrane but not with caveolin1

A. HeLa cells co-expressing FGFR2-GFP and either clathrin-dsRed (upper panels) or caveolin1-mRFP (lower panels), were incubated with FGF2 for 30 minutes, then fixed and analysed in dual-colour TIRF microscopy. High-magnification of selected regions from the cells shows overlay of green and red channels in yellow (merge), revealing that active FGFR2 colocalises with clathrin at the cell surface but not with caveolin1. Scale bars = 5 µm. **B**. Quantification of colocalisation was performed by analyzing the overlapping of clathrin/cavolin1 and FGFR2 spots. A control of random colocalisation is also shown (mean ± SEM, n = 12 cells) (*, $p < 0.05$; **, $p < 0.01$; ***, $p < 0.001$).

though the different stages of clathrin-mediated endocytosis have been extensively described, the exact order of recruitment of different proteins at the sites of CCV formation remains unclear. The striking colocalisation between FGFR2 and clathrin described in Subsection 3.3.3 can be explained by three non-mutually exclusive hypotheses: (1) the receptor can be recruited to sites of pre-formed clathrin at the plasma membrane; (2) CCPs can form where the receptor had previously clustered; and (3) clathrin and FGFR2 can be recruited simultaneously. To determine which of the three hypotheses best describes the dynamics of recruitment of FGFR2 and clathrin at sites of CME, HeLa cells co-expressing clathrin-dsRed and FGFR2-GFP were imaged in dual-colour TIRF microscopy upon FGF2 stimulation. The appearance of FGFR2 spots on the TIRF field relative to the appearance of a colocalising clathrin spot (or vice versa) was analyzed. As shown in Figure 3.14A, in most of the events analyzed, FGFR2 clusters were observed to form at sites of pre-existing clathrin. Clathrin was almost always found to sit on the plasma membrane at sites where the receptor would subsequently be recruited (Figure 3.14 A and B). A very small percentage (12%) of FGFR spots was also observed to appear simultaneously with clathrin. However, this could be due to the low time-resolution of the time-lapses, 1 frame/30 sec: the recruitment of clathrin and receptor at sites of CME might be separated by only a few seconds, seeming simultaneous when watched with a frame rate of 1 frame/30 sec. Interestingly, similar recruitment dynamics have also been observed for EGFR (Rappoport and Simon 2009), suggesting that recruitment to pre-existing CCPs could be a conserved mechanism across RTKs.

Figure 3.14. Activated FGFR2 is recruited at sites of pre-existing clathrin-coated pits

HeLa cells co-expressing FGFR2-GFP and clathrin-dsRed were imaged in simultaneous dual-colour TIRF microscopy (1 frame/30sec) upon stimulation with FGF2 for 15 min. **A**. Quantification analysis of percentage of clathrin-coated pits forming at pre-clustered FGFR2, FGFR2 spots recruited at pre-existing clathrin or FGFR2, and clathrin clustering simultaneously at the plasma membrane. **B**. Selected frames from a time-lapse sequence of two FGFR2 spots (top), two clathrin spots (middle), and merge of the two channels in yellow (bottom). C. Kymographic representation of the time series depicted in (B) showing that activated FGFR2 appears in the TIRF field and colocalises with clathrin which already existed prior to FGF stimulation (mean ± SEM, n = 33 cells) (*, $p < 0.05$; **, $p < 0.01$; ***, $p < 0.001$).

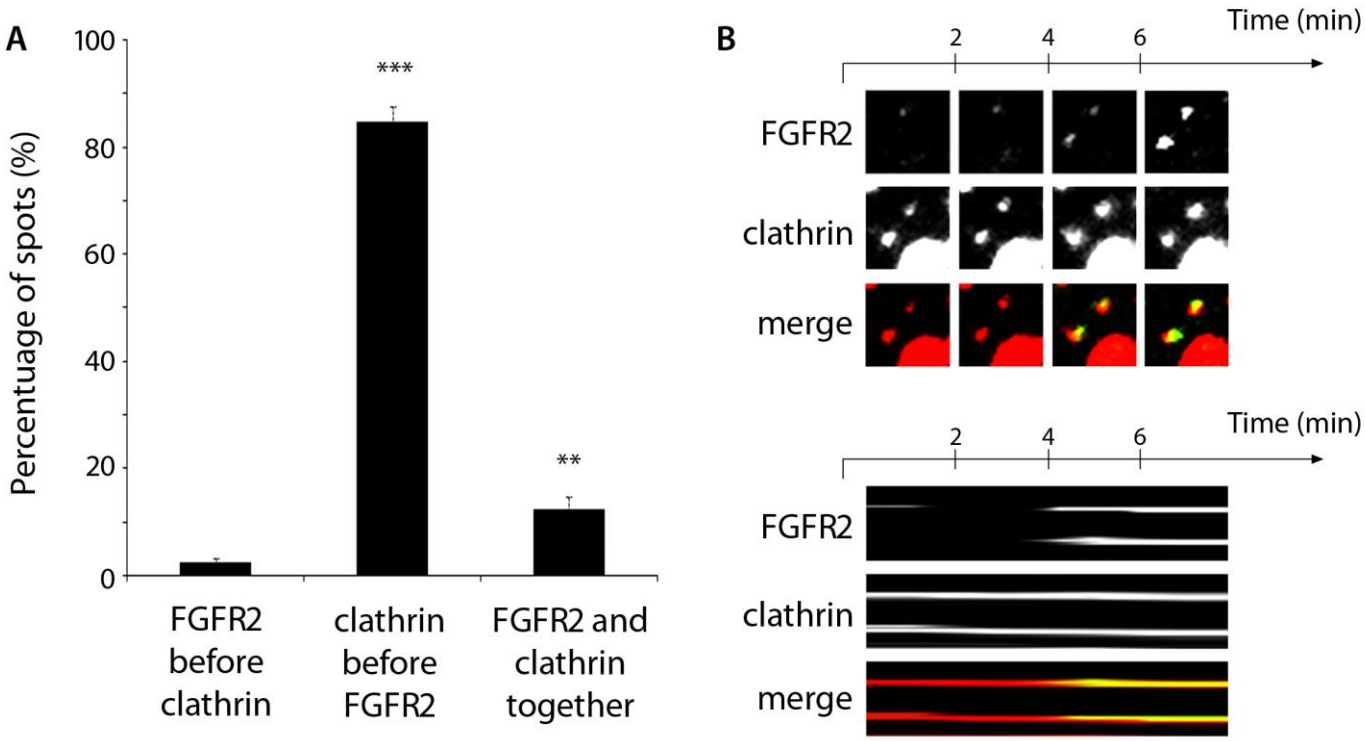

3.3.5 Conclusions

The results presented in this chapter show that FGFR2 is internalised through clathrin-mediated endocytosis. The first evidence of this came from analysis of the involvement of GTPase dynamin in the process of FGFR2 endocytosis. Treatment with the potent dynamin inhibitor Dynasore completely prevented receptor internalisation from the plasma membrane upon ligand stimulation, demonstrating that FGFR2 endocytosis occurs through a dynamin-dependent pathway. Two of the best characterized endocytosis pathways that are dynamin-dependent include clathrin-mediated and caveolar endocytosis. To assess whether activated FGFR2 enters cells through clathrin or caveolae, each of these endocytosis pathways was selectively inhibited by employing an RNAi-based approach. Silencing the expression of α-adaptin, a key component of CME machinery, resulted in impaired FGFR2 endocytosis. Conversely, silencing of caveolin1, the coat protein required for caveolar endocytosis, showed no effect on FGFR2 internalisation. In addition, by employing TIRF microscopy, active FGFR2 was shown to colocalise with clathrin at the cell surface, but not with caveolin1. This indicates that in response to ligand stimulation, the receptor forms clusters at the plasma membrane, specifically at sites of clathrin-mediated endocytosis, and not at caveolae membrane domains, further confirming that that FGFR2 enters cells through clathrin-mediated endocytosis and not through caveolae. Finally, the dynamics of recruitment of FGFR2 and clathrin at sites of CME was investigated and shown to be similar to that already described for other RTK family members: activated receptor accumulates at spots of clathrin that already existed prior to FGF stimulation.

3.4 FGFR signalling promotes CME through Src and Eps8

Internalisation and intracellular trafficking of RTKs through CME depend on their concentration in clathrin-coated pits on the plasma membranes. Therefore, the abundance of available clathrin on the cell surface is an important determinant for regulation of endocytosis. This assumption is further supported by a number of recent studies that directly associate activation of RTKs with an increase in plasma membrane clathrin-coated pits with a subsequent effect on receptor endocytosis. Wilde et al., for instance, showed that activated EGFR causes redistribution of clathrin to the cell periphery and, consequently, promotes EGFR uptake (Wilde et al. 1999). Similarly, nerve growth factor (NGF) has been demonstrated to signal through its receptor (Trk) to induce an increase of clathrin at the plasma membrane and promote clathrin-mediated endocytosis (Beattie et al. 2000). Even though the exact role of this process in the context of RTK has not yet been clarified, it may represent an important regulatory process by which receptors can control the pool of clathrin on the plasma membrane available for endocytosis, therefore modulating internalisation of receptors themselves. One of the goals of this project is to investigate whether a similar regulatory mechanism also controls endocytosis of FGFRs and to identify the effectors involved in this regulatory process.

3.4.1 FGFR2 activation induces recruitment of clathrin at the cell surface and promotes CME

To assess whether FGFR stimulation also caused clathrin redistribution, HeLa cells expressing FGFR2-GFP and clathrin-dsRed were imaged in TIRF microscopy before and 30 minutes after FGF2 stimulation. As depicted in Figure 3.15A, after FGF2 treatment there

was a marked increase in clathrin puncta at the plasma membrane. This increase was quantified in 30 cells (from 3 different experiments): for each cell imaged, a line was manually drawn around the external cell perimeter and the number of clathrin spots per surface area was calculated. In FGF2 treated cells, the average number of puncta per surface area was 203% of the non-treated control cells, a statistically significant result (p = 0.001) (Figure 3.15B). These observations demonstrated that FGF2 stimulation promotes recruitment of new clathrin at the plasma membrane.

To assess whether FGF2 signals through its receptor FGFR2 to induce this clathrin redistribution, cells were pre-treated with FGFR kinase inhibitor SU5402 and clathrin puncta were quantified before and after FGF2 stimulation, as described above. Quantification analysis is shown in Figure 3.15B and demonstrates that when receptor kinase activity is impaired, ligand stimulation fails to induce clathrin redistribution at the cell surface, indicating that FGF2 binds and activates FGFR2 to promote recruitment of new clathrin at the plasma membrane. Interestingly, the steady-state level of clathrin in non-stimulated cells does not appear to be altered by SU5402 treatment, suggesting that basal FGFR2 signalling does not regulate CME.

The next step was to define the biological role of the increase of plasma membrane clathrin-coated pits induced upon FGF2 stimulation. One possible scenario is that this new pool of clathrin is recruited from the cytoplasm to the cell surface to be employed in receptor endocytosis. To verify this, HeLa cells cotransfected with FGFR2-GFP and clathrin-dsRed were imaged in live-cell TIRF microscopy at a rate of 5 frames/second for 120 seconds before and 30 minutes after ligand addition. The density of endocytic events before and after FGF2 stimulation was quantified by counting the number of clathrin

spots disappearing from the TIRF field during each 120-second time-lapse. The analysis clearly showed a significant increment in the density of endocytosis events after FGF2 treatment (Figure 3.16A), confirming that the clathrin-coated pits recruited at the cell surface following ligand stimulation were actively involved in clathrin-mediated trafficking.

To further confirm this, the effect of FGF2 treatment on endocytosis of transferrin, a specific validated marker of clathrin-mediated endocytosis (Hanover et al. 1984), was examined. Unexpectedly, FGF2 stimulation did not result in an increase in transferrin uptake (Figure 3.16B), suggesting that the increased clathrin puncta undergoing endocytosis upon FGFR2 activation may represent a cargo-specific population of clathrin-coated pits.

Finally, to exclude that this effect was cell-line specific or due to overexpression conditions in our model system, similar studies were performed in cells endogenously expressing FGFR2, specifically LNCaps (Carstens et al. 1997). Even in the absence of expression of GFP-tagged FGFR2, FGF2 stimulation resulted in a similar increase in plasma membrane clathrin spot number (Figure 3.17).

Thus, these data demonstrated that, similar to other members of the RTK family, activated FGFR2 promotes recruitment of new clathrin at the plasma membrane, which in turn is required for CME.

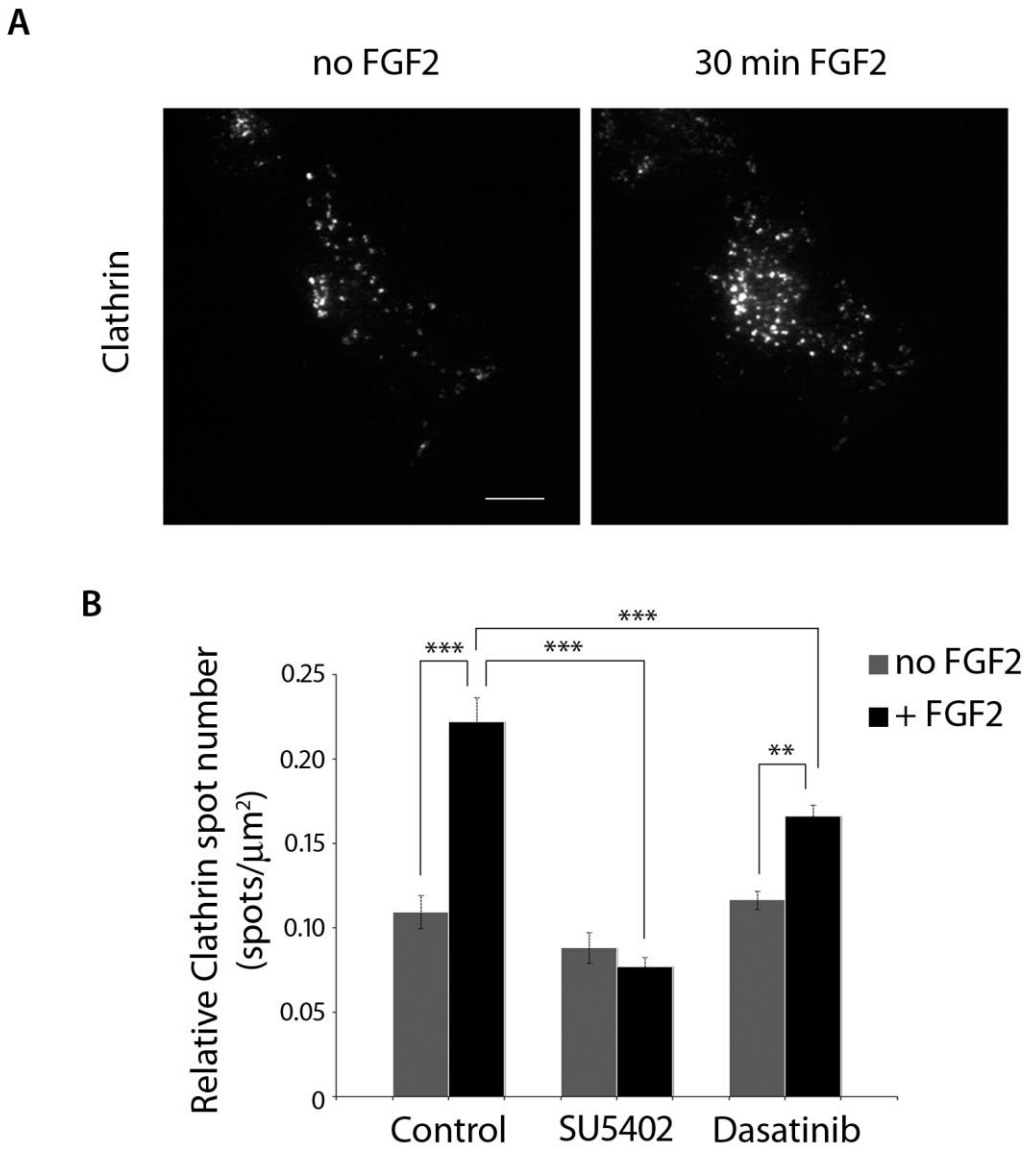

Figure 3.15. Activated FGFR2 signals through Src to promote an increase of CCPs at the plasma membrane

HeLa cells transiently transfected with FGFR2-GFP and clathrin-dsRed, and pre-incubated in the presence (or absence) of SU5402 or dasatinib were imaged in TIRF microscopy before and 30 minutes after ligand stimulation. **A**. Incubation with FGF2 induces a significant increase in the number of clathrin puncta at the plasma membrane. Scale bars = 5 µm. **B**. Quantification analysis of clathrin spot number normalised to cell surface area for the conditions described above reveals that the FGFR2-dependent increase of clathrin at the plasma membrane is Src-dependent and requires the kinase activity of the receptor (mean ± SEM; n = 30 cells for each condition in (B) (*, $p < 0.05$; **, $p < 0.01$; ***, $p < 0.001$).

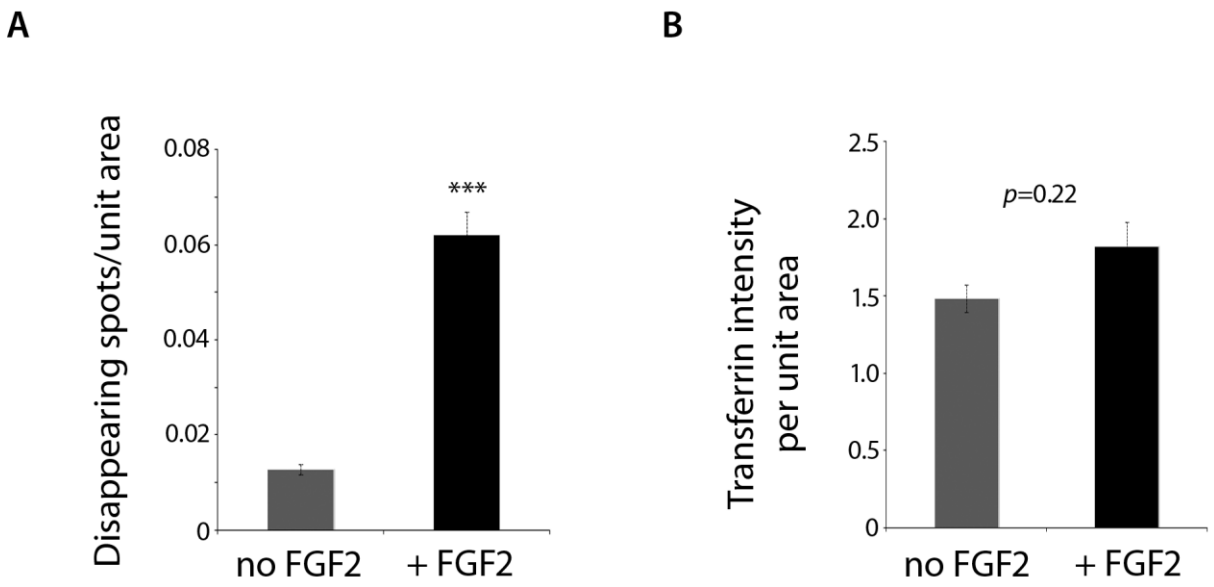

Figure 3.16. FGF2 treatment promotes clathrin-mediated endocytosis but does not result in an increase in transferrin uptake

A. HeLa cells co-expressing FGFR2-GFP and clathrin-dsRed were imaged in live-cell TIRF microscopy at 37°C for 2 minutes (5 frame/sec) before and 30 minutes after FGF2 stimulation. The experiment was performed in 24 cells and the total number of clathrin spots disappearing from the TIRF field was calculated, revealing a significant increment in the density of endocytosis events upon FGF2 addition. **B**. FGFR2-GFP expressing HeLa cells were incubated with transferrin-AlexaFluor546 and either stimulated with FGF2 or non-stimulated (control). The experiment in A was performed in 49 cells and transferrin fluorescence intensity was quantified (as described in Methods), showing that FGF2 stimulation does not induce an increase in transferrin uptake (mean ± SEM) (*, $p < 0.05$; **, $p < 0.01$; ***, $p < 0.001$)

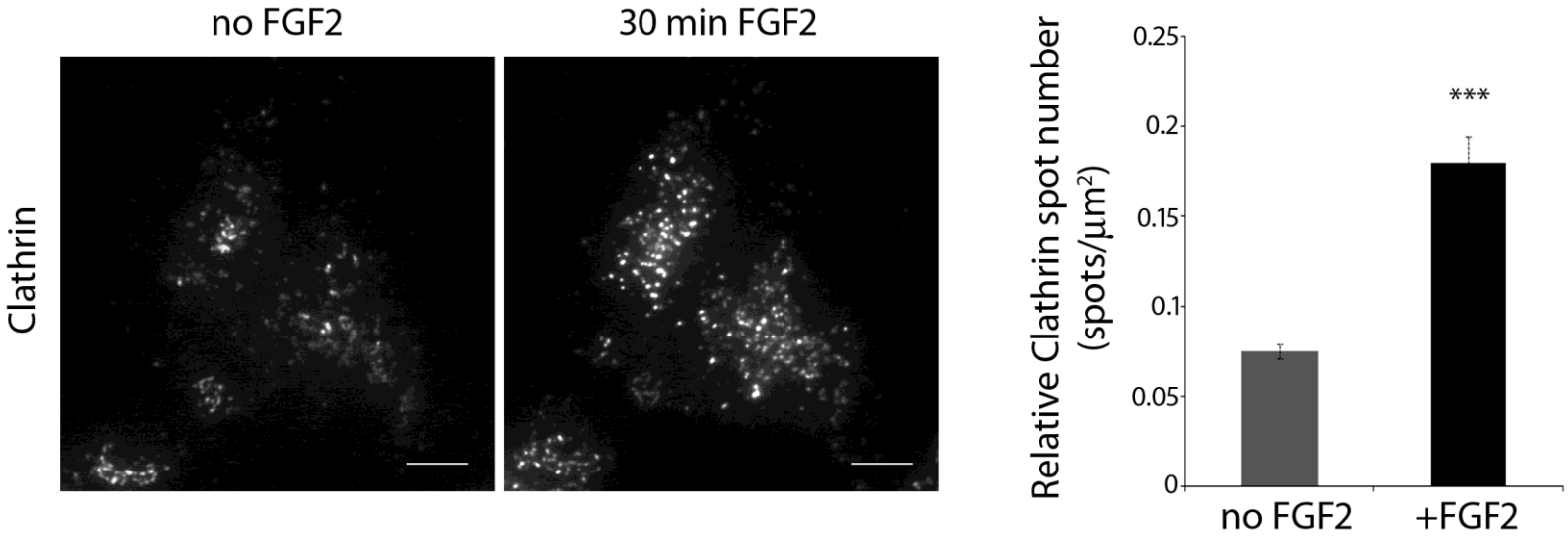

Figure 3.17. FGF2-dependent redistribution of CCPs at the cell surface in FGFR2-expressing LNCaP cells

A. LNCap cells endogenously expressing FGFR2 and transfected with clathrin-dsRed were imaged in TIRF microscopy before and 30 minutes after ligand stimulation. Incubation with FGF2 induces a clear increase in the number of clathrin spots at the plasma membrane. Scale bars = 5 µm. **B**. Quantification analysis of clathrin puncta before and after FGF stimulation confirms that the redistribution of clathrin at the cell surface induced by FGFR2 activation is not cell-line specific, and can occur via signalling through endogenous FGFR2 (mean ± SEM; n = 45 cells) (*, $p < 0.05$; **, $p < 0.01$; ***, $p < 0.001$).

3.4.2 FGF-dependent increase in CME is mediated by Src and Eps8

After demonstrating that FGFR2 signalling has a direct effect upon endocytic machinery by inducing clathrin redistribution, the involvement of effector molecules with a role in this regulatory feedback was investigated. The protein kinase Src is one of the candidate molecules having specific function in this mechanism of regulation. Wilde et al. in fact identified Src as responsible for regulating the cellular distribution of clathrin upon EGFR activation (Wilde et al. 1999). In addition, recently, Src has clearly emerged as one of the key downstream effectors in the FGFR signalling cascade, with implications for its role as a regulatory factor in FGFR trafficking. To investigate the role of Src in FGFR-dependent redistribution of clathrin, HeLa cells co-expressing FGFR2-GFP and clathrin-dsRed were treated with the Src family kinase (SFK) inhibitor Dasatinib and imaged in TIRF microscopy before and 30 minutes after FGF2 stimulation. Quantification analysis of clathrin puncta (Figure 3.15B) revealed that Dasatinib treatment significantly inhibits the increment in clathrin spots number upon FGFR2 stimulation, demonstrating that SFKs play a role in this process. Interestingly, Dasatinib treatment did not cause complete inhibition of clathrin recruitment, and a partial increase in plasma membrane clathrin-coated pits (around 30%) could still be observed. However, this result is consistent with the presence of alternative pathways downstream of FGFR2 that bypass Src involvement; thus, FGFR2 appears to signal through both Src-dependent and Src-independent pathways to regulate plasma membrane distribution of clathrin. Further, the basal level of clathrin puncta in non-stimulated conditions does not appear to be altered by Dasatinib treatment, suggesting that Src activity is not required for constitutive endocytosis.

As discussed in Section 1.4.2, active Src plays a key role in regulating FGFR2 transport to and from the plasma membrane (Sandilands et al. 2007). In characterizing targets for Src kinase with a role in the regulation of FGFR signalling and trafficking, Cunningham et al. recently identified a set of putative proteins (Cunningham et al. 2010). Among these, the multifunctional scaffold protein Eps8 was particularly interesting, since it has been shown to participate in CME (Taylor et al. 2011), in EGFR trafficking and signalling (Lanzetti et al. 2000), and in actin dynamics (Provenzano et al. 1998). Consistent with these observations and to further investigate the mutual relation between FGFR and Src, a series of TIRF studies was performed to assess whether Eps8, along with Src, was also responsible for regulating the distribution of clathrin upon FGFR2 activation. HeLa cells expressing FGFR2-GFP and clathrin-dsRed were treated with siRNA targeting Eps8, and the effect on FGF-dependent clathrin redistribution at the cell surface was examined. As depicted in Figure 3.18A, Eps8 silencing entirely prevented the increase in clathrin puncta at the plasma membrane upon FGFR activation. Importantly, the siRNA sequences used in this study were already employed and validated in the literature (Disanza et al. 2006). In addition, western blot analysis confirmed potent silencing of Eps8 expression without affecting the levels of negative control protein, tubulin (Figure 3.18B). Therefore, the recruitment of new clathrin at the plasma membrane is promoted by activated FGFR2 signalling though Src and Eps8.

Finally, to further confirm the role of Eps8 in CME, a series of biochemical studies were performed. Coimmunoprecipitation analyses revealed that Eps8 interacts with clathrin heavy chain, α-adaptin and dynamin2, all members of the endocytosis machinery (Doherty and McMahon 2009) (Figure 3.19A). Interestingly, similar results were also

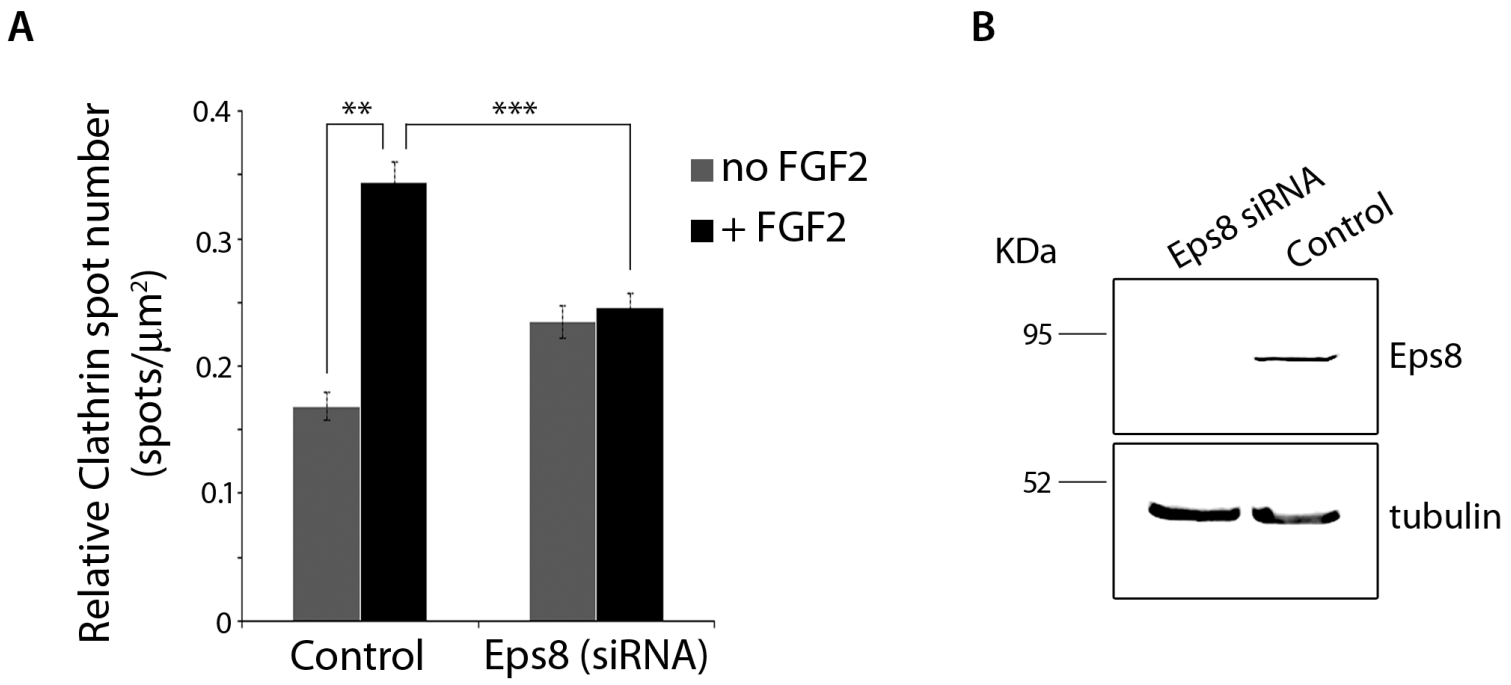

Figure 3.18. Activated FGFR2 signals through Eps8 to promote an increase of CCPs at the plasma membrane

HeLa cells transiently transfected with FGFR2-GFP and clathrin-dsRed and treated with siRNA against Eps8, were imaged in TIRF microscopy before and 30 minutes after ligand stimulation. **A**. Quantification analysis of clathrin spot number normalised to cell surface area for the conditions described above reveals that the FGFR2-dependent increase of clathrin at the plasma membrane is Eps8-dependent (mean ± SEM; n = 24 cells (*, $p < 0.05$; **, $p < 0.01$; ***, $p < 0.001$). **B**. Cellular extracts from HeLa cells treated with Eps8 siRNA were resolved by SDS-PAGE and analysed by immunoblotting with anti-Eps8 antibody (blot representative of 3 experiments).

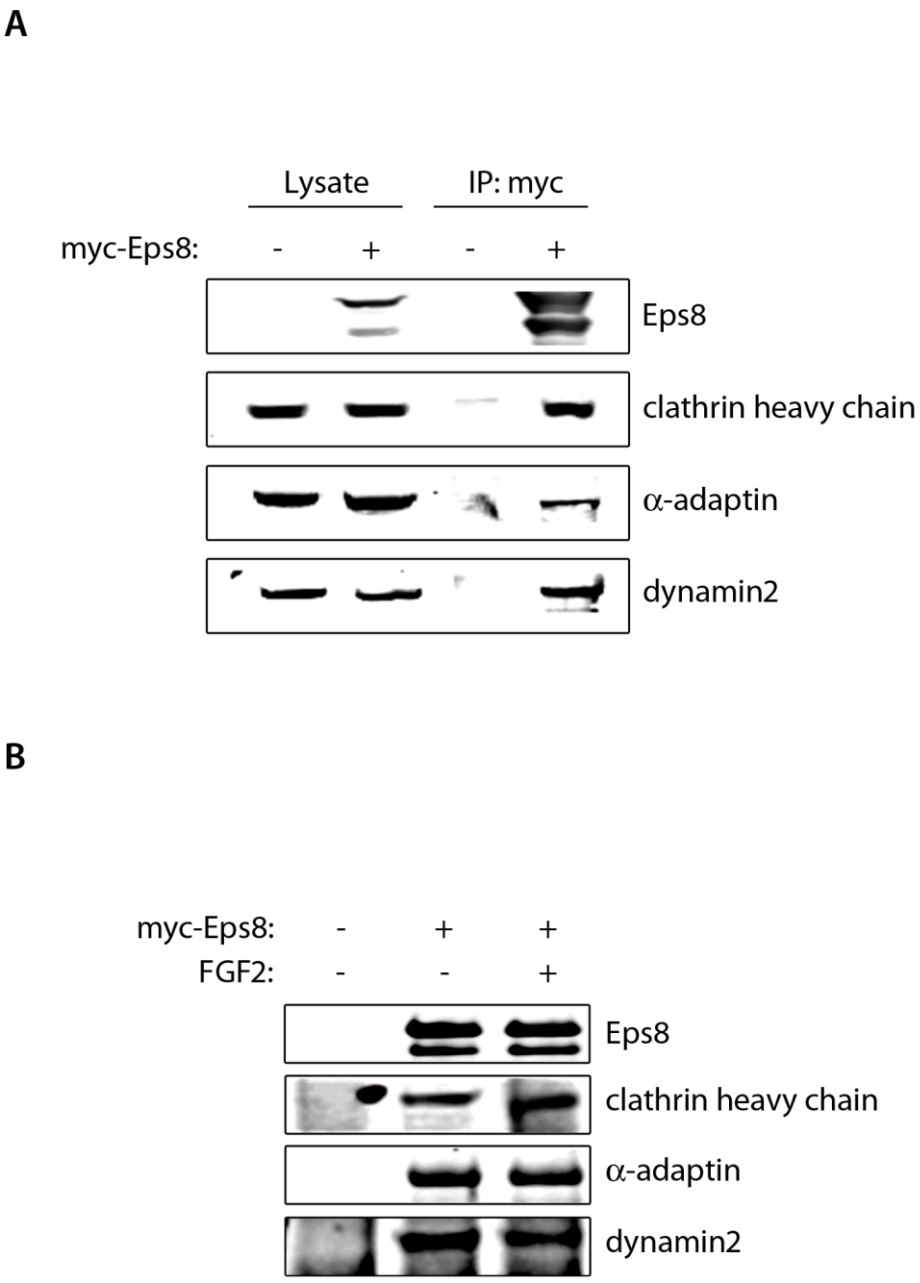

Figure 3.19. Eps8 interacts with AP2, clathrin and dynamin.

A. Cellular extracts from HeLa cells transiently overexpressing myc-Eps8 (where indicated) were immunoprecipitated with anti-myc antibody, resolved by SDS-PAGE and analysed by immunoblotting for the levels of specified proteins. **B**. Cellular extracts from HEK283T cells transiently transfected with myc-Eps8 (where indicated) were stimulated or not with FGF2, immunoprecipitated with anti-myc antibody, resolved by SDS-PAGE and analysed by immunoblotting for the levels of specified proteins.

obtained in HEK293, the cell line used to originally identify the connection between FGFR, Src and Eps8 (Cunningham et al. 2010) (Figure 3.19B). These findings demonstrate that Eps8 is incorporated into an endocytic machinery together with other key proteins, further confirming its role during the early phases of FGFR2 trafficking.

3.4.3 Conclusions

In this chapter, a novel mechanism of regulation of FGFRs trafficking was described. Using high-resolution TIRF microscopy, FGF2 was shown to signal through FGFR2 regulation of clathrin redistribution at the cell surface. As shown in Figure 3.15, FGF stimulation is sufficient to induce an increase in CCPs at the plasma membrane, and this process appears to be dependent on FGFR2 kinase activity. Since a similar phenomenon was observed for other members of RTKs, including EGFR (Wilde et al. 1999), Trk (Beattie et al. 2000), and IR (Corvera 1990), this may represent a mechanism conserved within the RTK family.

Clathrin exists as a heterogeneous population when in association with the plasma membrane: a small portion is actively involved in formation of clathrin-coated vesicles; the vast majority of clathrin, however, constitutes a static pool which is not immediately involved in CME (Rappoport et al. 2006). It is possible that the new clathrin recruited at the cell surface following FGFR2 activation may constitute the ‘dynamic’ pool. In such case, FGF-dependent activation of FGFR2 would result in an incremental CME process, generating a mechanism for regulating receptor trafficking. This hypothesis was validated by looking at the density of endocytosis events occurring at the cell surface upon FGF2 stimulation. As illustrated in Figure 3.16A, FGFR2 activation increases not only the number of CCPs at the plasma membrane, but also the number of CME events,

demonstrating that downstream FGFR signalling has a direct effect on endocytosis machinery. Interestingly though, FGFR2 activation had no effects on transferrin uptake (Figure 3.17B), suggesting that the CCPs recruited upon FGFR2 activation may represent a cargo-specific population. Although further investigation is needed, these observations may imply that the route of entry for activated RTKs is a cargo-specific pathway, which would be an entirely new scenario in the context of receptor-mediated, clathrin-mediated endocytosis. The results set forth in this chapter also show involvement of Src protein kinase in FGFR-dependent peripheral accumulation of clathrin. This finding is not surprising, as Src activity has already been implicated in the regulation of cellular distribution of clathrin upon activation of other growth factor receptors, such as EGFR. In line with these observations, and given the key role that Src plays in the FGFR signalling pathway, inhibition of Src kinase activity was shown to prevent increase in CCP number following FGFR2 activation (Figure 3.15B).

In a recent proteomic study (Cunningham et al. 2010), the scaffold protein Eps8 was identified as a target of Src kinase activity in response to FGFR2 activation. In the present study it was shown that Eps8, along with Src, plays a role in the FGFR2-dependent redistribution of CCPs at the cell surface, as downregulation of Eps8 expression by siRNA inhibits the increment of clathrin puncta at the plasma membrane (Figure 3.18). Furthermore, FGFR2 signalling through Src to Eps8 was shown to regulate distribution of CCPs at the plasma membrane and consequently to promote clathrin-mediated endocytosis. Finally, Eps8 was shown to interact with the CME machinery (Figure 3.19), further supporting its role in the early phases of FGFR2 endocytosis.

At present, the molecular mechanism by which Src and Eps8 mediate clathrin redistribution is not clear. As mentioned in the Introduction, Eps8 in the context of RTKs functions as scaffold protein for a number of signalling molecules, coordinating different signalling cascades. It would be interesting to determine whether regulation of clathrin redistribution observed upon FGFR2 activation also depends on additional signalling and adaptor molecules recruited by phosphorylated Eps8. In particular Rab5, whose function has already been associated with Eps8 (Lanzetti et al. 2000) is an interesting candidate, as it has been implicated in regulation of CME machinery (Bucci et al. 1992), and in the FGFR2 signal transduction pathway (Vecchione et al. 2007).

3.5 Regulation of FGFR2 trafficking and signalling through Src and Eps8

As described in detail in Section 1.4.2, Src and RTKs, the non-receptor tyrosine kinase Src is one of the main effectors downstream of FGFR, and it has been implicated as a key regulatory factor with both positive and negative roles in activation and termination of FGFR signalling. In addition, the first line of evidence suggesting a role for Src in the regulation of FGFR trafficking recently came from Sandilands et al., in which the kinase was shown to also control the transport of FGFR to and from the plasma membrane (Sandilands et al. 2007). In such a scenario, it may be speculated that Src-dependent regulation of receptor trafficking can in turn affect downstream signalling output, and that Src may be a key intermediate that operates at the crossroads of signalling and trafficking of FGFRs. In this chapter, the involvement of Src activity in the regulation of endocytosis and trafficking of FGFR2 is further investigated, providing new supporting evidence for reciprocal crosstalk between FGFR2 signalling and trafficking. Further, given identification of Eps8 as a target of Src-mediated phosphorylation in the FGFR signalling cascade (Cunningham et al. 2010) and its function in clathrin-mediated endocytosis of FGFR2, the potential role of Eps8 in regulating FGFR2 signalling and the early phases of endocytic receptor trafficking was also investigated.

3.5.1 Src kinase activity regulates early endocytic trafficking of FGFR2

The data described in Section 3.4 suggest a role for Src in the early phases of FGFR2 clathrin-mediated endocytosis. To further validate this observation, the effect of Src kinase activity inhibition on internalisation and trafficking of activated FGFR2 was studied. Chemical inhibition of Src activity was obtained using the selective Src family kinase (SFK) inhibitor Dasatinib (Lombardo L. J. et al. 2004), which has been previously shown to block

Src-mediated FGFR signalling and trafficking processes (Sandilands at al. 2007). In the presence of ligand, cells treated with the SFK inhibitor showed impaired receptor internalisation: following 30 minutes of stimulation, over 75% of the total amount of receptor was not endocytosed and still localised at the plasma membrane (Figure 3.20A and B). Src inhibition also affected the intracellular trafficking of FGFR2: higher magnifications of cells incubated with ligand for 30 minutes show that in Dasatinib treatment condition, the pool of internalised FGFR2 atypically and statically localises in peripheral compartments rather than in perinuclear regions, suggesting a role for Src in regulating early endocytic trafficking of activated FGFR2 (Figure 3.20A). To confirm these results, super-resolution confocal microscopy studies were also performed, providing detail at a resolution smaller than 50 nm. As shown in Figure 3.20C, super-resolution imaging of activated FGFR2-GFP in Dasatinib-treated cells revealed the clear presence of FGFR2-positive puncta localised in a peripheral endocytic compartment, confirming the role of Src in early endocytic trafficking of FGFR2.

3.5.2 Role of Eps8 on endocytic trafficking of FGFR2

Given the established role of Eps8 as a Src-dependent effector in FGFR signalling (Cunningham et al. 2010) and its importance in regulating redistribution of clathrin at the plasma membrane upon FGFR2 activation, the next step was to elucidate the role of this scaffold protein in FGFR2 trafficking. To do so, we monitored the effect of knocking down Eps8 gene expression on FGFR2 internalisation by using the established receptor trafficking assay. A new cell line with stable Eps8 shRNA expression was employed in

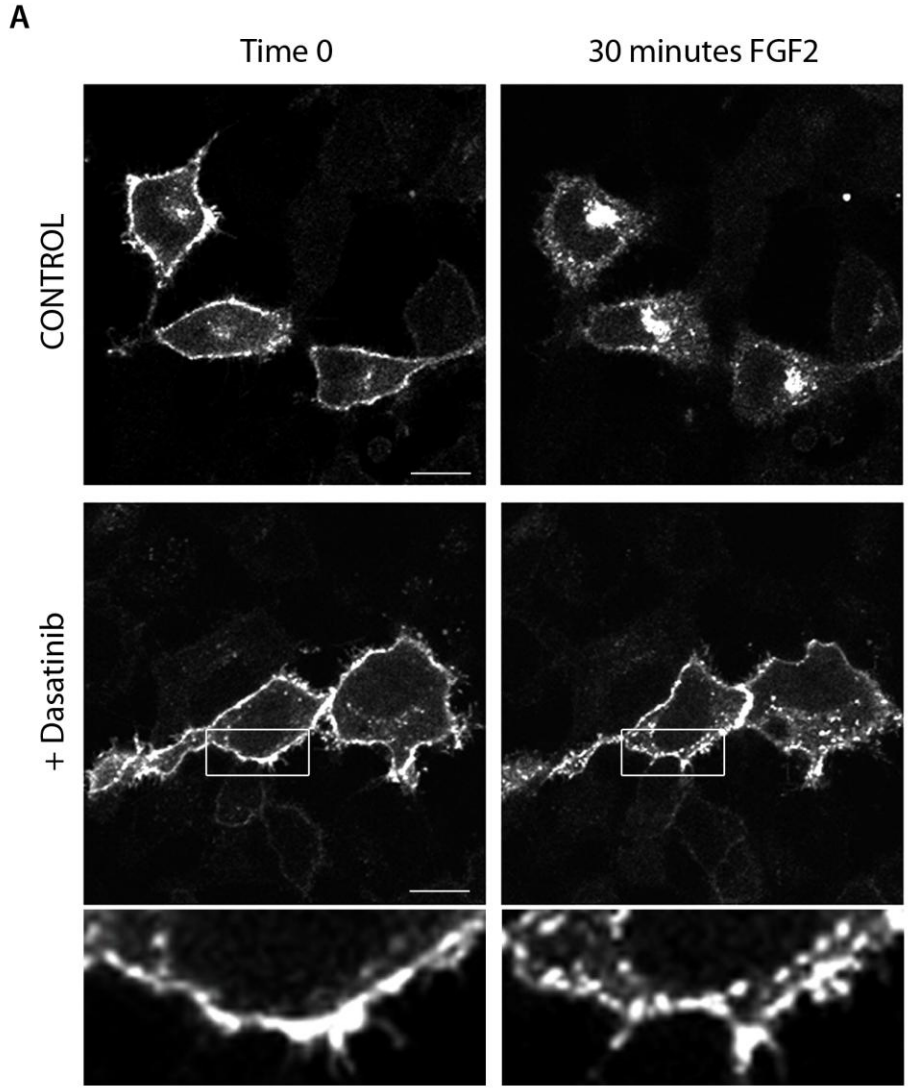
A
Time 0
30 minutes FGF2
CONTROL
+ Dasatinib

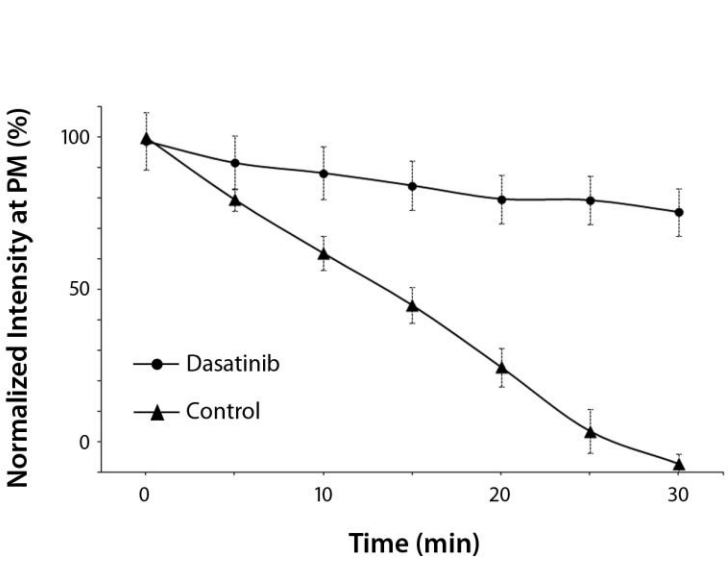
B
Normalized Intensity at PM (%)
100
50
0
Dasatinib
Control
0
10
20
30
Time (min)

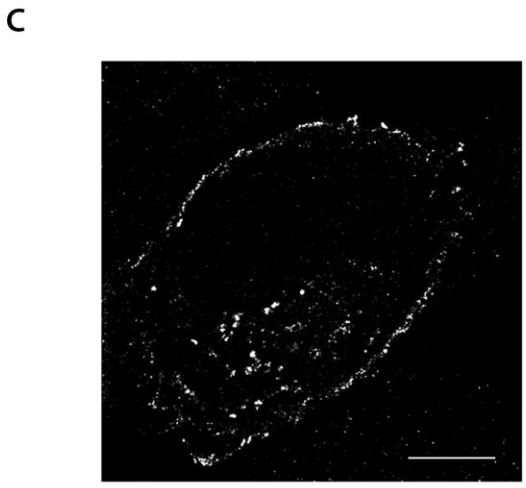
C

Figure 3.20. Src kinase activity is required for FGFR2 trafficking

A. HeLa cells transiently transfected with FGFR2-GFP and incubated for 30 minutes in the presence (lower panels) or absence (control, upper panels) of SFK inhibitor dasatinib were imaged in confocal microscopy for 30 minutes following FGF2 stimulation. The first (left panels) and last frame (right panels) of the time-lapse are shown, corresponding to conditions before and after FGF2 treatment, respectively. While in control cells activated FGFR2 undergoes efficient internalisation from the plasma membrane, dasatinib treatment prevents receptor endocytosis and trafficking toward peri-nuclear compartments. Higher magnifications of dasatinib-treated cells show that when Src activity is impaired, activated FGFR2 atypically and statically localises in the peripheral compartment rather than in peri-nuclear regions. Scale bars = 10 µm. **B**. The experiment in A was performed in 10 cells and FGFR2-GFP intensity in the PM region of the cells was quantified (as described in Methods) for each frame of the time-lapses and plotted as a function of time (mean ± SEM). **C**. Analysis of dasatinib-treated cells in super-resolution confocal microscopy reveals the presence of FGFR2-positive puncta localised in a peripheral endocytic compartment. Scale bars = 4 µm.

these studies. Although this Eps8 knock-down cell line was already validated in the literature (Disanza et al. 2006), western blot analysis was performed, confirming potent and selective silencing of Eps8 expression (Figure 3.21C). When FGFR2-GFP expressing Eps8 shRNA were stimulated with FGF2 ligand for 30 minutes, significant attenuation of receptor internalisation and trafficking toward perinuclear regions was observed (Figure 3.21A). Interestingly, similar to Src inhibitor treated cells, FGFR2 containing vesicles that did not leave thecell periphery were also observed upon ligand stimulation (Figure 3.21A). Further, quantification analysis of FGFR2 internalisation revealed that the effect of Eps8 silencing was not evident during the earliest phases of receptor trafficking, suggesting a potential role for Eps8 in regulating FGFR2 sorting through early endocytic compartments rather than the process of internalisation itself (Figure 3.21B). Thus, inhibition of Src and downregulation of Eps8 expression produce similar effects on FGFR2

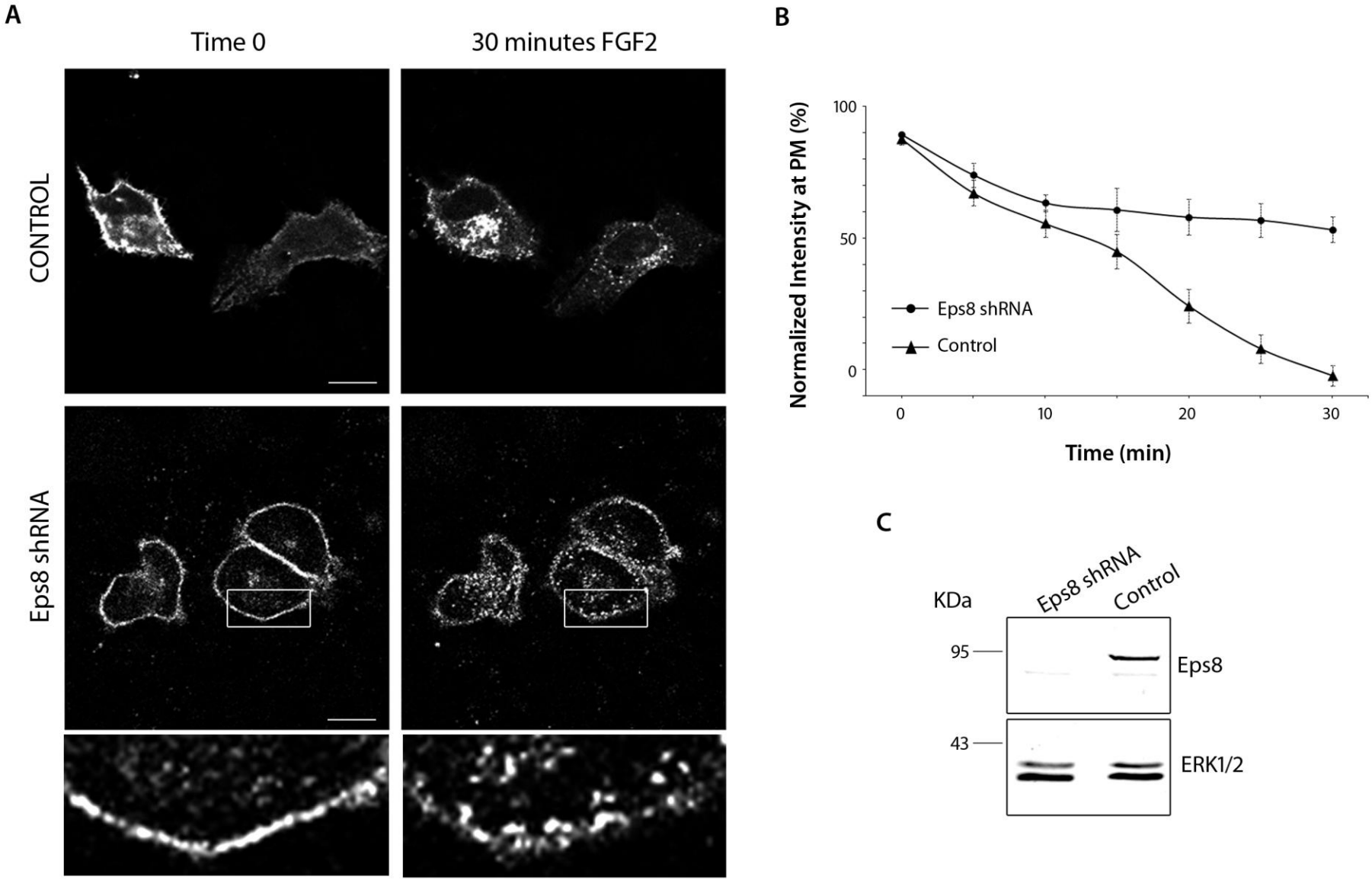
A
Time 0
30 minutes FGF2
CONTROL
Eps8 shRNA
B
Normalized Intensity at PM (%)
100
50
0
Eps8 shRNA
Control
0
10
20
30
Time (min)
C
KDa
Eps8 shRNA
Control
95
Eps8
43
ERK1/2

Figure 3.21. Silencing of Eps8 impairs FGFR2 trafficking

A. Eps8 knock-down HeLa cells (Eps8 shRNA) transiently transfected with FGFR2-GFP were imaged in confocal microscopy for 30 minutes following FGF2 stimulation. The first (left panels) and the last frame (right panels) of the time-lapse are shown, corresponding to conditions before and after FGF2 treatment, respectively. Similarly to dasatinib treatment, the absence of Eps8 prevents receptor internalisation and its trafficking toward peri-nuclear compartments. Higher magnifications of Eps8 knock-down cells show atypical peripheral localisation of FGFR-containing vesicles, suggesting a role for Eps8 in early endocytic trafficking of FGFR2. Scale bars = 10 µm. **B**. The experiment in A was performed in 8 cells, and FGFR2-GFP intensity in the PM region of the cells was quantified (as described in Methods) for each frame of the time-lapses and plotted as a function of time (mean ± SEM). **C**. Cellular extracts from Eps8 knock down (shRNA) or control vector (control) HeLa cells were resolved by SDS-PAGE and analysed by immunoblotting with anti-Eps8 antibody (blot representative of 3 experiments).

trafficking, further confirming a connection between Src kinase activity and Eps8 in the context of FGFR2 endocytosis.

Once established that Eps8 plays a role in regulating FGFR2 trafficking within a peripheral endocytic compartment, subcellular localisation of Eps8 action on the endocytic trafficking of FGFR2 was investigated. HeLa cells co-expressing FGFR2-GFP and Eps8-mCherry were imaged in dual-colour confocal microscopy at various times upon FGF2 stimulation. As shown in Figure 3.22A, in the absence of ligand, both Eps8 and FGFR2 localise in proximity to the plasma membrane. Interestingly, Eps8 staining revealed punctate structures, suggesting that Eps8 is associated with (or resides inside) peripheral vesicles. Colocalisation between Eps8 and FGFR2 at the cell periphery is maintained, although to a lesser extent, upon stimulation with FGF2 for 10 minutes (Figure 3.22B), when the first receptor-containing vesicles begin to form. However, following ligand incubation for longer periods (e.g. 30 minutes), FGFR2 redistributes away from the cell

periphery, trafficking toward perinuclear compartments, and colocalisation with Eps8 in peripheral vesicles is lost. Notably, when Eps8 is imaged with EEA1, a validated marker for early endosomes (Stenmark et al. 1996), clear colocalisation is observed (Figure 3.22C), suggesting that Eps8 localisation is restricted to the early endosomal system.

To further confirm early endosomal localisation of Eps8 action, a series of triple-labelling experiments was performed between activated FGFR2, following 10 minutes FGF2 stimulation, Eps8, and an early endosomal marker (transferrin upon 5 minutes incubation). As shown in Figure 3.22D, triple colocalisation revealed the presence of a region of overlap (in white) between the three proteins. Taken together, these data confirm that Eps8 specifically resides in the early endocytic compartments and that activated FGFR2 transits through this compartment during early phases of receptor trafficking, to be ultimately sorted toward perinuclear regions. This observation is consistent with findings from Burke et al. on EGFR endocytosis, where Eps8 was found to associate with internalised EGFR only at early time-point stimulation (10 minutes) (Burke et al. 2001 and unpublished data); this corresponds to the time at which EGFR accumulates in early endosomes.

Finally, to further validate the connection between Src kinase activity and Eps8 function within the peripheral endocytic system, colocalisation between the two proteins was studied. The result, depicted in Figure 3.23, revealed a striking overlap of Eps8 with constitutively active Src, specifically at the cell periphery, confirming evidence of localisation of Src/Eps8 action within the peripheral endocytic compartment.

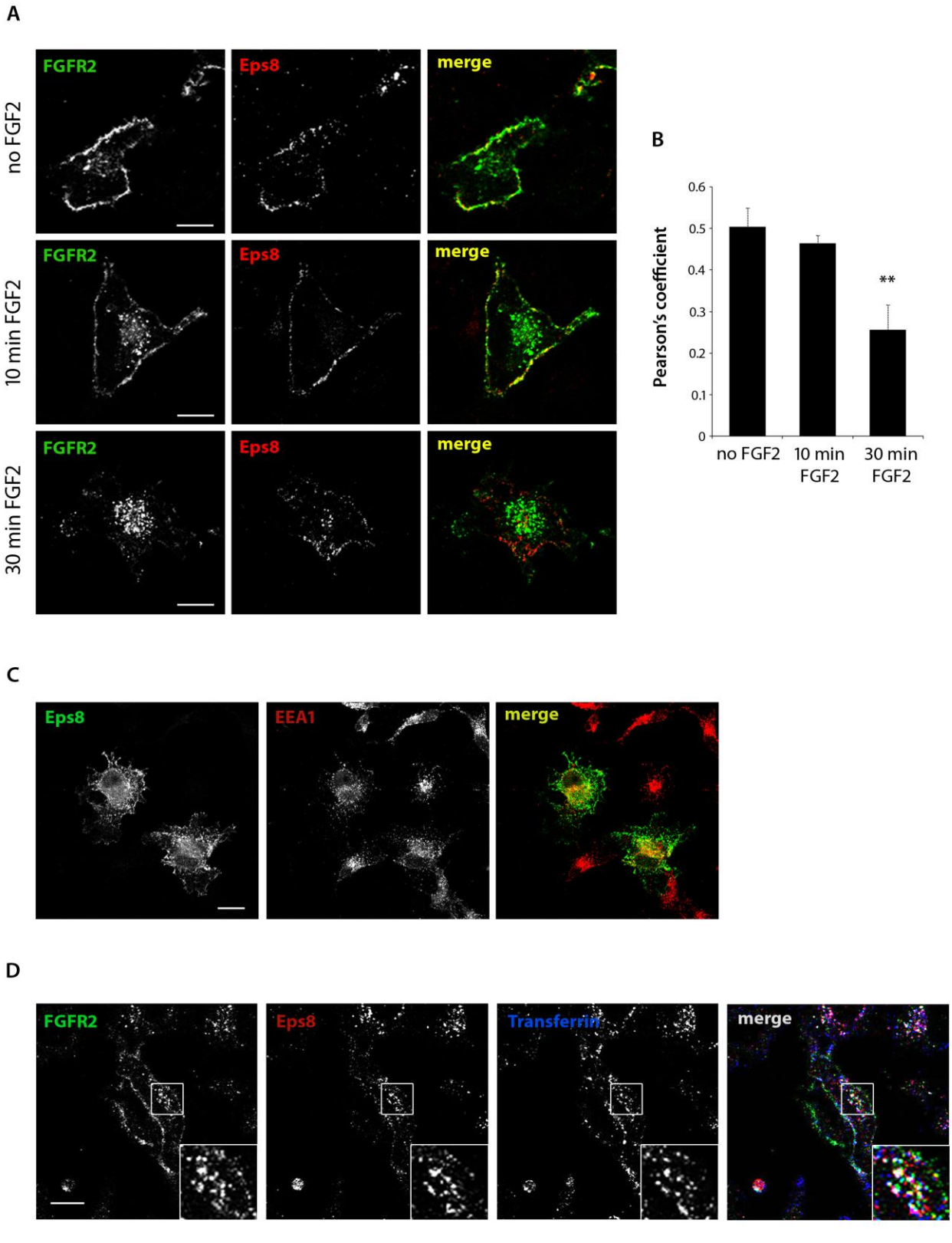
A
FGFR2
Eps8
merge
no FGF2
10 min FGF2
30 min FGF2
B
Pearson's coefficient
0.6
0.5
0.4
0.3
0.2
0.1
0
**
no FGF2
10 min FGF2
30 min FGF2
C
Eps8
EEA1
merge
D
FGFR2
Eps8
Transferrin
merge

Figure 3.22. Localisation of Eps8 action on FGFR2 trafficking is restricted to the early endosomal system

A. HeLa cells transfected with FGFR2-GFP and Eps8-mCherry were stimulated with FGF2 for either 10 or 30 minutes, or non-stimulated, then fixed and imaged in confocal microscopy. During the early stages of activation (up to 10min FGF2 stimulation), FGFR2 localises in peripheral compartments, where it colocalises with Eps8. Upon ligand incubation for longer periods (30 minutes), FGFR2 redistributes away from the cell periphery, while Eps8 localisation remains restricted to peripheral compartments, just beneath the plasma membrane. Scale bars = 10 µm **B**. Quantification analysis of colocalisation between FGFR2 and Eps8, showing significant overlap only during early phases of receptor activation, when both proteins localise in early endocytic compartments (mean ± SEM, *, $p < 0.05$; **, $p < 0.01$; ***, $p < 0.001$, n = 14 cells). **C**. Eps8-GFP expressing HeLa cells were fixed and immunostained for EEA1 and analysed in confocal microscopy. Scale bars = 10 µm. **D**. HeLa cells co-expressing FGFR2-GFP and Eps8-mCherry were stimulated with FGF2 10 minutes. Upon incubation with transferrin-AF633 during the latter 5 minutes of stimulation, cells were rinsed, fixed, and imaged in confocal microscopy. Higher-magnification images of selected regions from the cells show colocalisation (in white) of FGFR2, Eps8 and 5-min internalised transferrin, demonstrating that during the early phases of receptor trafficking, activated FGFR2 transits through the early endocytic compartments, where Eps8 specifically resides. Scale bars = 5 µm.

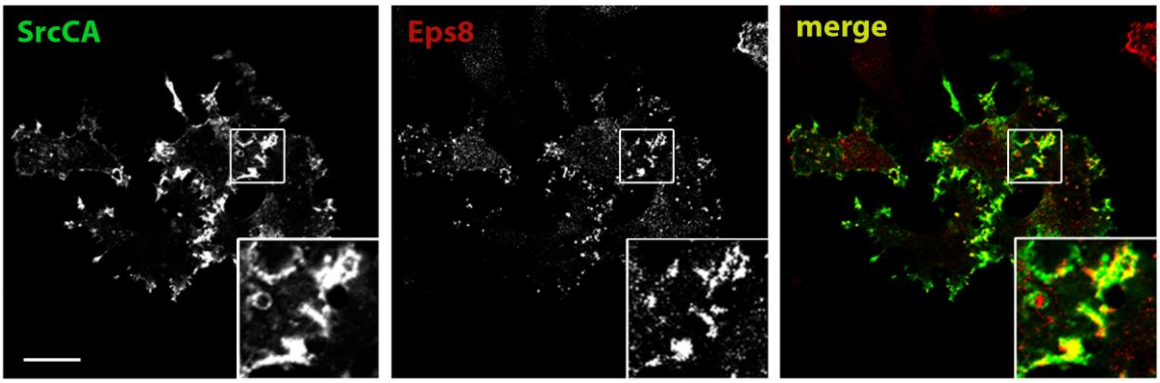

Figure 3.23. Colocalisation between Eps8 and active Src

HeLa cells co-expressing Eps8-mCherry and constitutive active Src (SrcCA) were fixed and immunostained for active Src (phospho416Src antibody), then analysed in confocal microscopy. Higher-magnification regions show clear colocalisation between active Src and Eps8 (in yellow). Scale bars = 5 µm.

3.5.3 Role of Eps8 in trafficking FGFR2 out of early endocytic system

Results illustrated thus far indicate that Eps8 may be important in regulating early phases of FGFR2 trafficking following endocytosis. A clear indication that Eps8 is important in ensuring correct transit of FGFR2 out of the early endocytic system came from a series of immunofluorescence analyses performed on the previously described Eps8 shRNA cell line. In these studies, the differential fate of activated FGFR2 in the presence or absenc eof Eps8 was investigated by analysing colocalisation of activated receptor with validated markers of the endocytic pathway (Figure 3.24). Consistent with the live-cell imaging investigations described earlier in this study, in scrambled shRNA (control) cells, upon stimulation with FGF2 ligand for 30 minutes, activated FGFR2 was found to accumulate to an intracellular region adjacent to the nucleus. Thus, analysis of colocalisation between activated FGFR2 and EEA1 revealed a very low extent of overlap (Figure 3.24A and B), confirming that following stimulation for 30 minutes, the internalised receptor is trafficked away from the early endocytic compartments. However, in the absence of Eps8 expression, the extent of colocalisation between FGFR2 and EEA1 significantly increases, demonstrating that Eps8 plays a critical role in sorting the receptor out of the early endocytic system.

As described in Section 1.3, Endocytosis and endocytic trafficking**,** the canonical endocytic pathway enables transport of RTKs from early endosomal compartments toward lysosomes for degradation and/or the recycling pathway. Thus, on the basis of the observations described above, it is possible that the role of Eps8 is to regulate the exit of FGFR2 from the peripheral early endosomes toward these late compartments. To confirm this hypothesis, localisation of activated FGFR2 was studied in relation to specific markers

for perinuclear recycling (Rab 11, Ullrich O. et al. 1996) and lysosomal degradative compartments (Lysotracker). As depicted in Figure 3.24 C–F, in control cells 30 minutes post stimulation, FGFR2 was found to accumulate in both the recycling and the degradative compartment, as demonstrated by the high degree of colocalisation with Rab11 and Lysotracker, respectively. This indicates that, similar to other members of the RTK family such as EGFR, activated FGFR2, upon transiting through the endosomal system, is either recycled back to the plasma membrane or sorted for degradation. However, in Eps8 knock-down cells, the extent of accumulation of activated receptor with both Rab11 and Lysotracker-positive compartments appears significantly reduced. This observation is consistent with the previously observed accumulation of receptor in early endosomal compartments in Eps8 knock-down condition. Thus, taken together, these findings demonstrate that Eps8 is required for trafficking activated FGFR2 out of the peripheral early endosomes and toward the degradative and perinuclear recycling compartments.

3.5.4 Role of Eps8 in FGFR2 signalling

As discussed in greater detail in Section 1.3.3, receptor endocytosis and signalling are tightly linked processes and they can profoundly influence each other. Thus, in light of the findings thus far, it is possible that Eps8, by controlling the early endocytic trafficking of FGFR2, can also influence the signalling activated downstream of the receptor. To investigate this issue, the output profile of FGFR2 signalling was analyzed upon FGF2 stimulation in the presence or absence of Eps8. Because activated FGFR2 signals through the RAS-MAPK pathway (Eswarakumar et al. 2005), phosphorylated ERK1/2 were used as indicators of duration and intensity of signalling activated downstream of the receptor.

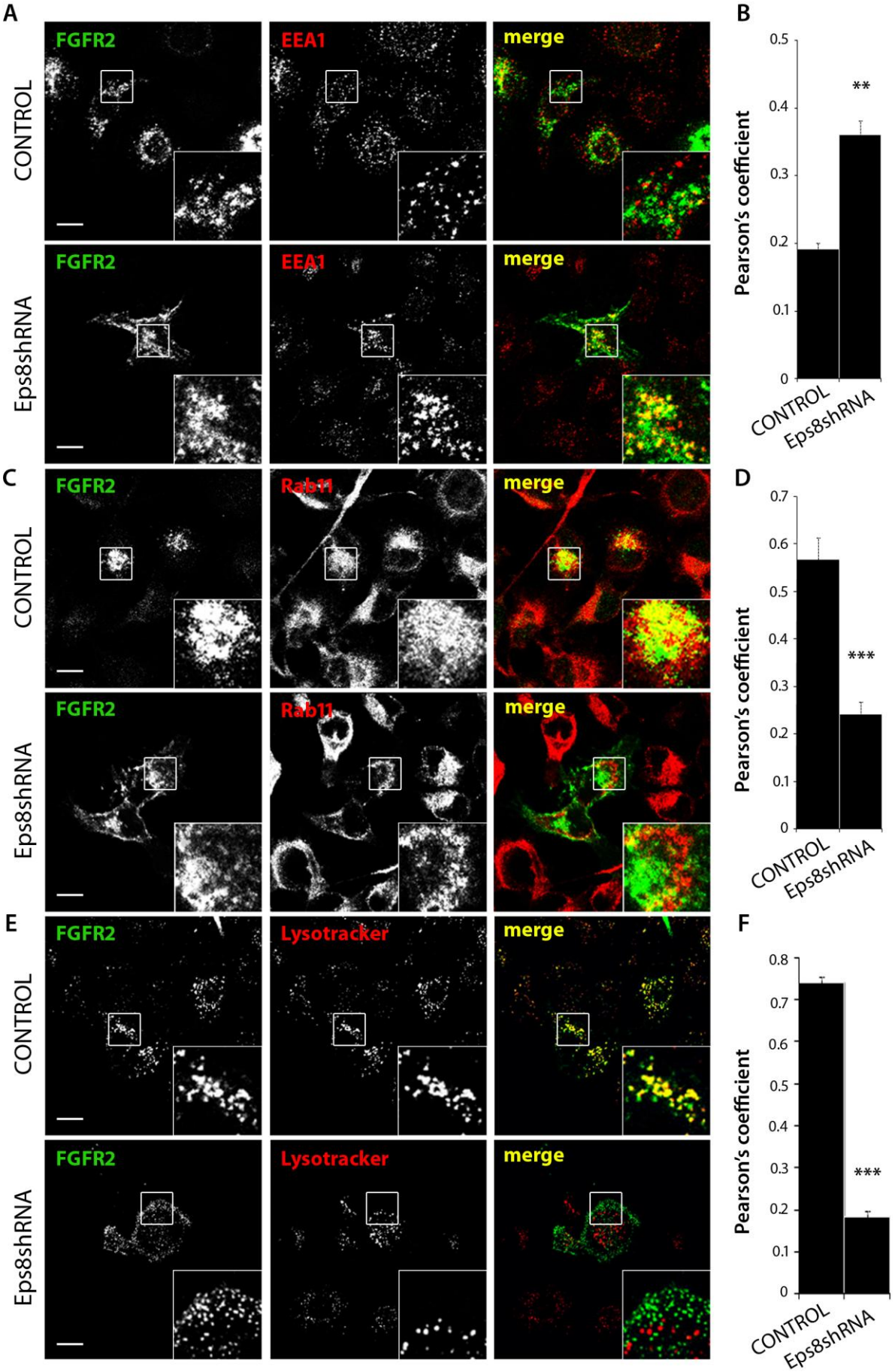
A
FGFR2
EEA1
merge
CONTROL
Eps8shRNA
B
Pearson's coefficient
0.5
0.4
0.3
0.2
0.1
0
**
CONTROL
Eps8shRNA
C
FGFR2
Rab11
merge
CONTROL
Eps8shRNA
D
Pearson's coefficient
0.7
0.6
0.5
0.4
0.3
0.2
0.1
0
***
CONTROL
Eps8shRNA
E
FGFR2
Lysotracker
merge
CONTROL
Eps8shRNA
F
Pearson's coefficient
0.8
0.7
0.6
0.5
0.4
0.3
0.2
0.1
0
***
CONTROL
Eps8shRNA

Figure 3.24. Eps8 is required for sorting activated FGFR2 out of peripheral early endosomes and toward degradative and peri-nuclear recycling compartments

Eps8 knock down (Eps8 shRNA) and vector control HeLa cells transiently transfected with FGFR2-GFP were stimulated with FGF2 for 30 minutes and immunostained for EEA1 (**A**) or Rab11 (**C**), or treated with LysoTracker-Red (**E**). Then, cells were fixed and analysed in confocal microscopy. Higher-magnification images of selected cell regions show that in absence of Eps8, active FGFR2 is retained in early endosomal compartments (EEA1-positive) and is prevented from sorting to both peri-nuclear recycling (Rab11-positive) and lysosomal degradative (LysoTracker-positive) compartments. Scale bars = 5 µm. (**B**, **D**, **F**) Colocalisation of active FGFR2 with EEA1, Rab11 or LysoTracker was quantified in control cells as 0.19 ± 0.02, 0.57 ± 0.04, and 0.74 ± 0.01, respectively, and in Eps8 knock down cells as 0.36 ± 0.04, 0.24 ± 0.05, and 0.18 ± 0.01, respectively (Pearson's coefficient, mean ± SEM, *, $p < 0.05$; **, $p < 0.01$; ***, $p < 0.001$, n = 18 cells).

As shown in Figure 3.25A, in control cells FGF2 stimulation promotes rapid appearance of the p44 form of activated ERK (ERK1), which was maximally induced at 5 minutes. In this condition, however, stimulation with FGF2 had no effect on the p42 form of ERK (ERK2), whose basal level was unchanged over time. In fact non-transfected HeLa cells subjected to overnight serum starvation show a basal level of expression of the p42 form of ERK (Figure 3.25C). When Eps8 expression was silenced, significant effects on pERK activation were observed. In fact, as depicted in Figure 3.25A and B, in Eps8 knock-down cells the FGF2-dependent amplification of the p44 form of ERK during early-phase activation was diminished. This observation suggests that Eps8 is important for FGFR2-dependent activation of the RAS-MAPK pathway during early phases of receptor endocytosis, probably via a feedback mechanism generated by the primary role of Eps8 in regulating transit of activated receptor through the early endocytic system. This finding also suggest that FGFR2 remains active upon endocytosis and continues to signal along

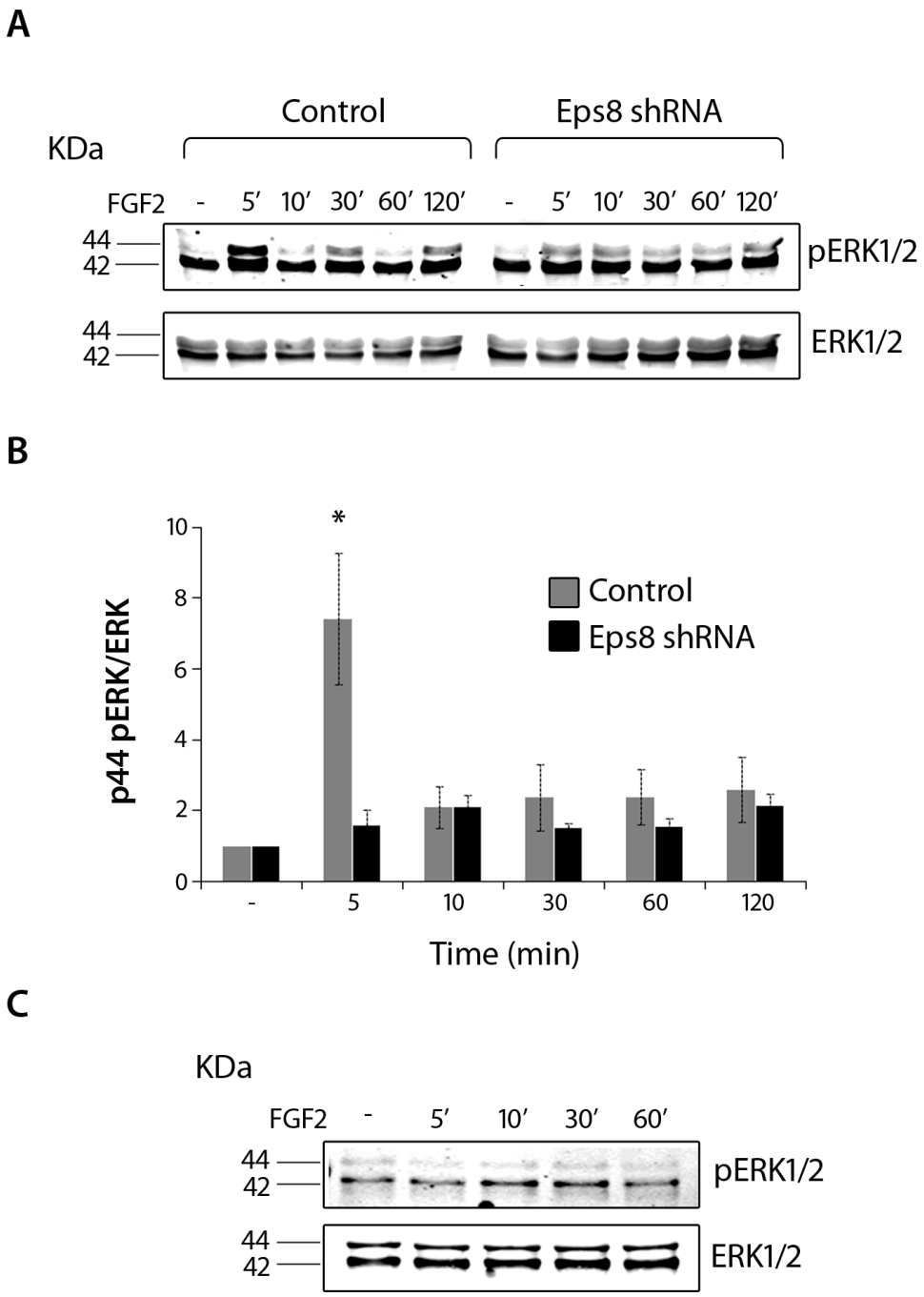

Figure 3.25. Eps8 regulates RAS-MAPK signalling pathway downstream of FGFR2

A. Eps8 knock down (Eps8 shRNA) and vector control HeLa cells transiently expressing FGFR2-GFP were lysed following stimulation with FGF2 for the indicated times. Cellular extracts were resolved by SDS-PAGE and analysed by immunoblotting for levels of specified proteins. The time-course of Erk1/2 phosphorylation in response to FGF2 shows significant attenuation of p44 ERK (ERK1) level at 5 minutes FGF2 stimulation in Eps8 knock down cells. **B**. Quantification analysis by densitometric scanning of western blots of p44 pERK level following FGF2 stimulation in Eps8 knock down (black) and vector control (gray) HeLa cells (mean ± SEM, *, $p < 0.05$; **, $p < 0.01$; ***, $p < 0.001$, n = 5 experiments). **C**. Non transfected HeLa cells were starved overnight in serum free media and lysed following stimulation with FGF2 for the indicated times. Cellular extracts where resolved by SDSPAGE and analysed by immunoblotting for the levels of specified proteins.

the endocytic pathway, similar to observations for other members of the RTK family, such as EGFR (Jiang and Sorkin 2002). Finally, the presence of a lower amplitude of signalling output which remains unaffected even in the absence of Eps8 indicates that activated FGFR2 can also signal through the RAS-MAPK pathway in an Eps8-independent manner.

3.5.5 Conclusions

The evidence presented in this chapter establishes Src kinase as a key regulator of early endocytic trafficking of FGFR2. Live-cell imaging studies revealed that functional Src activity is required for correct endocytosis of FGFR2 and its consequent trafficking toward perinuclear compartments. In fact, cells treated with the Src-family inhibitor Dasatinib showed impaired receptor internalisation as well as a clear defect in the redistribution of internalised receptor away from the cell periphery. Super-resolution imaging studies in Dasatinib-treated cells confirmed the importance of Src activity in ensuring regular endocytic trafficking of FGFR2, as demonstrated by the clear accumulation of receptor-containing vesicles in peripheral endocytic compartments upon 30 minutes' FGF2 stimulation.

The results presented in this chapter also demonstrate a role for the multifunctional scaffold protein Eps8 in FGFR2 trafficking. Involvement of Eps8 in the context of FGFR2 was already demonstrated by Cunningham et al., where the adaptor protein was characterized as target of Src-mediated phosphorylation in the FGFR signalling cascade (Cunningham et al. 2010). In the present study, clear evidence of the key role of Eps8 in regulating FGFR2 endocytosis came from real-time analysis of FGFR2 trafficking in KDEps8 cells. Similar to the result obtained in Dasatinib-treated cells, the absence of Eps8 led to impaired receptor trafficking and accumulation of FGFR2-positive puncta in a peripheral

endocytic compartment. The observation that silencing of Eps8 protein phenocopies the effect of Src kinase activity inhibition on FGFR2 trafficking further confirms the mechanistic link between FGFR2 activation, Src activity, and Eps8 function, specifically localised in an early endocytic compartment.

The precise role of Eps8 in regulating FGFR2 trafficking was also characterized by a series of colocalisation studies. The results show that Eps8 is required for trafficking the activated receptor out of early endosomal systems and toward degradative and the perinuclear recycling compartments. In fact, in the absence of the adaptor protein, the transit of activated receptor through the EEA1-positive compartments is blocked and FGFR2 accumulates at the cell periphery and is prevented from being trafficked to late lysosomal and recycling compartments.

Finally, the findings shown here provide new insight into the crosstalk between trafficking and signalling of FGFR2. Biochemical studies revealed that depletion of Eps8 severely inhibits the ability of FGFR2 to activate the RAS-MAPK pathway in its early phases, suggesting a role for Eps8 in regulating and also signalling downstream FGFR2. Whether this is an indirect consequence of Eps8-dependent regulation on receptor trafficking or a direct effect of Eps8 on downstream signalling output remains to be verified. In conclusion, these findings demonstrate that Src acts through Eps8 to regulate endocytosis and early endocytic trafficking of FGFR2, and that Eps8 functions as a key coordinator in the interplay between FGFR2 trafficking and signalling.

CHAPTER 4

DISCUSSION

RTKs undergo rapid and controlled internalisation from the cell surface in response to ligand binding (Le Roy and Wrana 2005, von Zastrow and Sorkin 2007). Endocytosis and trafficking of receptors along the endocytic pathway are known to act as major mechanisms for receptor downregulation, as they ultimately result in receptor proteolysis and termination of signalling (Beguinot et al. 1984, Stoscheck and Carpenter 1984). However they can also contribute to spatio-temporal regulation of signal transduction, by influencing the duration and correct subcellular location of the signalling output generated (von Zastrow and Sorkin 2007; Di Fiore and De Camilli 2001). Thus, it is not surprising that defects in the endocytic machinery may result in abnormal cell signalling (Bache et al. 2004, Parachoniak and Park 2012) and that deregulation of RTK endocytosis is emerging as a mechanism of oncogenic activation (Peschard and Park 2003).

FGF receptors represent a subfamily of RTKs with established roles in both the development and progression of cancer (Haugsten et al. 2010, Wesche et al. 2011). Although over the last three decades much effort has been dedicated to studying the signalling pathways activated by FGFRs, the endocytic pathway for FGFR internalisation and the subsequent intracellular trafficking of receptors are subjects that remain elusive and subject to controversy.

By employing living-cell–based assay systems, this thesis examines basic aspects of receptor trafficking, along with the contribution of downstream effectors in the FGFR signalling cascade. The endocytic route for internalisation of FGFR2 is unravelled using advanced optical microscopy techniques, and trafficking of the receptor along the endocytic pathway is visualized. Recruitment of FGFR2 and clathrin at the plasma membrane prior to internalisation is also evaluated and is demonstrated to have similar dynamics to that of other members of RTKs. Finally, Eps8 is characterised as a novel regulator of endocytosis, and trafficking of FGFR2 and its function are shown to be key in coordinating the interplay between FGFR2 trafficking and signalling.

In Section 3.1, characterisation of a suitable model system to study FGFR2 dynamics in living cells is described. This is a critical step, since our analysis is based on employment of an ectopically overexpressed FGFR2-GFP. Confocal microscopy analysis of FGFR2-GFP–expressing HeLa cells reveals correct targeting of the fusion protein both before and after FGF stimulation, validating HeLa as an adequate cell model for our live-cell imaging studies. These results also indicate that GFP-fused receptor is active and that tagging does not interfere with receptor functionality. It must also be underlined that HeLa cells have been previously shown to express very low levels of endogenously expressed FGFR2 (Ahmed et al. 2008). This demonstration is important, because the presence of endogenous FGFR2 could interfere with the correct functionality of the overexpressed counterpart, affecting our results.

In Section 3.2, development of live-cell imaging assays based on advanced optical microscopy methods is described and shown to be a necessary tool for exploring receptor trafficking within a live-cell context. In fact, in contrast to many studies, this work

investigates several aspects of receptor trafficking in real-time, by using an established living-cell–based assay system. This approach is important, because it allows visualization of spatial and temporal endocytic dynamics of the receptor within a live biological context. Published works regarding endocytic trafficking of FGFR employ antibody-labelling methods, limiting their analysis to fixed cell-based techniques (Belleudi et al. 2009, Belleudi et al. 2007, Citores et al. 1999, Marchese et al. 1998). Thus, the novelty of the present work relates to the fact that mechanisms are investigated in a real-time system, allowing the characterization of the endocytic trafficking of FGFR2. Visualization of the dynamics of activated FGFR2 trafficking in living cells reveals that the first receptor-containing vesicles begin to appear from the inner surface of the plasma membrane at 5 minutes after FGF2 addition. Thus, the process of FGFR2 internalisation occurs very rapidly, and interestingly, this process recalls the kinetics of internalisation of EGFR, which also undergoes internalisation already at 5 minutes following ligand stimulation (Schmidt-Glenewinkel et al. 2009). This observation suggests that different members of the RTK family share the same dynamics of internalisation, which may in turn reflect a common pathway of endocytosis, as demonstrated in Section 3.3. At late time points following ligand incubation, the entire pool of surface-bound receptors appears to be completely redistributed to intracellular perinuclear compartments. These intracellular regions correspond to perinuclear recycling and lysosomal compartments, as demonstrated in Section 3.5. This demonstrates that FGFR2 follows both degradation and recycling pathways, similar to other members of the RTK family, such as EGFR (Sorkin and Goh 2008) or PDGFR (Hellberg et al. 2009). It would be interesting to further investigate this characteristic and to evaluate to what extent FGFR2 is targeted to lysosomes for degradation rather than to the recycling pathway, or whether discrimination between the

two outcomes depends on any specific factor or molecular event, such as the process of receptor ubiquitination.

The live-cell trafficking assay developed in this study also reveals that the kinase activity of FGFR2 is required for receptor internalisation. The explanation for this observation is not entirely clear. In fact, the kinase domain of RTK is important for initiation of the intracellular signalling cascade, a process that occurs at the plasma membrane independently from endocytosis of the receptor itself. A plausible hypothesis would be that the phosphotyrosine residues generated by the receptor kinase domain serve to recruit signalling/adaptor molecules that play a role in the internalisation process. This would explain identification of constitutively active mutant RTKs which show enhanced endocytosis (Joffre et al. 2011), and identification of mutant receptors with inactive kinase which are unable to internalise properly (Sorokin et al. 1994).

Finally, TIRF microscopy reveals that FGFR2 forms clusters at the plasma membrane in response to ligand binding. By clustering together, activated receptors are physically concentrated in the same plasma membrane domains. Although this phenomenon is already described for other membrane-bound receptors, including members of the RTK family (Sako et al. 2000), its function within a cellular context has not yet been clarified. One possible explanation for this phenomenon is that it concentrates activated receptors in the same microdomains of the plasma membrane specialised for endocytosis, such as lipid rafts, caveolae, and clathrin-coated pits, resulting in enclosure of multiple receptors in the same endocytic vesicle. In this case, therefore, clustering plays an important role in the process of receptor endocytosis. Alternatively, a functional consequence of receptor assembly might be enhancement of signalling efficiency: by physically recruiting activated

receptors within domains enriched in signalling molecules, or by simply aggregating multiple receptors together and enabling them to trans-phosphorylate and activate each other. Future studies, based for instance on employment of single-molecule fluorescence methods, are necessary to further investigate the spatial organization of FGFR2 on the cell surface and to determine which of the three hypotheses best describes the functional role of receptor clustering at the plasma membrane.

In Section 3.3, confocal and TIRF microscopy techniques, combined with employment of inhibitors or siRNA sequences are used to define the endocytic pathway(s) by which FGFR2 is internalised and trafficked during the early phases of receptor activation. A number of previous reports on endocytosis of FGFRs implicated multiple endocytic pathways, including both clathrin-mediated and caveolar endocytosis (Gleizes et al. 1996, Marchese et al. 1998). Further, few studies find that internalisation of FGFRs proceeds independently of both clathrin and caveolin (Citores et al. 2001, Reilly et al. 2004). Thus, identification of the specific pathway(s) for internalisation of FGFRs remains controversial.

Data from the present work reveal that treatment of cells with the dynamin inhibitor Dynasore entirely blocked uptake of FGFR2. This is a clear demonstration that FGFR2 endocytosis occurs through a dynamin-dependent process. Similar to FGFR2, the majority of RTKs enter cells through a process which is dynamin-dependent. However, in some cases, such as that of EGFR (Orth et al. 2006) or PDGFR (Sadowski et al. 2013), involvement of multiple alternative pathways which are dynamin-independent has also been observed. Our analysis demonstrates that the dynamin-dependent route is the only one responsible for internalisation of FGFR2 and that no other alternative pathway

occurs. In fact, when visualized in confocal live-cell microscopy, Dynasore-treated cells revealed no intracellular trafficking of FGFR2 even following 30 minutes of ligand stimulation. It should also be emphasised that when dynamin activity was inhibited, receptor-containing vesicles could still be observed forming at the cell periphery, but they seemed to fail to leave the plasma membrane. This is further confirmation of the key role of GTPase dynamin during the early phases of FGFR2 endocytosis.

Having demonstrated that FGFR2 enters cells through a dynamin-dependent pathway, the next step was to unequivocally identify this specific pathway. Employment of a siRNA-based approach revealed that endocytosis of FGFR2 is completely blocked in cells silenced for α-adaptin. Thus, the presence of an intact functional AP2 complex is a necessary requisite for endocytosis of FGFR2, indicating that FGFR2 internalisation occurs through clathrin-mediated endocytosis. Conversely, no effect is observed in cells treated with caveolin1 siRNA, definitively excluding caveolar endocytosis as a potential alternative pathway for internalisation of FGFR2. Thus, the present work demonstrates for the first time that FGFR2 endocytosis occurs through CME and that no additional pathways function in parallel to it.

Results from Section 3.2 indicate that FGFR2 aggregates in clusters at the plasma membrane in response to ligand-mediated activation. In light of the demonstration that FGFR2 is internalised through CME, we hypothesize that receptor clustering on the cell surface specifically occurs at clathrin-coated pits (and conversely not at caveolae membrane domains). TIRF microscopy experiments verify this hypothesis, revealing that activated FGFR2 significantly colocalises with clathrin at the plasma membrane, whereas no colocalization is observed with caveolin1.

Further high resolution live-cell TIRF microscopy experiments also revealed the dynamics of recruitment of FGFR2 and clathrin at sites of prior CME internalisation. These results demonstrate that following stimulation, activated FGFR2 is recruited predominantly into pre-formed CCPs. Notably, similar dynamics of recruitment are observed for activated EGFR (Rappoport and Simon 2009), suggesting that this could be a conserved mechanism across RTK members.

In Section 3.4, another aspect of the dynamics of FGFR2 endocytosis is investigated. Preliminary observations reveal that in HeLa cells, FGF stimulation causes an increase in the number of CCPs at the cell surface. Notably, the same effect is also observed in another cell line, LNCaps, which endogenously expresses FGFR2 (Carstens et al. 1997), demonstrating that this is not a cell line-specific phenomenon and, more importantly, that it is not due to overexpression conditions in our model system. Further, when the kinase activity of FGFR2 is blocked by SU5402 inhibitor, redistribution of clathrin at the plasma membrane is prevented, suggesting that this process requires the functional kinase activity of the receptor to occur.

Formation of new clathrin coats induced by receptor activation is already described for other members of the RTK family, such as EGFR (Wilde et al. 1999) or NGFR (Beattie et al. 2000). However, the function of clathrin redistribution at the cellular level remains unclear. It is possible that the new pool of clathrin is recruited to the cell surface to be employed in the process of receptor endocytosis. In this scenario, the presence of FGF ligand on the extracellular matrix would ultimately result in an incremental CME process, therefore generating a mechanism for regulating receptor trafficking.

Real-time analysis of the number of clathrin spots disappearing from the TIRF field in response to FGF stimulation reveals that the presence of FGF ligand also induces an increase in the density of endocytic events, verifying our hypothesis on the role of the FGF-dependent redistribution of CCPs. Unexpectedly, however, no effect could be observed on the uptake of transferrin, suggesting that the increased clathrin puncta undergoing endocytosis upon FGFR2 activation may represent a cargo-specific population of clathrin-coated pits.

This latter result may have important implications. First, it implies that only a specific subset of productive CCPs is involved in endocytosis in response to ligand-dependent FGFR2 activation. This confirms the increasingly clear scenario of CCPs as a highly heterogeneous population of endocytic machines at the plasma membrane. Second, it suggests that this heterogeneity of CCPs not only depends on factors such as size, maturation rate, dynamics, (Merrifield et al. 2005, Rappoport et al. 2005, Yarar et al. 2005), but it can also reflect differences in their cargo content. Third, data from this thesis suggest for the first time that cargo-specific mechanisms, such as ligand-induced receptor activation and clustering, can affect the properties and dynamic behaviour of specific CCPs at the cell surface, a phenomenon already shown for G protein coupled receptors (GPCRs) (Puthenveedu and von Zastrow 2006).

Finally, data from Section 3.4 reveal that the kinase Src is required for the increase in CCP number following FGFR activation. This result is consistent with findings from Wilde et al. who identify Src as the kinase responsible for regulating cellular distribution of clathrin upon EGFR activation (Wilde et al. 1999). Interestingly, Src inhibition does not result in complete inhibition of clathrin recruitment upon FGF stimulation, suggesting the

possibility that this regulatory loop, important for regulating the process of CME, can bypass Src activity, proceeding through an alternative pathway.

In light of previous work from our laboratory that identified the protein Eps8 as an Src-dependent kinase substrate phosphorylated in response to FGF stimulation (Cunningham et al. 2010), and of this protein's documented roles in vesicle trafficking (Lanzetti et al. 2000), we set out to explore the possibility that Eps8, along with Src, could play a role in the redistribution of clathrin observed following FGF stimulation. Employment of a siRNA-based approach reveals that in the absence of Eps8, the increase in clathrin punctua at the cell surface upon ligand stimulation is prevented, confirming our hypothesis.

From the data described thus far, an updated picture of endocytic trafficking of FGFR2 is becoming clear: following ligand binding and activation, FGFR2 distribution at the plasma membrane changes and activated receptors specifically cluster at pre-formed CCPs. Here, the process of endocytosis begins, and receptors are enclosed into clathrin-coated vesicles and trafficked intracellularly. Simultaneously, signalling through Src to Eps8 by activated FGFR2 brings new CCPs at the plasma membrane and consequently promotes clathrin-mediated endocytosis. Having focused on basic aspects of FGFR2 endocytosis before the internalisation process, the next step in this research was to explore the intracellular fate of the receptor and how FGFR2 trafficking through specific intracellular compartments is regulated.

In Section 3.5, employment of a live-cell trafficking assay developed in this study, in combination with chemical inhibition of Src activity, reveals that Src plays an important role in intracellular trafficking of FGFR2. Following Dasatinib treatment, FGFR2-containing vesicles are observed to atypically and statically accumulate in peripheral compartments,

and redistribution toward perinuclear compartments is entirely prevented. These results suggest that Src is not essential for internalisation of FGFR2, but is required for early phases of receptor trafficking. Using super-resolution confocal microscopy, clear FGFR2-positive puncta are observed that localise at the cell periphery of Dasatinib-treated cells, further confirming the role of Src in regulating FGFR2 trafficking during its early phases.

In light of these findings, and of the mechanistic connection between Src and Eps8 previously demonstrated by our group (Cunningham et al. 2010), we hypothesize that Eps8 could represent an Src-dependent regulator of FGFR trafficking within the early endocytic system. Analysis of FGFR2 trafficking in a previously established Eps8 knockdown cell line confirms our hypothesis, revealing a Dasatinib-like phenotype: significant attenuation of FGFR2 trafficking with an accumulation of receptor-containing vesicles within a peripheral punctuate compartment.

The work presented in Section 3.5 clearly confirms the connection between Src kinase activity and Eps8 function in regulating FGFR2 trafficking within the peripheral endocytic system. In a series of colocalisation studies, FGFR2 is observed to colocalise with Eps8 and transferrin in peripheral early endosomes during early phases of trafficking, as well as with constitutively active Src. However, following ligand stimulation for 30 minutes, FGFR2 appears to redistribute away from the cell periphery and colocalisation with Eps8 in peripheral vesicles is lost.

A clear demonstration that Eps8 is required to sort FGFR2 out of the early endocytic system comes from a series of immunofluorescence analyses performed on the previously mentioned Eps8 shRNA cell line. These analyses reveal that in control cells 30 minutes post-stimulation, FGFR2 poorly colocalises with EEA1-positive compartments,

while it is found to localise to the Rab11 positive recycling compartment as well as degradative compartments. Conversely, in stimulated Eps8 knockdown cells, FGFR2 is observed to be retained in the early endosomes and redistribution to perinuclear recycling and degradative compartments is entirely prevented. Thus, these data demonstrate for the first time that activated FGFR2 traffics through the EEA1-positive compartment and follows both the slow recycling and degradative pathways, and that the transition from early endosomal to late lysosomal/recycling compartments is controlled by Eps8.

Emerging evidence suggests that receptor endocytosis and signalling are tightly linked processes and that they can profoundly influence each other (Di Fiore and De Camilli 2001, von Zastrow and Sorkin 2007). Considering this reciprocal regulation and the demonstrated role of Eps8 in controlling early endocytic trafficking of FGFR2, it is speculated that Eps8 could also play a role in regulating signalling downstream of FGFR2.

Biochemical analysis reveals that depletion of Eps8 severely inhibits the ability of FGFR2 to activate the RAS-MAPK pathway, confirming the role of Eps8 in mediating signalling by FGFR2 immediately following activation. Whether this is a direct effect of Eps8 on receptor signalling dynamics or a feedback effect of Eps8-dependent regulation on receptor trafficking through the early endocytic system remains to be determined. Interestingly, the significant effect of Eps8 depletion on signalling by FGFR2 is observed only at very early time points, specifically at 5 minutes post–FGF stimulation. Bearing in mind that during this early phase, receptors containing vesicles are still localised in the early endocytic system, this data also suggest that FGFR2 signalling through the RAS-MAPK pathway can occur from endosomes during receptor endocytosis, similar to what

has already been demonstrated for EGFR (Jiang and Sorkin 2002). Thus, in conclusion, the work presented in this thesis identifies Eps8 as a novel regulator of FGFR2 endocytosis and a key coordinator of the signalling and trafficking of FGFR2, specifically during early stages of activation.

CHAPTER 4

REFERENCE LIST

Abbas S, Rotmans G, Lowenberg B, Valk PJ. 2008. Exon 8 splice site mutations in the gene encoding the E3-ligase CBL are associated with core binding factor acute myeloid leukemias. Haematologica 93: 1595-1597.

Abella JV, Park M. 2009. Breakdown of endocytosis in the oncogenic activation of receptor tyrosine kinases. Am J Physiol Endocrinol Metab 296: E973-984.

Abella JV, Parachoniak CA, Sangwan V, Park M. 2010. Dorsal ruffle microdomains potentiate Met receptor tyrosine kinase signaling and down-regulation. J Biol Chem 285: 24956-24967.

Abulrob A, Lu Z, Baumann E, Vobornik D, Taylor R, Stanimirovic D, Johnston LJ. 2010. Nanoscale imaging of epidermal growth factor receptor clustering: effects of inhibitors. J Biol Chem 285: 3145-3156.

Adar R, Monsonego-Ornan E, David P, Yayon A. 2002. Differential activation of cysteine-substitution mutants of fibroblast growth factor receptor 3 is determined by cysteine localization. J Bone Miner Res 17: 860-868.

Adnane J, Gaudray P, Dionne CA, Crumley G, Jaye M, Schlessinger J, Jeanteur P, Birnbaum D, Theillet C. 1991. BEK and FLG, two receptors to members of the FGF family, are amplified in subsets of human breast cancers. Oncogene 6: 659-663.

Ahmed Z, Schuller AC, Suhling K, Tregidgo C, Ladbury JE. 2008. Extracellular point mutations in FGFR2 elicit unexpected changes in intracellular signalling. Biochem J 413: 37-49.

Ahn S, Kim J, Lucaveche CL, Reedy MC, Luttrell LM, Lefkowitz RJ, Daaka Y. 2002. Src-dependent tyrosine phosphorylation regulates dynamin self-assembly and ligand-induced endocytosis of the epidermal growth factor receptor. J Biol Chem 277: 26642-26651.

Alessi DR, Saito Y, Campbell DG, Cohen P, Sithanandam G, Rapp U, Ashworth A, Marshall CJ, Cowley S. 1994. Identification of the sites in MAP kinase kinase-1 phosphorylated by p74raf-1. EMBO J 13: 1610-1619.

Allen BL, Rapraeger AC. 2003. Spatial and temporal expression of heparan sulfate in mouse development regulates FGF and FGF receptor assembly. J Cell Biol 163: 637-648.

Alvarez JV, Greulich H, Sellers WR, Meyerson M, Frank DA. 2006. Signal transducer and activator of transcription 3 is required for the oncogenic effects of non-small-cell lung cancer-associated mutations of the epidermal growth factor receptor. Cancer Res 66: 3162-3168.

Amaya E, Musci TJ, Kirschner MW. 1991. Expression of a dominant negative mutant of the FGF receptor disrupts mesoderm formation in Xenopus embryos. Cell 66: 257-270.

Amaya E, Stein PA, Musci TJ, Kirschner MW. 1993. FGF signalling in the early specification of mesoderm in Xenopus. Development 118: 477-487.

Amit I, et al. 2007. A module of negative feedback regulators defines growth factor signaling. Nat Genet 39: 503-512.

Aviezer D, Hecht D, Safran M, Eisinger M, David G, Yayon A. 1994. Perlecan, basal lamina proteoglycan, promotes basic fibroblast growth factor-receptor binding, mitogenesis, and angiogenesis. Cell 79: 1005-1013.

Avraham R, Yarden Y. 2011. Feedback regulation of EGFR signalling: decision making by early and delayed loops. Nat Rev Mol Cell Biol 12: 104-117.

Avruch J, Khokhlatchev A, Kyriakis JM, Luo Z, Tzivion G, Vavvas D, Zhang XF. 2001. Ras activation of the Raf kinase: tyrosine kinase recruitment of the MAP kinase cascade. Recent Prog Horm Res 56: 127-155.

Babst M, Odorizzi G, Estepa EJ, Emr SD. 2000. Mammalian tumor susceptibility gene 101 (TSG101) and the yeast homologue, Vps23p, both function in late endosomal trafficking. Traffic 1: 248-258.

Bache KG, Slagsvold T, Stenmark H. 2004. Defective downregulation of receptor tyrosine kinases in cancer. EMBO J 23: 2707-2712.

Bange J, et al. 2002. Cancer progression and tumor cell motility are associated with the FGFR4 Arg(388) allele. Cancer Res 62: 840-847.

Barbieri MA, Roberts RL, Mukhopadhyay A, Stahl PD. 1996. Rab5 regulates the dynamics of early endosome fusion. Biocell 20: 331-338.

Barouch W, Prasad K, Greene L, Eisenberg E. 1997. Auxilin-induced interaction of the molecular chaperone Hsc70 with clathrin baskets. Biochemistry 36: 4303-4308.

Bashkirov PV, Akimov SA, Evseev AI, Schmid SL, Zimmerberg J, Frolov VA. 2008. GTPase cycle of dynamin is coupled to membrane squeeze and release, leading to spontaneous fission. Cell 135: 1276-1286.

Bates CM. 2011. Role of fibroblast growth factor receptor signaling in kidney development. Pediatr Nephrol 26: 1373-1379.

Beattie EC, Howe CL, Wilde A, Brodsky FM, Mobley WC. 2000. NGF signals through TrkA to increase clathrin at the plasma membrane and enhance clathrin-mediated membrane trafficking. J Neurosci 20: 7325-7333.

Beenken A, Mohammadi M. 2009. The FGF family: biology, pathophysiology and therapy. Nat Rev Drug Discov 8: 235-253.

Beermann A, Schroder R. 2008. Sites of Fgf signalling and perception during embryogenesis of the beetle Tribolium castaneum. Dev Genes Evol 218: 153-167.

Beguinot L, Lyall RM, Willingham MC, Pastan I. 1984. Down-regulation of the epidermal growth factor receptor in KB cells is due to receptor internalization and subsequent degradation in lysosomes. Proc Natl Acad Sci U S A 81: 2384-2388.

Beiman M, Shilo BZ, Volk T. 1996. Heartless, a Drosophila FGF receptor homolog, is essential for cell migration and establishment of several mesodermal lineages. Genes Dev 10: 2993-3002.

Belleudi F, Leone L, Maggio M, Torrisi MR. 2009. Hrs regulates the endocytic sorting of the fibroblast growth factor receptor 2b. Exp Cell Res 315: 2181-2191.

Belleudi F, Leone L, Nobili V, Raffa S, Francescangeli F, Maggio M, Morrone S, Marchese C, Torrisi MR. 2007. Keratinocyte growth factor receptor ligands target the receptor to different intracellular pathways. Traffic 8: 1854-1872.

Bellus GA, McIntosh I, Szabo J, Aylsworth A, Kaitila I, Francomano CA. 1996. Hypochondroplasia: molecular analysis of the fibroblast growth factor receptor 3 gene. Ann N Y Acad Sci 785: 182-187.

Bellus GA, et al. 1999. Severe achondroplasia with developmental delay and acanthosis nigricans (SADDAN): phenotypic analysis of a new skeletal dysplasia caused by a Lys650Met mutation in fibroblast growth factor receptor 3. Am J Med Genet 85: 53-65.

Blondeau F, et al. 2004. Tandem MS analysis of brain clathrin-coated vesicles reveals their critical involvement in synaptic vesicle recycling. Proc Natl Acad Sci U S A 101: 3833-3838.

Bonifacino JS, Traub LM. 2003. Signals for sorting of transmembrane proteins to endosomes and lysosomes. Annu Rev Biochem 72: 395-447.

Bonifacino JS, Hurley JH. 2008. Retromer. Curr Opin Cell Biol 20: 427-436.

Bottcher RT, Pollet N, Delius H, Niehrs C. 2004. The transmembrane protein XFLRT3 forms a complex with FGF receptors and promotes FGF signalling. Nat Cell Biol 6: 38-44.

Bouyain S, Longo PA, Li S, Ferguson KM, Leahy DJ. 2005. The extracellular region of ErbB4 adopts a tethered conformation in the absence of ligand. Proc Natl Acad Sci U S A 102: 15024-15029.

Bridge JA, et al. 2001. Fusion of the ALK gene to the clathrin heavy chain gene, CLTC, in inflammatory myofibroblastic tumor. Am J Pathol 159: 411-415.

Brodsky FM, Chen CY, Knuehl C, Towler MC, Wakeham DE. 2001. Biological basket weaving: formation and function of clathrin-coated vesicles. Annu Rev Cell Dev Biol 17: 517-568.

Brugge JS, Erikson RL. 1977. Identification of a transformation-specific antigen induced by an avian sarcoma virus. Nature 269: 346-348.

Bruno IG, Jin W, Cote GJ. 2004. Correction of aberrant FGFR1 alternative RNA splicing through targeting of intronic regulatory elements. Hum Mol Genet 13: 2409-2420.

Bucci C, Parton RG, Mather IH, Stunnenberg H, Simons K, Hoflack B, Zerial M. 1992. The small GTPase rab5 functions as a regulatory factor in the early endocytic pathway. Cell 70: 715-728.

Buday L, Downward J. 2007. Roles of cortactin in tumor pathogenesis. Biochim Biophys Acta 1775: 263-273.

Burgar HR, Burns HD, Elsden JL, Lalioti MD, Heath JK. 2002. Association of the signaling adaptor FRS2 with fibroblast growth factor receptor 1 (Fgfr1) is mediated by alternative splicing of the juxtamembrane domain. J Biol Chem 277: 4018-4023.

Burgess AW, Cho HS, Eigenbrot C, Ferguson KM, Garrett TP, Leahy DJ, Lemmon MA, Sliwkowski MX, Ward CW, Yokoyama S. 2003. An open-and-shut case? Recent insights into the activation of EGF/ErbB receptors. Mol Cell 12: 541-552.

Burke P, Schooler K, Wiley HS. 2001. Regulation of epidermal growth factor receptor signaling by endocytosis and intracellular trafficking. Mol Biol Cell 12: 1897-1910.

Campone M, et al. 2012. Phase II study of single-agent bosutinib, a Src/Abl tyrosine kinase inhibitor, in patients with locally advanced or metastatic breast cancer pretreated with chemotherapy. Ann Oncol 23: 610-617.

Cantley LC, Songyang Z. 1994. Specificity in recognition of phosphopeptides by src-homology 2 domains. J Cell Sci Suppl 18: 121-126.

Cardone MH, Roy N, Stennicke HR, Salvesen GS, Franke TF, Stanbridge E, Frisch S, Reed JC. 1998. Regulation of cell death protease caspase-9 by phosphorylation. Science 282: 1318-1321.

Care BR, Soula HA. 2011. Impact of receptor clustering on ligand binding. BMC Syst Biol 5: 48.

Carstens RP, Eaton JV, Krigman HR, Walther PJ, Garcia-Blanco MA. 1997. Alternative splicing of fibroblast growth factor receptor 2 (FGF-R2) in human prostate cancer. Oncogene 15: 3059-3065.

Cartwright CA, Kamps MP, Meisler AI, Pipas JM, Eckhart W. 1989. pp60c-src activation in human colon carcinoma. J Clin Invest 83: 2025-2033.

Cavallaro U, Christofori G. 2004. Cell adhesion and signalling by cadherins and Ig-CAMs in cancer. Nat Rev Cancer 4: 118-132.

Ceridono M, Belleudi F, Ceccarelli S, Torrisi MR. 2005. Tyrosine 769 of the keratinocyte growth factor receptor is required for receptor signaling but not endocytosis. Biochem Biophys Res Commun 327: 523-532.

Cha JY, Maddileti S, Mitin N, Harden TK, Der CJ. 2009. Aberrant receptor internalization and enhanced FRS2-dependent signaling contribute to the transforming activity of the fibroblast growth factor receptor 2 IIIb C3 isoform. J Biol Chem 284: 6227-6240.

Chang H, Stewart AK, Qi XY, Li ZH, Yi QL, Trudel S. 2005. Immunohistochemistry accurately predicts FGFR3 aberrant expression and t(4;14) in multiple myeloma. Blood 106: 353-355.

Chavrier P, Goud B. 1999. The role of ARF and Rab GTPases in membrane transport. Curr Opin Cell Biol 11: 466-475.

Chellaiah AT, McEwen DG, Werner S, Xu J, Ornitz DM. 1994. Fibroblast growth factor receptor (FGFR) 3. Alternative splicing in immunoglobulin-like domain III creates a receptor highly specific for acidic FGF/FGF-1. J Biol Chem 269: 11620-11627.

Chen H, Ma J, Li W, Eliseenkova AV, Xu C, Neubert TA, Miller WT, Mohammadi M. 2007. A molecular brake in the kinase hinge region regulates the activity of receptor tyrosine kinases. Mol Cell 27: 717-730.

Chen RH, Tung R, Abate C, Blenis J. 1993. Cytoplasmic to nuclear signal transduction by mitogen-activated protein kinase and 90 kDa ribosomal S6 kinase. Biochem Soc Trans 21: 895-900.

Chen YJ, Shen MR, Maa MC, Leu TH. 2008. Eps8 decreases chemosensitivity and affects survival of cervical cancer patients. Mol Cancer Ther 7: 1376-1385.

Cheng L, Zhang S, Davidson DD, MacLennan GT, Koch MO, Montironi R, Lopez-Beltran A. 2009. Molecular determinants of tumor recurrence in the urinary bladder. Future Oncol 5: 843-857.

Chesi M, Nardini E, Brents LA, Schrock E, Ried T, Kuehl WM, Bergsagel PL. 1997. Frequent translocation t(4;14)(p16.3;q32.3) in multiple myeloma is associated with increased expression and activating mutations of fibroblast growth factor receptor 3. Nat Genet 16: 260-264.

Cho JY, Guo C, Torello M, Lunstrum GP, Iwata T, Deng C, Horton WA. 2004. Defective lysosomal targeting of activated fibroblast growth factor receptor 3 in achondroplasia. Proc Natl Acad Sci U S A 101: 609-614.

Christensen C, Lauridsen JB, Berezin V, Bock E, Kiselyov VV. 2006. The neural cell adhesion molecule binds to fibroblast growth factor receptor 2. FEBS Lett 580: 3386-3390.

Christoforidis S, McBride HM, Burgoyne RD, Zerial M. 1999. The Rab5 effector EEA1 is a core component of endosome docking. Nature 397: 621-625.

Chu PY, et al. 2012. Expression of Eps8 correlates with poor survival in oral squamous cell carcinoma. Asia Pac J Clin Oncol 8: e77-81.

Citores L, Wesche J, Kolpakova E, Olsnes S. 1999. Uptake and intracellular transport of acidic fibroblast growth factor: evidence for free and cytoskeleton-anchored fibroblast growth factor receptors. Mol Biol Cell 10: 3835-3848.

Citores L, Khnykin D, Sorensen V, Wesche J, Klingenberg O, Wiedlocha A, Olsnes S. 2001. Modulation of intracellular transport of acidic fibroblast growth factor by mutations in the cytoplasmic receptor domain. J Cell Sci 114: 1677-1689.

Cobb MH, Sang BC, Gonzalez R, Goldsmith E, Ellis L. 1989. Autophosphorylation activates the soluble cytoplasmic domain of the insulin receptor in an intermolecular reaction. J Biol Chem 264: 18701-18706.

Cohen MM, Jr. 2006. The new bone biology: pathologic, molecular, and clinical correlates. Am J Med Genet A 140: 2646-2706.

Cohn MJ, Izpisua-Belmonte JC, Abud H, Heath JK, Tickle C. 1995. Fibroblast growth factors induce additional limb development from the flank of chick embryos. Cell 80: 739-746.

Collins BM, McCoy AJ, Kent HM, Evans PR, Owen DJ. 2002. Molecular architecture and functional model of the endocytic AP2 complex. Cell 109: 523-535.

Colvin JS, White AC, Pratt SJ, Ornitz DM. 2001. Lung hypoplasia and neonatal death in Fgf9-null mice identify this gene as an essential regulator of lung mesenchyme. Development 128: 2095-2106.

Cooper JA, King CS. 1986. Dephosphorylation or antibody binding to the carboxy terminus stimulates pp60c-src. Mol Cell Biol 6: 4467-4477.

Cornejo-Roldan LR, Roessler E, Muenke M. 1999. Analysis of the mutational spectrum of the FGFR2 gene in Pfeiffer syndrome. Hum Genet 104: 425-431.

Corvera S. 1990. Insulin stimulates the assembly of cytosolic clathrin onto adipocyte plasma membranes. J Biol Chem 265: 2413-2416.

Cotton LM, O'Bryan MK, Hinton BT. 2008. Cellular signaling by fibroblast growth factors (FGFs) and their receptors (FGFRs) in male reproduction. Endocr Rev 29: 193-216.

Couet J, Sargiacomo M, Lisanti MP. 1997. Interaction of a receptor tyrosine kinase, EGF-R, with caveolins. Caveolin binding negatively regulates tyrosine and serine/threonine kinase activities. J Biol Chem 272: 30429-30438.

Coupin GT, Muller CD, Remy-Kristensen A, Kuhry JG. 1999. Cell surface membrane homeostasis and intracellular membrane traffic balance in mouse L929 cells. J Cell Sci 112 (Pt 14): 2431-2440.

Courtneidge SA. 2002. Role of Src in signal transduction pathways. The Jubilee Lecture. Biochem Soc Trans 30: 11-17.

Creighton TE. 1984. Pathways and mechanisms of protein folding. Adv Biophys 18: 1-20.

Cross DA, Alessi DR, Cohen P, Andjelkovich M, Hemmings BA. 1995. Inhibition of glycogen synthase kinase-3 by insulin mediated by protein kinase B. Nature 378: 785-789.

Crowther RA, Finch JT, Pearse BM. 1976. On the structure of coated vesicles. J Mol Biol 103: 785-798.

Cunningham DL, Sweet SM, Cooper HJ, Heath JK. 2010. Differential phosphoproteomics of fibroblast growth factor signaling: identification of Src family kinase-mediated phosphorylation events. J Proteome Res 9: 2317-2328.

Damm EM, Pelkmans L, Kartenbeck J, Mezzacasa A, Kurzchalia T, Helenius A. 2005. Clathrin- and caveolin-1-independent endocytosis: entry of simian virus 40 into cells devoid of caveolae. J Cell Biol 168: 477-488.

Damon DH, Lobb RR, D'Amore PA, Wagner JA. 1989. Heparin potentiates the action of acidic fibroblast growth factor by prolonging its biological half-life. J Cell Physiol 138: 221-226.

Dan HC, Sun M, Kaneko S, Feldman RI, Nicosia SV, Wang HG, Tsang BK, Cheng JQ. 2004. Akt phosphorylation and stabilization of X-linked inhibitor of apoptosis protein (XIAP). J Biol Chem 279: 5405-5412.

Daniels MA, Teixeiro E, Gill J, Hausmann B, Roubaty D, Holmberg K, Werlen G, Hollander GA, Gascoigne NR, Palmer E. 2006. Thymic selection threshold defined by compartmentalization of Ras/MAPK signalling. Nature 444: 724-729.

David-Pfeuty T, Nouvian-Dooghe Y. 1990. Immunolocalization of the cellular src protein in interphase and mitotic NIH c-src overexpresser cells. J Cell Biol 111: 3097-3116.

De Camilli P, Takei K, McPherson PS. 1995. The function of dynamin in endocytosis. Curr Opin Neurobiol 5: 559-565.

Delezoide AL, Benoist-Lasselin C, Legeai-Mallet L, Le Merrer M, Munnich A, Vekemans M, Bonaventure J. 1998. Spatio-temporal expression of FGFR 1, 2 and 3 genes during human embryo-fetal ossification. Mech Dev 77: 19-30.

Dell'Angelica EC, Klumperman J, Stoorvogel W, Bonifacino JS. 1998. Association of the AP-3 adaptor complex with clathrin. Science 280: 431-434.

Dell KR, Williams LT. 1992. A novel form of fibroblast growth factor receptor 2. Alternative splicing of the third immunoglobulin-like domain confers ligand binding specificity. J Biol Chem 267: 21225-21229.

Deng CX, Wynshaw-Boris A, Shen MM, Daugherty C, Ornitz DM, Leder P. 1994. Murine FGFR-1 is required for early postimplantation growth and axial organization. Genes Dev 8: 3045-3057.

DeVore DL, Horvitz HR, Stern MJ. 1995. An FGF receptor signaling pathway is required for the normal cell migrations of the sex myoblasts in C. elegans hermaphrodites. Cell 83: 611-620.

Di Fiore PP, De Camilli P. 2001. Endocytosis and signaling. an inseparable partnership. Cell 106: 1-4.

Di Fiore PP, Scita G. 2002. Eps8 in the midst of GTPases. Int J Biochem Cell Biol 34: 1178-1183.

Dickinson RJ, Eblaghie MC, Keyse SM, Morriss-Kay GM. 2002. Expression of the ERK-specific MAP kinase phosphatase PYST1/MKP3 in mouse embryos during morphogenesis and early organogenesis. Mech Dev 113: 193-196.

Dikic I, Giordano S. 2003. Negative receptor signalling. Curr Opin Cell Biol 15: 128-135.

Disanza A, Frittoli E, Palamidessi A, Scita G. 2009. Endocytosis and spatial restriction of cell signaling. Mol Oncol 3: 280-296.

Disanza A, et al. 2006. Regulation of cell shape by Cdc42 is mediated by the synergic actin-bundling activity of the Eps8-IRSp53 complex. Nat Cell Biol 8: 1337-1347.

Doherty GJ, McMahon HT. 2009. Mechanisms of endocytosis. Annu Rev Biochem 78: 857-902.

Dorey K, Amaya E. 2010. FGF signalling: diverse roles during early vertebrate embryogenesis. Development 137: 3731-3742.

Dowd CJ, Cooney CL, Nugent MA. 1999. Heparan sulfate mediates bFGF transport through basement membrane by diffusion with rapid reversible binding. J Biol Chem 274: 5236-5244.

Duan DS, Werner S, Williams LT. 1992. A naturally occurring secreted form of fibroblast growth factor (FGF) receptor 1 binds basic FGF in preference over acidic FGF. J Biol Chem 267: 16076-16080.

Dudka AA, Sweet SM, Heath JK. 2010. Signal transducers and activators of transcription-3 binding to the fibroblast growth factor receptor is activated by receptor amplification. Cancer Res 70: 3391-3401.

Easton DF, et al. 2007. Genome-wide association study identifies novel breast cancer susceptibility loci. Nature 447: 1087-1093.

Eblaghie MC, Lunn JS, Dickinson RJ, Munsterberg AE, Sanz-Ezquerro JJ, Farrell ER, Mathers J, Keyse SM, Storey K, Tickle C. 2003. Negative feedback regulation of FGF signaling levels by Pyst1/MKP3 in chick embryos. Curr Biol 13: 1009-1018.

Engqvist-Goldstein AE, Warren RA, Kessels MM, Keen JH, Heuser J, Drubin DG. 2001. The actin-binding protein Hip1R associates with clathrin during early stages of endocytosis and promotes clathrin assembly in vitro. J Cell Biol 154: 1209-1223.

Eswarakumar VP, Lax I, Schlessinger J. 2005. Cellular signaling by fibroblast growth factor receptors. Cytokine Growth Factor Rev 16: 139-149.

Faham S, Hileman RE, Fromm JR, Linhardt RJ, Rees DC. 1996. Heparin structure and interactions with basic fibroblast growth factor. Science 271: 1116-1120.

Falasca M, Logan SK, Lehto VP, Baccante G, Lemmon MA, Schlessinger J. 1998. Activation of phospholipase C gamma by PI 3-kinase-induced PH domain-mediated membrane targeting. EMBO J 17: 414-422.

Favelyukis S, Till JH, Hubbard SR, Miller WT. 2001. Structure and autoregulation of the insulin-like growth factor 1 receptor kinase. Nat Struct Biol 8: 1058-1063.

Fazioli F, Minichiello L, Matoska V, Castagnino P, Miki T, Wong WT, Di Fiore PP. 1993. Eps8, a substrate for the epidermal growth factor receptor kinase, enhances EGF-dependent mitogenic signals. EMBO J 12: 3799-3808.

Ferguson SM, et al. 2009. Coordinated actions of actin and BAR proteins upstream of dynamin at endocytic clathrin-coated pits. Dev Cell 17: 811-822.

Ferrell JE, Jr., Bhatt RR. 1997. Mechanistic studies of the dual phosphorylation of mitogen-activated protein kinase. J Biol Chem 272: 19008-19016.

Flaumenhaft R, Moscatelli D, Rifkin DB. 1990. Heparin and heparan sulfate increase the radius of diffusion and action of basic fibroblast growth factor. J Cell Biol 111: 1651-1659.

Floyd S, De Camilli P. 1998. Endocytosis proteins and cancer: a potential link? Trends Cell Biol 8: 299-301.

Ford-Perriss M, Abud H, Murphy M. 2001. Fibroblast growth factors in the developing central nervous system. Clin Exp Pharmacol Physiol 28: 493-503.

Ford MG, Mills IG, Peter BJ, Vallis Y, Praefcke GJ, Evans PR, McMahon HT. 2002. Curvature of clathrin-coated pits driven by epsin. Nature 419: 361-366.

Ford MG, Pearse BM, Higgins MK, Vallis Y, Owen DJ, Gibson A, Hopkins CR, Evans PR, McMahon HT. 2001. Simultaneous binding of PtdIns(4,5)P2 and clathrin by AP180 in the nucleation of clathrin lattices on membranes. Science 291: 1051-1055.

Fra AM, Williamson E, Simons K, Parton RG. 1995. De novo formation of caveolae in lymphocytes by expression of VIP21-caveolin. Proc Natl Acad Sci U S A 92: 8655-8659.

Francavilla C, Cattaneo P, Berezin V, Bock E, Ami D, de Marco A, Christofori G, Cavallaro U. 2009. The binding of NCAM to FGFR1 induces a specific cellular response mediated by receptor trafficking. J Cell Biol 187: 1101-1116.

Franke TF. 2008. Intracellular signaling by Akt: bound to be specific. Sci Signal 1: pe29.

Furdui CM, Lew ED, Schlessinger J, Anderson KS. 2006. Autophosphorylation of FGFR1 kinase is mediated by a sequential and precisely ordered reaction. Mol Cell 21: 711-717.

Furthauer M, Lin W, Ang SL, Thisse B, Thisse C. 2002. Sef is a feedback-induced antagonist of Ras/MAPK-mediated FGF signalling. Nat Cell Biol 4: 170-174.

Gelsi-Boyer V, et al. 2005. Comprehensive profiling of 8p11-12 amplification in breast cancer. Mol Cancer Res 3: 655-667.

Gill JC, Moenter SM, Tsai PS. 2004. Developmental regulation of gonadotropin-releasing hormone neurons by fibroblast growth factor signaling. Endocrinology 145: 3830-3839.

Gillespie LL, Chen G, Paterno GD. 1995. Cloning of a fibroblast growth factor receptor 1 splice variant from Xenopus embryos that lacks a protein kinase C site important for the regulation of receptor activity. J Biol Chem 270: 22758-22763.

Gisselbrecht S, Skeath JB, Doe CQ, Michelson AM. 1996. heartless encodes a fibroblast growth factor receptor (DFR1/DFGF-R2) involved in the directional migration of early mesodermal cells in the Drosophila embryo. Genes Dev 10: 3003-3017.

Gleizes PE, Noaillac-Depeyre J, Dupont MA, Gas N. 1996. Basic fibroblast growth factor (FGF-2) is addressed to caveolae after binding to the plasma membrane of BHK cells. Eur J Cell Biol 71: 144-153.

Gorvel JP, Chavrier P, Zerial M, Gruenberg J. 1991. rab5 controls early endosome fusion in vitro. Cell 64: 915-925.

Gotoh N. 2008. Regulation of growth factor signaling by FRS2 family docking/scaffold adaptor proteins. Cancer Sci 99: 1319-1325.

Gotoh N, Laks S, Nakashima M, Lax I, Schlessinger J. 2004. FRS2 family docking proteins with overlapping roles in activation of MAP kinase have distinct spatial-temporal patterns of expression of their transcripts. FEBS Lett 564: 14-18.

Gould SE, Upholt WB, Kosher RA. 1995. Characterization of chicken syndecan-3 as a heparan sulfate proteoglycan and its expression during embryogenesis. Dev Biol 168: 438-451.

Grant BD, Donaldson JG. 2009. Pathways and mechanisms of endocytic recycling. Nat Rev Mol Cell Biol 10: 597-608.

Griffin K, Patient R, Holder N. 1995. Analysis of FGF function in normal and no tail zebrafish embryos reveals separate mechanisms for formation of the trunk and the tail. Development 121: 2983-2994.

Griner EM, Kazanietz MG. 2007. Protein kinase C and other diacylglycerol effectors in cancer. Nat Rev Cancer 7: 281-294.

Gross I, Bassit B, Benezra M, Licht JD. 2001. Mammalian sprouty proteins inhibit cell growth and differentiation by preventing ras activation. J Biol Chem 276: 46460-46468.

Grosshans BL, Ortiz D, Novick P. 2006. Rabs and their effectors: achieving specificity in membrane traffic. Proc Natl Acad Sci U S A 103: 11821-11827.

Gruenberg J. 2001. The endocytic pathway: a mosaic of domains. Nat Rev Mol Cell Biol 2: 721-730.

Gruenberg J, Stenmark H. 2004. The biogenesis of multivesicular endosomes. Nat Rev Mol Cell Biol 5: 317-323.

Guillonneau X, Regnier-Ricard F, Laplace O, Jonet L, Bryckaert M, Courtois Y, Mascarelli F. 1998. Fibroblast growth factor (FGF) soluble receptor 1 acts as a natural inhibitor of FGF2 neurotrophic activity during retinal degeneration. Mol Biol Cell 9: 2785-2802.

Guimond SE, Turnbull JE. 1999. Fibroblast growth factor receptor signalling is dictated by specific heparan sulphate saccharides. Curr Biol 9: 1343-1346.

Guy GR, Jackson RA, Yusoff P, Chow SY. 2009. Sprouty proteins: modified modulators, matchmakers or missing links? J Endocrinol 203: 191-202.

Habermann B. 2004. The BAR-domain family of proteins: a case of bending and binding? EMBO Rep 5: 250-255.

Hacohen N, Kramer S, Sutherland D, Hiromi Y, Krasnow MA. 1998. sprouty encodes a novel antagonist of FGF signaling that patterns apical branching of the Drosophila airways. Cell 92: 253-263.

Haines BP, Wheldon LM, Summerbell D, Heath JK, Rigby PW. 2006. Regulated expression of FLRT genes implies a functional role in the regulation of FGF signalling during mouse development. Dev Biol 297: 14-25.

Hall AB, Jura N, DaSilva J, Jang YJ, Gong D, Bar-Sagi D. 2003. hSpry2 is targeted to the ubiquitin-dependent proteasome pathway by c-Cbl. Curr Biol 13: 308-314.

Hammer JA, 3rd, Wu XS. 2002. Rabs grab motors: defining the connections between Rab GTPases and motor proteins. Curr Opin Cell Biol 14: 69-75.

Hanafusa H, Torii S, Yasunaga T, Nishida E. 2002. Sprouty1 and Sprouty2 provide a control mechanism for the Ras/MAPK signalling pathway. Nat Cell Biol 4: 850-858.

Hancock JF. 2003. Ras proteins: different signals from different locations. Nat Rev Mol Cell Biol 4: 373-384.

Hanneken A. 2001. Structural characterization of the circulating soluble FGF receptors reveals multiple isoforms generated by secretion and ectodomain shedding. FEBS Lett 489: 176-181.

Hanover JA, Willingham MC, Pastan I. 1984. Kinetics of transit of transferrin and epidermal growth factor through clathrin-coated membranes. Cell 39: 283-293.

Haugsten EM, Wiedlocha A, Olsnes S, Wesche J. 2010. Roles of fibroblast growth factor receptors in carcinogenesis. Mol Cancer Res 8: 1439-1452.

Haugsten EM, Sorensen V, Brech A, Olsnes S, Wesche J. 2005. Different intracellular trafficking of FGF1 endocytosed by the four homologous FGF receptors. J Cell Sci 118: 3869-3881.

Haugsten EM, Zakrzewska M, Brech A, Pust S, Olsnes S, Sandvig K, Wesche J. 2011. Clathrin- and dynamin-independent endocytosis of FGFR3--implications for signalling. PLoS One 6: e21708.

Hayer A, Stoeber M, Ritz D, Engel S, Meyer HH, Helenius A. 2010. Caveolin-1 is ubiquitinated and targeted to intralumenal vesicles in endolysosomes for degradation. J Cell Biol 191: 615-629.

Hellberg C, Schmees C, Karlsson S, Ahgren A, Heldin CH. 2009. Activation of protein kinase C alpha is necessary for sorting the PDGF beta-receptor to Rab4a-dependent recycling. Mol Biol Cell 20: 2856-2863.

Henley JR, Krueger EW, Oswald BJ, McNiven MA. 1998. Dynamin-mediated internalization of caveolae. J Cell Biol 141: 85-99.

Henne WM, Boucrot E, Meinecke M, Evergren E, Vallis Y, Mittal R, McMahon HT. 2010. FCHo proteins are nucleators of clathrin-mediated endocytosis. Science 328: 1281-1284.

Herold CI, et al. 2011. Phase II trial of dasatinib in patients with metastatic breast cancer using real-time pharmacodynamic tissue biomarkers of Src inhibition to escalate dosing. Clin Cancer Res 17: 6061-6070.

Herr AB, Ornitz DM, Sasisekharan R, Venkataraman G, Waksman G. 1997. Heparin-induced self-association of fibroblast growth factor-2. Evidence for two oligomerization processes. J Biol Chem 272: 16382-16389.

Hinrichsen L, Meyerholz A, Groos S, Ungewickell EJ. 2006. Bending a membrane: how clathrin affects budding. Proc Natl Acad Sci U S A 103: 8715-8720.

Hinsby AM, Berezin V, Bock E. 2004. Molecular mechanisms of NCAM function. Front Biosci 9: 2227-2244.

Hsu VW, Prekeris R. 2010. Transport at the recycling endosome. Curr Opin Cell Biol 22: 528-534.

Iba H, Takeya T, Cross FR, Hanafusa T, Hanafusa H. 1984. Rous sarcoma virus variants that carry the cellular src gene instead of the viral src gene cannot transform chicken embryo fibroblasts. Proc Natl Acad Sci U S A 81: 4424-4428.

Innocenti M, Tenca P, Frittoli E, Faretta M, Tocchetti A, Di Fiore PP, Scita G. 2002. Mechanisms through which Sos-1 coordinates the activation of Ras and Rac. J Cell Biol 156: 125-136.

Irby RB, Mao W, Coppola D, Kang J, Loubeau JM, Trudeau W, Karl R, Fujita DJ, Jove R, Yeatman TJ. 1999. Activating SRC mutation in a subset of advanced human colon cancers. Nat Genet 21: 187-190.

Itoh N, Ornitz DM. 2004. Evolution of the Fgf and Fgfr gene families. Trends Genet 20: 563-569.

Jackson CC, Medeiros LJ, Miranda RN. 2010. 8p11 myeloproliferative syndrome: a review. Hum Pathol 41: 461-476.

Jang JH, Shin KH, Park JG. 2001. Mutations in fibroblast growth factor receptor 2 and fibroblast growth factor receptor 3 genes associated with human gastric and colorectal cancers. Cancer Res 61: 3541-3543.

Jekely G, Sung HH, Luque CM, Rorth P. 2005. Regulators of endocytosis maintain localized receptor tyrosine kinase signaling in guided migration. Dev Cell 9: 197-207.

Jiang X, Sorkin A. 2002. Coordinated traffic of Grb2 and Ras during epidermal growth factor receptor endocytosis visualized in living cells. Mol Biol Cell 13: 1522-1535.

Jin C, Wang F, Wu X, Yu C, Luo Y, McKeehan WL. 2004. Directionally specific paracrine communication mediated by epithelial FGF9 to stromal FGFR3 in two-compartment premalignant prostate tumors. Cancer Res 64: 4555-4562.

Jing SQ, Spencer T, Miller K, Hopkins C, Trowbridge IS. 1990. Role of the human transferrin receptor cytoplasmic domain in endocytosis: localization of a specific signal sequence for internalization. J Cell Biol 110: 283-294.

Joffre C, Barrow R, Menard L, Calleja V, Hart IR, Kermorgant S. 2011. A direct role for Met endocytosis in tumorigenesis. Nat Cell Biol 13: 827-837.

Johnson DE, Williams LT. 1993. Structural and functional diversity in the FGF receptor multigene family. Adv Cancer Res 60: 1-41.

Johnson DE, Lu J, Chen H, Werner S, Williams LT. 1991. The human fibroblast growth factor receptor genes: a common structural arrangement underlies the mechanisms for generating receptor forms that differ in their third immunoglobulin domain. Mol Cell Biol 11: 4627-4634.

Johnson LN, Noble ME, Owen DJ. 1996. Active and inactive protein kinases: structural basis for regulation. Cell 85: 149-158.

Kalff A, Spencer A. 2012. The t(4;14) translocation and FGFR3 overexpression in multiple myeloma: prognostic implications and current clinical strategies. Blood Cancer J 2: e89.

Kalinina J, Dutta K, Ilghari D, Beenken A, Goetz R, Eliseenkova AV, Cowburn D, Mohammadi M. 2012. The alternatively spliced acid box region plays a key role in FGF receptor autoinhibition. Structure 20: 77-88.

Kamioka Y, Yasuda S, Fujita Y, Aoki K, Matsuda M. 2010. Multiple decisive phosphorylation sites for the negative feedback regulation of SOS1 via ERK. J Biol Chem 285: 33540-33548.

Kan M, Wu X, Wang F, McKeehan WL. 1999. Specificity for fibroblast growth factors determined by heparan sulfate in a binary complex with the receptor kinase. J Biol Chem 274: 15947-15952.

Kan M, Wang F, Xu J, Crabb JW, Hou J, McKeehan WL. 1993. An essential heparin-binding domain in the fibroblast growth factor receptor kinase. Science 259: 1918-1921.

Kannan K, Givol D. 2000. FGF receptor mutations: dimerization syndromes, cell growth suppression, and animal models. IUBMB Life 49: 197-205.

Kaplan JM, Mardon G, Bishop JM, Varmus HE. 1988. The first seven amino acids encoded by the v-src oncogene act as a myristylation signal: lysine 7 is a critical determinant. Mol Cell Biol 8: 2435-2441.

Kaplan KB, Swedlow JR, Varmus HE, Morgan DO. 1992. Association of p60c-src with endosomal membranes in mammalian fibroblasts. J Cell Biol 118: 321-333.

Kazazic M, Roepstorff K, Johannessen LE, Pedersen NM, van Deurs B, Stang E, Madshus IH. 2006. EGF-induced activation of the EGF receptor does not trigger mobilization of caveolae. Traffic 7: 1518-1527.

Kelly BT, McCoy AJ, Spate K, Miller SE, Evans PR, Honing S, Owen DJ. 2008. A structural explanation for the binding of endocytic dileucine motifs by the AP2 complex. Nature 456: 976-979.

Kennedy SG, Kandel ES, Cross TK, Hay N. 1999. Akt/Protein kinase B inhibits cell death by preventing the release of cytochrome c from mitochondria. Mol Cell Biol 19: 5800-5810.

Kirchhausen T, Harrison SC. 1981. Protein organization in clathrin trimers. Cell 23: 755-761.

Kiselyov VV, et al. 2003. Structural basis for a direct interaction between FGFR1 and NCAM and evidence for a regulatory role of ATP. Structure 11: 691-701.

Kishan KV, Scita G, Wong WT, Di Fiore PP, Newcomer ME. 1997. The SH3 domain of Eps8 exists as a novel intertwined dimer. Nat Struct Biol 4: 739-743.

Klagsbrun M. 1990. The affinity of fibroblast growth factors (FGFs) for heparin; FGF-heparan sulfate interactions in cells and extracellular matrix. Curr Opin Cell Biol 2: 857-863.

Klambt C, Glazer L, Shilo BZ. 1992. breathless, a Drosophila FGF receptor homolog, is essential for migration of tracheal and specific midline glial cells. Genes Dev 6: 1668-1678.

Knights V, Cook SJ. 2010. De-regulated FGF receptors as therapeutic targets in cancer. Pharmacol Ther 125: 105-117.

Koegl M, Zlatkine P, Ley SC, Courtneidge SA, Magee AI. 1994. Palmitoylation of multiple Src-family kinases at a homologous N-terminal motif. Biochem J 303 (Pt 3): 749-753.

Kolch W. 2000. Meaningful relationships: the regulation of the Ras/Raf/MEK/ERK pathway by protein interactions. Biochem J 351 Pt 2: 289-305.

Kouhara H, Hadari YR, Spivak-Kroizman T, Schilling J, Bar-Sagi D, Lax I, Schlessinger J. 1997. A lipid-anchored Grb2-binding protein that links FGF-receptor activation to the Ras/MAPK signaling pathway. Cell 89: 693-702.

Kovalenko D, Yang X, Nadeau RJ, Harkins LK, Friesel R. 2003. Sef inhibits fibroblast growth factor signaling by inhibiting FGFR1 tyrosine phosphorylation and subsequent ERK activation. J Biol Chem 278: 14087-14091.

Kremer NE, D'Arcangelo G, Thomas SM, DeMarco M, Brugge JS, Halegoua S. 1991. Signal transduction by nerve growth factor and fibroblast growth factor in PC12 cells requires a sequence of src and ras actions. J Cell Biol 115: 809-819.

Kurosu H, Choi M, Ogawa Y, Dickson AS, Goetz R, Eliseenkova AV, Mohammadi M, Rosenblatt KP, Kliewer SA, Kuro-o M. 2007. Tissue-specific expression of betaKlotho and fibroblast growth factor (FGF) receptor isoforms determines metabolic activity of FGF19 and FGF21. J Biol Chem 282: 26687-26695.

Kurosu H, et al. 2006. Regulation of fibroblast growth factor-23 signaling by klotho. J Biol Chem 281: 6120-6123.

Kwabi-Addo B, Ozen M, Ittmann M. 2004. The role of fibroblast growth factors and their receptors in prostate cancer. Endocr Relat Cancer 11: 709-724.

Kypta RM, Goldberg Y, Ulug ET, Courtneidge SA. 1990. Association between the PDGF receptor and members of the src family of tyrosine kinases. Cell 62: 481-492.

Lacy SE, Bonnemann CG, Buzney EA, Kunkel LM. 1999. Identification of FLRT1, FLRT2, and FLRT3: a novel family of transmembrane leucine-rich repeat proteins. Genomics 62: 417-426.

Lajeunie E, Heuertz S, El Ghouzzi V, Martinovic J, Renier D, Le Merrer M, Bonaventure J. 2006. Mutation screening in patients with syndromic craniosynostoses indicates that a

limited number of recurrent FGFR2 mutations accounts for severe forms of Pfeiffer syndrome. Eur J Hum Genet 14: 289-298.

Lanzetti L, Rybin V, Malabarba MG, Christoforidis S, Scita G, Zerial M, Di Fiore PP. 2000. The Eps8 protein coordinates EGF receptor signalling through Rac and trafficking through Rab5. Nature 408: 374-377.

Larsson H, Klint P, Landgren E, Claesson-Welsh L. 1999. Fibroblast growth factor receptor-1-mediated endothelial cell proliferation is dependent on the Src homology (SH) 2/SH3 domain-containing adaptor protein Crk. J Biol Chem 274: 25726-25734.

Le Roy C, Wrana JL. 2005. Signaling and endocytosis: a team effort for cell migration. Dev Cell 9: 167-168.

Lemmon MA, Schlessinger J. 2010. Cell signaling by receptor tyrosine kinases. Cell 141: 1117-1134.

Leppanen VM, Prota AE, Jeltsch M, Anisimov A, Kalkkinen N, Strandin T, Lankinen H, Goldman A, Ballmer-Hofer K, Alitalo K. 2010. Structural determinants of growth factor binding and specificity by VEGF receptor 2. Proc Natl Acad Sci U S A 107: 2425-2430.

Letessier A, et al. 2006. Frequency, prognostic impact, and subtype association of 8p12, 8q24, 11q13, 12p13, 17q12, and 20q13 amplifications in breast cancers. BMC Cancer 6: 245.

Levkowitz G, Waterman H, Zamir E, Kam Z, Oved S, Langdon WY, Beguinot L, Geiger B, Yarden Y. 1998. c-Cbl/Sli-1 regulates endocytic sorting and ubiquitination of the epidermal growth factor receptor. Genes Dev 12: 3663-3674.

Lew ED, Furdui CM, Anderson KS, Schlessinger J. 2009. The precise sequence of FGF receptor autophosphorylation is kinetically driven and is disrupted by oncogenic mutations. Sci Signal 2: ra6.

Li C, Guo H, Xu X, Weinberg W, Deng CX. 2001. Fibroblast growth factor receptor 2 (Fgfr2) plays an important role in eyelid and skin formation and patterning. Dev Dyn 222: 471-483.

Li C, Scott DA, Hatch E, Tian X, Mansour SL. 2007. Dusp6 (Mkp3) is a negative feedback regulator of FGF-stimulated ERK signaling during mouse development. Development 134: 167-176.

Li E, You M, Hristova K. 2006. FGFR3 dimer stabilization due to a single amino acid pathogenic mutation. J Mol Biol 356: 600-612.

Li HS, Stolz DB, Romero G. 2005. Characterization of endocytic vesicles using magnetic microbeads coated with signalling ligands. Traffic 6: 324-334.

Li L, Cohen SN. 1996. Tsg101: a novel tumor susceptibility gene isolated by controlled homozygous functional knockout of allelic loci in mammalian cells. Cell 85: 319-329.

Li W, Liu H, Zhou JS, Cao JF, Zhou XB, Choi AM, Chen ZH, Shen HH. 2012. Caveolin-1 inhibits expression of antioxidant enzymes through direct interaction with nuclear erythroid 2 p45-related factor-2 (Nrf2). J Biol Chem 287: 20922-20930.

Li X, Brunton VG, Burgar HR, Wheldon LM, Heath JK. 2004. FRS2-dependent SRC activation is required for fibroblast growth factor receptor-induced phosphorylation of Sprouty and suppression of ERK activity. J Cell Sci 117: 6007-6017.

Liang J, et al. 2002. PKB/Akt phosphorylates p27, impairs nuclear import of p27 and opposes p27-mediated G1 arrest. Nat Med 8: 1153-1160.

Lim CP, Cao X. 2006. Structure, function, and regulation of STAT proteins. Mol Biosyst 2: 536-550.

Lin BC, Wang M, Blackmore C, Desnoyers LR. 2007. Liver-specific activities of FGF19 require Klotho beta. J Biol Chem 282: 27277-27284.

Lin W, Furthauer M, Thisse B, Thisse C, Jing N, Ang SL. 2002. Cloning of the mouse Sef gene and comparative analysis of its expression with Fgf8 and Spry2 during embryogenesis. Mech Dev 113: 163-168.

Liu H, Chen B, Xiong H, Huang QH, Zhang QH, Wang ZG, Li BL, Chen Z, Chen SJ. 2004. Functional contribution of EEN to leukemogenic transformation by MLL-EEN fusion protein. Oncogene 23: 3385-3394.

Liu J, Huang C, Zhan X. 1999. Src is required for cell migration and shape changes induced by fibroblast growth factor 1. Oncogene 18: 6700-6706.

Lo TL, Fong CW, Yusoff P, McKie AB, Chua MS, Leung HY, Guy GR. 2006. Sprouty and cancer: the first terms report. Cancer Lett 242: 141-150.

Lombardo CR, Consler TG, Kassel DB. 1995. In vitro phosphorylation of the epidermal growth factor receptor autophosphorylation domain by c-src: identification of phosphorylation sites and c-src SH2 domain binding sites. Biochemistry 34: 16456-16466.

Lombardo LJ, et al. 2004. Discovery of N-(2-chloro-6-methyl- phenyl)-2-(6-(4-(2-hydroxyethyl)- piperazin-1-yl)-2-methylpyrimidin-4- ylamino)thiazole-5-carboxamide (BMS-354825), a dual Src/Abl kinase inhibitor with potent antitumor activity in preclinical assays. J Med Chem 47: 6658-6661.

Lowenstein EJ, Daly RJ, Batzer AG, Li W, Margolis B, Lammers R, Ullrich A, Skolnik EY, Bar-Sagi D, Schlessinger J. 1992. The SH2 and SH3 domain-containing protein GRB2 links receptor tyrosine kinases to ras signaling. Cell 70: 431-442.

Lu SY, Sheikh F, Sheppard PC, Fresnoza A, Duckworth ML, Detillieux KA, Cattini PA. 2008. FGF-16 is required for embryonic heart development. Biochem Biophys Res Commun 373: 270-274.

Luttrell DK, Luttrell LM, Parsons SJ. 1988. Augmented mitogenic responsiveness to epidermal growth factor in murine fibroblasts that overexpress pp60c-src. Mol Cell Biol 8: 497-501.

Maa MC, Leu TH, McCarley DJ, Schatzman RC, Parsons SJ. 1995. Potentiation of epidermal growth factor receptor-mediated oncogenesis by c-Src: implications for the etiology of multiple human cancers. Proc Natl Acad Sci U S A 92: 6981-6985.

Maa MC, Lee JC, Chen YJ, Lee YC, Wang ST, Huang CC, Chow NH, Leu TH. 2007. Eps8 facilitates cellular growth and motility of colon cancer cells by increasing the expression and activity of focal adhesion kinase. J Biol Chem 282: 19399-19409.

Macia E, Ehrlich M, Massol R, Boucrot E, Brunner C, Kirchhausen T. 2006. Dynasore, a cell-permeable inhibitor of dynamin. Dev Cell 10: 839-850.

Magee J, Cygler M. 2011. Interactions between kinase scaffold MP1/p14 and its endosomal anchoring protein p18. Biochemistry 50: 3696-3705.

Magnusson MK, Meade KE, Brown KE, Arthur DC, Krueger LA, Barrett AJ, Dunbar CE. 2001. Rabaptin-5 is a novel fusion partner to platelet-derived growth factor beta receptor in chronic myelomonocytic leukemia. Blood 98: 2518-2525.

Maher P. 1999. p38 mitogen-activated protein kinase activation is required for fibroblast growth factor-2-stimulated cell proliferation but not differentiation. J Biol Chem 274: 17491-17498.

Manning G, Young SL, Miller WT, Zhai Y. 2008. The protist, Monosiga brevicollis, has a tyrosine kinase signaling network more elaborate and diverse than found in any known metazoan. Proc Natl Acad Sci U S A 105: 9674-9679.

Mansukhani A, Dell'Era P, Moscatelli D, Kornbluth S, Hanafusa H, Basilico C. 1992. Characterization of the murine BEK fibroblast growth factor (FGF) receptor: activation by three members of the FGF family and requirement for heparin. Proc Natl Acad Sci U S A 89: 3305-3309.

Marais R, Wynne J, Treisman R. 1993. The SRF accessory protein Elk-1 contains a growth factor-regulated transcriptional activation domain. Cell 73: 381-393.

Marchese C, Mancini P, Belleudi F, Felici A, Gradini R, Sansolini T, Frati L, Torrisi MR. 1998. Receptor-mediated endocytosis of keratinocyte growth factor. J Cell Sci 111 (Pt 23): 3517-3527.

Marsh SK, Bansal GS, Zammit C, Barnard R, Coope R, Roberts-Clarke D, Gomm JJ, Coombes RC, Johnston CL. 1999. Increased expression of fibroblast growth factor 8 in human breast cancer. Oncogene 18: 1053-1060.

Mason I. 2007. Initiation to end point: the multiple roles of fibroblast growth factors in neural development. Nat Rev Neurosci 8: 583-596.

Mason JM, Morrison DJ, Bassit B, Dimri M, Band H, Licht JD, Gross I. 2004. Tyrosine phosphorylation of Sprouty proteins regulates their ability to inhibit growth factor signaling: a dual feedback loop. Mol Biol Cell 15: 2176-2188.

Matoskova B, Wong WT, Salcini AE, Pelicci PG, Di Fiore PP. 1995. Constitutive phosphorylation of eps8 in tumor cell lines: relevance to malignant transformation. Mol Cell Biol 15: 3805-3812.

Mattila MM, Harkonen PL. 2007. Role of fibroblast growth factor 8 in growth and progression of hormonal cancer. Cytokine Growth Factor Rev 18: 257-266.

Mayor S, Pagano RE. 2007. Pathways of clathrin-independent endocytosis. Nat Rev Mol Cell Biol 8: 603-612.

McLauchlan H, Newell J, Morrice N, Osborne A, West M, Smythe E. 1998. A novel role for Rab5-GDI in ligand sequestration into clathrin-coated pits. Curr Biol 8: 34-45.

McMahon HT, Boucrot E. 2011. Molecular mechanism and physiological functions of clathrin-mediated endocytosis. Nat Rev Mol Cell Biol 12: 517-533.

Meakin SO, MacDonald JI, Gryz EA, Kubu CJ, Verdi JM. 1999. The signaling adapter FRS-2 competes with Shc for binding to the nerve growth factor receptor TrkA. A model for discriminating proliferation and differentiation. J Biol Chem 274: 9861-9870.

Mehta PB, Robson CN, Neal DE, Leung HY. 2001. Keratinocyte growth factor activates p38 MAPK to induce stress fibre formation in human prostate DU145 cells. Oncogene 20: 5359-5365.

Merrifield CJ, Perrais D, Zenisek D. 2005. Coupling between clathrin-coated-pit invagination, cortactin recruitment, and membrane scission observed in live cells. Cell 121: 593-606.

Meyers EN, Lewandoski M, Martin GR. 1998. An Fgf8 mutant allelic series generated by Cre- and Flp-mediated recombination. Nat Genet 18: 136-141.

Meyers GA, Orlow SJ, Munro IR, Przylepa KA, Jabs EW. 1995. Fibroblast growth factor receptor 3 (FGFR3) transmembrane mutation in Crouzon syndrome with acanthosis nigricans. Nat Genet 11: 462-464.

Miaczynska M, Zerial M. 2002. Mosaic organization of the endocytic pathway. Exp Cell Res 272: 8-14.

Miaczynska M, Bar-Sagi D. 2010. Signaling endosomes: seeing is believing. Curr Opin Cell Biol 22: 535-540.

Miaczynska M, Christoforidis S, Giner A, Shevchenko A, Uttenweiler-Joseph S, Habermann B, Wilm M, Parton RG, Zerial M. 2004. APPL proteins link Rab5 to nuclear signal transduction via an endosomal compartment. Cell 116: 445-456.

Miki T, Fleming TP, Bottaro DP, Rubin JS, Ron D, Aaronson SA. 1991. Expression cDNA cloning of the KGF receptor by creation of a transforming autocrine loop. Science 251: 72-75.

Miki T, Bottaro DP, Fleming TP, Smith CL, Burgess WH, Chan AM, Aaronson SA. 1992. Determination of ligand-binding specificity by alternative splicing: two distinct growth factor receptors encoded by a single gene. Proc Natl Acad Sci U S A 89: 246-250.

Mim C, Unger VM. 2012. Membrane curvature and its generation by BAR proteins. Trends Biochem Sci 37: 526-533.

Min H, Danilenko DM, Scully SA, Bolon B, Ring BD, Tarpley JE, DeRose M, Simonet WS. 1998. Fgf-10 is required for both limb and lung development and exhibits striking functional similarity to Drosophila branchless. Genes Dev 12: 3156-3161.

Moffa AB, Ethier SP. 2007. Differential signal transduction of alternatively spliced FGFR2 variants expressed in human mammary epithelial cells. J Cell Physiol 210: 720-731.

Mohammadi M, Schlessinger J, Hubbard SR. 1996a. Structure of the FGF receptor tyrosine kinase domain reveals a novel autoinhibitory mechanism. Cell 86: 577-587.

Mohammadi M, Olsen SK, Ibrahimi OA. 2005. Structural basis for fibroblast growth factor receptor activation. Cytokine Growth Factor Rev 16: 107-137.

Mohammadi M, Dikic I, Sorokin A, Burgess WH, Jaye M, Schlessinger J. 1996b. Identification of six novel autophosphorylation sites on fibroblast growth factor receptor 1 and elucidation of their importance in receptor activation and signal transduction. Mol Cell Biol 16: 977-989.

Mohammadi M, Dionne CA, Li W, Li N, Spivak T, Honegger AM, Jaye M, Schlessinger J. 1992. Point mutation in FGF receptor eliminates phosphatidylinositol hydrolysis without affecting mitogenesis. Nature 358: 681-684.

Mohammadi M, McMahon G, Sun L, Tang C, Hirth P, Yeh BK, Hubbard SR, Schlessinger J. 1997. Structures of the tyrosine kinase domain of fibroblast growth factor receptor in complex with inhibitors. Science 276: 955-960.

Mohammadi M, Honegger AM, Rotin D, Fischer R, Bellot F, Li W, Dionne CA, Jaye M, Rubinstein M, Schlessinger J. 1991. A tyrosine-phosphorylated carboxy-terminal peptide of the fibroblast growth factor receptor (Flg) is a binding site for the SH2 domain of phospholipase C-gamma 1. Mol Cell Biol 11: 5068-5078.

Mongiovi AM, Romano PR, Panni S, Mendoza M, Wong WT, Musacchio A, Cesareni G, Di Fiore PP. 1999. A novel peptide-SH3 interaction. EMBO J 18: 5300-5309.

Monsonego-Ornan E, Adar R, Feferman T, Segev O, Yayon A. 2000. The transmembrane mutation G380R in fibroblast growth factor receptor 3 uncouples ligand-mediated receptor activation from down-regulation. Mol Cell Biol 20: 516-522.

Montesano R, Roth J, Robert A, Orci L. 1982. Non-coated membrane invaginations are involved in binding and internalization of cholera and tetanus toxins. Nature 296: 651-653.

Mori S, Ronnstrand L, Yokote K, Engstrom A, Courtneidge SA, Claesson-Welsh L, Heldin CH. 1993. Identification of two juxtamembrane autophosphorylation sites in the PDGF beta-receptor; involvement in the interaction with Src family tyrosine kinases. EMBO J 12: 2257-2264.

Mosesson Y, Mills GB, Yarden Y. 2008. Derailed endocytosis: an emerging feature of cancer. Nat Rev Cancer 8: 835-850.

Motley A, Bright NA, Seaman MN, Robinson MS. 2003. Clathrin-mediated endocytosis in AP-2-depleted cells. J Cell Biol 162: 909-918.

Murzin AG, Lesk AM, Chothia C. 1992. beta-Trefoil fold. Patterns of structure and sequence in the Kunitz inhibitors interleukins-1 beta and 1 alpha and fibroblast growth factors. J Mol Biol 223: 531-543.

Muthuswamy SK, Gilman M, Brugge JS. 1999. Controlled dimerization of ErbB receptors provides evidence for differential signaling by homo- and heterodimers. Mol Cell Biol 19: 6845-6857.

Nagase T, Nagase M, Hirose S, Ohmori K. 1998. Mutations in fibroblast growth factor receptor 2 gene and craniosynostotic syndromes in Japanese children. J Craniofac Surg 9: 162-170.

Nagendra HG, Harrington AE, Harmer NJ, Pellegrini L, Blundell TL, Burke DF. 2001. Sequence analyses and comparative modeling of fly and worm fibroblast growth factor receptors indicate that the determinants for FGF and heparin binding are retained in evolution. FEBS Lett 501: 51-58.

Nagy P, Jenei A, Kirsch AK, Szollosi J, Damjanovich S, Jovin TM. 1999. Activation-dependent clustering of the erbB2 receptor tyrosine kinase detected by scanning near-field optical microscopy. J Cell Sci 112 (Pt 11): 1733-1741.

Nakatsu F, Ohno H. 2003. Adaptor protein complexes as the key regulators of protein sorting in the post-Golgi network. Cell Struct Funct 28: 419-429.

Niehrs C, Pollet N. 1999. Synexpression groups in eukaryotes. Nature 402: 483-487.

Nielsen E, Severin F, Backer JM, Hyman AA, Zerial M. 1999. Rab5 regulates motility of early endosomes on microtubules. Nat Cell Biol 1: 376-382.

Nolen B, Taylor S, Ghosh G. 2004. Regulation of protein kinases; controlling activity through activation segment conformation. Mol Cell 15: 661-675.

Oh P, McIntosh DP, Schnitzer JE. 1998. Dynamin at the neck of caveolae mediates their budding to form transport vesicles by GTP-driven fission from the plasma membrane of endothelium. J Cell Biol 141: 101-114.

Olsen SK, Ibrahimi OA, Raucci A, Zhang F, Eliseenkova AV, Yayon A, Basilico C, Linhardt RJ, Schlessinger J, Mohammadi M. 2004. Insights into the molecular basis for fibroblast growth factor receptor autoinhibition and ligand-binding promiscuity. Proc Natl Acad Sci U S A 101: 935-940.

Olsen SK, Li JY, Bromleigh C, Eliseenkova AV, Ibrahimi OA, Lao Z, Zhang F, Linhardt RJ, Joyner AL, Mohammadi M. 2006. Structural basis by which alternative splicing modulates the organizer activity of FGF8 in the brain. Genes Dev 20: 185-198.

Ong SH, Hadari YR, Gotoh N, Guy GR, Schlessinger J, Lax I. 2001. Stimulation of phosphatidylinositol 3-kinase by fibroblast growth factor receptors is mediated by coordinated recruitment of multiple docking proteins. Proc Natl Acad Sci U S A 98: 6074-6079.

Ong SH, Guy GR, Hadari YR, Laks S, Gotoh N, Schlessinger J, Lax I. 2000. FRS2 proteins recruit intracellular signaling pathways by binding to diverse targets on fibroblast growth factor and nerve growth factor receptors. Mol Cell Biol 20: 979-989.

Onwuazor ON, Wen XY, Wang DY, Zhuang L, Masih-Khan E, Claudio J, Barlogie B, Shaughnessy JD, Jr., Stewart AK. 2003. Mutation, SNP, and isoform analysis of fibroblast growth factor receptor 3 (FGFR3) in 150 newly diagnosed multiple myeloma patients. Blood 102: 772-773.

Ornitz DM, Itoh N. 2001. Fibroblast growth factors. Genome Biol 2: REVIEWS3005.

Ornitz DM, Marie PJ. 2002. FGF signaling pathways in endochondral and intramembranous bone development and human genetic disease. Genes Dev 16: 1446-1465.

Ornitz DM, Yayon A, Flanagan JG, Svahn CM, Levi E, Leder P. 1992. Heparin is required for cell-free binding of basic fibroblast growth factor to a soluble receptor and for mitogenesis in whole cells. Mol Cell Biol 12: 240-247.

Orr-Urtreger A, Bedford MT, Burakova T, Arman E, Zimmer Y, Yayon A, Givol D, Lonai P. 1993. Developmental localization of the splicing alternatives of fibroblast growth factor receptor-2 (FGFR2). Dev Biol 158: 475-486.

Orth JD, Krueger EW, Weller SG, McNiven MA. 2006. A novel endocytic mechanism of epidermal growth factor receptor sequestration and internalization. Cancer Res 66: 3603-3610.

Ostman A, Bohmer FD. 2001. Regulation of receptor tyrosine kinase signaling by protein tyrosine phosphatases. Trends Cell Biol 11: 258-266.

Pandith AA, Shah ZA, Siddiqi MA. 2010. Oncogenic role of fibroblast growth factor receptor 3 in tumorigenesis of urinary bladder cancer. Urol Oncol.

Parachoniak CA, Park M. 2012. Dynamics of receptor trafficking in tumorigenicity. Trends Cell Biol 22: 231-240.

Parton RG, Way M, Zorzi N, Stang E. 1997. Caveolin-3 associates with developing T-tubules during muscle differentiation. J Cell Biol 136: 137-154.

Passos-Bueno MR, Wilcox WR, Jabs EW, Sertie AL, Alonso LG, Kitoh H. 1999. Clinical spectrum of fibroblast growth factor receptor mutations. Hum Mutat 14: 115-125.

Pearse BM. 1976. Clathrin: a unique protein associated with intracellular transfer of membrane by coated vesicles. Proc Natl Acad Sci U S A 73: 1255-1259.

Pelkmans L. 2005. Secrets of caveolae- and lipid raft-mediated endocytosis revealed by mammalian viruses. Biochim Biophys Acta 1746: 295-304.

Pelkmans L, Kartenbeck J, Helenius A. 2001. Caveolar endocytosis of simian virus 40 reveals a new two-step vesicular-transport pathway to the ER. Nat Cell Biol 3: 473-483.

Pelkmans L, Puntener D, Helenius A. 2002. Local actin polymerization and dynamin recruitment in SV40-induced internalization of caveolae. Science 296: 535-539.

Pellman D, Garber EA, Cross FR, Hanafusa H. 1985. An N-terminal peptide from p60src can direct myristylation and plasma membrane localization when fused to heterologous proteins. Nature 314: 374-377.

Peschard P, Park M. 2003. Escape from Cbl-mediated downregulation: a recurrent theme for oncogenic deregulation of receptor tyrosine kinases. Cancer Cell 3: 519-523.

Peters KG, Marie J, Wilson E, Ives HE, Escobedo J, Del Rosario M, Mirda D, Williams LT. 1992. Point mutation of an FGF receptor abolishes phosphatidylinositol turnover and Ca2+ flux but not mitogenesis. Nature 358: 678-681.

Plotnikov AN, Schlessinger J, Hubbard SR, Mohammadi M. 1999. Structural basis for FGF receptor dimerization and activation. Cell 98: 641-650.

Plotnikov AN, Hubbard SR, Schlessinger J, Mohammadi M. 2000. Crystal structures of two FGF-FGFR complexes reveal the determinants of ligand-receptor specificity. Cell 101: 413-424.

Pollock PM, et al. 2007. Frequent activating FGFR2 mutations in endometrial carcinomas parallel germline mutations associated with craniosynostosis and skeletal dysplasia syndromes. Oncogene 26: 7158-7162.

Polo S, Di Fiore PP. 2006. Endocytosis conducts the cell signaling orchestra. Cell 124: 897-900.

Ponseti IV. 1970. Skeletal growth in achondroplasia. J Bone Joint Surg Am 52: 701-716.

Popovici C, Roubin R, Coulier F, Pontarotti P, Birnbaum D. 1999. The family of Caenorhabditis elegans tyrosine kinase receptors: similarities and differences with mammalian receptors. Genome Res 9: 1026-1039.

Powers CJ, McLeskey SW, Wellstein A. 2000. Fibroblast growth factors, their receptors and signaling. Endocr Relat Cancer 7: 165-197.

Provenzano C, Gallo R, Carbone R, Di Fiore PP, Falcone G, Castellani L, Alema S. 1998. Eps8, a tyrosine kinase substrate, is recruited to the cell cortex and dynamic F-actin upon cytoskeleton remodeling. Exp Cell Res 242: 186-200.

Przylepa KA, et al. 1996. Fibroblast growth factor receptor 2 mutations in Beare-Stevenson cutis gyrata syndrome. Nat Genet 13: 492-494.

Purchio AF, Erikson E, Brugge JS, Erikson RL. 1978. Identification of a polypeptide encoded by the avian sarcoma virus src gene. Proc Natl Acad Sci U S A 75: 1567-1571.

Puri V, Watanabe R, Singh RD, Dominguez M, Brown JC, Wheatley CL, Marks DL, Pagano RE. 2001. Clathrin-dependent and -independent internalization of plasma membrane sphingolipids initiates two Golgi targeting pathways. J Cell Biol 154: 535-547.

Puthenveedu MA, von Zastrow M. 2006. Cargo regulates clathrin-coated pit dynamics. Cell 127: 113-124.

Pye DA, Kumar S. 1998. Endothelial and fibroblast cell-derived heparan sulphate bind with differing affinity to basic fibroblast growth factor. Biochem Biophys Res Commun 248: 889-895.

Rappoport JZ, Simon SM. 2008. A functional GFP fusion for imaging clathrin-mediated endocytosis. Traffic 9: 1250-1255.

—. 2009. Endocytic trafficking of activated EGFR is AP-2 dependent and occurs through preformed clathrin spots. J Cell Sci 122: 1301-1305.

Rappoport JZ, Benmerah A, Simon SM. 2005. Analysis of the AP-2 adaptor complex and cargo during clathrin-mediated endocytosis. Traffic 6: 539-547.

Rappoport JZ, Kemal S, Benmerah A, Simon SM. 2006. Dynamics of clathrin and adaptor proteins during endocytosis. Am J Physiol Cell Physiol 291: C1072-1081.

Rapraeger AC, Krufka A, Olwin BB. 1991. Requirement of heparan sulfate for bFGF-mediated fibroblast growth and myoblast differentiation. Science 252: 1705-1708.

Rashid S, Pilecka I, Torun A, Olchowik M, Bielinska B, Miaczynska M. 2009. Endosomal adaptor proteins APPL1 and APPL2 are novel activators of beta-catenin/TCF-mediated transcription. J Biol Chem 284: 18115-18128.

Raucci A, Laplantine E, Mansukhani A, Basilico C. 2004. Activation of the ERK1/2 and p38 mitogen-activated protein kinase pathways mediates fibroblast growth factor-induced growth arrest of chondrocytes. J Biol Chem 279: 1747-1756.

Rebscher N, Deichmann C, Sudhop S, Fritzenwanker JH, Green S, Hassel M. 2009. Conserved intron positions in FGFR genes reflect the modular structure of FGFR and reveal stepwise addition of domains to an already complex ancestral FGFR. Dev Genes Evol 219: 455-468.

Reilly JF, Mizukoshi E, Maher PA. 2004. Ligand dependent and independent internalization and nuclear translocation of fibroblast growth factor (FGF) receptor 1. DNA Cell Biol 23: 538-548.

Ren M, Qin H, Ren R, Tidwell J, Cowell JK. 2011. Src activation plays an important key role in lymphomagenesis induced by FGFR1 fusion kinases. Cancer Res 71: 7312-7322.

Resh MD. 1999. Fatty acylation of proteins: new insights into membrane targeting of myristoylated and palmitoylated proteins. Biochim Biophys Acta 1451: 1-16.

Ricotta D, Conner SD, Schmid SL, von Figura K, Honing S. 2002. Phosphorylation of the AP2 mu subunit by AAK1 mediates high affinity binding to membrane protein sorting signals. J Cell Biol 156: 791-795.

Robinson DR, Wu YM, Lin SF. 2000. The protein tyrosine kinase family of the human genome. Oncogene 19: 5548-5557.

Robinson ML. 2006. An essential role for FGF receptor signaling in lens development. Semin Cell Dev Biol 17: 726-740.

Rodriguez-Viciana P, Warne PH, Dhand R, Vanhaesebroeck B, Gout I, Fry MJ, Waterfield MD, Downward J. 1994. Phosphatidylinositol-3-OH kinase as a direct target of Ras. Nature 370: 527-532.

Roghani M, Moscatelli D. 2007. Prostate cells express two isoforms of fibroblast growth factor receptor 1 with different affinities for fibroblast growth factor-2. Prostate 67: 115-124.

Ross TS, Bernard OA, Berger R, Gilliland DG. 1998. Fusion of Huntingtin interacting protein 1 to platelet-derived growth factor beta receptor (PDGFbetaR) in chronic myelomonocytic leukemia with t(5;7)(q33;q11.2). Blood 91: 4419-4426.

Rossig L, Badorff C, Holzmann Y, Zeiher AM, Dimmeler S. 2002. Glycogen synthase kinase-3 couples AKT-dependent signaling to the regulation of p21Cip1 degradation. J Biol Chem 277: 9684-9689.

Rossig L, Jadidi AS, Urbich C, Badorff C, Zeiher AM, Dimmeler S. 2001. Akt-dependent phosphorylation of p21(Cip1) regulates PCNA binding and proliferation of endothelial cells. Mol Cell Biol 21: 5644-5657.

Roth TF, Porter KR. 1964. Yolk Protein Uptake in the Oocyte of the Mosquito Aedes Aegypti. L. J Cell Biol 20: 313-332.

Rothberg KG, Ying YS, Kolhouse JF, Kamen BA, Anderson RG. 1990. The glycophospholipid-linked folate receptor internalizes folate without entering the clathrin-coated pit endocytic pathway. J Cell Biol 110: 637-649.

Rothberg KG, Heuser JE, Donzell WC, Ying YS, Glenney JR, Anderson RG. 1992. Caveolin, a protein component of caveolae membrane coats. Cell 68: 673-682.

Rousseau F, Bonaventure J, Legeai-Mallet L, Pelet A, Rozet JM, Maroteaux P, Le Merrer M, Munnich A. 1994. Mutations in the gene encoding fibroblast growth factor receptor-3 in achondroplasia. Nature 371: 252-254.

Roy S, Plowman S, Rotblat B, Prior IA, Muncke C, Grainger S, Parton RG, Henis YI, Kloog Y, Hancock JF. 2005. Individual palmitoyl residues serve distinct roles in H-ras trafficking, microlocalization, and signaling. Mol Cell Biol 25: 6722-6733.

Rubin C, Litvak V, Medvedovsky H, Zwang Y, Lev S, Yarden Y. 2003. Sprouty fine-tunes EGF signaling through interlinked positive and negative feedback loops. Curr Biol 13: 297-307.

Rubin JS, Osada H, Finch PW, Taylor WG, Rudikoff S, Aaronson SA. 1989. Purification and characterization of a newly identified growth factor specific for epithelial cells. Proc Natl Acad Sci U S A 86: 802-806.

Rubino M, Miaczynska M, Lippe R, Zerial M. 2000. Selective membrane recruitment of EEA1 suggests a role in directional transport of clathrin-coated vesicles to early endosomes. J Biol Chem 275: 3745-3748.

Ryan PJ, Paterno GD, Gillespie LL. 1998. Identification of phosphorylated proteins associated with the fibroblast growth factor receptor type I during early Xenopus development. Biochem Biophys Res Commun 244: 763-767.

Sadowski L, Jastrzebski K, Kalaidzidis Y, Heldin CH, Hellberg C, Miaczynska M. 2013. Dynamin Inhibitors Impair Endocytosis and Mitogenic Signaling of PDGF. Traffic.

Sako Y, Minoghchi S, Yanagida T. 2000. Single-molecule imaging of EGFR signalling on the surface of living cells. Nat Cell Biol 2: 168-172.

Sandilands E, Akbarzadeh S, Vecchione A, McEwan DG, Frame MC, Heath JK. 2007. Src kinase modulates the activation, transport and signalling dynamics of fibroblast growth factor receptors. EMBO Rep 8: 1162-1169.

Sasaki A, Taketomi T, Wakioka T, Kato R, Yoshimura A. 2001. Identification of a dominant negative mutant of Sprouty that potentiates fibroblast growth factor- but not epidermal growth factor-induced ERK activation. J Biol Chem 276: 36804-36808.

Schaeffer HJ, Catling AD, Eblen ST, Collier LS, Krauss A, Weber MJ. 1998. MP1: a MEK binding partner that enhances enzymatic activation of the MAP kinase cascade. Science 281: 1668-1671.

Schenck A, Goto-Silva L, Collinet C, Rhinn M, Giner A, Habermann B, Brand M, Zerial M. 2008. The endosomal protein Appl1 mediates Akt substrate specificity and cell survival in vertebrate development. Cell 133: 486-497.

Schlessinger J, Plotnikov AN, Ibrahimi OA, Eliseenkova AV, Yeh BK, Yayon A, Linhardt RJ, Mohammadi M. 2000. Crystal structure of a ternary FGF-FGFR-heparin complex reveals a dual role for heparin in FGFR binding and dimerization. Mol Cell 6: 743-750.

Schmees C, Villasenor R, Zheng W, Ma H, Zerial M, Heldin CH, Hellberg C. 2012. Macropinocytosis of the PDGF beta-receptor promotes fibroblast transformation by H-RasG12V. Mol Biol Cell 23: 2571-2582.

Schmidt-Glenewinkel H, Reinz E, Eils R, Brady NR. 2009. Systems biological analysis of epidermal growth factor receptor internalization dynamics for altered receptor levels. J Biol Chem 284: 17243-17252.

Schmidt A, Hall A. 2002. Guanine nucleotide exchange factors for Rho GTPases: turning on the switch. Genes Dev 16: 1587-1609.

Schnitzer JE, Oh P. 1994. Albondin-mediated capillary permeability to albumin. Differential role of receptors in endothelial transcytosis and endocytosis of native and modified albumins. J Biol Chem 269: 6072-6082.

Schoorlemmer J, Goldfarb M. 2001. Fibroblast growth factor homologous factors are intracellular signaling proteins. Curr Biol 11: 793-797.

Schuller AC, Ahmed Z, Ladbury JE. 2008. Extracellular point mutations in FGFR2 result in elevated ERK1/2 activation and perturbation of neuronal differentiation. Biochem J 410: 205-211.

Schultheiss KP, Craddock BP, Tong M, Seeliger M, Miller WT. 2013. Metazoan-like signaling in a unicellular receptor tyrosine kinase. BMC Biochem 14: 4.

Scita G, Di Fiore PP. 2010. The endocytic matrix. Nature 463: 464-473.

Scita G, Nordstrom J, Carbone R, Tenca P, Giardina G, Gutkind S, Bjarnegard M, Betsholtz C, Di Fiore PP. 1999. EPS8 and E3B1 transduce signals from Ras to Rac. Nature 401: 290-293.

Scita G, Tenca P, Areces LB, Tocchetti A, Frittoli E, Giardina G, Ponzanelli I, Sini P, Innocenti M, Di Fiore PP. 2001. An effector region in Eps8 is responsible for the activation of the Rac-specific GEF activity of Sos-1 and for the proper localization of the Rac-based actin-polymerizing machine. J Cell Biol 154: 1031-1044.

Seghezzi G, Patel S, Ren CJ, Gualandris A, Pintucci G, Robbins ES, Shapiro RL, Galloway AC, Rifkin DB, Mignatti P. 1998. Fibroblast growth factor-2 (FGF-2) induces vascular endothelial growth factor (VEGF) expression in the endothelial cells of forming capillaries: an autocrine mechanism contributing to angiogenesis. J Cell Biol 141: 1659-1673.

Shatz M, Liscovitch M. 2008. Caveolin-1: a tumor-promoting role in human cancer. Int J Radiat Biol 84: 177-189.

Shi E, Kan M, Xu J, Wang F, Hou J, McKeehan WL. 1993. Control of fibroblast growth factor receptor kinase signal transduction by heterodimerization of combinatorial splice variants. Mol Cell Biol 13: 3907-3918.

Shimizu A, Tada K, Shukunami C, Hiraki Y, Kurokawa T, Magane N, Kurokawa-Seo M. 2001. A novel alternatively spliced fibroblast growth factor receptor 3 isoform lacking the acid box domain is expressed during chondrogenic differentiation of ATDC5 cells. J Biol Chem 276: 11031-11040.

Shimoaka T, Ogasawara T, Yonamine A, Chikazu D, Kawano H, Nakamura K, Itoh N, Kawaguchi H. 2002. Regulation of osteoblast, chondrocyte, and osteoclast functions by fibroblast growth factor (FGF)-18 in comparison with FGF-2 and FGF-10. J Biol Chem 277: 7493-7500.

Shishido E, Higashijima S, Emori Y, Saigo K. 1993. Two FGF-receptor homologues of Drosophila: one is expressed in mesodermal primordium in early embryos. Development 117: 751-761.

Shtiegman K, Yarden Y. 2003. The role of ubiquitylation in signaling by growth factors: implications to cancer. Semin Cancer Biol 13: 29-40.

Sigal CT, Zhou W, Buser CA, McLaughlin S, Resh MD. 1994. Amino-terminal basic residues of Src mediate membrane binding through electrostatic interaction with acidic phospholipids. Proc Natl Acad Sci U S A 91: 12253-12257.

Sigismund S, Argenzio E, Tosoni D, Cavallaro E, Polo S, Di Fiore PP. 2008. Clathrin-mediated internalization is essential for sustained EGFR signaling but dispensable for degradation. Dev Cell 15: 209-219.

Simons K, Toomre D. 2000. Lipid rafts and signal transduction. Nat Rev Mol Cell Biol 1: 31-39.

Singh S, Singh M, Mak IW, Turcotte R, Ghert M. 2012. Investigation of FGFR2-IIIC signaling via FGF-2 ligand for advancing GCT stromal cell differentiation. PLoS One 7: e46769.

Slamon DJ. 1987. Proto-oncogenes and human cancers. N Engl J Med 317: 955-957.

Sleeman M, Fraser J, McDonald M, Yuan S, White D, Grandison P, Kumble K, Watson JD, Murison JG. 2001. Identification of a new fibroblast growth factor receptor, FGFR5. Gene 271: 171-182.

So CW, Lin M, Ayton PM, Chen EH, Cleary ML. 2003. Dimerization contributes to oncogenic activation of MLL chimeras in acute leukemias. Cancer Cell 4: 99-110.

Sommer A, Rifkin DB. 1989. Interaction of heparin with human basic fibroblast growth factor: protection of the angiogenic protein from proteolytic degradation by a glycosaminoglycan. J Cell Physiol 138: 215-220.

Sorkin A. 2004. Cargo recognition during clathrin-mediated endocytosis: a team effort. Curr Opin Cell Biol 16: 392-399.

Sorkin A, Von Zastrow M. 2002. Signal transduction and endocytosis: close encounters of many kinds. Nat Rev Mol Cell Biol 3: 600-614.

Sorkin A, Goh LK. 2008. Endocytosis and intracellular trafficking of ErbBs. Exp Cell Res 314: 3093-3106.

Sorokin A, Mohammadi M, Huang J, Schlessinger J. 1994. Internalization of fibroblast growth factor receptor is inhibited by a point mutation at tyrosine 766. J Biol Chem 269: 17056-17061.

Soubeyran P, Kowanetz K, Szymkiewicz I, Langdon WY, Dikic I. 2002. Cbl-CIN85-endophilin complex mediates ligand-induced downregulation of EGF receptors. Nature 416: 183-187.

Spinola M, et al. 2005. FGFR4 Gly388Arg polymorphism and prognosis of breast and colorectal cancer. Oncol Rep 14: 415-419.

Spivak-Kroizman T, Lemmon MA, Dikic I, Ladbury JE, Pinchasi D, Huang J, Jaye M, Crumley G, Schlessinger J, Lax I. 1994. Heparin-induced oligomerization of FGF molecules is responsible for FGF receptor dimerization, activation, and cell proliferation. Cell 79: 1015-1024.

Stan RV, Roberts WG, Predescu D, Ihida K, Saucan L, Ghitescu L, Palade GE. 1997. Immunoisolation and partial characterization of endothelial plasmalemmal vesicles (caveolae). Mol Biol Cell 8: 595-605.

Stauber DJ, DiGabriele AD, Hendrickson WA. 2000. Structural interactions of fibroblast growth factor receptor with its ligands. Proc Natl Acad Sci U S A 97: 49-54.

Stehelin D, Fujita DJ, Padgett T, Varmus HE, Bishop JM. 1977. Detection and enumeration of transformation-defective strains of avian sarcoma virus with molecular hybridization. Virology 76: 675-684.

Steinberg F, Zhuang L, Beyeler M, Kalin RE, Mullis PE, Brandli AW, Trueb B. 2010. The FGFRL1 receptor is shed from cell membranes, binds fibroblast growth factors (FGFs), and antagonizes FGF signaling in Xenopus embryos. J Biol Chem 285: 2193-2202.

Stenmark H, Aasland R, Toh BH, D'Arrigo A. 1996. Endosomal localization of the autoantigen EEA1 is mediated by a zinc-binding FYVE finger. J Biol Chem 271: 24048-24054.

Stimpson HE, Toret CP, Cheng AT, Pauly BS, Drubin DG. 2009. Early-arriving Syp1p and Ede1p function in endocytic site placement and formation in budding yeast. Mol Biol Cell 20: 4640-4651.

Storm SM, Cleveland JL, Rapp UR. 1990. Expression of raf family proto-oncogenes in normal mouse tissues. Oncogene 5: 345-351.

Stoscheck CM, Carpenter G. 1984. Down regulation of epidermal growth factor receptors: direct demonstration of receptor degradation in human fibroblasts. J Cell Biol 98: 1048-1053.

Sudhop S, Coulier F, Bieller A, Vogt A, Hotz T, Hassel M. 2004. Signalling by the FGFR-like tyrosine kinase, Kringelchen, is essential for bud detachment in Hydra vulgaris. Development 131: 4001-4011.

Suga H, Dacre M, de Mendoza A, Shalchian-Tabrizi K, Manning G, Ruiz-Trillo I. 2012. Genomic survey of premetazoans shows deep conservation of cytoplasmic tyrosine kinases and multiple radiations of receptor tyrosine kinases. Sci Signal 5: ra35.

Sun X, Meyers EN, Lewandoski M, Martin GR. 1999. Targeted disruption of Fgf8 causes failure of cell migration in the gastrulating mouse embryo. Genes Dev 13: 1834-1846.

Takeya T, Hanafusa H. 1983. Structure and sequence of the cellular gene homologous to the RSV src gene and the mechanism for generating the transforming virus. Cell 32: 881-890.

Tanaka A, Fujita DJ. 1986. Expression of a molecularly cloned human c-src oncogene by using a replication-competent retroviral vector. Mol Cell Biol 6: 3900-3909.

Tang TL, Freeman RM, Jr., O'Reilly AM, Neel BG, Sokol SY. 1995. The SH2-containing protein-tyrosine phosphatase SH-PTP2 is required upstream of MAP kinase for early Xenopus development. Cell 80: 473-483.

Tatosyan AG, Mizenina OA. 2000. Kinases of the Src family: structure and functions. Biochemistry (Mosc) 65: 49-58.

Tavormina PL, Shiang R, Thompson LM, Zhu YZ, Wilkin DJ, Lachman RS, Wilcox WR, Rimoin DL, Cohn DH, Wasmuth JJ. 1995. Thanatophoric dysplasia (types I and II) caused by distinct mutations in fibroblast growth factor receptor 3. Nat Genet 9: 321-328.

Tavormina PL, et al. 1999. A novel skeletal dysplasia with developmental delay and acanthosis nigricans is caused by a Lys650Met mutation in the fibroblast growth factor receptor 3 gene. Am J Hum Genet 64: 722-731.

Taylor JGt, et al. 2009. Identification of FGFR4-activating mutations in human rhabdomyosarcomas that promote metastasis in xenotransplanted models. J Clin Invest 119: 3395-3407.

Taylor MJ, Perrais D, Merrifield CJ. 2011. A high precision survey of the molecular dynamics of mammalian clathrin-mediated endocytosis. PLoS Biol 9: e1000604.

Tefft JD, Lee M, Smith S, Leinwand M, Zhao J, Bringas P, Jr., Crowe DL, Warburton D. 1999. Conserved function of mSpry-2, a murine homolog of Drosophila sprouty, which negatively modulates respiratory organogenesis. Curr Biol 9: 219-222.

Teis D, Wunderlich W, Huber LA. 2002. Localization of the MP1-MAPK scaffold complex to endosomes is mediated by p14 and required for signal transduction. Dev Cell 3: 803-814.

Thorley JA, McKeating JA, Rappoport JZ. 2010. Mechanisms of viral entry: sneaking in the front door. Protoplasma 244: 15-24.

Tice DA, Biscardi JS, Nickles AL, Parsons SJ. 1999. Mechanism of biological synergy between cellular Src and epidermal growth factor receptor. Proc Natl Acad Sci U S A 96: 1415-1420.

Tomlinson DC, Knowles MA. 2010. Altered splicing of FGFR1 is associated with high tumor grade and stage and leads to increased sensitivity to FGF1 in bladder cancer. Am J Pathol 177: 2379-2386.

Torii S, Kusakabe M, Yamamoto T, Maekawa M, Nishida E. 2004. Sef is a spatial regulator for Ras/MAP kinase signaling. Dev Cell 7: 33-44.

Traub LM. 2009. Tickets to ride: selecting cargo for clathrin-regulated internalization. Nat Rev Mol Cell Biol 10: 583-596.

Traverse S, Gomez N, Paterson H, Marshall C, Cohen P. 1992. Sustained activation of the mitogen-activated protein (MAP) kinase cascade may be required for differentiation of PC12 cells. Comparison of the effects of nerve growth factor and epidermal growth factor. Biochem J 288 (Pt 2): 351-355.

Turner N, Grose R. 2010. Fibroblast growth factor signalling: from development to cancer. Nat Rev Cancer 10: 116-129.

Ullrich A, Schlessinger J. 1990. Signal transduction by receptors with tyrosine kinase activity. Cell 61: 203-212.

Ullrich O, Reinsch S, Urbe S, Zerial M, Parton RG. 1996. Rab11 regulates recycling through the pericentriolar recycling endosome. J Cell Biol 135: 913-924.

Ungewickell E, Branton D. 1981. Assembly units of clathrin coats. Nature 289: 420-422.

Ungewickell E, Ungewickell H, Holstein SE, Lindner R, Prasad K, Barouch W, Martin B, Greene LE, Eisenberg E. 1995. Role of auxilin in uncoating clathrin-coated vesicles. Nature 378: 632-635.

Urakawa I, Yamazaki Y, Shimada T, Iijima K, Hasegawa H, Okawa K, Fujita T, Fukumoto S, Yamashita T. 2006. Klotho converts canonical FGF receptor into a specific receptor for FGF23. Nature 444: 770-774.

Vainikka S, Joukov V, Wennstrom S, Bergman M, Pelicci PG, Alitalo K. 1994. Signal transduction by fibroblast growth factor receptor-4 (FGFR-4). Comparison with FGFR-1. J Biol Chem 269: 18320-18326.

Van Der Sluijs P, Hull M, Zahraoui A, Tavitian A, Goud B, Mellman I. 1991. The small GTP-binding protein rab4 is associated with early endosomes. Proc Natl Acad Sci U S A 88: 6313-6317.

Vecchione A, Cooper HJ, Trim KJ, Akbarzadeh S, Heath JK, Wheldon LM. 2007. Protein partners in the life history of activated fibroblast growth factor receptors. Proteomics 7: 4565-4578.

Verbeek BS, Vroom TM, Adriaansen-Slot SS, Ottenhoff-Kalff AE, Geertzema JG, Hennipman A, Rijksen G. 1996. c-Src protein expression is increased in human breast cancer. An immunohistochemical and biochemical analysis. J Pathol 180: 383-388.

Vetter IR, Wittinghofer A. 2001. The guanine nucleotide-binding switch in three dimensions. Science 294: 1299-1304.

von Zastrow M, Sorkin A. 2007. Signaling on the endocytic pathway. Curr Opin Cell Biol 19: 436-445.

Wang F, Kan M, Yan G, Xu J, McKeehan WL. 1995a. Alternately spliced NH2-terminal immunoglobulin-like Loop I in the ectodomain of the fibroblast growth factor (FGF) receptor 1 lowers affinity for both heparin and FGF-1. J Biol Chem 270: 10231-10235.

Wang F, Kan M, Xu J, Yan G, McKeehan WL. 1995b. Ligand-specific structural domains in the fibroblast growth factor receptor. J Biol Chem 270: 10222-10230.

Wang J, Yu W, Cai Y, Ren C, Ittmann MM. 2008. Altered fibroblast growth factor receptor 4 stability promotes prostate cancer progression. Neoplasia 10: 847-856.

Ward CW, Lawrence MC, Streltsov VA, Adams TE, McKern NM. 2007. The insulin and EGF receptor structures: new insights into ligand-induced receptor activation. Trends Biochem Sci 32: 129-137.

Ware MF, Tice DA, Parsons SJ, Lauffenburger DA. 1997. Overexpression of cellular Src in fibroblasts enhances endocytic internalization of epidermal growth factor receptor. J Biol Chem 272: 30185-30190.

Waterman H, Yarden Y. 2001. Molecular mechanisms underlying endocytosis and sorting of ErbB receptor tyrosine kinases. FEBS Lett 490: 142-152.

Webster MK, D'Avis PY, Robertson SC, Donoghue DJ. 1996. Profound ligand-independent kinase activation of fibroblast growth factor receptor 3 by the activation loop mutation responsible for a lethal skeletal dysplasia, thanatophoric dysplasia type II. Mol Cell Biol 16: 4081-4087.

Wei K, Xu Y, Tse H, Manolson MF, Gong SG. 2011. Mouse FLRT2 interacts with the extracellular and intracellular regions of FGFR2. J Dent Res 90: 1234-1239.

Wei L, Hubbard SR, Hendrickson WA, Ellis L. 1995. Expression, characterization, and crystallization of the catalytic core of the human insulin receptor protein-tyrosine kinase domain. J Biol Chem 270: 8122-8130.

Weinstein DC, Marden J, Carnevali F, Hemmati-Brivanlou A. 1998. FGF-mediated mesoderm induction involves the Src-family kinase Laloo. Nature 394: 904-908.

Wesche J, Haglund K, Haugsten EM. 2011. Fibroblast growth factors and their receptors in cancer. Biochem J 437: 199-213.

Wheldon LM, Haines BP, Rajappa R, Mason I, Rigby PW, Heath JK. 2010. Critical role of FLRT1 phosphorylation in the interdependent regulation of FLRT1 function and FGF receptor signalling. PLoS One 5: e10264.

Wheldon LM, Khodabukus N, Patey SJ, Smith TG, Heath JK, Hajihosseini MK. 2011. Identification and characterization of an inhibitory fibroblast growth factor receptor 2 (FGFR2) molecule, up-regulated in an Apert Syndrome mouse model. Biochem J 436: 71-81.

Wiedemann M, Trueb B. 2000. Characterization of a novel protein (FGFRL1) from human cartilage related to FGF receptors. Genomics 69: 275-279.

Wiesmann C, Ultsch MH, Bass SH, de Vos AM. 1999. Crystal structure of nerve growth factor in complex with the ligand-binding domain of the TrkA receptor. Nature 401: 184-188.

Wilde A, Beattie EC, Lem L, Riethof DA, Liu SH, Mobley WC, Soriano P, Brodsky FM. 1999. EGF receptor signaling stimulates SRC kinase phosphorylation of clathrin, influencing clathrin redistribution and EGF uptake. Cell 96: 677-687.

Wilkie AO, Morriss-Kay GM, Jones EY, Heath JK. 1995. Functions of fibroblast growth factors and their receptors. Curr Biol 5: 500-507.

Willingham MC, Jay G, Pastan I. 1979. Localization of the ASV src gene product to the plasma membrane of transformed cells by electron microscopic immunocytochemistry. Cell 18: 125-134.

Wong A, Lamothe B, Lee A, Schlessinger J, Lax I. 2002. FRS2 alpha attenuates FGF receptor signaling by Grb2-mediated recruitment of the ubiquitin ligase Cbl. Proc Natl Acad Sci U S A 99: 6684-6689.

Wright TJ, Mansour SL. 2003. FGF signaling in ear development and innervation. Curr Top Dev Biol 57: 225-259.

Xu H, Lee KW, Goldfarb M. 1998. Novel recognition motif on fibroblast growth factor receptor mediates direct association and activation of SNT adapter proteins. J Biol Chem 273: 17987-17990.

Yamaguchi F, Saya H, Bruner JM, Morrison RS. 1994a. Differential expression of two fibroblast growth factor-receptor genes is associated with malignant progression in human astrocytomas. Proc Natl Acad Sci U S A 91: 484-488.

Yamaguchi H, Hendrickson WA. 1996. Structural basis for activation of human lymphocyte kinase Lck upon tyrosine phosphorylation. Nature 384: 484-489.

Yamaguchi TP, Harpal K, Henkemeyer M, Rossant J. 1994b. fgfr-1 is required for embryonic growth and mesodermal patterning during mouse gastrulation. Genes Dev 8: 3032-3044.

Yan G, Fukabori Y, McBride G, Nikolaropolous S, McKeehan WL. 1993. Exon switching and activation of stromal and embryonic fibroblast growth factor (FGF)-FGF receptor genes in prostate epithelial cells accompany stromal independence and malignancy. Mol Cell Biol 13: 4513-4522.

Yap LF, Jenei V, Robinson CM, Moutasim K, Benn TM, Threadgold SP, Lopes V, Wei W, Thomas GJ, Paterson IC. 2009. Upregulation of Eps8 in oral squamous cell carcinoma promotes cell migration and invasion through integrin-dependent Rac1 activation. Oncogene 28: 2524-2534.

Yarar D, Waterman-Storer CM, Schmid SL. 2005. A dynamic actin cytoskeleton functions at multiple stages of clathrin-mediated endocytosis. Mol Biol Cell 16: 964-975.

Yayon A, Klagsbrun M, Esko JD, Leder P, Ornitz DM. 1991. Cell surface, heparin-like molecules are required for binding of basic fibroblast growth factor to its high affinity receptor. Cell 64: 841-848.

Yayon A, Zimmer Y, Shen GH, Avivi A, Yarden Y, Givol D. 1992. A confined variable region confers ligand specificity on fibroblast growth factor receptors: implications for the origin of the immunoglobulin fold. EMBO J 11: 1885-1890.

Yeh BK, Igarashi M, Eliseenkova AV, Plotnikov AN, Sher I, Ron D, Aaronson SA, Mohammadi M. 2003. Structural basis by which alternative splicing confers specificity in fibroblast growth factor receptors. Proc Natl Acad Sci U S A 100: 2266-2271.

Yu H, Rosen MK, Shin TB, Seidel-Dugan C, Brugge JS, Schreiber SL. 1992. Solution structure of the SH3 domain of Src and identification of its ligand-binding site. Science 258: 1665-1668.

Yu K, Herr AB, Waksman G, Ornitz DM. 2000. Loss of fibroblast growth factor receptor 2 ligand-binding specificity in Apert syndrome. Proc Natl Acad Sci U S A 97: 14536-14541.

Yusoff P, Lao DH, Ong SH, Wong ES, Lim J, Lo TL, Leong HF, Fong CW, Guy GR. 2002. Sprouty2 inhibits the Ras/MAP kinase pathway by inhibiting the activation of Raf. J Biol Chem 277: 3195-3201.

Zha J, Harada H, Yang E, Jockel J, Korsmeyer SJ. 1996. Serine phosphorylation of death agonist BAD in response to survival factor results in binding to 14-3-3 not BCL-X(L). Cell 87: 619-628.

Zhan X, Plourde C, Hu X, Friesel R, Maciag T. 1994. Association of fibroblast growth factor receptor-1 with c-Src correlates with association between c-Src and cortactin. J Biol Chem 269: 20221-20224.

Zhang Y, McKeehan K, Lin Y, Zhang J, Wang F. 2008. Fibroblast growth factor receptor 1 (FGFR1) tyrosine phosphorylation regulates binding of FGFR substrate 2alpha (FRS2alpha) but not FRS2 to the receptor. Mol Endocrinol 22: 167-175.

Zisman-Rozen S, Fink D, Ben-Izhak O, Fuchs Y, Brodski A, Kraus MH, Bejar J, Ron D. 2007. Downregulation of Sef, an inhibitor of receptor tyrosine kinase signaling, is common to a variety of human carcinomas. Oncogene 26: 6093-6098.

APPENDIX

PUBLISHED PAPERS

Debbie L. Cunningham, Andrew J. Creese, **Giulio Auciello**, Steve M. M. Sweet, Tulin Tatar, Joshua Z. Rappoport, Melissa M. Grant, John K., 2013. Novel Binding Partners and Differentially Regulated Phosphorylation Sites Clarify Eps8 as a Multi-Functional Adaptor . *PLOS ONE*

Auciello G, Cunningham DL, Tatar T, Heath JK, Rappoport JZ., 2013. Regulation of fibroblast growth factor receptor signalling and trafficking by Src and Eps8. *J Cell Sci*. 126(Pt 2):613-24

Veltman DM, **Auciello G**, Spence HJ, Machesky LM, Rappoport JZ, Insall RH., 2011. Functional analysis of Dictyostelium IBARa reveals a conserved role of the I-BAR domain in endocytosis. *Biochem J*. 436(1):45-52

Mardakheh FK, **Auciello G**, Dafforn TR, Rappoport JZ, Heath JK., 2010. Nbr1 is a novel inhibitor of ligand-mediated receptor tyrosine kinase degradation. *Mol Cell Biol*. 30(24):5672-85

OPEN ACCESS Freely available online

PLOS ONE

Novel Binding Partners and Differentially Regulated Phosphorylation Sites Clarify Eps8 as a Multi-Functional Adaptor

Debbie L. Cunningham[1], Andrew J. Creese[1,2], Giulio Auciello[3], Steve M. M. Sweet[1¤], Tulin Tatar[1,3], Joshua Z. Rappoport[3], Melissa M. Grant[2], John K. Heath[1]*

1 Cancer Research UK Growth Factor Signalling Group, School of Biosciences, College of Life and Environmental Sciences, University of Birmingham, Birmingham, United Kingdom, **2** School of Dentistry, College of Medical and Dental Sciences, University of Birmingham, Birmingham, United Kingdom, **3** School of Biosciences, College of Life and Environmental Sciences, University of Birmingham, Birmingham, United Kingdom

Abstract

Eps8 is involved in both cell signalling and receptor trafficking. It is a known phosphorylation substrate for two proteins involved in the fibroblast growth factor receptor (FGFR) signalling pathway: the receptor itself and Src. Here we report a differential proteomic analysis of Eps8 aimed to identify specific FGFR and Src family kinase dependent phosphosites and co-associated phosphodependent binding partners. This study reveals a total of 22 Eps8 pTyr and pSer/Thr phosphorylation sites, including those that are dependent on Src family and FGFR kinase activity. Peptide affinity purification of proteins that bind to a selection of the pTyr phosphosites has identified a range of novel Eps8 binding partners including members of the intracellular vesicle trafficking machinery (clathrin and AP-2), proteins which have been shown to regulate activated receptor trafficking (NBR1 and Vav2), and proteins involved in receptor signalling (IRS4 and Shp2). Collectively this study significantly extends the understanding of Eps8 post-translational modification by regulated phosphorylation, identifies novel Eps8 binding partners implicated in receptor trafficking and signalling, and confirms the functions of Eps8 at the nexus of receptor signalling and vesicular trafficking.

Citation: Cunningham DL, Creese AJ, Auciello G, Sweet SMM, Tatar T, et al. (2013) Novel Binding Partners and Differentially Regulated Phosphorylation Sites Clarify Eps8 as a Multi-Functional Adaptor. PLoS ONE 8(4): e61513. doi:10.1371/journal.pone.0061513

Editor: Chandra Verma, Bioinformatics Institute, Singapore

Received October 8, 2012; **Accepted** March 9, 2013; **Published** April 23, 2013

Funding: This work was supported by CRUK (grant no. RCCS13677), www.cancerresearchuk.org/; MRC PhD studentship www.mrc.ac.uk/; and FP6 Endotrack (grant no. REAZ 12101), www.endotrack.org/. The funders had no role in study design, data collection and analysis, decision to publish, or preparation of the manuscript

Competing Interests: The authors have declared that no competing interests exist.

* E-mail: J.K.Heath@bham.ac.uk

¤ Current address: Genome Damage and Stability Centre, The University of Sussex, Brighton, United Kingdom

Introduction

Eps8 is involved in modulating cell signalling and receptor trafficking, via its range of protein interactions. When bound in a complex with Abi1and Sos1, Eps8 participates in signal transduction from Ras to Rac, leading to actin remodelling [1]. The SH3 domain of Eps8 binds Abi1 [1,2] and, essential to its role in Rac activation, Sos1 binds the C-terminal effector region [3]. Coexpression of this Eps8-Abi1-Sos1 tri-complex has been correlated with advanced stage ovarian cancer, shown to be attributed to increased Rac-induced cell migration [4]. Interaction with the RabGAP, RN-Tre, via its SH3 domain, disrupts this tri-complex enabling Eps8 to participate in receptor trafficking via de-activation of Rab5 [5]. In addition, Eps8 is involved in actin capping and bundling via its interactions with IRSp53 and monomeric actin [6,7].

Eps8 was originally identified as a novel phosphorylation substrate for the epidermal growth factor receptor (EGFR) and is also phosphorylated upon activation of other tyrosine kinases including fibroblast growth factor receptor (FGFR), platelet-derived growth factor (PDGF) and erbB-2 [8]. It has since been identified as a phosphorylation substrate for Src [9] and elevated expression of Eps8 has been observed in v-Src transformed cells [9,10] and a variety of human cancers [11,12,13]. Phosphorylation is an important post-translational modification in the regulation of protein-protein interactions constituting cellular signal transduction, and aberrant regulation of phosphorylation can lead to malignancy. Indeed, constitutive phosphorylation of Eps8 has been found in a range of tumour cell lines [14].

Previously, we used quantitative proteomics to identify candidate mediators of FGFR signalling which are targets for Src family kinase (SFK)–mediated phosphorylation and functionally implicated in trafficking of activated FGFRs [15]. Eps8 was one such protein identified in this survey.

Collectively these features identify Eps8 as a potential target for transmitting FGFR and Src mediated signalling events to downstream effectors which warranted a detailed investigation of both FGFR and SFK mediated phosphorylation of Eps8 and analysis of phospho-dependent Eps8 binding partners to identify further candidate effectors and provide some insight into the possible pathways that these phosphorylation events influence. Using quantitative mass spectrometry techniques [16,17,18] coupled with chemical inhibition of FGFR and SFK kinase activity we have carried out phosphopeptide mapping of Eps8 in

order to identify FGFR and SFK-regulated phosphorylation sites. In addition, differentially recruited phosphodependent protein partners have been identified using quantitative peptide pull down (PPD) assays. This technique has revealed many novel Eps8 binding partners including insulin-receptor substrate 4 (IRS4). Previous proteomic studies have implicated IRS4 in FGFR signalling [19,20]. Here we have identified IRS4 as a novel binding partner for an Eps8 peptide containing phosphorylated Tyr252. Furthermore, we show that the interaction between Eps8 and IRS4 and their colocalisation within cells is increased following FGFR activation which coincides with tyrosine phosphorylation of both Eps8 and IRS4.

These results significantly expand the range of proteins implicated to interact with Eps8, illustrating further its role as a multi-functional adaptor molecule mediating FGFR and Src kinase signalling.

Materials and Methods

Cell Culture

Human embryonic kidney epithelial 293T cells and mouse NIH 3T3s were cultured at 37°C, 5% CO_2 in DMEM containing 2 mM L-Glutamine (Lonza), supplemented with 0.1 mg/ml streptomycin, 0.2 U/ml penicillin (Sigma), and 10% v/v fetal calf serum (Labtech International). For SILAC labelling, 293T cells were cultured in SILAC DMEM (Thermo Fisher Scientific) supplemented with either 0.1 mg/ml "light" isotopically normal L-Lysine and L-Arginine (R0K0) (Sigma), "medium" $^{13}C_6$ L-Lysine and 4,4,5,5-D4 L-Lysine (R6K4), or "heavy" $^{13}C_6$ $^{15}N_4$ L-Arginine and $^{13}C_6$ $^{15}N_2$ L-Lysine (R10K8) (Goss Scientific), 0.5 mg/ml proline (Sigma), 0.1 mg/ml streptomycin, 0.2 U/ml penicillin, and 10% v/v dialysed fetal bovine serum (Labtech International).

Cloning and Transfection

The human open reading frames for Eps8 and IRS4 were supplied in Gateway (Invitrogen^{TM}) pDONR vectors from Open Biosystems. The insert encoding Eps8 was cloned into the Gateway compatible mammalian expression vector, Myc-PRK5 (gift from Laura Machesky) using Gateway cloning. The insert encoding IRS4 was cloned into the Gateway mammalian expression vector, pDEST53 (GFP-tag) using Gateway cloning. Eps8-mCherry was a gift from Giorgio Scita (IFOM University of Milan, Milan, Italy). HEK 293T cells were transfected using Genejuice (Novagen) and NIH 3T3 cells were transfected using Lipofectamine2000 (Invitrogen) according to manufacturer's instructions. Cells were allowed to overexpress transfected protein for 48 h.

Cell Treatment and Cell Lysis

Following overnight serum starvation in media containing 0.1% serum, cells were either pre-treated with SU6656, dasatinib or SU5402 for 30 min, followed by addition of 20 ng/ml FGF2, or treated as above in the absence of chemical inhibitor. For experiments where cells were treated with sodium pervanadate, 2 mM sodium pervanadate was added to the media for 20 min prior

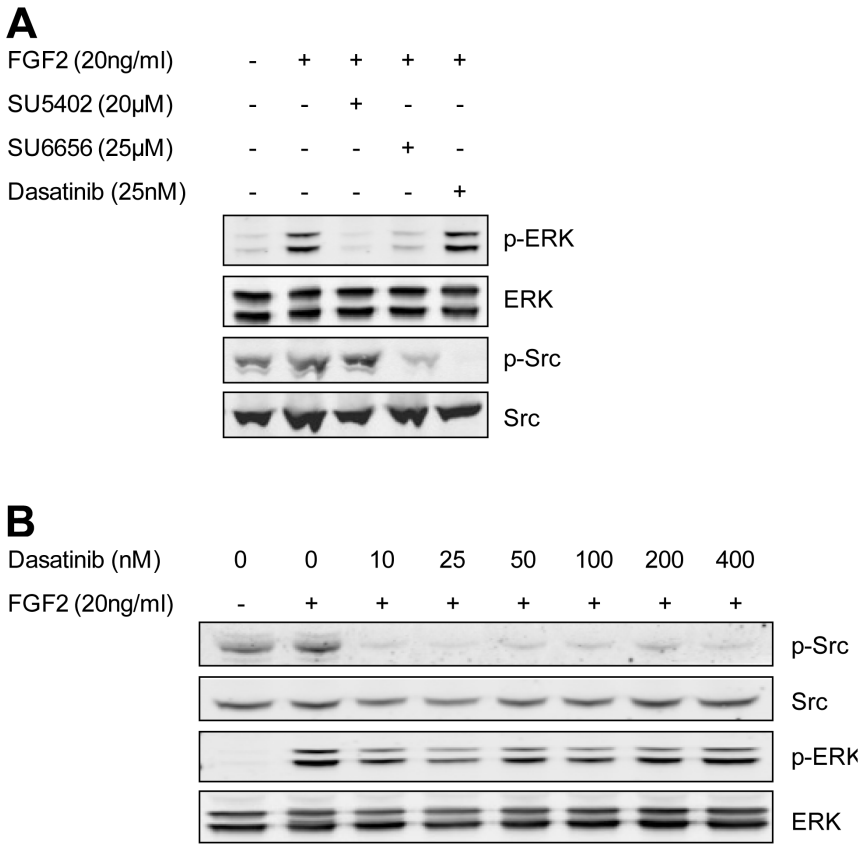

Figure 1. Chemical inhibition of Src kinase and FGFR kinase activity. A) HEK 293T cells were treated with SU5402, SU6656, or dasatinib 30 min prior to addition of FGF2 for 15 min. Cells were lysed and analysed by western blotting. B) HEK 293T cells were treated with increasing concentrations of dasatinib for 30 min prior to addition of FGF2 for 15 min. Cells were lysed and analysed by western blotting.
doi:10.1371/journal.pone.0061513.g001

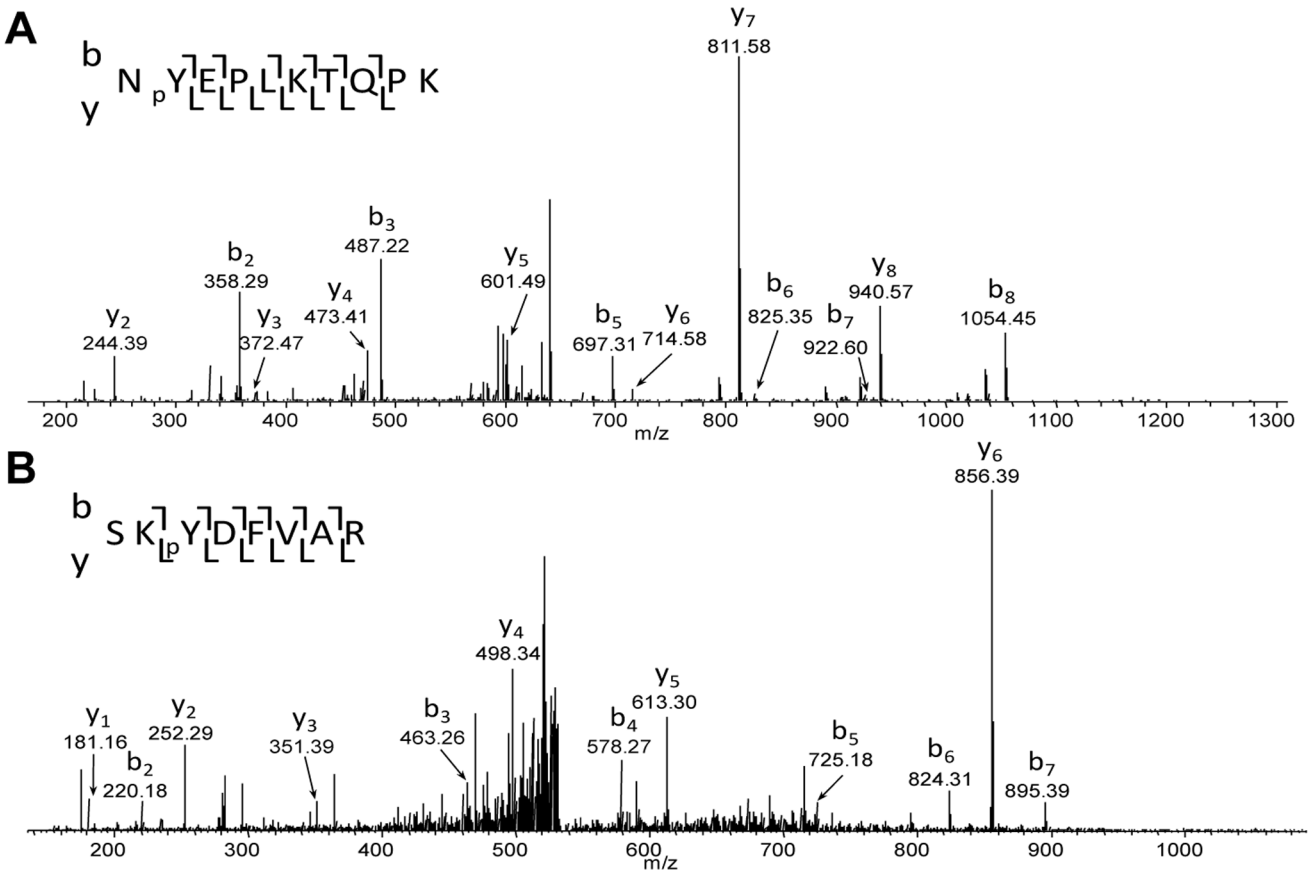

Figure 2. Representative mass spectra for identification and site localisation of tyrosine phosphorylation on Eps8. A) Eps8 is phosphorylated on residue 525. B) Eps8 is phosphorylated on residue 540. pY indicates phosphotyrosine.
doi:10.1371/journal.pone.0061513.g002

to FGF2 stimulation. Cell lysis and measurement of total protein concentrations were performed as described previously [15].

Immunoprecipitation and Western Blotting

Antibodies were purchased from Roche (Myc 9E10), Santa Cruz (Eps8 sc-1841; Clathrin HC sc-12734; Vav2 sc-20803; Shp2 sc-424; IRS4 sc-100854; AP-2 sc-10761; PHB sc-28259; PHB2 sc-133094; ERK sc-94; p-ERK sc-7383), NEB (Src 2110, p-Src 2101, STAT3 9139), and Abcam (NBR1 ab55474). For IPs, antibodies were conjugated to Protein G Dynabeads (Invitrogen), as per manufacturer's instructions. For SILAC anti-Myc IPs, anti-Myc antibody was further cross-linked to the beads: the conjugated Dynabeads were washed twice in a 10-fold excess of 0.2 M triethanolamine pH8.2. Beads were then resuspended in a 10-fold excess of freshly prepared 20 mM dimethyl pimelidate dihydrochloride (DMP) (Sigma) and mixed for 30 mins at room temperature followed by washing in a ten-fold excess of 50 mM Tris/HCl for 15 mins at room temperature and further washes (x3) in a 10-fold excess of PBS/0.1% Tween 20 (PBS-T). Cross-linked beads were resuspended in PBS, prior to addition of whole cell lysate (WCL). WCLs were mixed at 4°C with anti-Myc beads for 30 min, prior to washing. For SILAC experiments, WCLs from the heavy, medium, and light cell populations were immunoprecipitated separately (10 mg WCL) and beads were mixed following five washes in a 20-fold excess of lysis buffer. Following addition of reduced sample buffer, samples were boiled for 5 min, run on 4–12% Bis-Tris gels (Invitrogen) and Coomassie stained. Western blotting was performed as previously described [15].

Peptide Pull Downs

Phosphorylated and non-phosphorylated peptide pairs were synthesised by Alta Bioscience, Birmingham, UK. Each peptide was synthesised with an N-terminal desthiobiotin. Peptides were bound to MyOne Streptavidin Dynabeads (Invitrogen) (2.5 μg/50 μl beads) by incubating at room temperature for 1 hour. Peptide-bound beads were washed for 15 min×5 in a 20-fold excess of PBS-T. Heavy SILAC labelled (R10K8) WCL (10 mg) was incubated with 50 μl beads bound to the phosphorylated peptide, medium SILAC labelled (R6K4) WCL (10 mg) was incubated with 50 μl beads bound to the non-phosphorylated peptide, and light SILAC labelled (R0K0) WCL (10 mg) was incubated with 50 μl beads without peptide, overnight at 4°C. PPDs were washed at least 5 times in a 20-fold excess of PBS-T. Beads from each peptide pair and a non-peptide control were combined. Following addition of reduced sample buffer, protein samples were run on 4–12% Bis-Tris gels (Invitrogen) and Coomassie stained.

Trypsin Digestion and Phosphopeptide Enrichment of Samples

Trypsin digestion was carried out as previously described [15,21]. From the excised band corresponding to Eps8, phosphopeptides were enriched using TiO_2 tips (GLSciences), according to the manufacturer's instructions. All resulting peptide mixtures were analysed by liquid chromatography tandem mass spectrometry (LC-MS/MS).

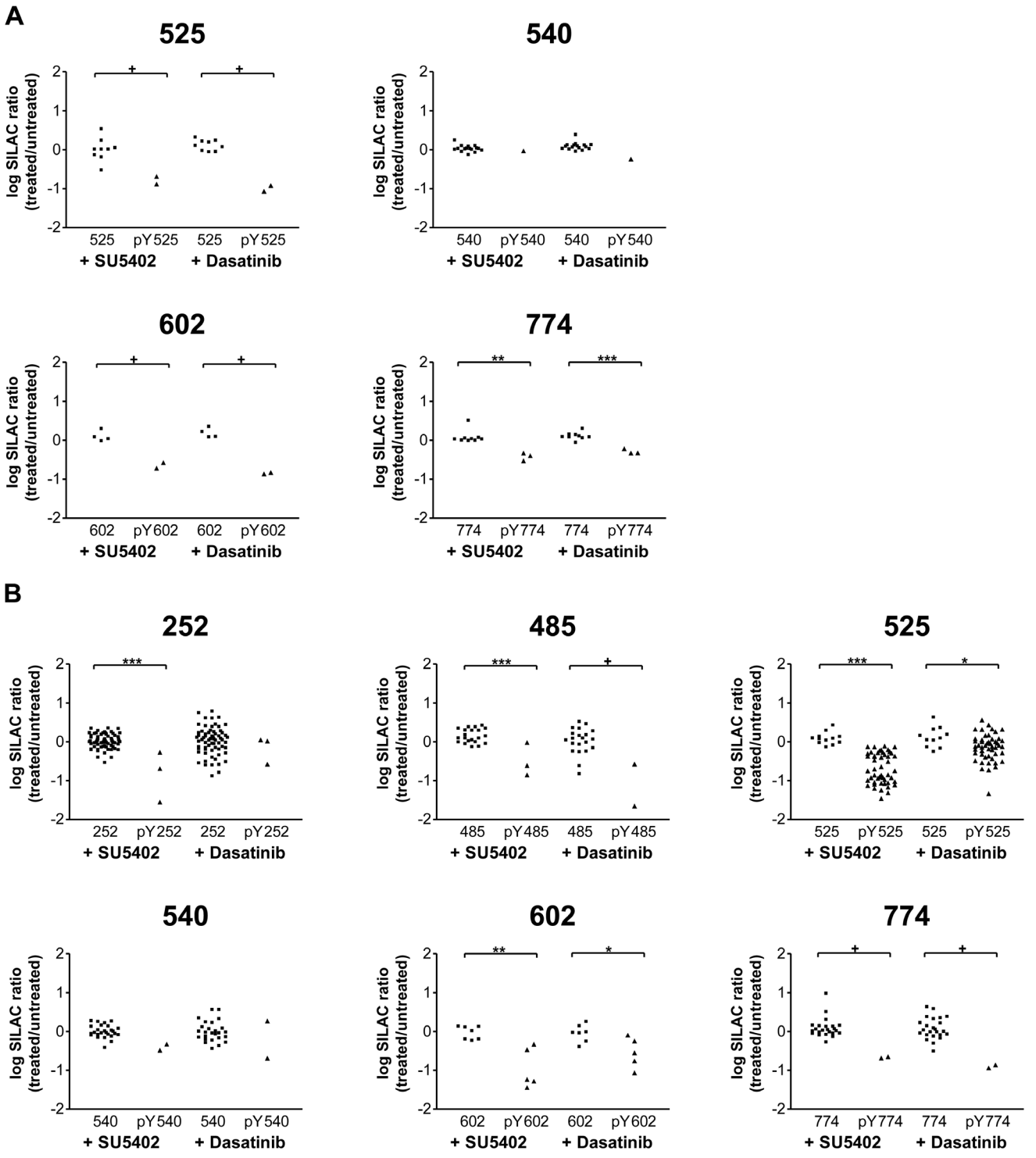

Figure 3. Differential regulation of tyrosine phosphorylation on Eps8. Heavy, medium and light SILAC labelled HEK 293T cells were treated with either 25 nM dasatinib, 20 μM SU5402, or no inhibitor, prior to FGF2 stimulation (20 ng/ml; 15 min). Myc-Eps8 was immunoprecipitated and the resulting sample was run on an SDS-PAGE gel and, following in-gel trypsin digestion and phophopeptide enrichment, analysed by mass spectrometry. Each graph represents specific residues on Eps8 as indicated. Each data point represents a single peptide identification. *P* values were calculated by an unpaired t-test (0.01–0.05 = *; 0.001–0.01 = **; <0.001 = ***). +, the median of the ratios is<the cut-off value of 0.57 and is deemed significantly changed (see Method S1). A) Experiment was carried out in the absence of sodium pervanadate. B) Experiment was carried out in the presence of 2 mM sodium pervanvadate.
doi:10.1371/journal.pone.0061513.g003

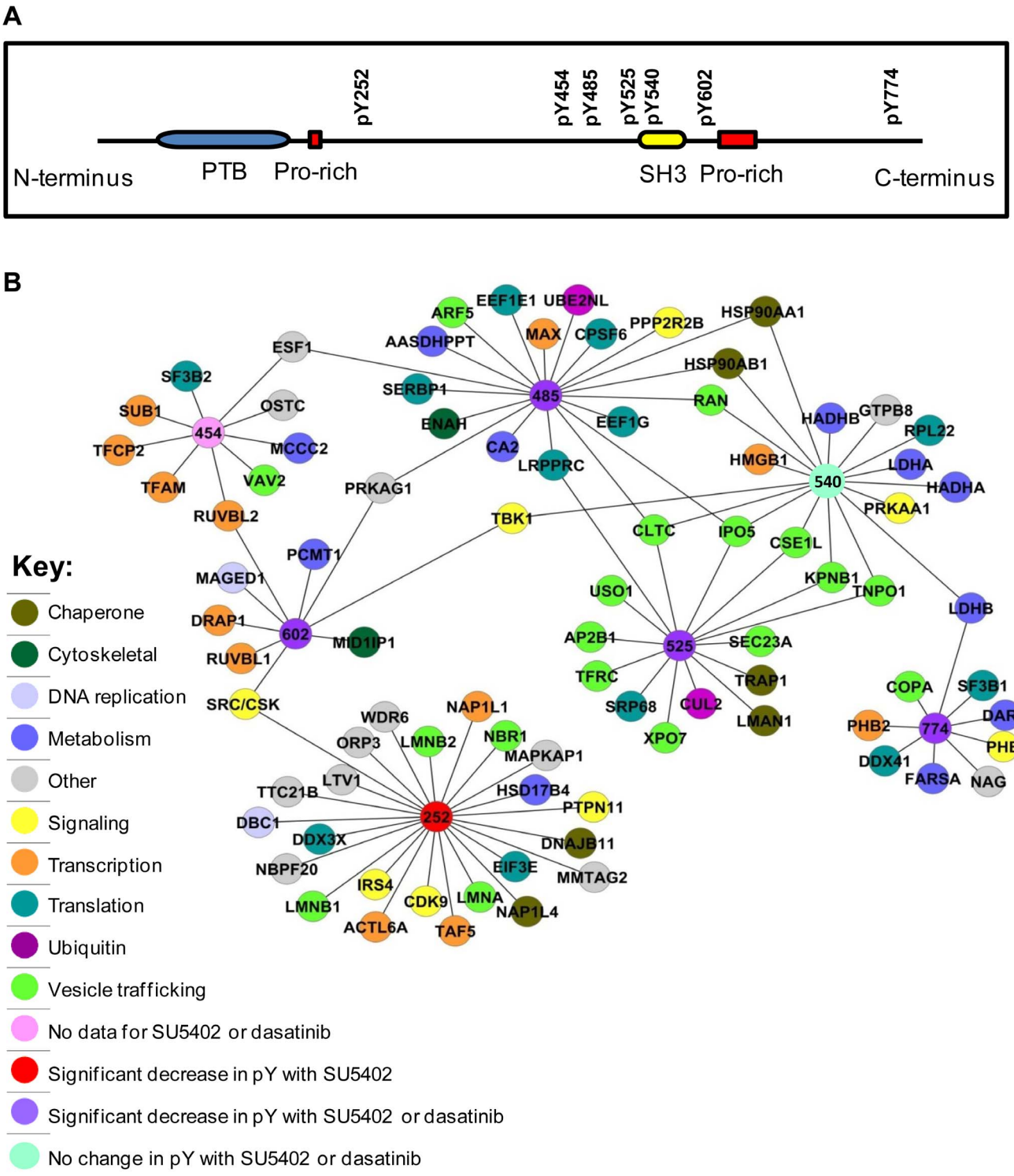

Figure 4. Protein-peptide interaction network for proteins binding specifically to phosphotyrosine-containing Eps8 peptides. A) Schematic diagram showing locations of the pY residues within the domain structure of Eps8. B) Using SILAC we carried out quantitative peptide pull-down assays from FGF2 stimulated (20 ng/ml; 15 min) HEK 293T cells to compare protein-peptide interactions for phosphotyrosine versus non-phosphotyrosine containing Eps8 peptides. Proteins interacting preferentially to phosphotyrosine peptides have been plotted in an interaction network.
doi:10.1371/journal.pone.0061513.g004

Mass Spectrometry

On-line liquid chromatography was performed by use of an Dionex Ultimate 3000 LC system (Thermo Fisher Scientific). Peptides were loaded onto an Acclaim PepMap 100 C18 resolving column (15 cm length;75 μm internal diameter; LC Packings, USA) and separated over a 40 minute gradient from 3.2% to 44%

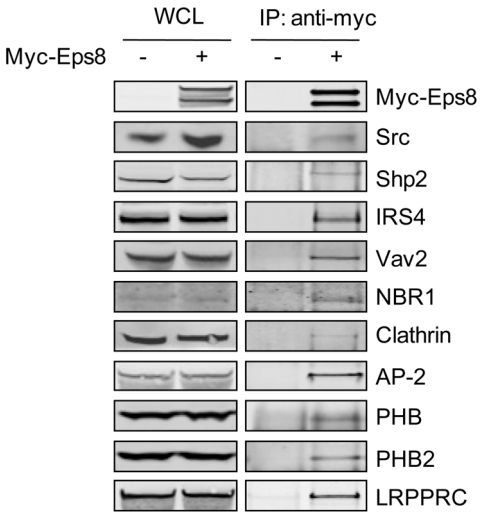

Figure 5. Full-length Eps8 interacts with a range of proteins identified in the peptide pull down assays. HEK 293T cells were either transfected with Myc-Eps8 or left untransfected. Cells were stimulated with 20 ng/ml FGF2 for 15 min and immunoprecipitated using an anti-Myc antibody. Western blot analysis was carried out on whole cell lysate and immunoprecipitation samples using antibodies against the indicated proteins.
doi:10.1371/journal.pone.0061513.g005

acetonitrile (Baker, Holland). Peptides eluted directly (350 nL/min) via a Triversa nanospray source (Advion Biosciences, NY, USA) into a LTQ Orbitrap Velos mass spectrometer (Thermo Fisher Scientific). The mass spectrometer alternated between a full FT-MS scan (m/z 380-1600) and subsequent CID MS/MS scans of the twenty most abundant ions. Survey scans were acquired in the Orbitrap cell with a resolution of 60,000 at m/z 400. Precursor ions were isolated and subjected to CID in the linear ion trap. Isolation width was 2 Th. Only multiply-charged precursor ions were selected for MS/MS. CID was performed with helium gas at a normalized collision energy of 35%. Precursor ions were activated for 10 ms. Data acquisition was controlled by Xcalibur 2.1 software.

Identification and Quantification of Peptide and Proteins

Mass spectra were processed using the MaxQuant software (version 1.0.13.13) [22,23]. Data were searched, using MASCOT version 2.2 (Matrix Science), against a concatenated database consisting of the human IPI database (version 3.72) supplemented with common contaminants (including keratins, trypsin, BSA) and the reversed-sequence version of the same database. The human database contained 173,046 protein entries (86,523 of which were reversed-sequence versions). The search parameters were: minimum peptide length 6, peptide tolerance 7 ppm, mass tolerance 0.5 Da, cleavage enzyme trypsin/P, and a total of 2 missed cleavages were allowed. Carbamidomethyl (C) was set as a fixed modification and oxidation (M), acetylation (Protein N-term),

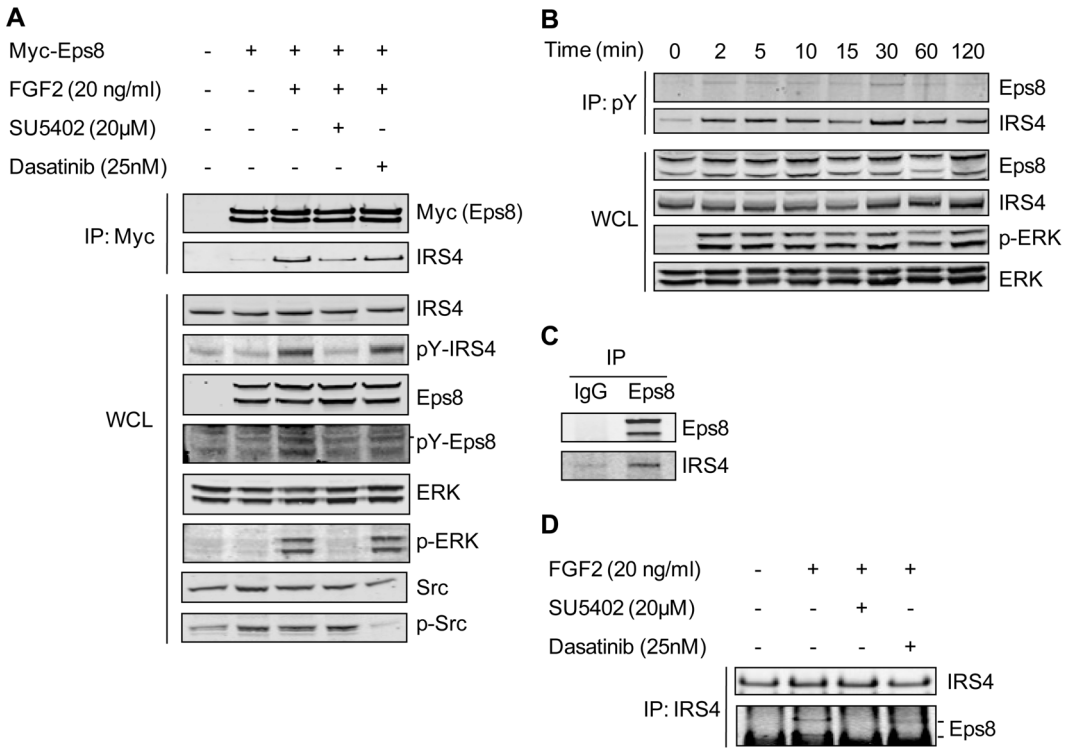

Figure 6. Eps8 and IRS4 interact in an FGF2 dependent manner that correlates with an increase in their tyrosine phosphorylation. A) HEK293T cells transfected with Myc-Eps8 were stimulated with 20 ng/ml FGF2 for 15 min either following 30 min pretreatment with SU5402 or dasatinib or in the absence of inhibitors. Anti-Myc immunoprecipitation and whole cell lysate samples were analysed by western blotting. B) HEK293T cells were stimulated with 20 ng/ml FGF2 for different lengths of time and tyrosine phosphorylated proteins were immunoprecipitated. Anti-pY immunoprecipitation and whole cell lysate samples were analysed by western blotting. C) HEK 293T cells were stimulated with 20 ng/ml FGF2 for 15 min and immnoprecipitations carried out using antibodies to either Eps8 or rabbit IgG. Resulting IP samples were analysed by western blotting. d) Following 30 min treatment with SU5402 or dasatinib and stimulation with 20 ng/ml FGF2 for a further 15 min, endogenous IRS4 was immunoprecipitated from HEK293T cells. Resulting IP samples were analysed by western blotting.
doi:10.1371/journal.pone.0061513.g006

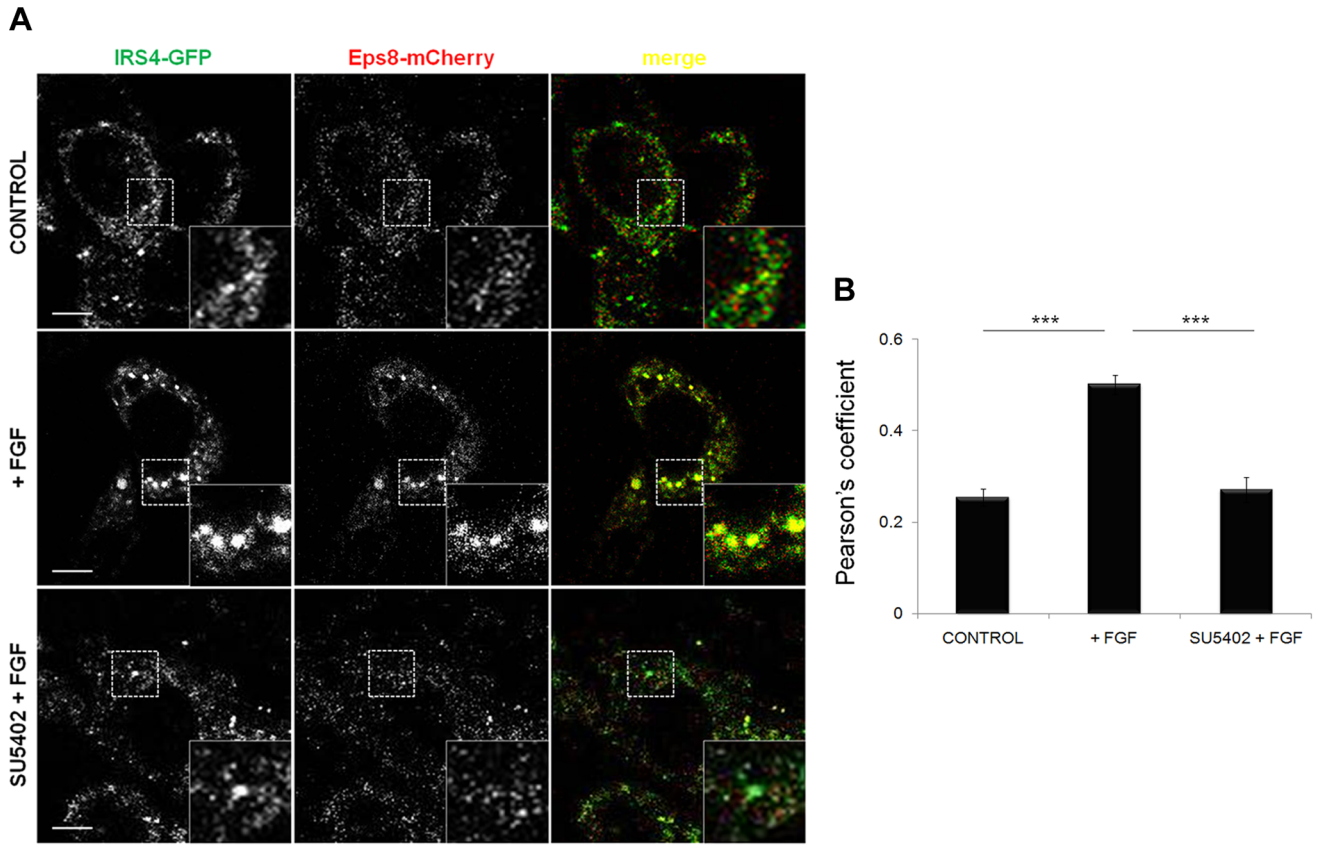

Figure 7. Eps8 and IRS4 colocalise within cells in an FGF2 dependent manner. NIH 3T3 cells were co-transfected with IRS4-GFP and Eps8-mCherry. Cells stimulated with FGF2 (20 ng/ml) in the presence and absence of SU5402 (25 μM) were compared to unstimulated cells (control). A) Confocal microscopy was used to visualise the localisation of IRS4 and Eps8. B) The colocalisation (Pearson's coefficient) between IRS4 and Eps8 is significantly increased in the presence of FGF2 and absence of SU5402 (Pearson's coefficient, mean±SEM, n = 42 cells. Scale bars = 5 μm. ***, $P<0.001$).
doi:10.1371/journal.pone.0061513.g007

Phospho (ST), and Phospho (Y) were set as variable modifications. The appropriate SILAC labels were selected and the maximum labelled amino acids was set to 3.

All experiments were filtered to have a peptide and protein false-discovery rate (FDR) below 1%. Within the MaxQuant output, phosphorylation sites were considered to be localised correctly if the localisation score (PTM score) was at least 0.85 (85%). Additional information is listed in Method S1.

Confocal Microscopy and Quantification Analysis

Cells were fixed in 4% paraformaldehyde (PFA; Electron Microscopy Sciences) in PBS for 10 min prior to analysis. Confocal laser microscopy was performed with an inverted microscope (Zeiss LSM 710) using a 40×1.3NA oil-immersion objective and a Transmission-Photomultiplier LSM T-PMT. Data analysis was performed using NIS-Elements Imaging Software version 3.2 (Nikon). The experiment was repeated 3 times and an image that represented the phenotype of most of the cells was selected.

Results and Discussion

Effects of SU5402 and Dasatinib on Eps8 Phosphorylation

Eps8 is a phosphorylation substrate for FGFR [8] and Src [9]. To identify the residues upon which these phosphorylation events take place we have used a targeted mass spectrometric approach. A quantitative SILAC technique coupled with chemical inhibition of FGFR or SFK activity has been used to examine any differential regulation in the phosphorylation of Eps8. Dasatinib is an SFK/ABL kinase inhibitor approved for use in patients with chronic myelogenous leukemia [24]. Here, dasatinib has been used to inhibit SFK activity in preference to SU6656 [25], which was our previous inhibitor of choice prior to dasatinib becoming commercially available [15]. At concentrations needed to inhibit Src kinase activity in HEK 293T cells, SU6656 also shows some inhibition of FGFR activation, as measured by levels of phosphorylated ERK (Figure 1A). Dasatinib does not show inhibition of FGFR induced ERK activity, even at high concentrations (Figure 1B). SU5402, has been used to inhibit the tyrosine kinase activity of FGFR1 [26] and does not have any effect on phospho-Src levels (Figure 1A). Using these compounds has allowed us to differentiate between SFK-mediated and FGFR-mediated phosphorylation events on Eps8 by comparing levels of phosphorylation in the presence of dasatinib and SU5402.

We transfected three populations of HEK 293T cells, grown in either 'Light' R0K0, 'Medium' R6K4, or 'Heavy' R10K8 SILAC media, with Myc-Eps8. Cells were either left untreated (R0K0) or pre-treated with SU5402 (R6K4) or dasatinib (R10K8) for 30 min before stimulation with FGF2 for a further 15 min. Prior to mass spectrometric analysis, phosphopeptide enrichment was carried out on immunoprecipitated Myc-Eps8.

A total of 22 distinct sites of phosphorylation (18 serines and 4 tyrosines) on Eps8 were identified (Table S1). Representative mass spectra for two of the identified phosphopeptides are shown in Figure 2 (see Figure S3 for additional spectra). The log-ratios for each identification of phosphorylated peptide and non-phosphorylated counterpart peptide are plotted in Figure 3 (tyrosine residues) and Figure S1 (serine residues) and provide a visual comparison of the relative ratios and number of peptide identifications between non-treated and inhibitor treated samples. Statistical methods for determining differential phosphorylation are discussed by de la Fuente van Bentem *et al.* [27]. Our preferred statistical method for deciding differential phosphorylation between samples is to use a t-test to directly compare non-phosphorylated and phosphorylated counterpart peptides. However, the t-test has only been applied when there are three or more replicates for each peptide. Another method to determine differential phosphorylation is to select a cut-off for significant statistics which is based on p-values determined from a test sample (Method S1). This has been applied when only two identifications have been made. Of the 4 tyrosine residues identified, 3 phosphotyrosine containing peptides (pY525, pY602, pY774) had reduced SILAC ratios compared to their unphosphorylated counterpart in the presence of both SU5402 and dasatinib, indicating that the tyrosine phosphorylation on these particular sites within Eps8 are sensitive to both FGFR and SFK activity (Figure 3A).

Eps8 contains 20 tyrosine residues, and according to the PhosphositePlus database [28], 9 of them have been found in their phosphorylated form in the human protein. It may be that under our experimental conditions in which the cells were stimulated with FGF2, only the 4 tyrosines that we have identified are phosphorylated. However, it is also possible that the levels of some phosphopeptides remain too low for mass spectrometric detection. Thus, in an attempt to increase the number of phosphorylated tyrosine residues identified, prior to FGF2 stimulation, cells were treated with sodium pervanadate to inhibit tyrosine phosphatase activity and maximise the levels of tyrosine phosphorylated peptides. Under these conditions, an additional 3 phosphotyrosine containing peptides were identified, and the majority of the previously identified phosphopeptides were present in greater abundance (Figure 3B). Several additional serine residues were also identified (Figure S1). Of the tyrosine residues identified, 5 phosphotyrosine peptides (pY252, pY485, pY525, pY540, pY602, pY774) had a reduced SILAC ratio in the presence of SU5402 indicating that these particular sites within Eps8 are regulated by FGFR kinase activity (Figure 3B). Four (pY485, pY525, pY602, pY774) also had a reduced SILAC ratios in the presence of dasatinib, indicating that these sites are regulated by SFK activity (Figure 3B). One phosphopeptide (pY454) was identified but was of too low abundance for ratio calculation. Data obtained in the absence and presence of sodium pervandate were in agreement in terms of the differential regulation of phosphorylation on these sites. In the absence of tyrosine phosphatase activity, the number of phosphotyrosine peptide identification events for site pY525 was hugely increased, suggesting that this site is readily phosphorylated but has a high turnover rate. Phosphorylation and dephosphorylation of proteins at distinct sites can act as a molecular switch regulating the association and disassociation of interacting proteins. It may be that the Y525 is an important regulatory site that is required to be turned over at a high frequency rate in order to allow Eps8 function.

Our experiments have identified 16 of the 20 tyrosines present within the human form of Eps8, the remainder being in regions of the protein that were not detected. The total sequence coverage of Eps8 is 68%. In the presence of FGF2, 7 of these tyrosine residues are phosphorylated and for 6 of these a SILAC ratio could be calculated. Residue pY540 shows no change in phosphorylation due to the presence of the inhibitors, residue pY252 shows a decrease in phosphorylation only in the presence of the FGFR inhibitor, and the phosphorylation on residues pY485, pY525, pY602, and pY774 are decreased in the presence of both the FGFR and SFK inhibitor.

Phosphotyrosine Specific Interactions

In the presence of FGF2, we have identified specific sites of tyrosine phosphorylation on Eps8. We have demonstrated differential phosphorylation events on a number of these sites that are dependent on activity of FGFR or SFKs. The distribution of these sites on Eps8 is shown graphically in Figure 4A. Our aim was to then further characterise these sites by identifying phospho-dependent protein binding partners. To identify such potential pTyr-dependent interacting partners for these residues in Eps8, which may be involved in cellular processes downstream of FGFR, we used a quantitative proteomic peptide pulldown (PPD) approach [18]. Peptides containing the desired tyrosine residues were synthesised in their phosphorylated and non-phosphorylated forms. Using SILAC, we incubated heavy labelled (R10K8) HEK 293T cell lysates with phosphorylated peptide, medium labelled (R6K4) lysates with non-phosphorylated peptide, and light lysates (R0K0) were used as a no peptide control. All cells were treated with FGF2 for 15 min prior to lysis. The huge advantage of using SILAC over other techniques is that the specific binders can still be identified in the presence of many non-specific proteins. Typically a pull-down experiment will isolate not only specific interactors but also background proteins that are binding to the bead matrix. Proteins with SILAC ratios close to 1:1 can be discarded and only those proteins that are significantly enriched in one of the populations are regarded as 'hits'. To qualify as a pY-dependent binder in these PPD experiments, proteins had to have a $H_{pY}/M_{non\text{-}pY}$ and $H_{pY}/L_{control}$ ratio at least 2 standard deviations higher than the median (95% confidence). H/M and H/L ratios for all proteins identified in each PPD experiment are plotted in Figure S2. There are instances when peptides are identified only in the heavy state and, therefore, not assigned a ratio. In these cases, the mass spectra were manually checked to identify pY-peptide specific interactors. Eighty-five distinct proteins with a range of cellular functions were identified for the 7 pY-peptides (Figure 4B; Table S2).

We have identified a number of SH2 or PTB domain-containing proteins from our PPD assays which are likely to be direct interacting partners for our phosphotyrosine peptides. These proteins include known phosphotyrosine-binding proteins Shp2 (PTPN11), Vav2 and Insulin receptor substrate 4 (IRS4). In addition, four heavy labelled peptides identified as common to both Src and CSK were enriched in the pY-PPD for residues 252 and 602. From this data it is not possible to discriminate between these two proteins as they have high sequence homology, however, Eps8 is known to bind to Src [9]. STAT3, another SH2 domain containing protein, was identified in the pY525 PPD, with a significantly increased $H_{pY}/M_{non\text{-}pY}$ ratio (>95% confidence) and an increased $H_{pY}/L_{control}$ (>93% confidence). As both ratios were not >95% confidence, STAT3 was not included in Figure 4B and Table S2.

IRS4, Shp2 and WDR6 were identified as a potential novel binding partners for the pY252 peptide. IRS4 acts as an interface between receptor tyrosine kinases, such as IGF1R [29] and FGFR1 [19], and SH2-containing intracellular signalling molecules. It contains an IRS PTB domain, through which it can bind

to phosphorylated proteins. IRS4 is known to interact with both Shp2 [30] and WDR6 [31,32,33], and all these proteins have been implicated in FGFR signalling [19,20,34].

Eps8 has been shown to regulate receptor endocytosis via its interaction with RN-Tre [5]. When bound to Eps8, RN-Tre, a RabGAP, acts on Rab5 to inhibit EGFR internalisation [5]. We have found several potential Eps8 binding proteins that also play a role in endocytosis. Clathrin heavy chain was enriched preferentially with pY485, pY525 and pY540 peptides, and a component of the adaptor protein complex 2 (AP-2), AP-2 complex subunit beta-1 (AP2B1), with the pY525 peptide. AP-2 is involved in clathrin-dependent endocytosis in which cargo proteins become incorporated into clathrin-coated vesicles (CCVs) which fuse with the early endosome. Recently Eps8 has been shown to be recruited to clathrin-coated structures at the plasma membrane [35] and, furthermore, we have found that FGFR activation promotes clathrin-mediated endocytosis through Eps8 and Src [36]. Vav2, found enriched for pY454, regulates EGFR receptor endocytosis and degradation [37] and NBR1, found enriched for pY252, regulates the degradation of receptor tyrosine kinases [38]. These proteins are potential novel Eps8 interactors that may act downstream of FGFR.

Proteins involved in vesicular trafficking to and from the Golgi apparatus include Arf5, a protein involved in vesicle budding from the Golgi, identified in the pY485 PPD, coatamer subunit alpha (COPA) in the pY774 PPD and both Sec23A and general vesicular transport factor p115 (USO1) in the pY525 PPD.

A cluster of proteins involved in nucleocytoplasmic transport were found bound to pY485, pY525, and pY540: the small GTPase Ran, Importin-5 (IPO5), importin subunit beta 1 (KPNB1), Exportin-2 (CSE1L), Exportin-7 (XPO7), and Transportin-1 (TNPO1). A number of these proteins are known to bind, either in isolation, or together with an adapter protein, to nuclear localisation signals (NLSs) in cargo proteins. As an NLS is a positively charged sequence, it is possible that these proteins can bind preferentially to peptides containing basic residues. Peptide 540 is a potential candidate for this, having 4 lysine residues in close proximity. However, each of these proteins is enriched specifically for the pY form of the peptide, arguing against lysine-dependent binding. Eps8 contains a putative NLS between residues 299–309 [8], but has not been reported to be present in the nucleus.

Out of the many proteins identified that have functions in protein trafficking, whether it be from the plasma membrane, to and from the Golgi, or to and from the nucleus, a significant number of them are associated with the pY525 peptide. Interestingly this is the site that we find to have a high turnover rate, suggesting a functional role in a dynamic cellular process.

MAPKAP1 (Sin1) was recruited to the pY252 peptide. MAPKAP1 interacts with mammalian target of rapamycin (mTOR) and is found in the mTOR complex 2 (mTORC2) [39,40,41]. Interestingly, Eps8 has been shown to regulate the expression of FAK via the mTor/STAT3 pathway [11]. Eps8 overexpression leading to increased activity of FAK via this pathway has been shown to promote disease progression in colon cancer [11]. MAPKAP1 may be a physical link to this pathway. As previously mentioned, STAT3 was also identified in the pY525 PPD. Additionally, STAT3 has been linked to FGFR in tumour cells where it can interact with amplified receptor [42].

Other potentially interesting putative Eps8 binding partners that we have identified that could link Eps8 to FGFR signalling include LRPPRC, which has previously been co-purified with the FGFR complex [43], and PHB which is required for Ras-mediated Raf-MEK-ERK activation [44].

Several RNA-binding proteins have been found in our PPDs. It has been reported previously that RNA-binding proteins can bind preferentially to the negative charge on the phosphorylated peptides, thus appearing as specific binders when they are actually contaminants [18].

Novel Eps8 Binding Partners

Without further validation proteins identified in peptide pull-down assays can only be described as potential interactors. It may be that the interactions are not biologically relevant, or when the full length protein is in its folded conformation the interactions detected between peptide and protein are not sterically possible. In addition contaminants arising from interactions with the bead matrix may be present. Common IP contaminants, described as the 'bead proteome' are listed and scored in the 'protein frequency library' (used to identify the frequency with which proteins appear in a subset of IPs using a particular type of beads) [45,46]. This library can help in discriminating between those proteins that are true interactors and those that may be bead contaminants. The majority of proteins identified both here, and with a high frequency (68–92%) in experiments compiled in the protein frequency library [46] are RNA-binding proteins: 60S ribosomal protein (RPL22), SERBP1, ATP-dependent RNA helicase DDX3X, splicing factor 3B subunits 1 and 2 (SF3B1, SF3B2), DEAD box protein 41 (DDX41). Hence further validation is required to identify 'true' protein-protein interactions.

In an attempt to further validate potential protein-protein interactions we used co-immunoprecipitation to pull down Myc-tagged Eps8 protein from FGF2 stimulated HEK 293T cells and probed for proteins of interest (Figure 5). The interactions between Eps8 and AP-2 and clathrin, proteins important in clathrin-mediated endocytosis, have been confirmed. This further supports evidence that Eps8 plays an important role in endocytic trafficking. In addition, we confirm the novel interactions between Eps8 and Shp2, Vav2, NBR1, LRPPRC, PHB, PHB2 and IRS4. It must be noted that, although co-immunoprecipitation experiments such as these can confirm protein-protein interactions it is acknowledged that they detect both direct and indirect interactions.

The Novel Interaction between Eps8 and IRS4 is FGF2 Dependent

FGF2 activation of FGFR1 and FGF7 activation of FGFR2 results in phosphorylation of IRS4 on residue 921 [19,20]. Phosphorylation of IRS4 promotes the formation of a complex with Shc, which may link IRS4 directly to activated receptor, and also allows recruitment of Grb2, PLCγ and PI3K thus promoting downstream signalling [19]. In our PPDs IRS4 was identified as a potential novel binding partner for the Eps8 peptide containing phosphorylated Tyr252, a residue shown to be sensitive to the addition of the FGFR kinase inhibitor, SU5402 and not the SFK inhibitor, dasatinib (Figures 3 and 4). Furthermore, the Eps8-IRS4 protein-protein interaction was confirmed by subsequent co-immunoprecipitation experiments with Myc-Eps8 in FGF2 stimulated cells (Figure 5). Next, as eluded to in the peptide pull down assays, we investigated whether the Eps8-IRS4 interaction within cells is dependent upon FGF2 activation and, therefore, sensitive to the addition of SU5402 but not dasatinib. Co-immunoprecipitation experiments were performed in the presence and absence of FGF2, SU5402 and dasatinib (Figure 6). The association between Myc-Eps8 and IRS4 increases in the presence of FGF2 (Figure 6A). Pre-treatment with SU5402 causes an inhibition of this interaction, indicating this increased association is due to activation of the FGF receptor. This FGF2 dependent

increase in the association is not affected by the presence of dasatinib and, therefore, not dependent on SFK phosphorylation. An increase in phosphorylation of both Eps8 and IRS4 is seen upon FGF2 activation as previously reported [8,19]. Both Eps8 and IRS4 are tyrosine phosphorylated in response to FGF2 in HEK 293T cells (Figure 6A) and remain so throughout the duration of receptor activation (Figure 6B). The interaction between Eps8 and IRS4 has been confirmed using endogenous levels of both proteins (Figure 6C). Co-immunoprecipitation of endogenous levels of Eps8 and IRS4 only in the presence of FGF2 and FGF2 with dasatinib, both conditions where FGF receptor is active, confirm that this interaction is FGF dependent (Figure 6D) as seen with overexpressed Eps8. Cell imaging data using fluorescently tagged proteins confirm these results. Following FGF2 stimulation, Eps8 colocalises with IRS4 in NIH 3T3 cells within the cytoplasm (Figure 7). This colocalisation is decreased following the addition of SU5402 indicating that it is dependent upon activated FGFR. These data, together with the peptide pull down data suggests that the interaction between Eps8 and IRS4 may occur on residue 252 of Eps8 when it is a phosphorylated state and whose phosphorylation is dependent upon FGFR activation.

Conclusions

Here we have used quantitative proteomics to study the phosphorylation of Eps8 and phosphotyrosine dependent binding of proteins to it. Clusters of proteins with distinct cellular functions have been identified, including a large number involved in trafficking, either from the cell membrane, the Golgi or from cytoplasm to nucleus and vice versa. Most of the proteins identify are potential novel interactors, and further studies are needed to validate some of these interactions. The validated interactions between Eps8 and clathrin and AP-2, provide further evidence to support the role of Eps8 in receptor mediated endocytosis. Also, the interaction between Eps8 and IRS4, together with the knowledge that IRS4 is involved in downstream signalling from the FGF receptor, is an interesting lead into the role of Eps8 in FGFR signalling. In conclusion, Eps8 is a multi-functional adaptor protein which may have the capabilities of integrating receptor trafficking, cellular signalling, and protein degradation.

Supporting Information

Figure S1 Differential regulation of serine phosphorylation on Eps8. Heavy, medium and light SILAC labelled HEK 293T cells were treated with either dasatinib, SU5402, or no inhibitor, prior to FGF2 stimulation. Myc-Eps8 was immunoprecipitated and the resulting sample was run on an SDS-PAGE gel and, following in-gel trypsin digestion and phophopeptide enrichment, analysed by mass spectrometry. Each graph represents specific residues on Eps8 as indicated. Each data point represents a single peptide identification. *P* values were calculated by an unpaired t-test (0.01–0.05 = *; 0.001–0.01 = **; <0.001 = ***). +, the median of the ratios is outside the significance cut-off values (<0.57 or >1.75) and is deemed significantly changed (see) A) Experiment was carried out in the absence of sodium pervanadate. B) Experiment was carried out in the presence of 2 mM sodium pervanvadate.
(PDF)

Figure S2 Relative SILAC ratios for proteins identified in peptide pull down assays. Biotinylated Eps8 peptides containing the desired tyrosine residues (the residue number is indicated at the top of each plot) were synthesised in their phosphorylated and non-phosphorylated forms. Three peptide pull down assays for each residue were performed. Using SILAC, we incubated heavy labelled (R10K8) HEK 293T cell lysates with phosphorylated peptide, medium labelled (R6K4) lysates with non-phosphorylated peptide, and light lysates (R0K0) were used as a no peptide control. All cells were treated with FGF2 for 15 min prior to lysis. Following washing, the beads from each assay were combined, the resulting sample run on an SDS-PAGE gel and, following in-gel trypsin digestion, analysed by mass spectrometry. Each graph represents specific residues on Eps8 as indicated. Each data point represents a single protein identification and is shown as a function of its $H_{pY}/M_{non\text{-}pY}$ and $H_{pY}/L_{control}$ ratios. Those proteins with both ratios at least 2 standard deviations higher than the median (95% confidence) are shown in red and are considered pY-specific binders (these protein are named in Figure 4).
(PDF)

Figure S3 Additional Mass Spectra of Phosphorylated Peptides Identified.
(PDF)

Table S1 Phosphorylated Peptides and non-Phosphorylated Counterpart Peptides Identified in Triple SILAC (+/− SU5402/dasatinib) Experiments.
(XLS)

Table S2 Proteins Identified as pY-specific binders in SILAC peptide pull down (PPD) experiments.
(XLS)

Method S1 Supplementary details regarding Peptide and Protein Identification and Quantification.
(DOC)

Acknowledgments

The authors would like to gratefully acknowledge Sue Brewer and Cleidiane Zampronio for technical support.

Author Contributions

Conceived and designed the experiments: DLC GA SMMS JZR JKH. Performed the experiments: DLC AJC GA TT. Analyzed the data: DLC MMG. Wrote the paper: DLC JKH.

References

1. Scita G, Nordstrom J, Carbone R, Tenca P, Giardina G, et al. (1999) EPS8 and E3B1 transduce signals from Ras to Rac. Nature 401: 290–293.
2. Biesova Z, Piccoli C, Wong WT (1997) Isolation and characterization of e3B1, an eps8 binding protein that regulates cell growth. Oncogene 14: 233–241.
3. Scita G, Tenca P, Areces LB, Tocchetti A, Frittoli E, et al. (2001) An effector region in Eps8 is responsible for the activation of the Rac-specific GEF activity of Sos-1 and for the proper localization of the Rac-based actin-polymerizing machine. J Cell Biol 154: 1031–1044.
4. Chen H, Wu X, Pan ZK, Huang S (2010) Integrity of SOS1/EPS8/ABI1 tricomplex determines ovarian cancer metastasis. Cancer Res 70: 9979–9990.
5. Lanzetti L, Rybin V, Malabarba MG, Christoforidis S, Scita G, et al. (2000) The Eps8 protein coordinates EGF receptor signalling through Rac and trafficking through Rab5. Nature 408: 374–377.
6. Disanza A, Carlier MF, Stradal TE, Didry D, Frittoli E, et al. (2004) Eps8 controls actin-based motility by capping the barbed ends of actin filaments. Nat Cell Biol 6: 1180–1188.
7. Disanza A, Mantoani S, Hertzog M, Gerboth S, Frittoli E, et al. (2006) Regulation of cell shape by Cdc42 is mediated by the synergic actin-bundling activity of the Eps8-IRSp53 complex. Nat Cell Biol 8: 1337–1347.

8. Fazioli F, Minichiello L, Matoska V, Castagnino P, Miki T, et al. (1993) Eps8, a substrate for the epidermal growth factor receptor kinase, enhances EGF-dependent mitogenic signals. EMBO J 12: 3799–3808.
9. Maa MC, Lai JR, Lin RW, Leu TH (1999) Enhancement of tyrosyl phosphorylation and protein expression of eps8 by v-Src. Biochim Biophys Acta 1450: 341–351.
10. Gallo R, Provenzano C, Carbone R, Di Fiore PP, Castellani L, et al. (1997) Regulation of the tyrosine kinase substrate Eps8 expression by growth factors, v-Src and terminal differentiation. Oncogene 15: 1929–1936.
11. Maa MC, Lee JC, Chen YJ, Lee YC, Wang ST, et al. (2007) Eps8 facilitates cellular growth and motility of colon cancer cells by increasing the expression and activity of focal adhesion kinase. J Biol Chem 282: 19399–19409.
12. Wang H, Patel V, Miyazaki H, Gutkind JS, Yeudall WA (2009) Role for EPS8 in squamous carcinogenesis. Carcinogenesis 30: 165–174.
13. Yap LF, Jenei V, Robinson CM, Moutasim K, Benn TM, et al. (2009) Upregulation of Eps8 in oral squamous cell carcinoma promotes cell migration and invasion through integrin-dependent Rac1 activation. Oncogene 28: 2524–2534.
14. Matoskova B, Wong WT, Salcini AE, Pelicci PG, Di Fiore PP (1995) Constitutive phosphorylation of eps8 in tumor cell lines: relevance to malignant transformation. Mol Cell Biol 15: 3805–3812.
15. Cunningham DL, Sweet SM, Cooper HJ, Heath JK (2010) Differential phosphoproteomics of fibroblast growth factor signaling: identification of Src family kinase-mediated phosphorylation events. J Proteome Res 9: 2317–2328.
16. Blagoev B, Kratchmarova I, Ong SE, Nielsen M, Foster LJ, et al. (2003) A proteomics strategy to elucidate functional protein-protein interactions applied to EGF signaling. Nat Biotechnol 21: 315–318.
17. Amanchy R, Kalume DE, Pandey A (2005) Stable isotope labeling with amino acids in cell culture (SILAC) for studying dynamics of protein abundance and posttranslational modifications. Sci STKE 2005: pl2.
18. Schulze WX, Mann M (2004) A novel proteomic screen for peptide-protein interactions. J Biol Chem 279: 10756–10764.
19. Hinsby AM, Olsen JV, Mann M (2004) Tyrosine phosphoproteomics of fibroblast growth factor signaling: a role for insulin receptor substrate-4. J Biol Chem 279: 46438–46447.
20. Luo Y, Yang C, Jin C, Xie R, Wang F, et al. (2009) Novel phosphotyrosine targets of FGFR2IIIb signaling. Cell Signal 21: 1370–1378.
21. Shevchenko A, Tomas H, Havlis J, Olsen JV, Mann M (2006) In-gel digestion for mass spectrometric characterization of proteins and proteomes. Nat Protoc 1: 2856–2860.
22. Cox J, Mann M (2008) MaxQuant enables high peptide identification rates, individualized p.p.b.-range mass accuracies and proteome-wide protein quantification. Nat Biotechnol 26: 1367–1372.
23. Cox J, Matic I, Hilger M, Nagaraj N, Selbach M, et al. (2009) A practical guide to the MaxQuant computational platform for SILAC-based quantitative proteomics. Nat Protoc 4: 698–705.
24. Kantarjian H, Jabbour E, Grimley J, Kirkpatrick P (2006) Dasatinib. Nat Rev Drug Discov 5: 717–718.
25. Blake RA, Broome MA, Liu X, Wu J, Gishizky M, et al. (2000) SU6656, a selective src family kinase inhibitor, used to probe growth factor signaling. Mol Cell Biol 20: 9018–9027.
26. Mohammadi M, McMahon G, Sun L, Tang C, Hirth P, et al. (1997) Structures of the tyrosine kinase domain of fibroblast growth factor receptor in complex with inhibitors. Science 276: 955–960.
27. de la Fuente van Bentem S, Mentzen WI, de la Fuente A, Hirt H (2008) Towards functional phosphoproteomics by mapping differential phosphorylation events in signaling networks. Proteomics 8: 4453–4465.
28. Hornbeck PV, Chabra I, Kornhauser JM, Skrzypek E, Zhang B (2004) PhosphoSite: A bioinformatics resource dedicated to physiological protein phosphorylation. Proteomics 4: 1551–1561.
29. Qu BH, Karas M, Koval A, LeRoith D (1999) Insulin receptor substrate-4 enhances insulin-like growth factor-I-induced cell proliferation. J Biol Chem 274: 31179–31184.
30. Escribano O, Fernandez-Moreno MD, Zueco JA, Menor C, Fueyo J, et al. (2003) Insulin receptor substrate-4 signaling in quiescent rat hepatocytes and in regenerating rat liver. Hepatology 37: 1461–1469.
31. Chiba T, Yao J, Higami Y, Shimokawa I, Hosokawa M, et al. (2007) Identification of differentially expressed genes in senescence-accelerated mouse testes by suppression subtractive hybridization analysis. Mamm Genome 18: 105–112.
32. Chiba T, Inoue D, Mizuno A, Komatsu T, Fujita S, et al. (2009) Identification and characterization of an insulin receptor substrate 4-interacting protein in rat brain: implications for longevity. Neurobiol Aging 30: 474–482.
33. Sano H, Liu SC, Lane WS, Piletz JE, Lienhard GE (2002) Insulin receptor substrate 4 associates with the protein IRAS. J Biol Chem 277: 19439–19447.
34. Saxton TM, Henkemeyer M, Gasca S, Shen R, Rossi DJ, et al. (1997) Abnormal mesoderm patterning in mouse embryos mutant for the SH2 tyrosine phosphatase Shp-2. EMBO J 16: 2352–2364.
35. Taylor MJ, Perrais D, Merrifield CJ (2011) A high precision survey of the molecular dynamics of mammalian clathrin-mediated endocytosis. PLoS Biol 9: e1000604.
36. Auciello G, Cunningham DL, Tatar T, Heath JK and Rappoport JZ (2012) Regulation of fibroblast growth factor receptor signalling and trafficking by Src and Eps8. J Cell Sci doi: 10.1242/jcs.116228.
37. Thalappilly S, Soubeyran P, Iovanna JL, Dusetti NJ (2010) VAV2 regulates epidermal growth factor receptor endocytosis and degradation. Oncogene 29: 2528–2539.
38. Mardakheh FK, Auciello G, Dafforn TR, Rappoport JZ, Heath JK (2010) Nbr1 is a novel inhibitor of ligand-mediated receptor tyrosine kinase degradation. Mol Cell Biol 30: 5672–5685.
39. Pearce LR, Huang X, Boudeau J, Pawlowski R, Wullschleger S, et al. (2007) Identification of Protor as a novel Rictor-binding component of mTOR complex-2. Biochem J 405: 513–522.
40. Jacinto E, Facchinetti V, Liu D, Soto N, Wei S, et al. (2006) SIN1/MIP1 maintains rictor-mTOR complex integrity and regulates Akt phosphorylation and substrate specificity. Cell 127: 125–137.
41. Yang Q, Inoki K, Ikenoue T, Guan KL (2006) Identification of Sin1 as an essential TORC2 component required for complex formation and kinase activity. Genes Dev 20: 2820–2832.
42. Dudka AA, Sweet SM, Heath JK (2010) Signal transducers and activators of transcription-3 binding to the fibroblast growth factor receptor is activated by receptor amplification. Cancer Res 70: 3391–3401.
43. DiSorbo D, Shi EG, McKeehan WL (1988) Purification form human hepatoma cells of a 130-kDa membrane glycoprotein with properties of the heparin-binding growth factor receptor. Biochem Biophys Res Commun 157: 1007–1014.
44. Rajalingam K, Wunder C, Brinkmann V, Churin Y, Hekman M, et al. (2005) Prohibitin is required for Ras-induced Raf-MEK-ERK activation and epithelial cell migration. Nat Cell Biol 7: 837–843.
45. Trinkle-Mulcahy L, Boulon S, Lam YW, Urcia R, Boisvert FM, et al. (2008) Identifying specific protein interaction partners using quantitative mass spectrometry and bead proteomes. J Cell Biol 183: 223–239.
46. Boulon S, Ahmad Y, Trinkle-Mulcahy L, Verheggen C, Cobley A, et al. (2010) Establishment of a protein frequency library and its application in the reliable identification of specific protein interaction partners. Mol Cell Proteomics 9: 861–879.

Regulation of fibroblast growth factor receptor signalling and trafficking by Src and Eps8

Giulio Auciello[1,2], Debbie L. Cunningham[1], Tulin Tatar[1,2], John K. Heath[1,2] and Joshua Z. Rappoport[2,*]

[1]CRUK Growth Factor Group, University of Birmingham, Edgbaston, Birmingham B15 2TT, UK
[2]School of Biosciences, University of Birmingham, Edgbaston, Birmingham B15 2TT, UK
*Author for correspondence (j.rappoport@bham.ac.uk)

Accepted 13 November 2012
Journal of Cell Science 126, 613–624

doi: 10.1242/jcs.116228

Summary

Fibroblast growth factor receptors (FGFRs) mediate a wide spectrum of cellular responses that are crucial for development and wound healing. However, aberrant FGFR activity leads to cancer. Activated growth factor receptors undergo stimulated endocytosis, but can continue to signal along the endocytic pathway. Endocytic trafficking controls the duration and intensity of signalling, and growth factor receptor signalling can lead to modifications of trafficking pathways. We have developed live-cell imaging methods for studying FGFR dynamics to investigate mechanisms that coordinate the interplay between receptor trafficking and signal transduction. Activated FGFR enters the cell following recruitment to pre-formed clathrin-coated pits (CCPs). However, FGFR activation stimulates clathrin-mediated endocytosis; FGF treatment increases the number of CCPs, including those undergoing endocytosis, and this effect is mediated by Src and its phosphorylation target Eps8. Eps8 interacts with the clathrin-mediated endocytosis machinery and depletion of Eps8 inhibits FGFR trafficking and immediate Erk signalling. Once internalized, FGFR passes through peripheral early endosomes en route to recycling and degredative compartments, through an Src- and Eps8-dependent mechanism. Thus Eps8 functions as a key coordinator in the interplay between FGFR signalling and trafficking. This work provides the first detailed mechanistic analysis of growth factor receptor clustering at the cell surface through signal transduction and endocytic trafficking. As we have characterised the Src target Eps8 as a key regulator of FGFR signalling and trafficking, and identified the early endocytic system as the site of Eps8-mediated effects, this work provides novel mechanistic insight into the reciprocal regulation of growth factor receptor signalling and trafficking.

Key words: Eps8, FGFR, Clathrin, Endocytosis, Src

Introduction

Ligand-mediated activation of receptor tyrosine kinases (RTKs) initiates a signal transduction cascade that leads to a broad spectrum of cellular responses including differentiation, proliferation, survival and migration. These responses are initiated by recruitment of adaptors, scaffold and signalling proteins to the phosphorylated cytoplasmic tail of the receptor (Greenfield et al., 1989; Ullrich and Schlessinger, 1990; Heldin, 1995). Receptor activation also acts as the initiating stimulus for endocytosis of RTKs following ligand binding and this can occur via a variety of routes including both clathrin-mediated endocytosis (CME) and clathrin-independent endocytosis (CIE) (von Zastrow and Sorkin, 2007; Le Roy and Wrana, 2005). Endocytosis and subsequent trafficking to intracellular compartments have been considered to be principally mechanisms of signal attenuation: the former by controlling the number of receptors available for activation on the plasma membrane, the latter by sorting the internalized receptors into the intralumenal vesicles of multivescicular bodies (MVBs) where receptor proteolysis takes place and signalling is terminated (Stoscheck and Carpenter, 1984; Beguinot et al., 1984). There is mounting evidence, however, that signalling from internalized receptors persists along the endocytic pathway, and that endocytosis and intracellular trafficking mechanisms have a powerful influence on the spatial and temporal dynamics of the signal (von Zastrow and Sorkin, 2007; Di Fiore and De Camilli, 2001; Kholodenko, 2002; Polo and Di Fiore, 2006; Sorkin and Von Zastrow, 2002; Disanza et al., 2009; Sandilands and Frame, 2008) which influences biological outcomes (Zhang et al., 2000). Alternatively, recent evidence suggests that for at least some RTKs, signalling primarily occurs immediately following ligand binding prior to endocytosis (Sousa et al., 2012; Brankatschk et al., 2012). It is also possible that regulated endocytosis and intracellular trafficking of activated RTKs shape the identity of the signal as confinement within intracellular compartments provides a mechanism for regulating the composition of receptor-associated protein complexes. These considerations place emphasis on understanding the molecular mechanisms that coordinate activated RTK signalling and trafficking as key determinants of the biological outcomes of receptor activation.

Fibroblast growth factor receptors (FGFRs) represent a subfamily of 4 highly conserved RTKs (FGFR1, FGFR2, FGFR3 and FGFR4) that regulates fundamental cellular processes, including proliferation, differentiation and angiogenesis (Burgess and Maciag, 1989; Basilico and Moscatelli, 1992). FGFR activation initiates signalling through a number of pathways including the well characterised Ras/Raf/ERK and PI3 kinase/PDK/Akt pathways (Mason, 1994). Of particular interest is the occurrence of somatic or germ-line mutations in FGFRs which modify the dynamics of signal propagation via mechanisms such as hyper-sensitivity of kinase activation, ligand-independent dimerization or receptor

Journal of Cell Science

amplification (Grose and Dickson, 2005; Wesche et al., 2011; Turner and Grose, 2010; Beenken and Mohammadi, 2009). These findings indicate that understanding the mechanisms of FGFR endocytosis and trafficking, and their impact on signalling dynamics, is an important goal in understanding both pathological and physiological FGFR biology. We have previously demonstrated a critical role for non receptor tyrosine kinases of the Src family (SFKs) in shaping FGFR trafficking and signalling dynamics (Sandilands et al., 2007). Src is recruited to activated fibroblast growth factor receptor complexes through the adaptor protein factor receptor substrate 2 (FRS2) at the plasma membrane. This localisation requires both active Src and FGFR kinases, which are interdependent. Internalization of activated FGFRs involves release from complexes containing activated Src and trafficking into multiple intracellular compartments including RhoB and Rab5 endosomes via a mechanism(s) which require an intact actin cytoskeleton (Sandilands et al., 2007). Chemical and genetic inhibition studies showed strikingly different requirements for Src family kinases in FGFR-mediated signalling; activation of the phosphoinositide-3 kinase–Akt pathway is severely attenuated, whereas activation of the extracellular-signal-regulated kinase pathway is delayed in its initial phase and fails to attenuate. These findings show that Src kinase activity and Src substrates that mediate exit of activated FGFRs from the plasma membrane are critical determinants of the early phases of FGFR signal propagation.

In detailing Src substrates that are phosphorylated in the early phases of FGFR activation, in order to identify candidates for mediating Src-regulated trafficking, we identified the multifunctional scaffolding protein Eps8 as a prominent target of Src kinase activity (Cunningham et al., 2010). Eps8 is an attractive subject for further scrutiny as it has well documented roles in regulating the actin cytoskeleton (Provenzano et al., 1998) and has been implicated in trafficking of the epidermal growth factor receptor (EGFR) (Di Fiore and Scita, 2002). Furthermore, EGFR signalling through Src has previously been shown as a mechanism for regulating the cellular distribution of clathrin (Wilde et al., 1999). It is accordingly of interest to understand the functions of Eps8 in regulating FGFR trafficking and signalling dynamics.

In this study, we have performed a detailed series of analyses to investigate the mechanisms responsible for the coordinated trafficking and signalling of activated FGFR. We have specifically characterised the mechanisms controlling FGFR endocytosis and endocytic trafficking in the early phases of FGFR activation and in particular we have focused on the role of Src acting through Eps8. Eps8 is thus identified as a key mediator of the early phases of activated FGFR trafficking and signalling relevant to regulation of clathrin-mediated endocytosis, trafficking out of the early endosome into the perinuclear recycling compartment, and FGF-mediated pErk signalling.

Results

FGFR is internalized though an FGFR-kinase- and dynamin-dependent pathway

Different pathways have been implicated in the endocytosis of activated RTKs (von Zastrow and Sorkin, 2007; Le Roy and Wrana, 2005). Thus, we first set out to document the mechanism by which FGFR is trafficked following activation. We employed live-cell confocal microscopy to analyse the trafficking of activated FGFR2 in HeLa cells, which express very low levels of endogenous FGFR2 (Ahmed et al., 2008), using a GFP-tagged form of FGFR2 which was previously validated in published studies from John Ladbury's laboratory (Schüller et al., 2008). As depicted in Fig. 1A, live-cell confocal imaging demonstrates that following FGF stimulation, FGFR2–GFP undergoes rapid internalization from the plasma membrane and eventually traffics to a peri-nuclear endocytic compartment. This redistribution away from the cell periphery did not occur in the absence of ligand addition, and SU5402, a potent inhibitor of FGFR kinase activity, completely prevented FGF stimulated internalization (Fig. 1A,B) (Sun et al., 1999). Therefore, the cellular localisation and behaviour of GFP-tagged FGFR2 reflects that of endogenous protein. Thus, we have applied this quantitative and robust assay for trafficking of activated RTKs in live cells to the analysis of the routes of FGFR endocytosis and endocytic trafficking.

Several endocytosis pathways have been implicated in the internalization of activated FGFRs (Marchese et al., 1998; Citores et al., 1999; Belleudi et al., 2007; Gleizes et al., 1996; Haugsten et al., 2011). The large GTPase dynamin has been clearly demonstrated to be a crucial regulator of numerous endocytosis pathways (Doherty and McMahon, 2009). Therefore, we assessed whether inhibition of dynamin function with the potent dynamin inhibitor Dynasore affected the ligand induced endocytosis of FGFR (Macia et al., 2006). Importantly, control endocytosis studies verified the efficacy of Dynasore treatment in our systems (supplementary material Fig. S1A). As depicted in Fig. 1C,D, treatment with Dynasore completely prevented internalization of FGFR following FGF stimulation. Therefore, activated FGFRs undergo dynamin-dependent endocytosis.

FGFR is internalized through clathrin-mediated endocytosis

Two of the main endocytosis pathways that are dynamin dependent include clathrin-mediated endocytosis and entry via caveolae (Doherty and McMahon, 2009). We employed an RNAi-based approach utilising previously published siRNA which we have previously employed to silence expression of α-adaptin, a critical component of the clathrin-mediated endocytosis machinery, in HeLa cells (Rappoport and Simon, 2008; Rappoport and Simon, 2009), or caveolin1 (Li et al., 2012), which is required for caveolae formation (Rothberg et al., 1992). Control experiments revealed that α-adaptin siRNA treatment significantly inhibited transferrin endocytosis (supplementary material Fig. S1B) and potently reduced expression of α-adaptin (supplementary material Fig. S1C). Similarly, siRNA targeting caveolin1 significantly inhibited endocytosis of cholera toxin B sub-unit (supplementary material Fig. S2A) and decreased caveolin1 protein levels (supplementary material Fig. S2B). Importantly, these siRNA reagents did not reduce expression of control protein. Therefore, the utility of these inhibitory strategies has been sufficiently validated in our systems for usage in live-cell imaging studies.

As demonstrated in Fig. 2A,B, treatment with α-adaptin siRNA clearly prevented endocytosis of FGFR following FGF treatment. However, silencing of caveolin1 expression had no effect on the internalization of FGFR following stimulation (Fig. 2C,D). Thus, these results show that active FGFR enters cells via clathrin-mediated endocytosis and not through caveolae.

In order to verify the potential for clathrin-mediated endocytosis of activated FGFR we performed a series of

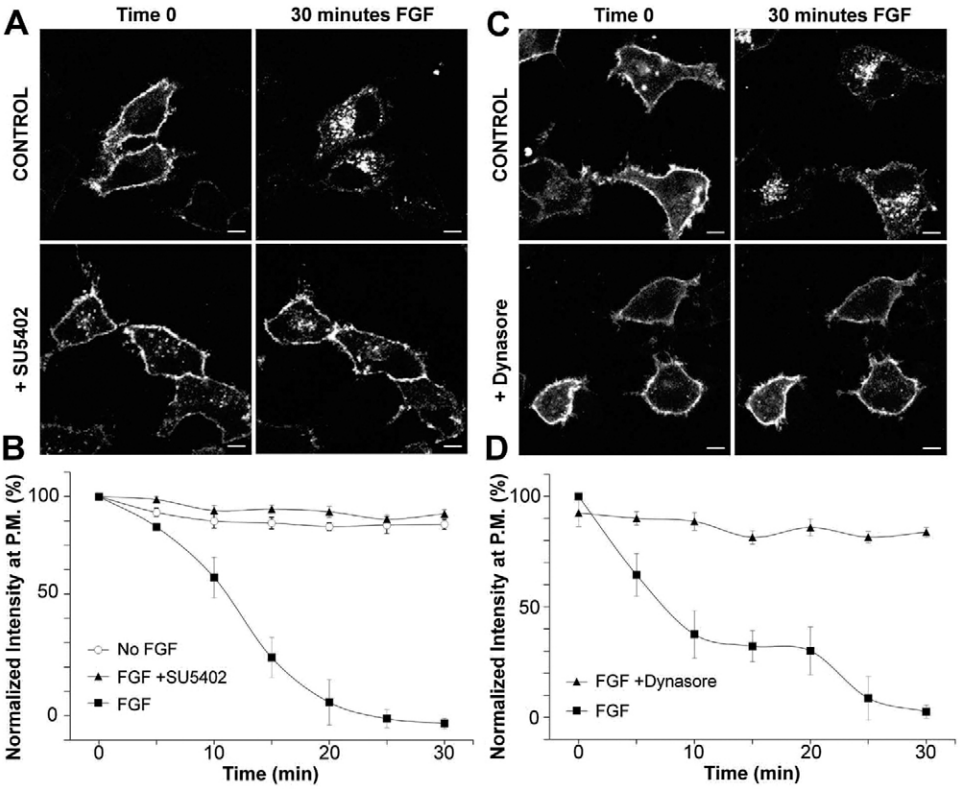

Fig. 1. Active FGFR is internalized through dynamin-dependent endocytosis. HeLa cells transiently transfected with FGFR2-GFP were incubated for 5 minutes in the presence or absence of SU5402 (**A**) or for 30 minutes in the presence or absence of Dynasore inhibitor (**C**) and imaged using confocal live-cell microscopy at 37℃ for 30 minutes following stimulation with FGF2 + heparin. The first and the last frames are shown, corresponding to the situations before and after FGF2 treatment, respectively. Scale bars: 5 μm. (**B**,**D**) The experiments shown in A and C were performed in many cells and the relative FGFR2–GFP intensity in the PM region of the cells was calculated (as described in the Materials and Methods) for each frame of the time-lapse sequence and plotted as a function of time (means ± s.e.m., $n=14$ cells).

colocalisation studies with known markers for these same two endocytosis pathways. Total internal reflection fluorescence (TIRF) microscopy permits selective illumination of the plasma-membrane-associated region with a depth of penetration of only ~100 nm (Axelrod, 2008; Mattheyses et al., 2010) and has emerged as the technique of choice for imaging trafficking

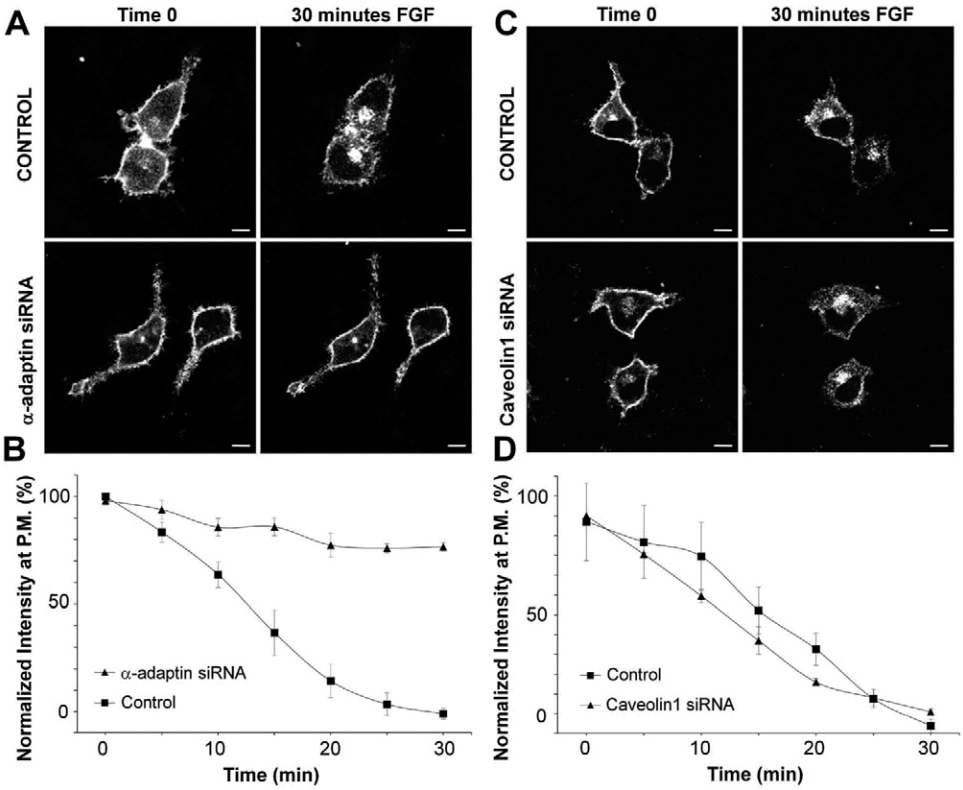

Fig. 2. Active FGFR enters cells by clathrin-mediated endocytosis and not through caveolae. HeLa cells were co-transfected with FGFR2–GFP and α-adaptin siRNA (**A**) or caveolin1 siRNA (**C**) and confocal live-cell microscopy was performed at 37℃ for 30 minutes following stimulation with FGF2 + heparin. Scale bars: 5 μm. (**B**,**D**) The experiments shown in A and C were performed in many cells and a quantification of FGFR2–GFP intensity in the PM region of the cells as function of time was performed (means ± s.e.m., $n=10$ cells).

processes at the plasma membrane such as endocytosis (Rappoport, 2008), and the dynamics of activated RTKs (Rappoport and Simon, 2009). As depicted in Fig. 3, TIRF microscopy reveals that following FGF stimulation FGFR2–GFP significantly colocalises with clathrin–dsRed (Fig. 3A,B), a previously validated marker for sites of clathrin-mediated endocytosis (Engqvist-Goldstein et al., 2001). Furthermore, consistent with our RNAi studies (Fig. 2), no significant colocalisation was observed between FGFR and a red-tagged caveolin1 fusion protein known to mark caveolae at the cell surface (Damm et al., 2005). Therefore, these two lines of evidence support the conclusion that activated FGFR enters cells primarily via clathrin-mediated endocytosis. It should be noted though that, as in our previous studies of EGFR trafficking by TIRF microscopy (Rappoport and Simon, 2009), colocalisation of activated FGFR and clathrin at the plasma membrane persists following time points where a majority of the receptor has been internalised. This could either suggest differences between endocytosis kinetics between the adherent and lateral plasma membranes, or reflect the presence of a population of growth factor receptor that does not undergo endocytosis following activation, possibly signalling through clathrin-coated pits (CCPs).

Live-cell TIRF microscopy can be employed to visualise the dynamics of RTKs at the plasma membrane, and our previous results demonstrated that following activation EGFR clusters at pre-formed CCPs prior to endocytosis (Rappoport and Simon, 2009). Three non-mutually exclusive hypothesis could describe the dynamics leading to colocalisation of activated FGFR and clathrin: FGFR could be recruited to CCPs, CCPs could form at the sites of receptor clustering, and clathrin and FGFR could accumulate simultaneously. When two-colour live-cell TIRF was performed on cells expressing FGFR2–GFP and clathrin–dsRed, it was observed that the vast majority of receptor clusters form at the sites of pre-existing clathrin (Fig. 4). In nearly all cases clathrin was observed at the site where subsequently FGFR would cluster. Thus, it seems that recruitment to pre-existing CCPs represents an emerging paradigm for the dynamics of activated RTKs.

FGFR activation promotes clathrin-mediated endocytosis through Src and Eps8

Previous evidence has identified Src as involved in the redistribution of clathrin to the cell periphery following RTK activation (Wilde et al., 1999). Therefore, we assessed whether FGFR stimulation regulated clathrin-mediated endocytosis. As depicted in Fig. 5, stimulation of cells with FGF led to a striking increase in the number of clathrin spots on the plasma membrane (Fig. 5A,B). Furthermore, this also increased the density of endocytosis events as gauged by established TIRF microscopy based criteria (Fig. 5D) (Rappoport, 2008). Interestingly, FGF treatment did not result in an increase in transferrin entry,

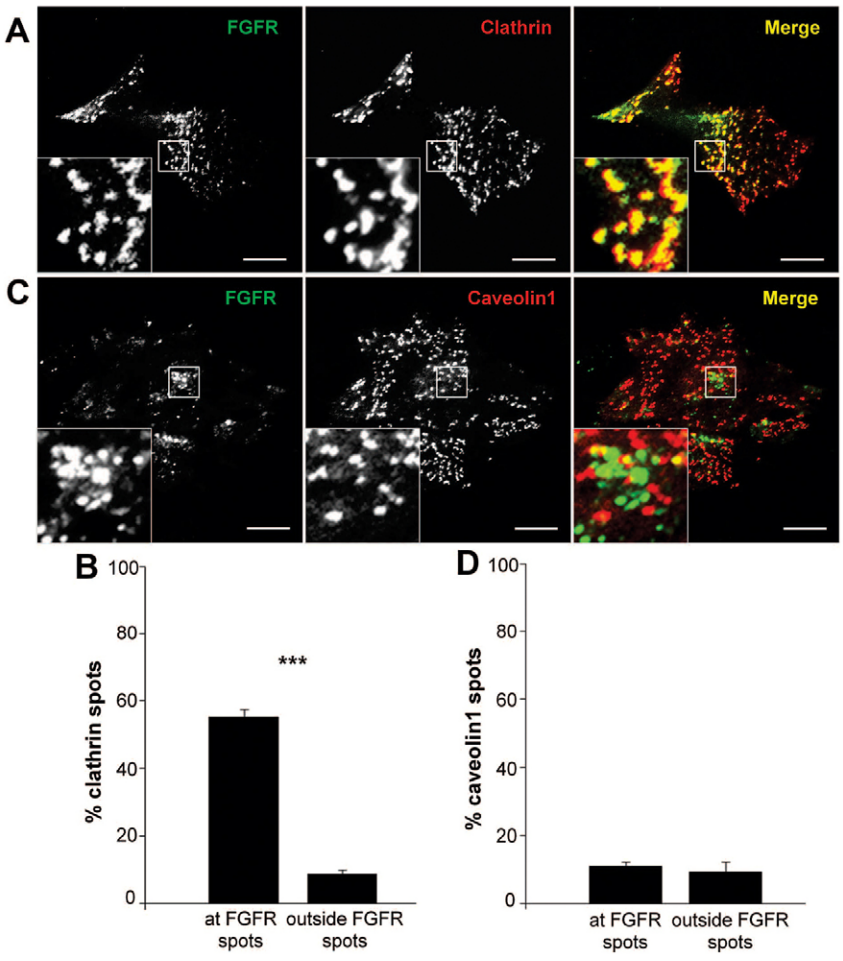

Fig. 3. Activated FGFR colocalises with clathrin at the plasma membrane but not with caveolin1. HeLa cells co-transfected with FGFR2–GFP and clathrin–dsRed (**A**) or caveolin1–mRFP (**C**) were stimulated with FGF2 + heparin for 15 minutes, then fixed and analysed using dual-colour TIRF microscopy. Higher-magnification images (insets) of selected regions of the cells show overlap of FGFR and clathrin/caveolin1 in yellow. Scale bars: 5 μm. (**B**,**D**) Quantification of colocalisation was performed by analysing the overlap of each clathrin or cavolin1 spot with an FGFR one. A control of random colocalisation is also shown (means ± s.e.m., n=24 cells). *P<0.05; **P<0.01; ***P<0.001.

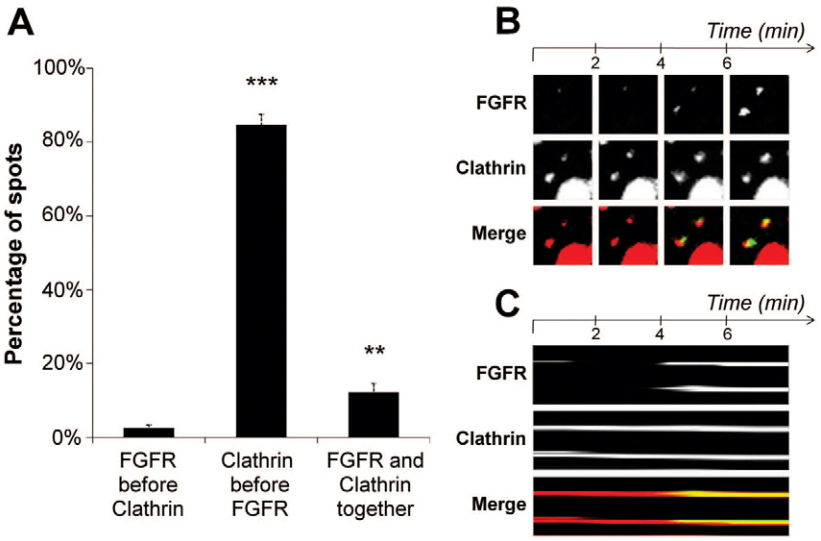

Fig. 4. Activated FGFR clusters at sites of pre-formed clathrin-coated pits. HeLa cells co-expressing FGFR2–GFP and clathrin–dsRed were imaged using simultaneous two-colour TIRF microscopy at 37℃ (1 frame/30 sec) after stimulation with FGF2 + heparin. (**B**) Selected frames from a time-lapse sequence of two FGFR spots (top) and two clathrin spots (middle), and the merged images (bottom) showing the overlap of the two channels in yellow. (**C**) The kymographic representation of the spots shown in B reveals that FGFR appears in the TIRF field and colocalises with pre-existing clathrin. (**A**) Quantification of the percentage of clathrin clusters forming at pre-existing FGFR spots, of FGFR spots recruited at pre-formed clathrin clusters or FGFR and clathrin clustering simultaneously at the plasma membrane (means ± s.e.m., $n=33$ cells). *$P<0.05$; **$P<0.01$; ***$P<0.001$.

suggesting that the increased endocytosis observed following FGFR activation may reflect a cargo specific pathway (supplementary material Fig. S3).

The increase in clathrin-mediated endocytosis was a direct consequence of receptor activity, and not an alternative effect of FGF treatment, as SU5402 completely abrogated the ability of

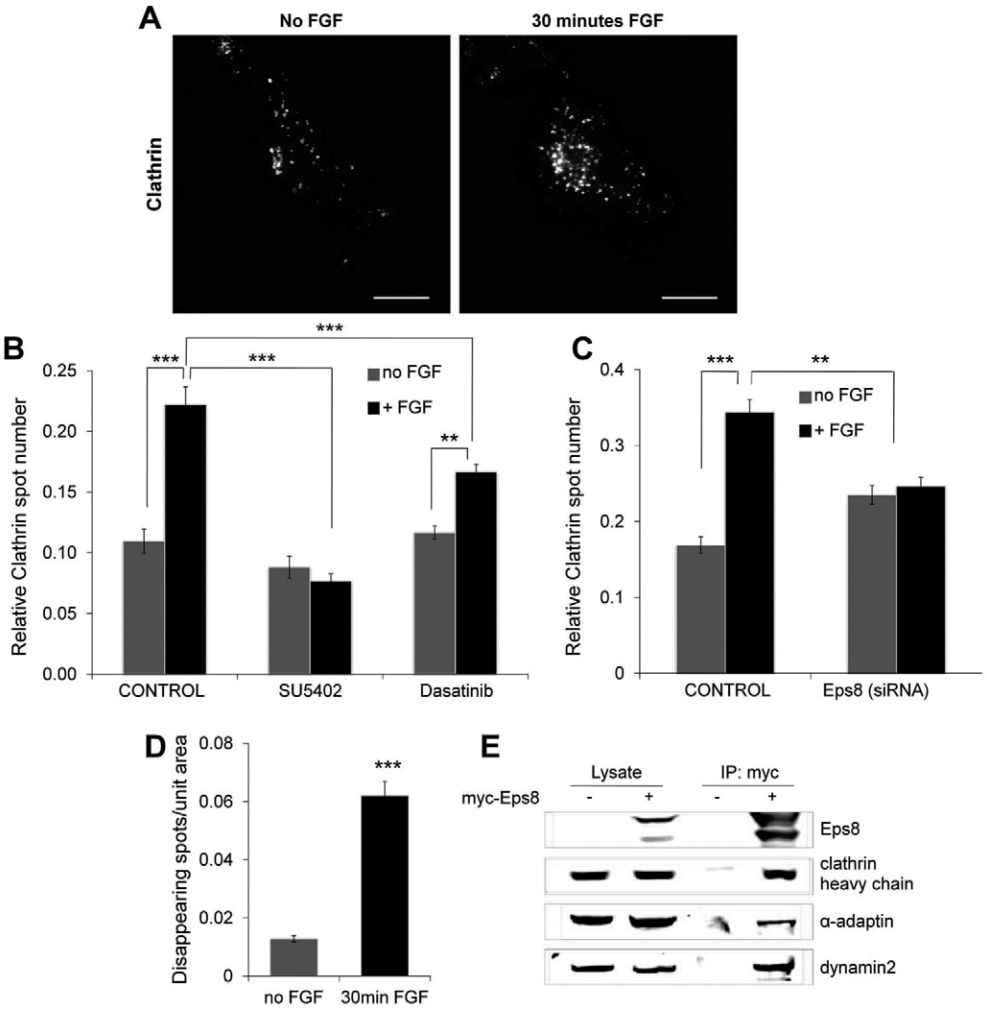

Fig. 5. FGFR activation promotes clathrin-mediated endocytosis via Src and Eps8. (**A**–**C**) HeLa cells transiently expressing FGFR2–GFP and clathrin–dsRed and incubated in the presence or absence of SU5402 (5 minutes), Dasatinib inhibitor (30 minutes) or treated with Eps8 siRNA, were analysed using TIRF microscopy before and 30 minutes after stimulation with FGF2 + heparin. (A) Upon FGF stimulation, cells show a significant increase in the number of clathrin spots on the plasma membrane. Scale bars: 5 µm. (B,C) Quantification of the clathrin spots for the different conditions described above reveals that the FGF-dependent increase of clathrin at the plasma membrane is both Src and Eps8 dependent, and requires the full kinase activity of the receptor. (**D**) HeLa cells expressing FGFR2–GFP and Clathrin–dsRed were imaged using live-cell TIRF microscopy at 37℃ for 2 minutes (1 frame/200 msec) before and 30 minutes after stimulation with FGF2 + heparin. Quantification of the clathrin spots disappearing from the TIRF field shows a significant increase in the density of endocytic events upon FGF stimulation (means ± s.e.m., $n=30$ cells for each condition in B and C, $n=24$ cells in D. *$P<0.05$; **$P<0.01$; ***$P<0.001$. (**E**) Cellular extracts from HeLa cells transfected with myc–Eps8 (where indicated) were immunoprecipitated with anti-myc, resolved by SDS-PAGE and analysed by immunoblotting for the levels of specified proteins.

FGF addition to increase clathrin spot number at the plasma membrane (Fig. 5B). However, as SU5402 treatment in unstimulated cells did not alter the steady state number of clathrin spots on the cell surface, it can be inferred that basal FGFR signalling does not regulate the baseline level of clathrin-mediated endocytosis. Treatment with the Src family kinase inhibitor Dasatinib, which we have previously shown inhibits Src-dependent FGFR signalling and trafficking events (Sandilands et al., 2007), significantly inhibited the ability of FGFR stimulation to increase clathrin spot numbers (Fig. 5B). However, Dasatinib treatment in unstimulated cells did not reduce the number of CCPs, suggesting that SFK activity is not required for constitutive endocytosis.

Our previously published work identified that Eps8 is phosphorylated in a Src-dependent manner following FGFR activation (Cunningham et al., 2010). Furthermore, Eps8 has been implicated as playing a role in clathrin-mediated endocytosis (Taylor et al., 2011). Consistent with these observations, treatment with Eps8 siRNA completely prevented the increased number of clathrin spots following FGFR activation (Fig. 5C). Importantly, the sequence employed to silencing Eps8 was employed in previously published studies from the laboratory of Giorgio Scita (Disanza et al., 2006), and western blot analysis revealed that siRNA targeting Eps8 potently reduced Eps8 protein levels without affecting expression on negative control protein, tubulin (supplementary material Fig. S4A). Therefore, FGFR signalling through Src to Eps8 appears to be important in recruiting new clathrin at plasma membrane, consequently promoting clathrin-mediated endocytosis. This provides evidence for a biologically relevant link between FGFR-mediated signalling and membrane trafficking mediated through Src and Eps8. Furthermore, we have performed similar studies in LNCap cells (supplementary material Fig. S5), which have previously been shown to endogenously express FGFR2 (Carstens et al., 1997). These studies revealed that in the absence of expression of GFP-tagged FGFR treatment of cells with FGF2 resulted in a significant increase in plasma membrane clathrin spot number. Therefore, these results demonstrate this effect is not cell line specific, and can occur via signalling through endogenous FGFR2.

In order to verify the suggested link between Eps8 and clathrin-mediated endocytosis we performed a series of biochemical studies. Co-immunoprecipitation analyses demonstrated that Eps8 associates with clathrin heavy chain, α-adaptin and dynamin2 (Fig. 5E), all proteins involved in clathrin-mediated endocytosis (Doherty and McMahon, 2009). This suggests that Eps8 is capable of being incorporated into a complex with several members of the endocytosis machinery, further supporting its role in early phases of trafficking following receptor activation. These associations were also observed in similar studies performed in HEK293 cells, the proteomic platform we previously employed to identify the connection between FGFR, Src and Eps8 (Cunningham et al., 2010) (supplementary material Fig. S6). Furthermore, in this model we observed that interactions between Eps8 and the machinery for clathrin-mediated endocytosis occur with and without FGF stimulation.

FGFR early endocytic trafficking requires SFK kinase activity

As the above data suggesting a role for Src and Eps8 in the early phases of FGFR signalling and clathrin-mediated endocytosis, we studied the effects of Src inhibition on trafficking of activated FGFR. As depicted in Fig. 6, treatment with Dasatinib resulted in

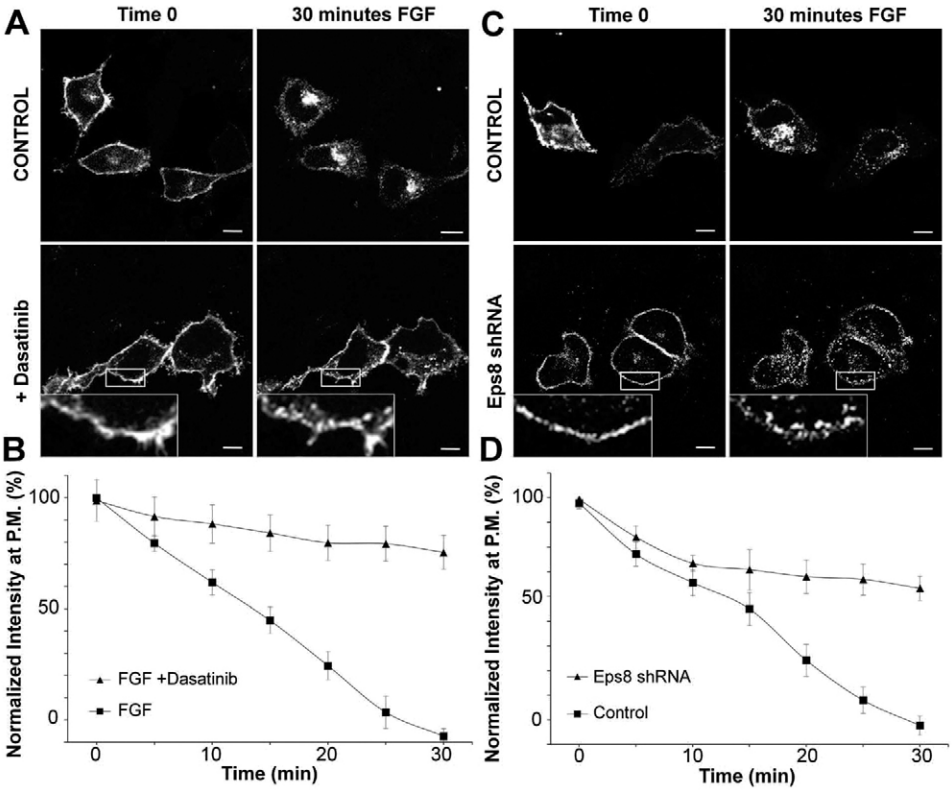

Fig. 6. Inhibition of Src kinase activity and silencing of Eps8 impair the trafficking of FGFR. (**A**) HeLa cells transiently expressing FGFR2–GFP were incubated for 30 minutes in the presence or absence of Dasatinib and imaged by confocal live-cell microscopy at 37℃ for 30 minutes following stimulation with FGF2 + heparin. (**C**) Eps8 knockdown cells (Eps8 shRNA) transiently expressing FGFR2–GFP were stimulation with FGF2 + heparin and imaged as in A. The first and the last frame of the time-lapse sequences are shown in A and C. Scale bars: 5 μm. Higher-magnification images of selected regions from the cells (insets) show an atypical peripheral localisation of FGFR-containing vesicles. (**B**,**D**) The quantification of FGFR2–GFP intensity in the PM region of the cells as a function of time shows an impaired trafficking of FGFR in both Src-inhibited and Eps8shRNA cells (means ± s.e.m., $n=16$ cells).

pronounced effects on the behaviour of FGFR2–GFP following FGF stimulation. Almost complete inhibition of redistribution of FGFR from the cell periphery was observed (Fig. 6A,B). However, high magnification imaging of the plasma-membrane-associated region (see Fig. 6A, inset) revealed the presence of numerous peripheral puncta containing FGFR following stimulation. This would support our evidence for a role of Src-kinase-dependent processes in regulating early endocytic trafficking of activated FGFR.

The role of Eps8 in endocytic trafficking of FGFR

Given the potential role of Eps8 as a downstream effector of Src-kinase-mediated processes, we next studied the consequences of Eps8 depletion on activated FGFR trafficking. In order to assess a role for Eps8 in this process, we made use of a HeLa cell line engineered with stable silencing of Eps8 expression which was previously validated in published studies from the laboratory of Giorgio Scita (Disanza et al., 2006). Western blotting studies confirmed potent and specific silencing of Eps8 in these cells, relative to control (supplementary material Fig. S4B). Similar to our observations in cells treated with the Src inhibitor (Fig. 6A,B), shRNA-mediated reduction in the expression of Eps8 also inhibited trafficking of activated FGFR away from the cellular periphery and towards the perinuclear region (Fig. 6C,D). Furthermore, peripheral FGFR-positive puncta were observed in Eps8 knockdown cells, identical to those observed following Dasatinib treatment (see Fig. 6C, inset). Interestingly, an effect of Eps8 depletion was not apparent at the earliest time points following FGF addition; accumulation of FGFR in a peripheral compartment, rather than direct inhibition of FGFR endocytosis was evident. Thus, inhibition of Src function and silencing of Eps8 result in similar effects on FGFR trafficking further supporting a mechanistic connection between FGFR activation, Src kinase activity and Eps8 function, specifically localised in a peripheral endocytic compartment.

In order to further characterise the potential localisation of Eps8 action on the endocytic trafficking of FGFR we simultaneously visualised both in cells at various times following FGF addition. As depicted in Fig. 7, prior to stimulation both FGFR and Eps8 are observed primarily close to the lateral plasma membrane, consistent with our other observations. However, while FGFR and Eps8 colocalise to a

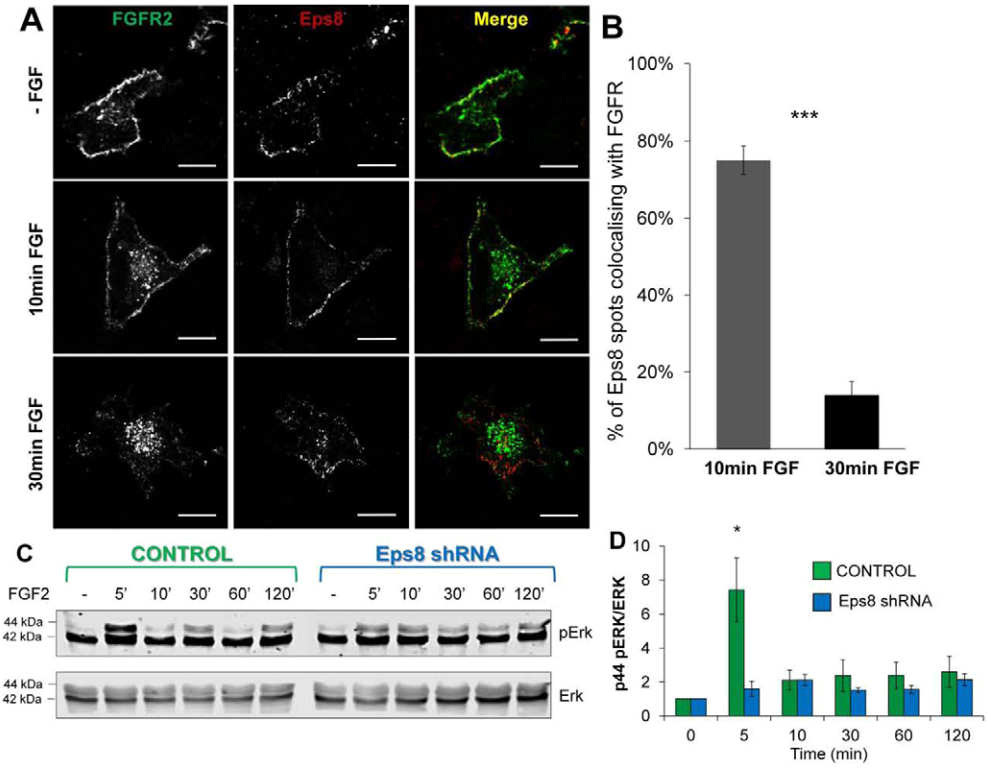

Fig. 7. During early stages of trafficking Eps8 colocalises with FGFR and is required for signal transduction through the MAPK cascade. HeLa cells transiently expressing FGFR2–GFP and Eps8–mCherry were either stimulated with FGF2 + heparin for 10 or 30 minutes, or not stimulated, then fixed and analysed using confocal microscopy. (**A**) During the early stages of activation (10 min FGF), FGFR primarily localises in early endosomal compartments, where it colocalises with Eps8. 30 minutes after FGF addition, FGFR redistributes to the perinuclear region, whereas Eps8 still resides in peripheral compartments, just beneath the plasma membrane. Scale bars: 5 µm. (**B**) Quantification demonstrates significant colocalisation of FGFR and Eps8 only during early phases of receptor activation, where they both localise in early endocytic compartments (means ± s.e.m., $n=14$ cells). (**C**) Eps8 knockdown and vector control HeLa cells transiently expressing FGFR2–GFP were lysed following stimulation with FGF2 + heparin for the indicated times. Cellular extracts where resolved by SDS-PAGE and analysed by immunoblotting for the levels of the specified proteins. The time course of Erk phosphorylation in response to FGF shows a significant attenuation of p44 ERK signal at early times (5 minutes) in Eps8 knockdown cells. (**D**) Quantification of p44 pERK levels following FGF stimulation in Eps8 knockdown (blue) and vector control HeLa (green) cells (means ± s.e.m., $n=5$ experiments) by densitometric scanning of western blots. *$P<0.05$; **$P<0.01$; ***$P<0.001$.

very large degree in peripheral vesicles 10 minutes post-stimulation, once FGFR traffics into the juxtanuclear compartment this coincidence is lost. Quantification revealed that 30 minutes following addition of FGF, Eps8 is retained at the periphery and no longer colocalises with the juxtanuclear pool of FGFR (Fig. 7B). Similarly, Eps8 colocalises with EEA1, a marker for early endosomes (Stenmark et al., 1996) (data not shown). Therefore it appears that Eps8 resides in the early endocytic system, and that activated receptors move through this compartment following endocytosis.

To further elucidate the site of action of Src/Eps8 in FGFR trafficking we performed a series of other colocalisation studies. As depicted in supplementary material Fig. S7, triple colocalisation of activated FGFR, following 10 minutes FGF treatment, Eps8, and transferrin, following a 5 minute incubation places Eps8 in a common early endocytic compartment shared by activated growth factor receptors and transferrin/transferrin receptor. Additionally, in supplementary material Fig. S8 colocalisation between Eps8 and constitutively active Src in the cell periphery, further support our evidence of an early endocytic compartment regulated by Src and Eps8.

The role of Eps8 in FGFR signalling

As we have clearly identified a role for Eps8 in the early endocytic trafficking of FGFR, we next tested whether Eps8 regulated FGFR signalling as well. As depicted in Fig. 7C,D, stimulation with FGF results in a rapid appearance of the p44 form of activated ERK which reaches maximum amplitude at 5 minutes and then declines. In this system, the p42 form of ERK exhibits tonic basal activation and does not respond to FGF stimulation. In fact p42/ERK is apparent in non-transfected HeLa cells subjected to overnight serum starvation (supplementary material Fig. S9). In cells stably silenced for Eps8 expression the FGF-mediated activation of p44 ERK was blunted during the initiating (5 minute) phase of the FGF response. Thus, these findings show that functional Eps8 is required for early phase activation of the Ras/Raf/ERK pathway during the period in which activated FGFRs are recruited away from the plasma membrane. This finding also suggests that activated FGFR can connect to the Ras/Raf/ERK pathway in an Eps8-independent manner which results in lower amplitude signals. Thus this suggests that Eps8 coordinates the signalling and trafficking of FGFR immediately following activation.

The role of Eps8 in trafficking FGFR out of the early endosome

In order to further characterise the role of Eps8 in FGFR trafficking, we performed a series of colocalisation studies with well characterised markers within the endocytic system. As in our previous live-cell imaging studies, 30 minutes following activation FGFR was observed to localise to an intracellular region adjacent to the nucleus (Fig. 8A). Thus, the extent of colocalisation between FGFR and EEA1, was very low 30 minutes post-stimulation (Fig. 8B). However, in the Eps8 knockdown cells the extent of colocalisation between FGFR and EEA1 was significantly higher (Fig. 8B), suggesting that Eps8 functions to permit exit of FGFR from peripheral early endosomes. Similarly, while clear colocalisation was observed between FGFR and Rab11 (Fig. 8C), a marker for the peri-nuclear recycling compartment (Ullrich et al., 1996), in control cells 30 minutes post-stimulation, this was significantly reduced in the Eps8 knockdown cells (Fig. 8D). Finally, we performed similar studies employing Lysotracker as a marker for endocytic degradative compartments (Fig. 8E,F), and found that silencing of Eps8 significantly reduced colocalisation of FGFR and Lysotracker 30 minutes post-stimulation. Finally, super-resolution imaging of FGFR–GFP in Dasatinib treated cells 30 minutes after FGF addition revealed clearly the presence of FGFR in peripheral diffraction limited puncta (supplementary material Fig. S10). Therefore, these results demonstrate that Eps8 is required for the trafficking of activated FGFR out of the early endocytic system and into the peri-nuclear recycling compartment and degradative compartment(s).

Discussion

Growth factor receptors undergo regulated internalization from the cell surface in response to ligand binding (von Zastrow and Sorkin, 2007; Le Roy and Wrana, 2005). Endocytosis and subsequent degradation represent strategies to attenuate signalling of RTK, and alterations in receptor trafficking have emerged as a mechanism of oncogenic activation (Peschard and Park, 2003). Here we have applied imaging based assays for studying endocytosis and trafficking of FGFRs with cells expressing a previously validated GFP-tagged FGFR2 (Schüller et al., 2008). Through use of this system we have demonstrated the interplay between RTK signalling and trafficking, and identified a mechanistic role for Eps8 in mediating clathrin-mediated endocytosis, endocytic trafficking, and MAP kinase signalling. We have demonstrated that receptor trafficking is regulated through signalling transduction pathways downstream of receptor activation, and that the location of the activated receptor within the endocytic system has significant implications on the amplitude of signalling readouts.

Although FGFs are extremely relevant in both development and cancer progression, very little is known about FGFR trafficking (Marchese et al., 1998; Citores et al., 1999; Belleudi et al., 2007; Gleizes et al., 1996; Haugsten et al., 2011). Our data have shown that internalization of FGFR was severely reduced in cells treated with the dynamin inhibitor Dynasore (Fig. 1), indicating that endocytosis of activated receptor occurs through a dynamin-dependent pathway. Using a siRNA approach we observed a complete block of FGFR endocytosis in cells silenced for α-adaptin, whereas no effect was detected in cells treated with caveolin1 siRNA (Fig. 2). We further confirmed these observations by analysing the colocalisation of FGFR with clathrin or caveolin1 at the plasma membrane using TIRF microscopy. Following stimulation, activated FGFR significantly colocalises with clathrin at the cells surface, while no colocalisation with caveolin1 was observed (Fig. 3). Thus, these results identified clathrin-mediated endocytosis as the major pathway for FGFR internalization. Further analyses via live cell TIRF microscopy demonstrated that, like activated EGFR (Rappoport and Simon, 2009), following stimulation FGFR is recruited into pre-formed CCPs (Fig. 4), suggesting that this may be a mechanism conserved across multiple different RTKs.

The next phase of our studies was to characterise mechanistic links between FGFR signalling and trafficking. Src plays a central role in FGFR signalling pathway and has been previously suggested to regulate FGFR trafficking (Sandilands et al., 2007). Previous analyses from our laboratory identified putative Src targets involved in the regulation of FGFRs signalling and

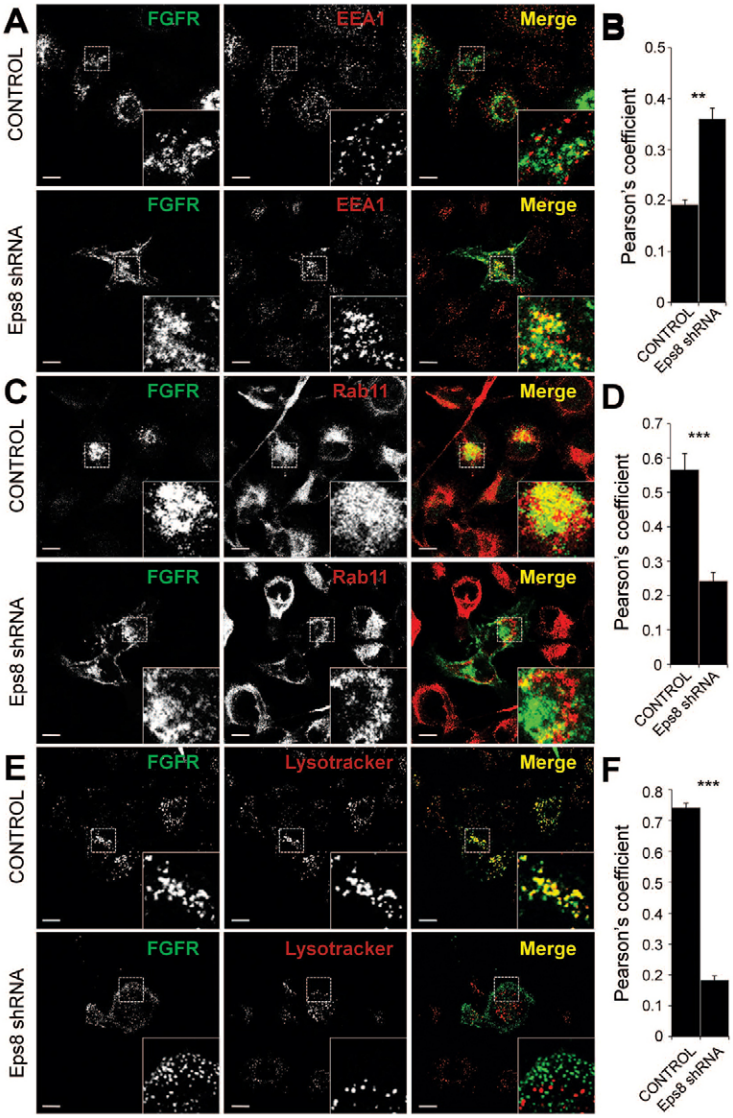

Fig. 8. Eps8 is required for the trafficking of activated FGFR out of the early endocytic system and into the peri-nuclear recycling and late degradative compartments. Eps8 knockdown and vector control HeLa cells transiently expressing FGFR2–GFP were fixed following stimulation with FGF2 + heparin for 30 minutes, immunostained for EEA1 (**A**) or Rab11 (**C**) or treated with LysoTracker Red (**E**) and analysed by confocal microscopy. Higher-magnification images of selected regions from the cells (insets) show that in Eps8 knockdown cells, where receptor trafficking is impaired, FGFR is retained in the peripheral compartment (EEA1) and prevented from sorting to the peri-nuclear recycling compartment (Rab11) and to the lysosomal degradative compartment (LysoTracker). Scale bars: 5 μm. (**B**,**D**,**F**) Colocalisation between FGFR and EEA1, Rab11 or LysoTracker was quantified in control cells as 0.19±0.02, 0.57±0.04, and 0.74±0.01, respectively, and in Eps8 knockdown cells as 0.36±0.04, 0.24±0.05 and 0.18±0.01, respectively (Pearson's correlation coefficient; means ± s.e.m., n=18 cells).

trafficking (Cunningham et al., 2010). In particular the protein Eps8, previously implicated in vesicle trafficking (Lanzetti et al., 2000), was identified as a Src-dependent kinase substrate phosphorylated in response to FGF stimulation. Therefore, we analysed potential roles for Eps8 in the trafficking and signalling of activated FGFR.

Previously it was shown that EGFR activation, signalling through Src, increased the peripheral accumulation of clathrin (Wilde et al., 1999). Our work demonstrates that FGFR activation increases both the number of CCPs and the events of clathrin-mediated endocytosis (Fig. 5). Furthermore, we have demonstrated that Src kinase activity and Eps8 are required for the increase in CCP number following FGFR activation (Fig. 5). Interestingly though, while FGFR activation stimulated clathrin-mediated endocytosis, it did not increase transferrin uptake (supplementary material Fig. S3). Thus, the route of entry for activated RTKs may exist as a cargo specific pathway.

Consistent with live cell imaging studies (Taylor et al., 2011), our biochemical studies demonstrated that Eps8 interacts with the clathrin-mediated endocytosis machinery (Fig. 5). Interestingly, similar studies in HEK293 cells demonstrated these interactions are not FGF2 stimulus dependent (supplementary material Fig. S6). However, we have also identified roles for Src and Eps8 in the further endocytic trafficking of FGFR. Following Dasatinib treatment, FGFR containing vesicles were observed to accumulate at the cell periphery, confirming the role for Src in the early endocytic trafficking of FGFRs (Fig. 6). Similarly, in Eps8 knockdown cells we observed a Dasatinib-like phenotype: a strong inhibition of FGFR trafficking with a pool of receptor localised in a peripheral punctuate compartment (Fig. 6). Thus, this is consistent with our hypothesis that Eps8 is a Src-dependent regulator of FGFR trafficking within the early endocytic system.

Further supporting a role for Eps8 in exit from the early endocytic system, during the early stages of trafficking FGFR significantly colocalises with Eps8 just beneath the plasma membrane (Fig. 7). Furthermore, Eps8 colocalised with FGFR and transferrin in peripheral early endosomes (supplementary material Fig. S7), as well as with constitutively active Src (supplementary material Fig. S8). However, 30 minutes post-stimulation the juxtanuclear pool of FGFR clearly did not colocalise with Eps8 which was retained in a peripheral compartment (Fig. 7). Similarly, exit from the EEA1 early

endosome was significantly reduced when Eps8 expression was silenced (Fig. 8). Finally, 30 minutes post-stimulation FGFR was found to localise to the Rab11-positive peri-nuclear recycling compartment, as well as degradative compartments, in stimulated control cells, and this was prevented in Eps8 knockdown cells (Fig. 8). Thus, activated receptors traffics through the Eps8/EEA1-positive peripheral compartment en route to the PNRC and late endosome/lysosome, and in the absence of Eps8 this is prevented.

Finally, we sought to determine if there is a concomitant feedback into FGFR2 signalling mediated through Eps8. Silencing of Eps8 expression had significant effects on a burst in Erk activation through the p44 form immediately following receptor activation (Fig. 7), suggesting that, consistent with recent work with EGFR (Sousa et al., 2012; Brankatschk et al., 2012), FGFR signalling through the MAP kinase pathway can occur prior to/during receptor endocytosis. Importantly, the p42/Erk band revealed in our studies, which was not Eps8 sensitive, is chronically active in HeLa cells (supplementary material Fig. S9). Finally, super-resolution imaging on a Leica gSTED system further elucidated the site of Eps8/Src-dependent FGFR trafficking (supplementary material Fig. S10). In Dasatinib treated cells FGFR clearly resides in peripheral puncta. Therefore, taken together these results identify Eps8 as a key mediator of activated FGFR trafficking and signalling, and identify the peripheral early endocytic compartment as a key crossroads in the regulation of RTKs.

The interplay between receptor tyrosine kinase signalling and trafficking has been emerging an area critical to understanding fundamental aspects of cell biology as well as how mis-regulation of either could potentially lead to pathological conditions, such as developmental defects or chronic disease. Our studies point to a response arc leading from RTK activation through Src via Eps8. Evidence supporting this hypothesis has been gained from a variety of studies, and is based upon work in other signalling systems, suggesting potential widespread significance. In our studies we have demonstrated that following activation FGFR enters the cell via clathrin-mediated endocytosis. FGF stimulation increases the number of CCPs, and events of clathrin-mediated endocytosis. Furthermore, both the FGF-dependent increase in clathrin at the plasma membrane and the early endocytic trafficking of activated FGFR depend upon Src and Eps8. FGFR traffics through an Eps8-positive early endocytic compartment on the way to the PNRC and lysosome, and in the absence of Eps8, FGFR is retained in peripheral early endosomes. Eps8 is also required for early phase pErk activation, placing this event early in the trafficking of activated FGFR. Therefore, FGFR activation induces alterations in signalling and trafficking that are mediated by Src acting through Eps8, and this alters both early endocytic trafficking and downstream MAPK signalling. Thus, the correlation between Src- and Eps8-dependent FGFR signalling and trafficking suggests a direct link between the two. However, validation and elucidation of the direct mechanistic coupling between FGFR signalling and trafficking and the precise role(s) of Src and Eps8 await further work in this area. In conclusion, while our data suggest that signalling through activated FGFR promotes clathrin-mediated endocytosis, and that this effect depends on Src/Eps8, the initial wave of FGFR endocytosis, although clearly clathrin dependant, does not seem to critically rely upon Src/Eps8. Finally, as constitutive endocytosis and the steady state production of clathrin-coated vesicles do not seem to be Src/Eps8 dependant, the endocytic cargo removed from the plasma membrane in FGF treated cells mediated by Src/Eps8 remains presently elusive.

Materials and Methods

Plasmids, siRNA and antibodies

The construct encoding GFP-tagged FGFR2IIIc (FGFR2–GFP) was a gift from J. Ladbury (M.D. Anderson Cancer Center, The University of Texas). DsRed-tagged clathrin light chain A (clathrin-dsRed) was a gift from T. Kirchhausen (Harvard Medical School, Boston, MA). Caveolin1-mRFP was a gift from A. Helenius (ETH Institute of Biochemistry, Zurich, Switzerland). Eps8-mCherry was a gift from Giorgio Scita (IFOM University of Milan, Milan, Italy). Constitutively active Src was provided by Margaret Frame (Edinburgh Cancer Research UK Centre). siRNA oligos targeting α-adaptin (sequence 5′-AAGAGCAUGUGCACGCUGGCCA-3′), caveolin1 (SmartPool l-003467) and Eps8 (sequence 5′-TGCAGACCC-TAGTATACCG-3′) were purchased from Dharmacon. Antibodies used were: anti-Rab11 (Invitrogen); anti-EEA1 (Abcam); anti-caveolin1 (BD Biosciences); anti-α-adaptin (Santa Cruz); anti-α-tubulin (Sigma); α-ERK1/2 and α-pERK (Santa Cruz); α-Eps8 (Abcam); anti-phospho-Src family (Tyr416; Cell Signaling); IRDye680 and IRDye800 conjugated secondary antibodies (Odyssey).

Cells and transfection

Eps8 shRNA and control shRNA HeLa cells were a gift from Giorgio Scita (IFOM University of Milan, Milan, Italy). HeLa and LNCaP cells were propagated in DMEM (Invitrogen) supplemented with 10% FBS (Labtech International) in a 5% CO_2 atmosphere at 37℃. DNA and siRNA transfection was performed by using Lipofectamine 2000 transfection reagent (Invitrogen) according to the manufacturer's protocol. At 48 hours post-transfection, cells were serum-starved for 30 min and then stimulated with 20 μg/ml Heparin (Sigma) and 50 ng/ml FGF2 for the indicated times. For the inhibition assays cells were either treated with 25 μM SU5402 (Calbiochem) for 5 min, 80 μM Dynasore (Sigma) for 30 min or 50 nM Dasatinib (Sellek Chemicals) for 30 min or treated as above in the absence of drug before FGF stimulation. For live-cell imaging, cells were washed once and the medium removed was replaced with prewarmed (37℃) imaging medium [10 mM HEPES–Hank's balanced salt solution (HBSS; Sigma) pH 7.4].

Laser scanning confocal microscopy and total internal reflection fluorescence microscopy

Confocal laser was performed with an inverted microscope (Eclipse Ti, Nikon A1R) at 37℃ using a 60× 1.45 NA oil-immersion objective and 12-bit CCD camera (Ixon 1M EMCCD). GFP constructs were excited with an argon ion 457–514 nm laser, mRFP and dsRed constructs with a Green Diode 561 nm laser. Images were prepared with NIS-Elements Imaging Software version 3.2 (Nikon). TIRF microscopy was performed with the system described above as well as with an inverted microscope (IX81, Olympus) using a 60× 1.49 NA oil-immersion objective and a 12-bit CCD camera (ORCA-R^2 C10600, Hamamatsu). GFP constructs were excited with a 491-50 Diode type laser, dsRed constructs with a 561-50 DPSS type laser. Images were analysed and prepared with Xcellence Advanced Lice Cell Imaging System version 1.1 (Olympus). Super-resolution imaging was performed on a gSTED system (Leica) and image stacks were deconvolved using Huygens linked within the Leica software.

Immunofluorescence

Cells grown on coverslips were fixed in 4% paraformaldehyde in TBS for 10 min, washed in TBS/100 mM glycine and permeabilised with TBS/0.1% saponin/20 mM glycine. After blocking with TBS/0.1% saponin/10% FCS, cells were incubated with primary antibodies, then washed and incubated with secondary antibodies. After staining, the coverslips were mounted in Hydromount (National Diagnostic) and imaged by using a Zeiss LSM 710 confocal microscope, a 40× 1.3NA oil-immersion objective and a Transmission-Photomultiplier LSM T-PMT. Each experiment was repeated a minimum of three times and an image that represented the phenotype of most of the cells was selected. For lysosomal staining, cells were incubated with 75 nM LysoTracker Red (Molecular Probes) for 30 minutes and immediately imaged in imaging media at room temperature.

Transferrin and cholera toxin B uptake assay

Following serum-starvation for 30 min, cells were incubated at 37℃ in either Alexa-Fluor-546–transferrin (Invitrogen), or Alexa-Fluor-555–cholera-toxin-B (Invitrogen). Cells were then rinsed, fixed and analysed by using a Nikon TE300 inverted epi-fluorescence microscope using an 60× 1.40 NA oil-immersion objective and a cooled CCD camera (Hamamatsu C4742-98-12WRB). For the triple colocalisation, HeLa cells were incubated with Alexa-Fluor-633–transferrin (Invitrogen) for 5 minutes, in order to mark the early endosomes. Cells were then rinsed, fixed and analysed using confocal microscopy.

Quantification analysis

For the trafficking assays FGFR2–GFP intensity in the plasma-membrane-associated region of the cells was calculated for each frame of the time-lapse sequences (1 frame/5 min). From each time point, a background value was subtracted, corresponding to the cytosolic fluorescence intensity before the stimulation with FGF (time=0 min). Cells were treated with a red membrane stain (data not shown) in order to define the plasma-membrane-associated region. For the colocalisation analysis, each spot of FGFR, clathrin, caveolin1 and Eps8 was identified and a circle was drawn around it. Spots were identified as colocalising when most of the fluorescence intensity of the pixels within the circular regions fitted in both the channels. For quantification of transferrin and cholera toxin uptake, cells randomly located on the coverslips were scanned at fixed intensity settings below pixel-saturation, and the total cellular intensity was determined. Data analysis was performed using either NIS-Elements Imaging Software version 3.2 (Nikon) or Xcellence Advanced Lice Cell Imaging System version 1.1 (Olympus).

Biochemical assays

Cultures of HeLa or Hek293T cells were lysed in lysis buffer (50 mM Tris-HCl pH 7.4, 150 mM NaCl, 1% Triton TX-100, 1 mM sodium orthovanadate, 50 mM sodium fluoride, 25 mM β-glycerophosphate) supplemented with complete mini protease inhibitors cocktail (Roche). The extracts were resolved by a 4–12% NuPAGE Bis-Tris SDS gel (Invitrogen) and transferred to Immobilon PVDF-FL membrane (Millipore). The membrane was blocked in methanol and incubated with primary antibodies overnight at 4℃. After washing in PBS 0.1% Tween-20 the membrane was incubated with secondary antibodies for 1 hour at room temperature followed by washing and detected using an Odyssey infrared imaging system (Li-COR). For the immunoprecipitation assay, cells were lysed and prepared as described. The extracts were immunoprecipitated with dynabeads (Invitrogen) crosslinked with anti-myc antibody. Supernatants were loaded on a 4–12% NuPAGE Bis-Tris SDS gel (Invitrogen) and subjected to immunoblot analysis with indicated antibodies. Quantification by densitometric scanning of western blots was performed using Odyssey Application Software version 3.0 (Li-COR). Since the primary antibodies used in this analysis detected both the 42 kDa and 44 kDa form of ERK/pERK, two bands were visualized and captured. The relative p44 phosphoERK levels shown in Fig. 7D were calculated by normalizing, for each point of the time course, the relative optical density value of the p44 phosphoERKs band to the corresponding total p44 ERK value.

Acknowledgements

The authors would like to thank Giorgio Scita (IFOM-IEO) for sharing reagents and expertise, and Sylwia Krawczyk and the rest of the Rappoport and Heath laboratories for helpful discussion. The Nikon A1R/TIRF microscope used in this research was obtained through the Birmingham Science City Translational Medicine Clinical Research and Infrastructure Trials Platform, with support from Advantage West Midlands (AWM). The funders had no role in study design, data collection and analysis, decision to publish, or preparation of the manuscript.

Funding

This work was supported by the Biotechnology and Biological Sciences Research Council [new investigator project grant number BB/H002308/1 to J.Z.R.]; Cancer Research UK [programme grant number C80/A10171 to J.K.H.]; and a Ph.D. studentship from the Medical Research Council [training grant reference number G0900175 to G.A.]. Deposited in PMC for release after 6 months.

Supplementary material available online at
http://jcs.biologists.org/lookup/suppl/doi:10.1242/jcs.116228/-/DC1

References

Ahmed, Z., Schüller, A. C., Suhling, K., Tregidgo, C. and Ladbury, J. E. (2008). Extracellular point mutations in FGFR2 elicit unexpected changes in intracellular signalling. *Biochem. J.* **413**, 37-49.

Axelrod, D. (2008). Total internal reflection fluorescence microscopy. In *Methods Cell Biol.* Vol. 89 (ed. J. J. Correia and H. William Detrich, III), pp. 169-221.

Basilico, C. and Moscatelli, D. (1992). The FGF family of growth factors and oncogenes. *Adv. Cancer Res.* **59**, 115-165.

Beenken, A. and Mohammadi, M. (2009). The FGF family: biology, pathophysiology and therapy. *Nat. Rev. Drug Discov.* **8**, 235-253.

Beguinot, L., Lyall, R. M., Willingham, M. C. and Pastan, I. (1984). Down-regulation of the epidermal growth factor receptor in KB cells is due to receptor internalization and subsequent degradation in lysosomes. *Proc. Natl. Acad. Sci. USA* **81**, 2384-2388.

Belleudi, F., Leone, L., Nobili, V., Raffa, S., Francescangeli, F., Maggio, M., Morrone, S., Marchese, C. and Torrisi, M. R. (2007). Keratinocyte growth factor receptor ligands target the receptor to different intracellular pathways. *Traffic* **8**, 1854-1872.

Brankatschk, B., Wichert, S. P., Johnson, S. D., Schaad, O., Rossner, M. J. and Gruenberg, J. (2012). Regulation of the EGF transcriptional response by endocytic sorting. *Sci. Signal.* **5**, ra21.

Burgess, W. H. and Maciag, T. (1989). The heparin-binding (fibroblast) growth factor family of proteins. *Annu. Rev. Biochem.* **58**, 575-602.

Carstens, R. P., Eaton, J. V., Krigman, H. R., Walther, P. J. and Garcia-Blanco, M. A. (1997). Alternative splicing of fibroblast growth factor receptor 2 (FGF-R2) in human prostate cancer. *Oncogene* **15**, 3059-3065.

Citores, L., Wesche, J., Kolpakova, E. and Olsnes, S. (1999). Uptake and intracellular transport of acidic fibroblast growth factor: evidence for free and cytoskeleton-anchored fibroblast growth factor receptors. *Mol. Biol. Cell* **10**, 3835-3848.

Cunningham, D. L., Sweet, S. M., Cooper, H. J. and Heath, J. K. (2010). Differential phosphoproteomics of fibroblast growth factor signaling: identification of Src family kinase-mediated phosphorylation events. *J. Proteome Res.* **9**, 2317-2328.

Damm, E. M., Pelkmans, L., Kartenbeck, J., Mezzacasa, A., Kurzchalia, T. and Helenius, A. (2005). Clathrin- and caveolin-1-independent endocytosis: entry of simian virus 40 into cells devoid of caveolae. *J. Cell Biol.* **168**, 477-488.

Di Fiore, P. P. and De Camilli, P. (2001). Endocytosis and signaling. an inseparable partnership. *Cell* **106**, 1-4.

Di Fiore, P. P. and Scita, G. (2002). Eps8 in the midst of GTPases. *Int. J. Biochem. Cell Biol.* **34**, 1178-1183.

Disanza, A., Mantoani, S., Hertzog, M., Gerboth, S., Frittoli, E., Steffen, A., Berhoerster, K., Kreienkamp, H. J., Milanesi, F., Di Fiore, P. P. et al. (2006). Regulation of cell shape by Cdc42 is mediated by the synergic actin-bundling activity of the Eps8-IRSp53 complex. *Nat. Cell Biol.* **8**, 1337-1347.

Disanza, A., Frittoli, E., Palamidessi, A. and Scita, G. (2009). Endocytosis and spatial restriction of cell signaling. *Mol. Oncol.* **3**, 280-296.

Doherty, G. J. and McMahon, H. T. (2009). Mechanisms of endocytosis. *Annu. Rev. Biochem.* **78**, 857-902.

Engqvist-Goldstein, A. E., Warren, R. A., Kessels, M. M., Keen, J. H., Heuser, J. and Drubin, D. G. (2001). The actin-binding protein Hip1R associates with clathrin during early stages of endocytosis and promotes clathrin assembly in vitro. *J. Cell Biol.* **154**, 1209-1224.

Gleizes, P. E., Noaillac-Depeyre, J., Dupont, M. A. and Gas, N. (1996). Basic fibroblast growth factor (FGF-2) is addressed to caveolae after binding to the plasma membrane of BHK cells. *Eur. J. Cell Biol.* **71**, 144-153.

Greenfield, C., Hiles, I., Waterfield, M. D., Federwisch, M., Wollmer, A., Blundell, T. L. and McDonald, N. (1989). Epidermal growth factor binding induces a conformational change in the external domain of its receptor. *EMBO J.* **8**, 4115-4123.

Grose, R. and Dickson, C. (2005). Fibroblast growth factor signaling in tumorigenesis. *Cytokine Growth Factor Rev.* **16**, 179-186.

Haugsten, E. M., Zakrzewska, M., Brech, A., Pust, S., Olsnes, S., Sandvig, K. and Wesche, J. (2011). Clathrin- and dynamin-independent endocytosis of FGFR3 - implications for signalling. *PLoS ONE* **6**, e21708.

Heldin, C. H. (1995). Dimerization of cell surface receptors in signal transduction. *Cell* **80**, 213-223.

Kholodenko, B. N. (2002). MAP kinase cascade signaling and endocytic trafficking: a marriage of convenience? *Trends Cell Biol.* **12**, 173-177.

Lanzetti, L., Rybin, V., Malabarba, M. G., Christoforidis, S., Scita, G., Zerial, M. and Di Fiore, P. P. (2000). The Eps8 protein coordinates EGF receptor signalling through Rac and trafficking through Rab5. *Nature* **408**, 374-377.

Le Roy, C. and Wrana, J. L. (2005). Clathrin- and non-clathrin-mediated endocytic regulation of cell signalling. *Nat. Rev. Mol. Cell Biol.* **6**, 112-126.

Li, W., Liu, H., Zhou, J. S., Cao, J. F., Zhou, X. B., Choi, A. M., Chen, Z. H. and Shen, H. H. (2012). Caveolin-1 inhibits expression of antioxidant enzymes through direct interaction with nuclear erythroid 2 p45-related factor-2 (Nrf2). *J. Biol. Chem.* **287**, 20922-20930.

Macia, E., Ehrlich, M., Massol, R., Boucrot, E., Brunner, C. and Kirchhausen, T. (2006). Dynasore, a cell-permeable inhibitor of dynamin. *Dev. Cell* **10**, 839-850.

Marchese, C., Mancini, P., Belleudi, F., Felici, A., Gradini, R., Sansolini, T., Frati, L. and Torrisi, M. R. (1998). Receptor-mediated endocytosis of keratinocyte growth factor. *J. Cell Sci.* **111**, 3517-3527.

Mason, I. J. (1994). The ins and outs of fibroblast growth factors. *Cell* **78**, 547-552.

Mattheyses, A. L., Simon, S. M. and Rappoport, J. Z. (2010). Imaging with total internal reflection fluorescence microscopy for the cell biologist. *J. Cell Sci.* **123**, 3621-3628.

Peschard, P. and Park, M. (2003). Escape from Cbl-mediated downregulation: a recurrent theme for oncogenic deregulation of receptor tyrosine kinases. *Cancer Cell* **3**, 519-523.

Polo, S. and Di Fiore, P. P. (2006). Endocytosis conducts the cell signaling orchestra. *Cell* **124**, 897-900.

Provenzano, C., Gallo, R., Carbone, R., Di Fiore, P. P., Falcone, G., Castellani, L. and Alemà, S. (1998). Eps8, a tyrosine kinase substrate, is recruited to the cell cortex and dynamic F-actin upon cytoskeleton remodeling. *Exp. Cell Res.* **242**, 186-200.

Rappoport, J. Z. (2008). Focusing on clathrin-mediated endocytosis. *Biochem. J.* **412**, 415-423.

Rappoport, J. Z. and Simon, S. M. (2008). A functional GFP fusion for imaging clathrin-mediated endocytosis. *Traffic* **9**, 1250-1255.

Rappoport, J. Z. and Simon, S. M. (2009). Endocytic trafficking of activated EGFR is AP-2 dependent and occurs through preformed clathrin spots. *J. Cell Sci.* **122**, 1301-1305.

Rothberg, K. G., Heuser, J. E., Donzell, W. C., Ying, Y. S., Glenney, J. R. and Anderson, R. G. (1992). Caveolin, a protein component of caveolae membrane coats. *Cell* **68**, 673-682.

Sandilands, E. and Frame, M. C. (2008). Endosomal trafficking of Src tyrosine kinase. *Trends Cell Biol.* **18**, 322-329.

Sandilands, E., Akbarzadeh, S., Vecchione, A., McEwan, D. G., Frame, M. C. and Heath, J. K. (2007). Src kinase modulates the activation, transport and signalling dynamics of fibroblast growth factor receptors. *EMBO Rep.* **8**, 1162-1169.

Schüller, A. C., Ahmed, Z., Levitt, J. A., Suen, K. M., Suhling, K. and Ladbury, J.-E. (2008). Indirect recruitment of the signalling adaptor Shc to the fibroblast growth factor receptor 2 (FGFR2). *Biochem. J.* **416**, 189-199.

Sorkin, A. and Von Zastrow, M. (2002). Signal transduction and endocytosis: close encounters of many kinds. *Nat. Rev. Mol. Cell Biol.* **3**, 600-614.

Sousa, L. P., Lax, I., Shen, H., Ferguson, S. M., De Camilli, P. and Schlessinger, J. (2012). Suppression of EGFR endocytosis by dynamin depletion reveals that EGFR signaling occurs primarily at the plasma membrane. *Proc. Natl. Acad. Sci. USA* **109**, 4419-4424.

Stenmark, H., Aasland, R., Toh, B. H. and D'Arrigo, A. (1996). Endosomal localization of the autoantigen EEA1 is mediated by a zinc-binding FYVE finger. *J. Biol. Chem.* **271**, 24048-24054.

Stoscheck, C. M. and Carpenter, G. (1984). Down regulation of epidermal growth factor receptors: direct demonstration of receptor degradation in human fibroblasts. *J. Cell Biol.* **98**, 1048-1053.

Sun, L., Tran, N., Liang, C., Tang, F., Rice, A., Schreck, R., Waltz, K., Shawver, L. K., McMahon, G. and Tang, C. (1999). Design, synthesis, and evaluations of substituted 3-[(3- or 4-carboxyethylpyrrol-2-yl)methylidenyl]indolin-2-ones as inhibitors of VEGF, FGF, and PDGF receptor tyrosine kinases. *J. Med. Chem.* **42**, 5120-5130.

Taylor, M. J., Perrais, D. and Merrifield, C. J. (2011). A high precision survey of the molecular dynamics of mammalian clathrin-mediated endocytosis. *PLoS Biol.* **9**, e1000604.

Turner, N. and Grose, R. (2010). Fibroblast growth factor signalling: from development to cancer. *Nat. Rev. Cancer* **10**, 116-129.

Ullrich, A. and Schlessinger, J. (1990). Signal transduction by receptors with tyrosine kinase activity. *Cell* **61**, 203-212.

Ullrich, O., Reinsch, S., Urbé, S., Zerial, M. and Parton, R. G. (1996). Rab11 regulates recycling through the pericentriolar recycling endosome. *J. Cell Biol.* **135**, 913-924.

von Zastrow, M. and Sorkin, A. (2007). Signaling on the endocytic pathway. *Curr. Opin. Cell Biol.* **19**, 436-445.

Wesche, J., Haglund, K. and Haugsten, E. M. (2011). Fibroblast growth factors and their receptors in cancer. *Biochem. J.* **437**, 199-213.

Wilde, A., Beattie, E. C., Lem, L., Riethof, D. A., Liu, S. H., Mobley, W. C., Soriano, P. and Brodsky, F. M. (1999). EGF receptor signaling stimulates SRC kinase phosphorylation of clathrin, influencing clathrin redistribution and EGF uptake. *Cell* **96**, 677-687.

Zhang, Y., Moheban, D. B., Conway, B. R., Bhattacharyya, A. and Segal, R. A. (2000). Cell surface Trk receptors mediate NGF-induced survival while internalized receptors regulate NGF-induced differentiation. *J. Neurosci.* **20**, 5671-5678.

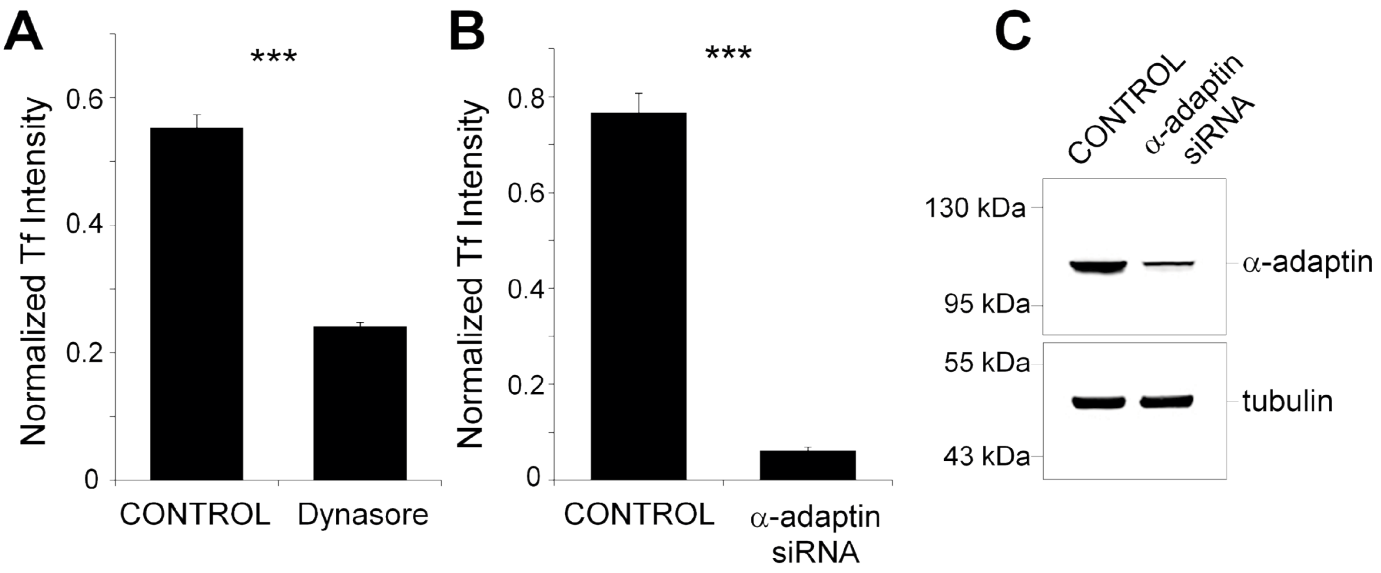

Fig S1. Silencing α-adaptin subunit of AP2 complex or inhibition of GTPase dynamin significantly reduces transferrin uptake. HeLa cells overexpressing FGFR2-GFP were either incubated for 30 minutes in the presence or absence of Dynasore inhibitor (**A**), or treated with α-adaptin siRNA (**B**). Following incubation with transferrin-Alexa-Fluor-546 (Tf) for 15 minutes at 37°C, cells were rinsed, fixed and analysed by epifluorescence microscopy. The quantification of Tf fluorescence intensity shows that both Dynasore activity and α-adaptin siRNA treatment significantly reduce transferrin entry (mean ± s.e.m., *n*=26 cells in (A), *n*=24 cells in (B) (**P*<0.05; ***P*<0.01; ****P*<0.001). (**C**) Western blot of lysates from HeLa cells transfected with α-adaptin siRNA and probed with anti-α-adaptin antibody shows potent silencing (mean ± s.e.m., *n*=3 experiments).

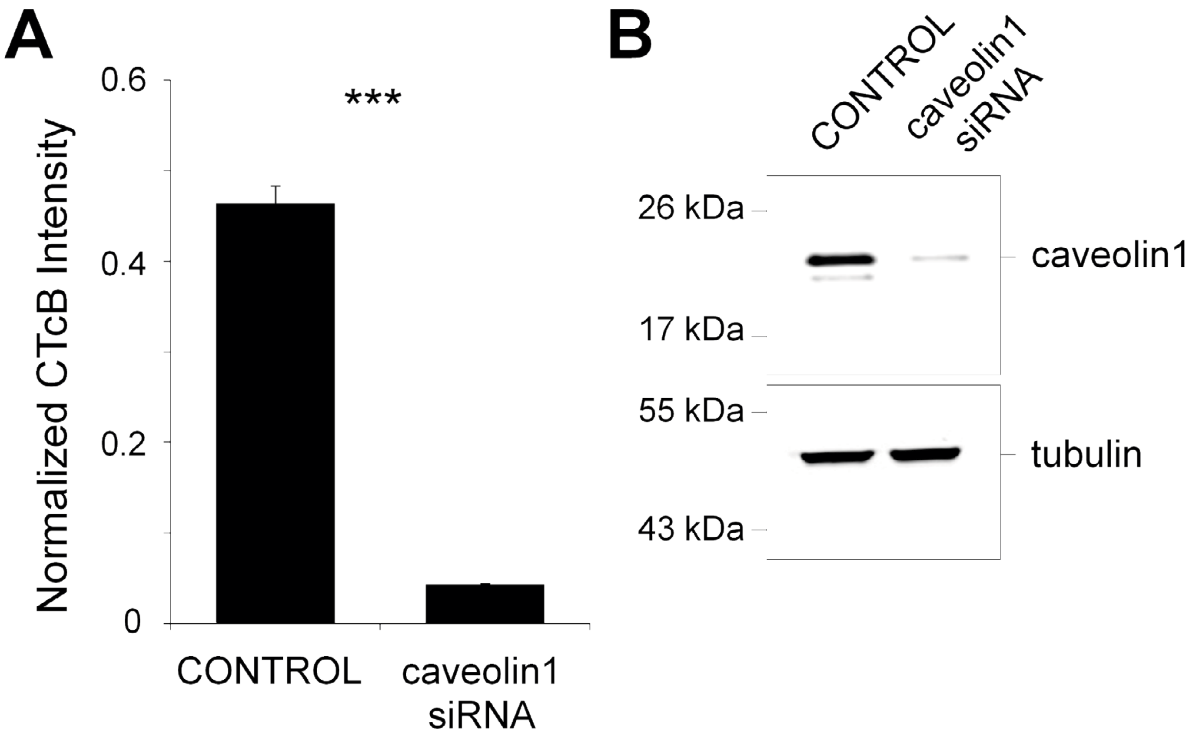

Fig S2. Silencing of caveolin1 leads to a significant reduction of choleratoxinB uptake. (**A**) HeLa cells overexpressing FGFR2-GFP were treated with caveolin1 siRNA. Following incubation with choleratoxinB-Alexa-Fluor-555 (CTcB) for 15 minutes at 37°C, cells were rinsed, fixed and analysed in epifluorescence microscopy. The quantification of CTcB fluorescence intensity shows that caveolin1 siRNA treatment leads to a significant reduction in cholera toxin uptake (mean ± s.e.m., *n*=15 cells; **P*<0.05; ***P*<0.01; ****P*<0.001). (**B**) Western blot of lysates from HeLa cells transfected with caveolin1 siRNA and probed with anti cav1 antibody shows potent silencing (mean ± s.e.m., *n*=3 experiments).

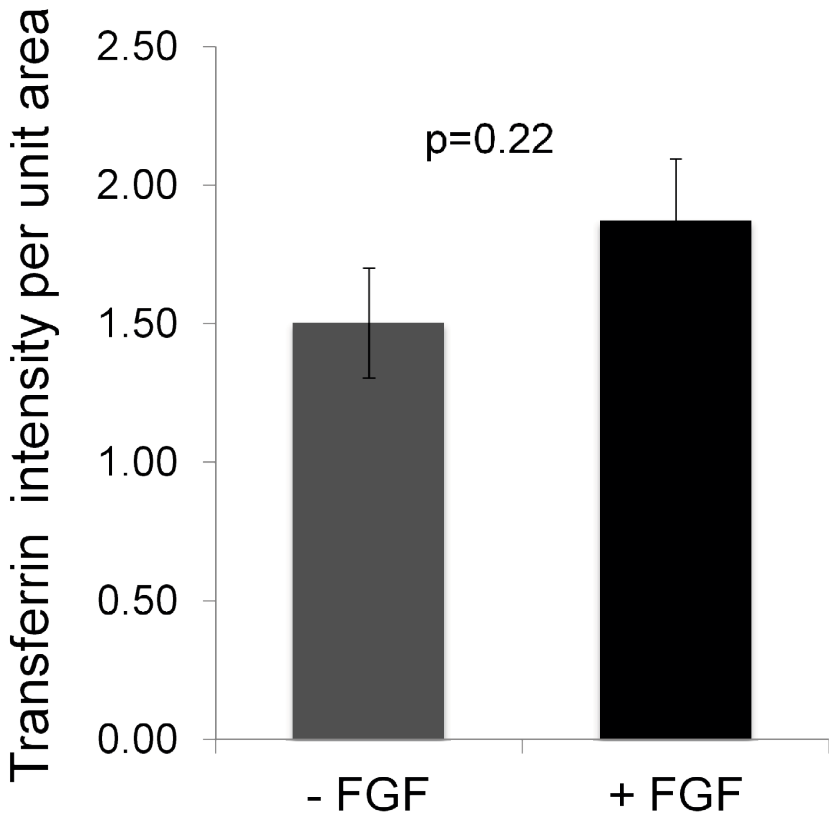

Fig S3. FGF treatment does not result in an increase in transferrin uptake. HeLa cells transiently expressing FGFR2-GFP were either stimulated with FGF2 + heparin for 15 minutes, or not stimulated, at 37°C in the presence of transferrin-Alexa-Fluor-546. Cells were then rinsed, fixed and analysed by epifluorescence microscopy. Quantification of transferrin fluorescence intensity demonstrates that FGF stimulation does not induce a significant increase in transferrin entry (mean ± s.e.m., *n*=49 cells each condition).

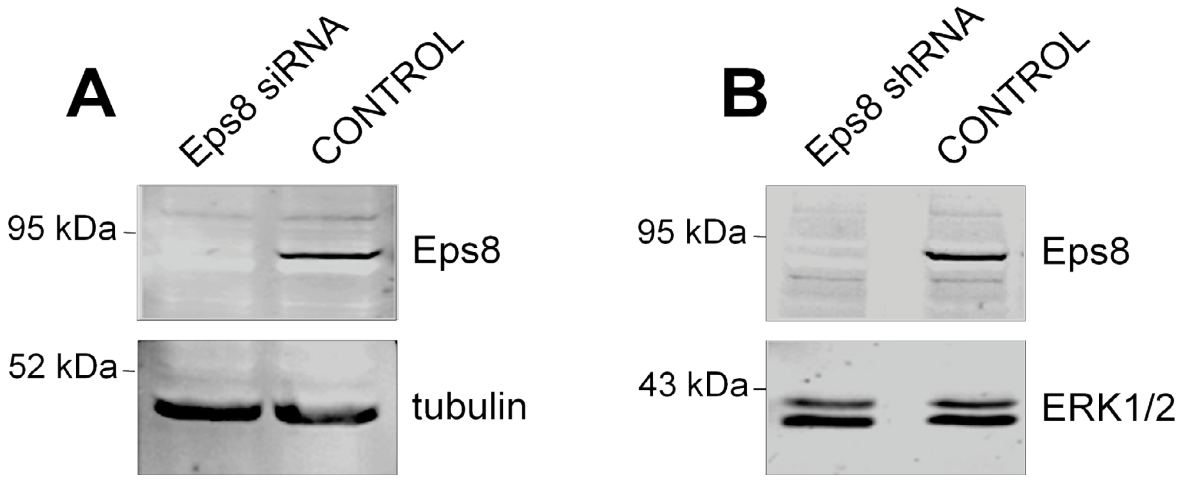

Fig S4. Eps8 expression is significantly silenced in the Eps8 knock down cell line and in Eps8 siRNA-treated HeLa cells. Cellular extracts from HeLa cells transfected with Eps8 siRNA (**A**) or from Eps8 knock down (shRNA) or control vector (control) HeLa cells (**B**) were resolved by SDS-PAGE and analysed by immunoblotting with anti-Eps8 antibody (mean ± s.e.m., *n*=3 experiments).

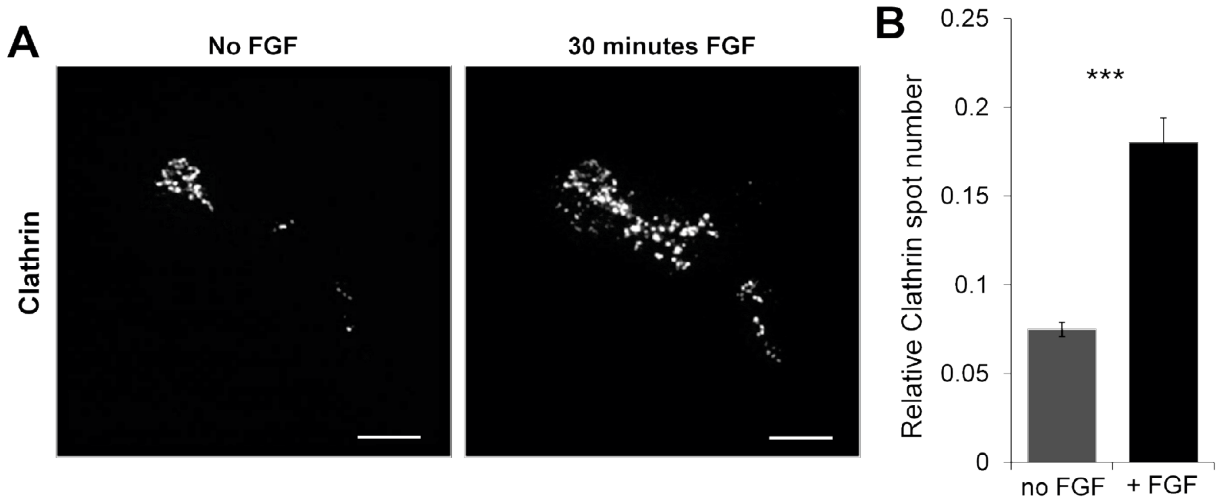

Fig S5. FGF-dependent peripheral accumulation of CCPs in FGFR-expressing LNCaP cells. LNCaP cells endogenously expressing FGFR2 and transfected with Clathrin-dsRed were analysed by TIRF microscopy before and 30 minutes after stimulation with FGF2 + heparin. (**A**) Upon FGF stimulation, cells show a significant increase in the number of clathrin spots on the plasma membrane. Scale bars: 5 μm. (**B**) Quantification analysis of clathrin spot number before and after FGF stimulation (mean ± s.e.m., *n*=45 cells; **P*<0.05; ***P*<0.01; ****P*<0.001).

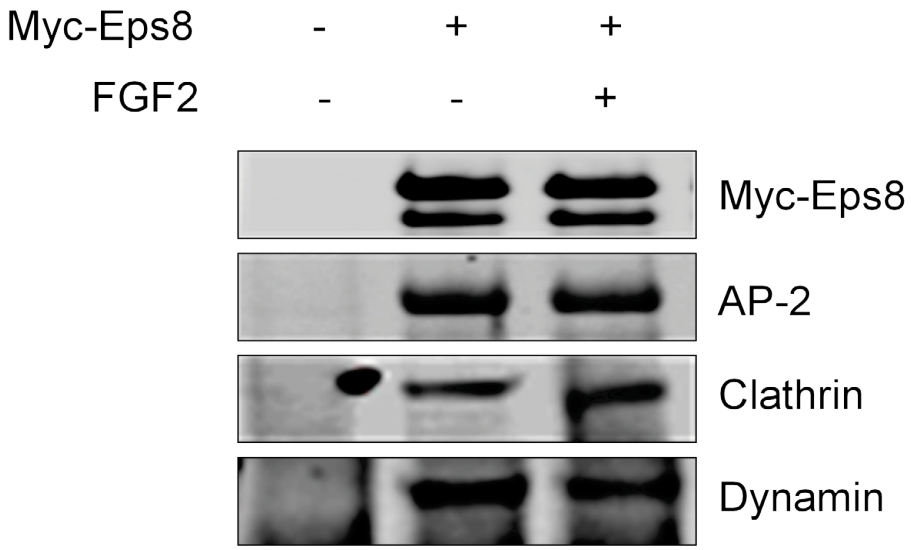

Fig S6. AP-2, Clathrin, and Dynamin interact with Eps8 in an FGF2-independent manner in HEK293T cells. Cellular extracts from HEK293T cells transfected with myc-Eps8 (where indicated) and stimulated or not with 20 ng/ml FGF + 10 μg/ml heparin for 15 min, were immunoprecipitated with anti-myc antibody, resolved by SDS-PAGE and analysed by immunoblotting for the levels of specified proteins.

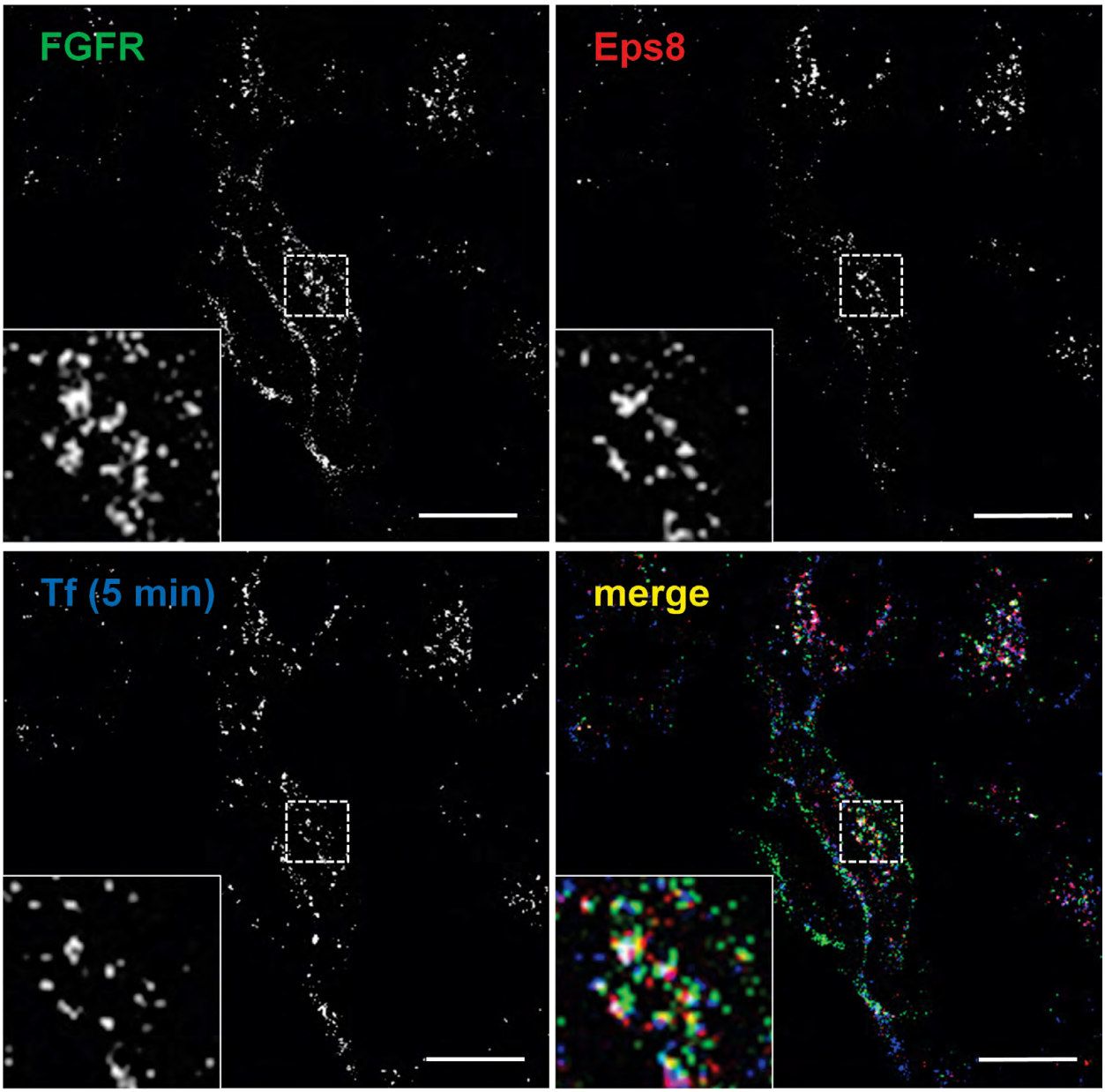

Fig S7. During early stages of trafficking FGFR colocalises with Eps8 in the early endosomal compartment. HeLa cells transiently expressing FGFR2-GFP and Eps8-mCherry were stimulated with FGF + heparin for 10 minutes. Following incubation with transferrin-Alexa-Fluor-633 (Tf) during the last 5 minutes of stimulation, cells were rinsed, fixed and analysed by confocal microscopy. Higher-magnification in merged image of selected regions from the cells show overlap of FGFR, Eps8 and 5 min internalized transferrin in white, demonstrating that during the early stages of activation (10 min FGF), FGFR colocalises with Eps8 within the early endocytic compartment. Scale bars=5 μm.

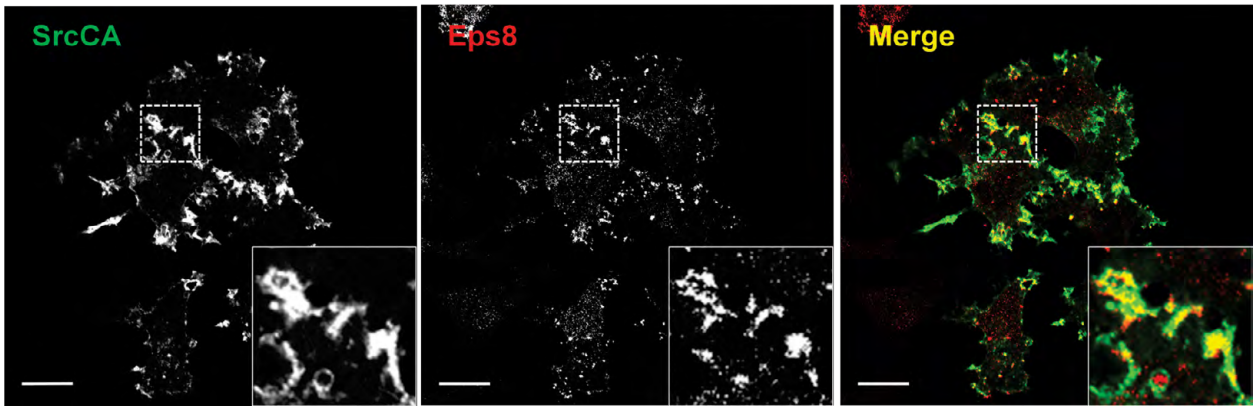

Fig S8. Colocalisation of Eps8 with active Src. HeLa cells transiently expressing constitutive active Src (SrcCA) and Eps8-mCherry were immunostained for active Src (P416Src antibody) and imaged in confocal microscopy. Higher-magnification merged image of selected regions from the cells show overlap of active Src and Eps8 in yellow. Scale bars=5 μm.

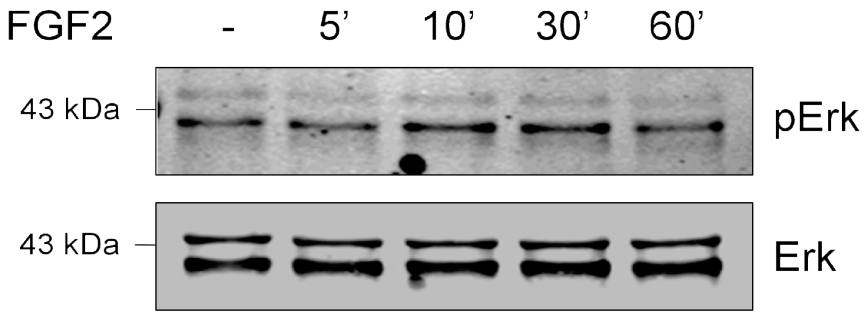

Fig S9. FGF-dependent kinetics of ERK phosphorylation in non-transfected HeLa cells. HeLa cells starved overnight in serum-free media were lysed following stimulation with FGF2 + heparin for the indicated times. Cellular extracts where resolved by SDS-PAGE and analysed by immunoblotting for the levels of specified proteins.

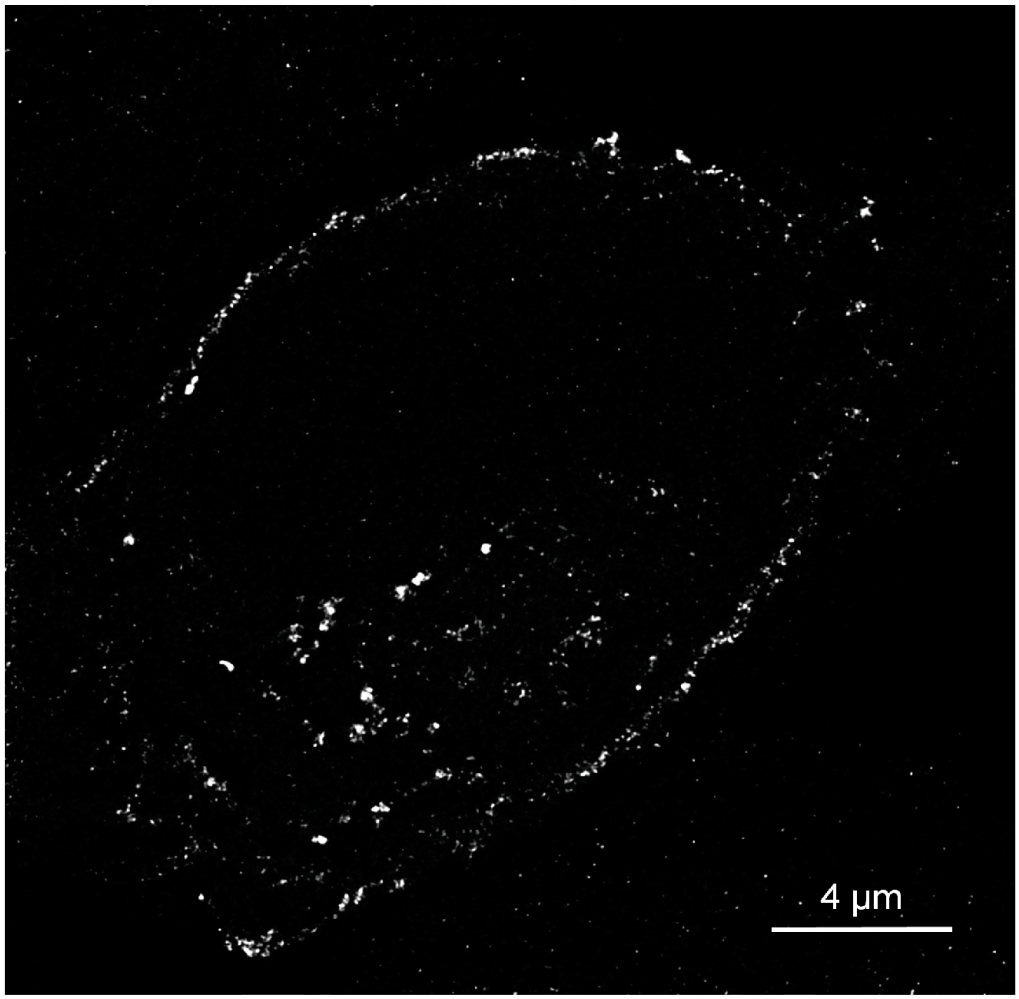

Fig S10. Super-resolution analysis of FGFR-containing vesicles in Dasatinib-treated HeLa cells. HeLa cells transiently expressing FGFR2-GFP and incubated for 30 minutes in the presence of Dasatinib inhibitor were stimulated with FGF2 + heparin for 30 minutes, fixed and analysed by super-resolution confocal microscopy on a Leica gSTED system followed by stack deconvolution. The high resolution image reveals the presence of a population of FGFR-containing vesicles accumulating at the cell periphery following Src inhibition.

BJ www.biochemj.org

BJ Cell

Biochem. J. (2011) **436**, 45–52 (Printed in Great Britain) doi:10.1042/BJ20101684

multimedia online data

Functional analysis of *Dictyostelium* IBARa reveals a conserved role of the I-BAR domain in endocytosis

Douwe M. VELTMAN*, Giulio AUCIELLO†, Heather J. SPENCE*, Laura M. MACHESKY*, Joshua Z. RAPPOPORT† and Robert H. INSALL*[1]

*Beatson Institute for Cancer Research, Switchback Road, Bearsden, Glasgow G61 1BD, U.K., and †School of Biosciences, University of Birmingham, Edgbaston, Birmingham B15 2TT, U.K.

I-BAR (inverse-Bin/amphiphysin/Rvs)-domain-containing proteins such as IRSp53 (insulin receptor substrate of 53 kDa) associate with outwardly curved membranes and connect them to proteins involved in actin dynamics. Research on I-BAR proteins has focussed on possible roles in filopod and lamellipod formation, but their full physiological function remains unclear. The social amoeba *Dictyostelium* encodes a single I-BAR/SH3 (where SH3 is Src homology 3) protein, called IBARa, along with homologues of proteins that interact with IRSp53 family proteins in mammalian cells, providing an excellent model to study its cellular function. Disruption of the gene encoding IBARa leads to a mild defect in development, but filopod and pseudopod dynamics are unaffected. Furthermore, ectopically expressed IBARa does not induce filopod formation and does not localize to filopods. Instead, IBARa associates with clathrin puncta immediately before they are endocytosed. This role is conserved: human BAIAP2L2 (brain-specific angiogenesis inhibitor 1-associated protein 2-like 2) also tightly co-localizes with clathrin plaques, although its homologues IRSp53 and IRTKS (insulin receptor tyrosine kinase substrate) associate with other punctate structures. The results from the present study suggest that I-BAR-containing proteins help generate the membrane curvature required for endocytosis and implies an unexpected role for IRSp53 family proteins in vesicle trafficking.

Key words: brain-specific angiogenesis inhibitor 1-associated protein 2-like 2 (BAIAP2L2), clathrin, endocytosis, inverse-Bin/amphiphysin/Rvs (I-BAR) domain, insulin receptor substrate of 53 kDa (IRSp53), insulin receptor tyrosine kinase substrate (IRTKS).

INTRODUCTION

The organization of many cellular structures depends on the coupling between membranes and the cytoskeleton. Adapter proteins with membrane-binding domains play an important role in this coupling. The BAR (Bin/amphiphysin/Rvs) domain folds into an elongated α-helical structure and binds membranes *in vitro* and *in vivo* [1]. BAR domains are unique in their curvature. Classical BAR and F-BAR (FCH-BAR) domains have a concave surface and preferentially bind to membranes with inward (positive) curvature, such as the outside face of vesicles [2,3]. Accordingly, proteins with these domains, such as amphiphysin and syndapin, are involved in vesicular processes such as clathrin-mediated endocytosis and endosomal recycling [3,4].

Conversely, I-BAR (inverse-BAR) domains have a convex surface and bind to outward (negative) membrane curvature [5,6]. Ectopical expression of I-BAR proteins in cultured cells generates numerous amounts of filopodia and the purified I-BAR domain is sufficient to tubulate membranes *in vitro*. The inside face of a filopodium contains strong negative curvature and these observations have led to the view that I-BAR proteins such as MIM (missing in metastasis) and IRSp53 (insulin receptor substrate of 53 kDa) play a role in filopodia formation.

Dictyostelium encodes a single I-BAR-domain-containing protein (Dictybase code DDB_G0274805). The *Dictyostelium* genome also encodes homologues of various proteins that have been reported to interact with I-BAR proteins in mammalian systems, in particular SCAR–WAVE [where WAVE is WASP (Wiskott–Aldrich syndrome protein) verprolin homologous] [7–9]. The presence of these proteins, in the absence of redundant paralogues, makes *Dictyostelium* ideal to study the functional role of I-BAR proteins.

The results of the present study reveal an unexpected conserved role for I-BAR domains in clathrin-mediated endocytosis, and thus that the specific curvature of the I-BAR domain does not limit its physiological function to protrusion formation.

EXPERIMENTAL

Bioinformatics

Novel I-BAR domain proteins were identified by searching GenBank® (http://blast.ncbi.nlm.nih.gov/Blast.cgi) using BLASTP and TBLASTN with I-BAR domains of known family members. Alignments of obtained sequences were performed with ClustalX and phylogenetic trees were drawn with Treeview.

Strains and constructs

An *ibrA* knockout was generated in AX2 (sDM8) and in AX3 (sDM7) as follows. The full-length *ibrA* gene amplified from cDNA was cloned into pDONR221. A floxed blasticidin-resistance cassette was ligated in between the unique MunI

Abbreviations used: BAIAP2L2, brain-specific angiogenesis inhibitor 1-associated protein 2-like 2; BAR, Bin/amphiphysin/Rvs; DIC, differential interference contrast; GFP, green fluorescent protein; I-BAR, inverse-BAR; IRSp53, insulin receptor substrate of 53 kDa; IRTKS, insulin receptor tyrosine kinase substrate; MIM, missing in metastasis; mRFP, monomeric red fluorescent protein; NA, numerical aperture; SH3, Src homology 3; TIRF, total internal reflection; WASP, Wiskott–Aldrich syndrome protein; WAVE, WASP verprolin homologous.

[1] To whom correspondence should be addressed (email r.insall@beatson.gla.ac.uk).

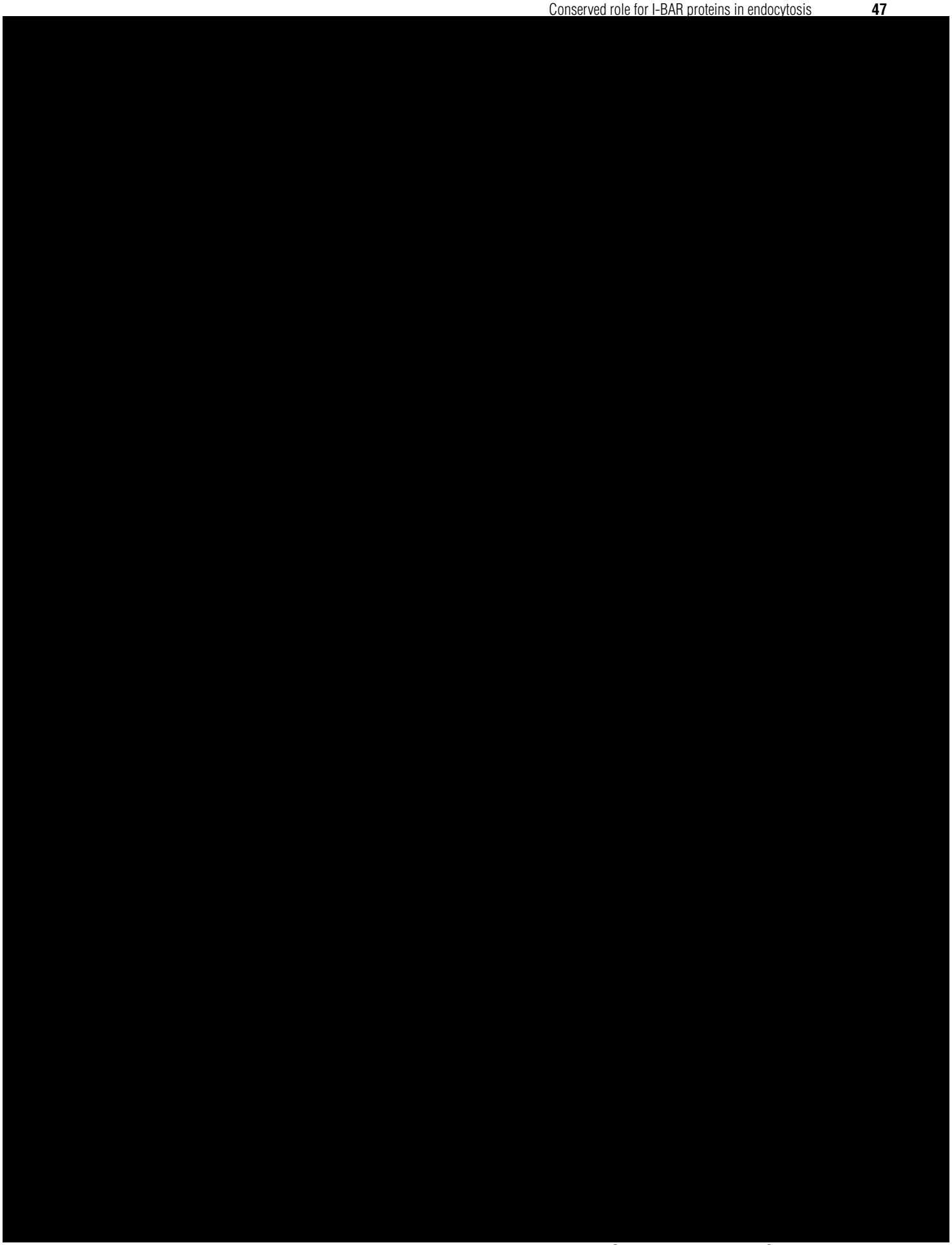

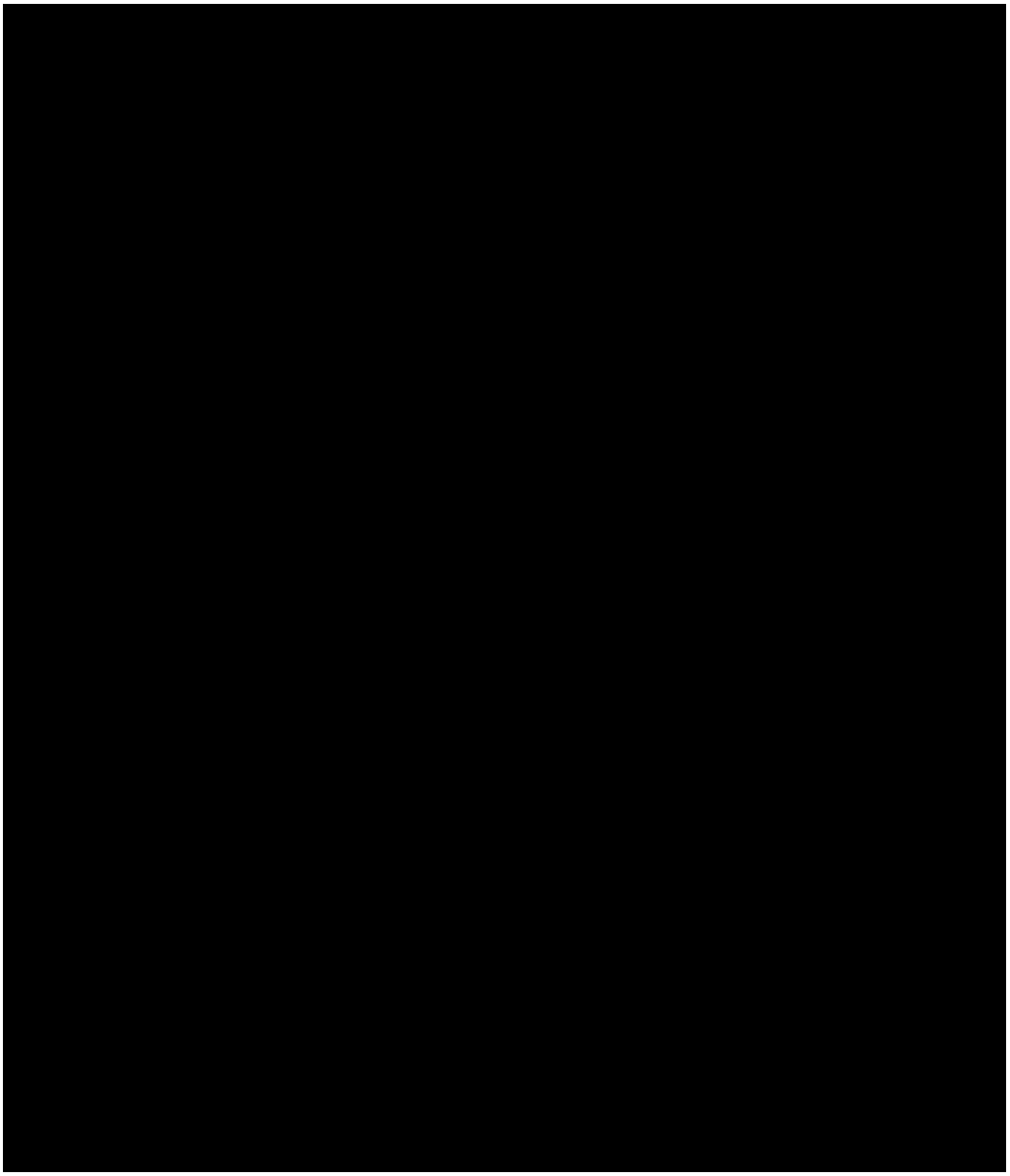

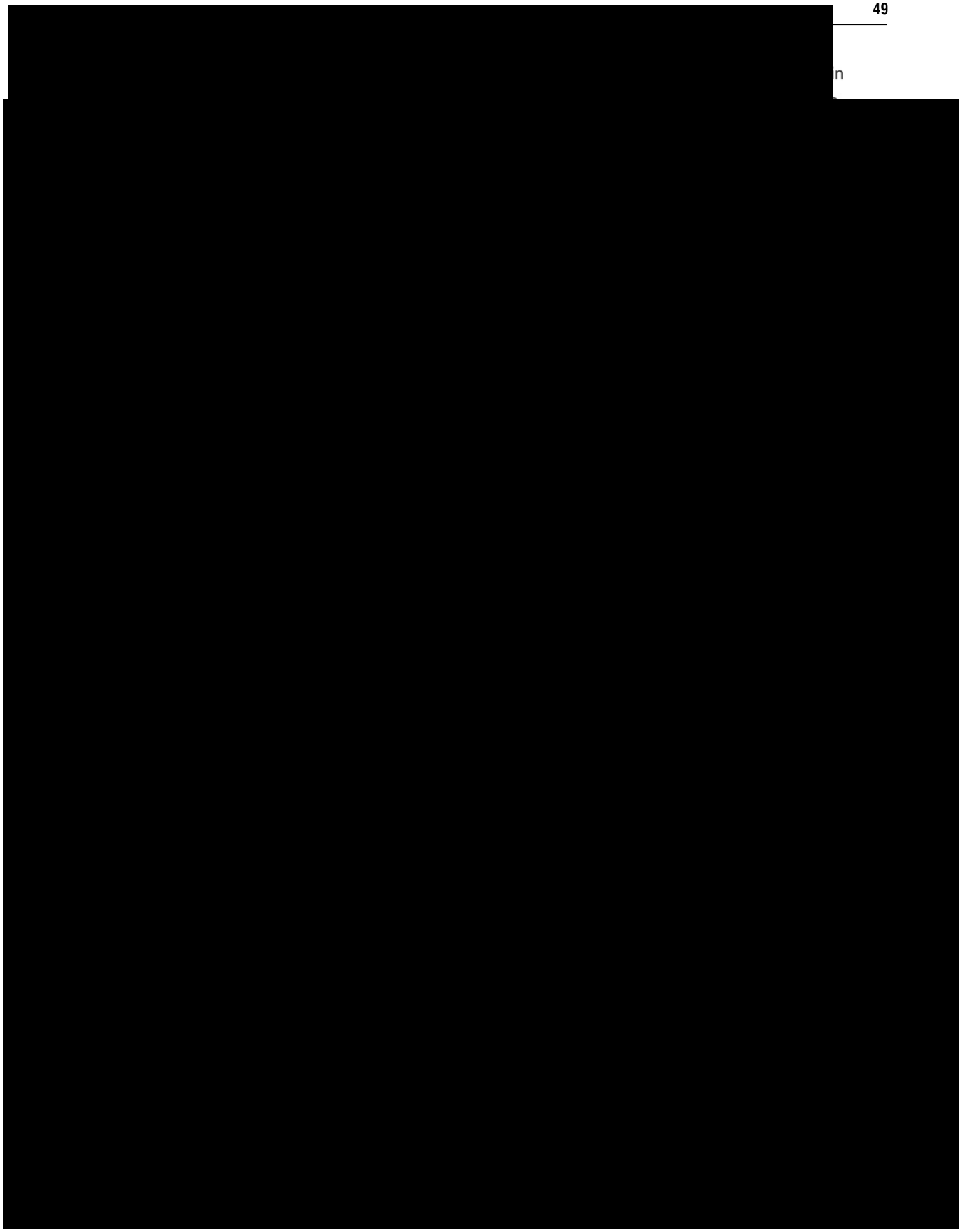

[redacted]

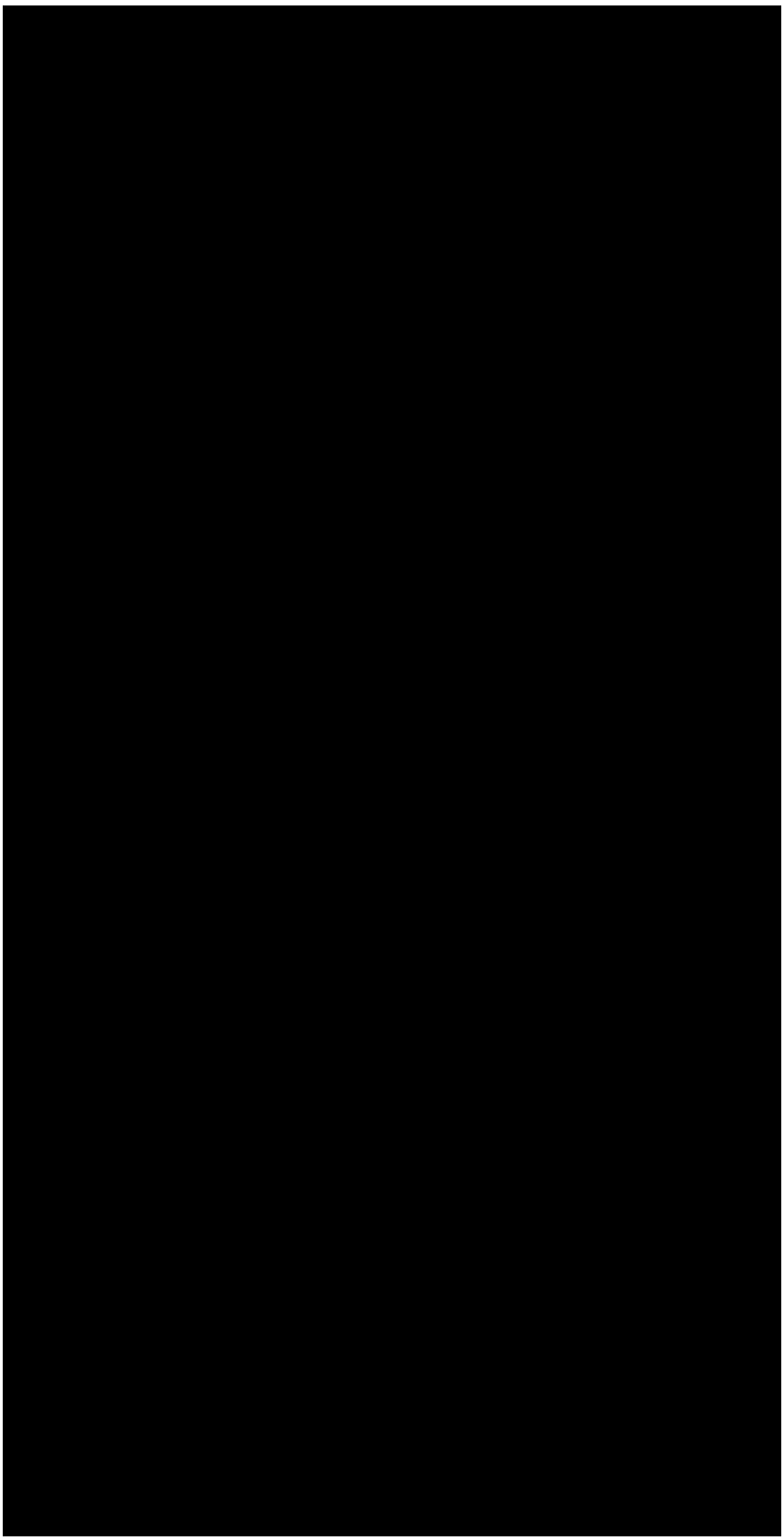

[redacted]

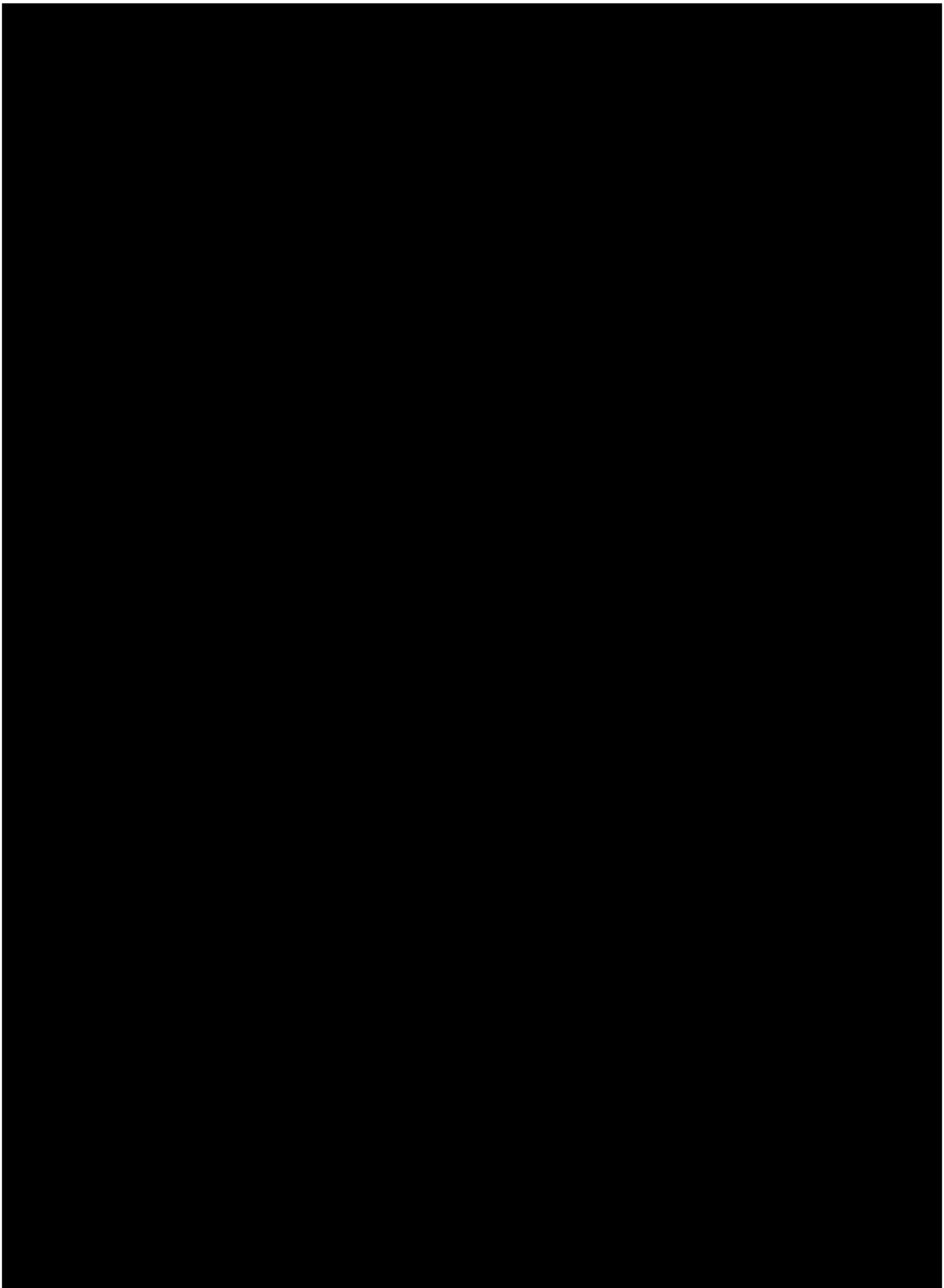

[redacted]

Biochem. J. (2011) **436**, 45–52 (Printed in Great Britain) doi:10.1042/BJ20101684

multimedia online data

SUPPLEMENTARY ONLINE DATA

Functional analysis of *Dictyostelium* IBARa reveals a conserved role of the I-BAR domain in endocytosis

Douwe M. VELTMAN*, Giulio AUCIELLO†, Heather J. SPENCE*, Laura M. MACHESKY*, Joshua Z. RAPPOPORT† and Robert H. INSALL*[1]

*Beatson Institute for Cancer Research, Switchback Road, Bearsden, Glasgow G61 1BD, U.K., and †School of Biosciences, University of Birmingham, Edgbaston, Birmingham B15 2TT, U.K.

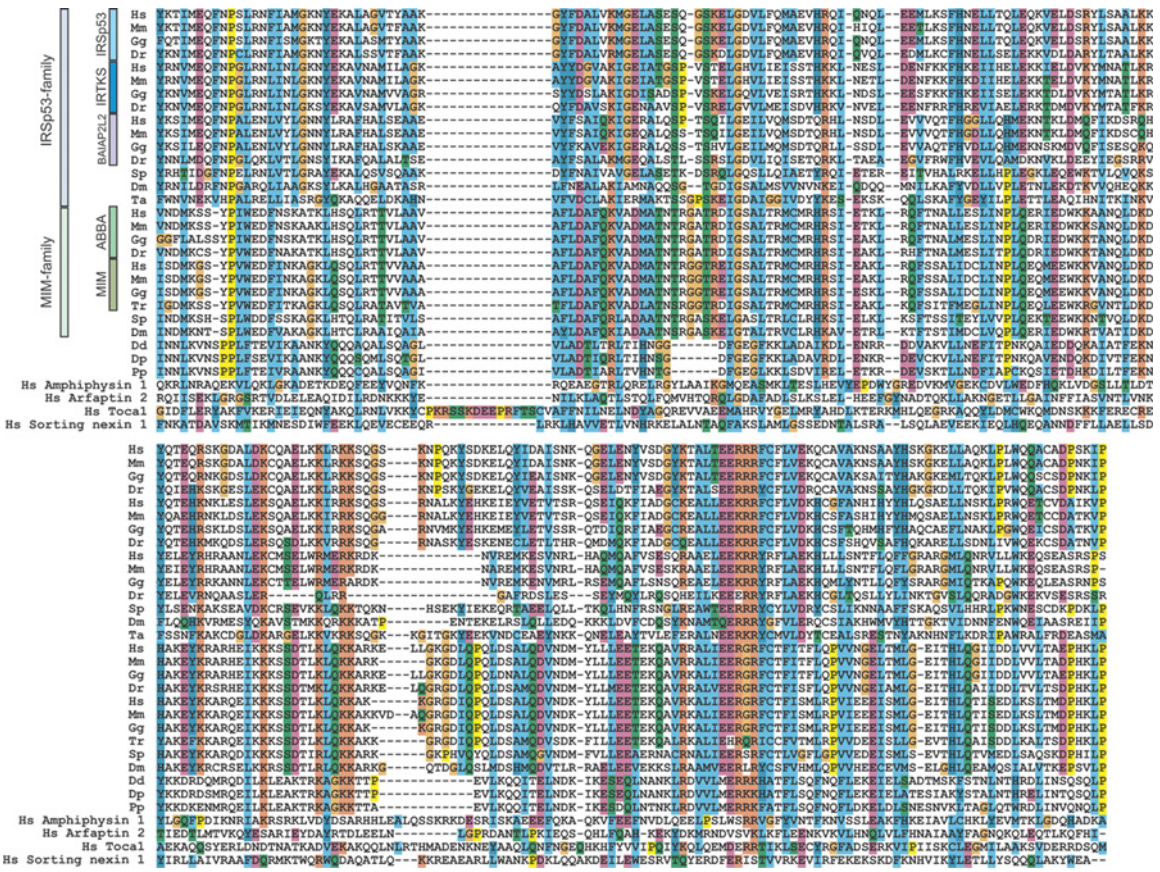

Figure S1 Alignment of the I-BAR domain

I-BAR domains from the indicated organisms were aligned in ClustalX. Residues are coloured according to the standard ClustalX colour scheme. The second half of the domain is shown below the first. Species abbreviations are as follows: Hs, *Homo sapiens*; Mm, *Mus musculus*; Gg, *Gallus gallus*; Dr, *Danio rerio*; Tr, *Takifugu rubripes*; Sp, *Strongylocentrotus purpuratus*; Dm, *Drosophila melanogaster*; Ta, *Trichoplax adhaerens*; Dd, *Dictyostelium discoideum*; Dp, *Dictyostelium purpureum*; and Pp, *Polysphondylium pallidum*.

[1] To whom correspondence should be addressed (email r.insall@beatson.gla.ac.uk).

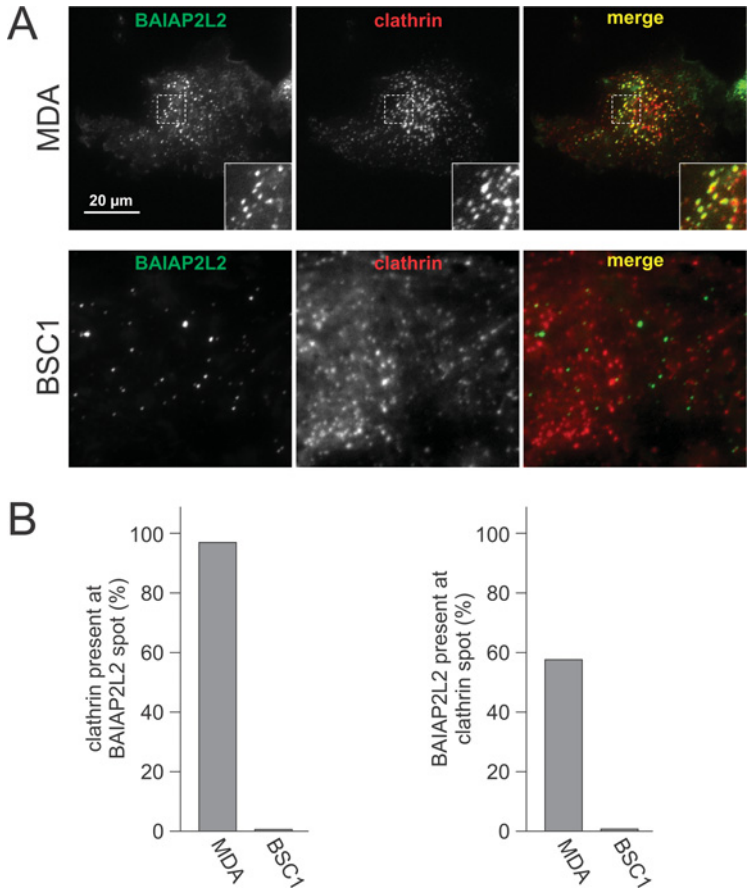

Figure S2 Co-localization between clathrin and BAIAP2L2

(**A**) Co-expression of fluorescently tagged clathrin with BAIAP2L2 in MDA MB231 cells and BSC1 cells. (**B**) For each clathrin spot in the respective strains, it was determined if BAIAP2L2 was also present at that position and vice versa.

Received 14 October 2010/28 February 2011; accepted 14 March 2011
Published as BJ Immediate Publication 14 March 2011, doi:10.1042/BJ20101684

MOLECULAR AND CELLULAR BIOLOGY, Dec. 2010, p. 5672–5685 Vol. 30, No. 24
0270-7306/10/$12.00 doi:10.1128/MCB.00878-10

Nbr1 Is a Novel Inhibitor of Ligand-Mediated Receptor Tyrosine Kinase Degradation▽

Faraz K. Mardakheh,[1] Giulio Auciello,[1,2] Tim R. Dafforn,[2] Joshua Z. Rappoport,[2] and John K. Heath[1]*

CRUK Growth Factor Group, School of Biosciences, University of Birmingham, Edgbaston, Birmingham B15 2TT, United Kingdom,[1] and School of Biosciences, University of Birmingham, Edgbaston, Birmingham B15 2TT, United Kingdom[2]

Received 28 July 2010/Returned for modification 21 September 2010/Accepted 28 September 2010

Neighbor of BRCA1 (Nbr1) is a highly conserved multidomain scaffold protein with proposed roles in endocytic trafficking and selective autophagy. However, the exact function of Nbr1 in these contexts has not been studied in detail. Here we investigated the role of Nbr1 in the trafficking of receptor tyrosine kinases (RTKs). We report that ectopic Nbr1 expression inhibits the ligand-mediated lysosomal degradation of RTKs, and this is probably done via the inhibition of receptor internalization. Conversely, the depletion of endogenous NBR1 enhances RTK degradation. Analyses of truncation mutations demonstrated that the C terminus of Nbr1 is essential but not sufficient for this activity. Moreover, the C terminus of Nbr1 is essential but not sufficient for the localization of the protein to late endosomes. We demonstrate that the C terminus of Nbr1 contains a novel membrane-interacting amphipathic α-helix, which is essential for the late endocytic localization of the protein but not for its effect on RTK degradation. Finally, autophagic and late endocytic localizations of Nbr1 are independent of one another, suggesting that the roles of Nbr1 in each context might be distinct. Our results define Nbr1 as a negative regulator of ligand-mediated RTK degradation and reveal the interplay between its various regions for protein localization and function.

Receptor tyrosine kinases (RTKs) are a major superfamily of membrane-spanning growth factor receptors with intrinsic kinase activity, which regulate fundamental cellular processes such as proliferation, migration, differentiation, and survival. RTKs include, among others, insulin-like growth factor receptor (IGFR), epidermal growth factor (EGF) receptor (EGFR), fibroblast growth factor (FGF) receptor (FGFR), vascular endothelial growth factor receptor (VEGFR), and platelet-derived growth factor receptor (PDGFR) (26). Most RTKs are activated by the binding of their cognate ligands, which induces receptor dimerization and the autophosphorylation of specific tyrosine residues within the kinase domain and the C-terminal cytoplasmic tail, as well as the phosphorylation of constitutively associated scaffold proteins such as FRS2. This results in the recruitment and subsequent phosphorylation of other signaling molecules, the assembly of multiprotein signaling complexes, and the ultimate activation of downstream signal transduction pathways. Such pathways include, among others, the RAS/mitogen-activated protein kinase (MAPK) cascade also known as the extracellular signal-regulated kinase (ERK) pathway, the phosphatidylinositol-3-OH kinase (PI3K)/AKT pathway, and the phospholipase C (PLC)/protein kinase C (PKC) pathway (26). These signaling pathways in turn act on a variety of transcription factors, the activities of which define the particular cellular outcome of a given stimulation.

Signaling from RTKs is tightly regulated by a variety of extrinsic and intrinsic control mechanisms, the deregulation of which is a major contributor to most cancers (35). In particular, endocytic trafficking has emerged as a key regulator of RTK signaling (30). Internalization is often triggered by ligand binding and the activation of RTKs on the cell surface. Receptor internalization occurs through clathrin-dependent or -independent mechanisms followed by trafficking through different vesicular compartments once inside the cell (30).

Endocytic trafficking can regulate RTK signaling at least at two levels. First, it can result in selective pathway propagation or downregulation by compartmentalization. For example, the removal of activated RTKs from the plasma membrane results in the termination of those downstream signaling pathways which require plasma membrane-associated molecules. These include the PLC/PKC and the PI3K/AKT pathways, both of which require phosphatidylinositol-4,5-phosphate ($PI45P_2$) as a substrate, which is absent in endosomes (8). In contrast, ERK1/2 signaling is not limited to plasma membrane. In fact, many studies suggested that full ERK1/2 activation depends on the endocytosis of RTKs (10, 11, 14, 34). This has been attributed to the ERK1/2 propagating scaffolding complex P14-MP1, which is localized specifically to late endosomes (19, 32, 33). Another example of specific endosomal signal propagation has been shown for AKT. The adaptor protein-containing pleckstrin homology (PH) domain, the PTB domain, and leucine zipper motif 1 (APPL1) can bind specifically to AKT on early endosomes and enhance its activity (25). APPL1 also binds to the AKT substrate glycogen synthase kinase 3β (GSK-3β) and increases its phosphorylation by AKT without affecting the phosphorylation of another AKT substrate, tuberous sclerosis complex protein 2 (TSC2), thereby providing pathway selectivity (25).

Second, it is well established that endocytosis can act to

* Corresponding author. Mailing address: CRUK Growth Factor Group, School of Biosciences, University of Birmingham, Edgbaston, Birmingham B15 2TT, United Kingdom. Phone: 44 121 414 7533. Fax: 44 121 414 4534. E-mail: j.k.heath@bham.ac.uk.

▽ Published ahead of print on 11 October 2010.

downregulate RTK signaling by trafficking receptors to lysosomes for degradation. En route, signaling receptors are removed from the limiting membrane of endosomes and enclosed within intraluminal vesicles of multivesicular bodies (MVBs), rendering them unable to interact with signaling molecules and susceptible to degradation by lysosomal hydrolyses (22, 30). MVB formation begins in early endosomes and continues in late endosomes before mature MVBs are finally fused with lysosomes (22). MVB sorting of RTKs depends on ubiquitination by specific ubiquitin ligases such as CBL, followed by the concerted action of the endosomal sorting complex required for transport (ESCRT) proteins, which direct ubiquitinated cargos to the intraluminal vesicles of MVBs (22). The importance of RTK regulation by MVB sorting and lysosomal degradation is manifested by the fact that a variety of cancer-associated genetic and epigenetic alterations specifically target this pathway (18). Once internalized, however, the lysosomal degradation route is not the only available itinerary for RTKs. Internalized receptors can undergo recycling back to the plasma membrane for reusage, and the balance between recycling and lysosomal targeting can be a crucial determinant of the signaling outcome (27, 28).

Nbr1 is a ubiquitously expressed multidomain scaffold protein of 988 amino acids with ~90% conservation between mouse and human (4, 37). It contains an N-terminal phox/Bem1p (PB1) domain, a ZZ-type zinc finger (ZZ), a coiled-coiled (CC) region, and a C-terminal ubiquitin association (UBA) domain capable of binding to both K48- and K63-type polyubiquitin chains (9, 36). The PB1 domain of NBR1 can bind to the open catalytic domain of the giant muscle kinase titin and regulate its downstream signaling in muscle cells (12). In addition, the PB1 domain can heterodimerize with the PB1 domain of P62/sequestosome-1 (SQSTM1) (12), another scaffold protein of similar architecture with proposed roles in endosomal trafficking (7) and selective autophagy (2, 21). A role in selective autophagy has also been proposed for NBR1, as it was shown to associate with the mammalian homologue of Atg8, an essential autophagosomal protein also known as microtubule-associated protein 1 light chain 3 (LC3) (9, 36). A main LC3-interacting region (LIR) as well as a secondary LC3-interacting region (LIR2) were identified in NBR1 (9), and it was proposed previously that similarly to P62, NBR1 can act as a specific adaptor for ubiquitinated cargos destined for degradation by autophagosomes (9, 36). Recently, an *in vivo* role for NBR1 in the regulation of bone mass and density has been revealed by its genetic truncation in mice (38).

We recently reported that NBR1 associates with Spred2, a negative regulator of ERK1/2 signaling downstream of RTKs (15). We showed that Spred2 activity is dependent on its interaction with NBR1 and that Spred2 downregulates ERK1/2 signaling downstream of FGFR by targeting the receptor to the lysosomal degradation pathway (15). These results led us to propose NBR1 as a novel regulator of RTK trafficking, but it remained unclear whether the protein had any effect on RTK trafficking on its own. Here we investigated the role of NBR1 in the context of RTK trafficking in more detail. We show that ectopic Nbr1 expression inhibits the ligand-mediated lysosomal degradation of endogenous RTKs. Live-cell imaging revealed that this effect is probably due to the inhibition of receptor internalization from the cell surface. In contrast, small interfering RNA (siRNA) depletion of endogenous NBR1 enhances receptor degradation. The C terminus of Nbr1 is essential but not sufficient for this function. Similarly, the C terminus of Nbr1 is essential but not sufficient for the late endocytic localization of the protein. We also show that in addition to the UBA domain, the C terminus of Nbr1 contains a membrane-interacting amphipathic α-helix, which is necessary for the late endocytic localization of the protein but not for its effect and RTK degradation. Finally, we demonstrate that the late endocytic and autophagic localizations of Nbr1 are independent, suggesting that the function of Nbr1 in each context might be distinct. Our results establish Nbr1 as a novel negative regulator of RTK trafficking and reveal the relationship between its different regions for protein localization and function.

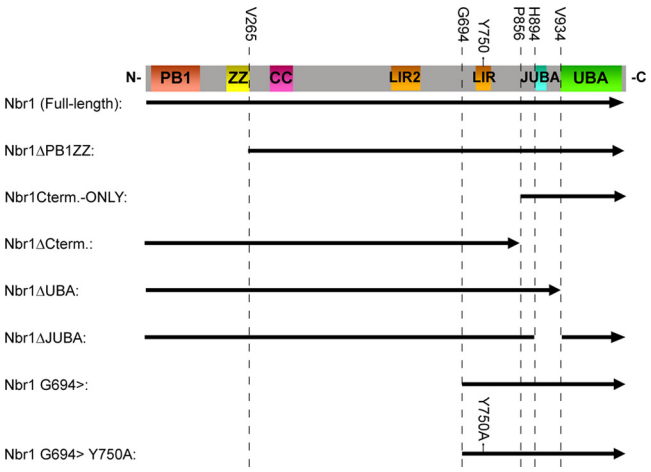

FIG. 1. Schematic representation of Nbr1 mutations used in this study. The arrow is in an N- to C-terminal direction. The indicated amino acids are the first or last included residues in the constructs. Nbr1 regions are represented linearly (the JUBA label applies to the cyan portion).

MATERIALS AND METHODS

Plasmid constructs. A schematic representation of Nbr1 constructs described in the study can be found in Fig. 1. N-terminally Myc- and green fluorescent protein (GFP)-tagged full-length mouse Nbr1 constructs as well as an N-terminally glutathione *S*-transferase (GST)-tagged C-terminal-only Nbr1 mutation (P856-Y988) construct were described previously (15). All N- and C-terminal truncation mutation constructs were made by Gateway cloning (Invitrogen) according to the manufacturer's instructions and as described previously (31). Briefly, forward and reverse primers with in-frame gateway 5′ overhangs corresponding to the beginning and end of a target sequence were used in a PCR to generate Gateway-compatible coding fragments. These fragments were then recombined into the Gateway pDONR201 entry vector (Invitrogen) using the BP clonase enzyme (Invitrogen). Myc-tagged constructs were generated by recombining entry vectors into a Myc-pRK5 gateway destination vector described previously (31) using the LR clonase enzyme (Invitrogen). GFP-tagged constructs were similarly generated by using the pcDNA DEST53 destination vector (Invitrogen). The Y750A point mutation was generated by site-directed mutagenesis using overlapping forward and reverses primers harboring the specific mutation in the middle. Finally, the Nbr1 juxta-UBA (JUBA) deletion mutation was generated from a full-length coding construct using primers with AgeI restriction digestion site 5′ overhangs. These forward and reverse primers were targeted to just after and just before the JUBA coding sequence, respectively, and were used in a PCR to amplify the whole construct minus the JUBA coding sequence. The linear product was then circularized by AgeI digestion (NEB) and

self-ligation using T4 ligase (Invitrogen). The C-terminally GFP-tagged EGFR construct was described previously (3, 23).

Reagents and antibodies. Mouse monoclonal anti-NBR1 antibodies were purchased from Abcam and Abnova (clone 6B11). Mouse monoclonal antibody against LAMP2 (clone H4B4) was also obtained from Abcam. Mouse monoclonal anti-Myc tag antibody (clone 9E10) was obtained from Roche. Rabbit monoclonal anti-Myc tag (clone 71D10) antibody was obtained from Cell Signaling Technology. Anti-EGFR, GST, EEA1, cleaved procyclic acidic repetitive protein (PARP), and cleaved CASP-9 rabbit polyclonal antibodies were also obtained from Cell Signaling Technology. Rabbit polyclonal anti-FGFR2 (Bek), ERK1, and mouse monoclonal anti-pERK1/2 (clone E4) antibodies were obtained from Santa Cruz Biotechnology Inc. Mouse monoclonal anti-α-tubulin (clone DM 1A) was obtained from Sigma. All fluorescently labeled (Alexa Fluor 488, Alexa Fluor 594, and Texas Red) secondary antibodies were obtained from Invitrogen. Horseradish peroxidase-conjugated anti-mouse and anti-rabbit IgG secondary antibodies were obtained from Amersham Biosciences Inc. IRDye infrared anti-mouse and anti-rabbit IgG secondary antibodies were obtained from Li-COR Biosciences.

EGF was purchased from Sigma. z-VAD-FMK and bafilomycin-A1 (BafA) were also obtained from Sigma. Nontargeting control and NBR1 siRNAs were purchased from Santa Cruz Biotechnology Inc. The custom-made JUBA peptide was obtained from Alta Bioscience. The GST-tagged PH domain of PLC-δ1 (PIP_2 Grip) was purchased from Echelon Inc. Membrane lipid strips, phosphatidylinositol-phosphate (PIP) arrays, and all phospholipids apart from phosphatidylcholine were also purchased from Echelon Inc. Phosphatidylcholine was purchased from Avanti Polar Lipids Inc.

Cell culture, transfection, stimulation, lysis, and Western blotting. Cell culture and transfections were performed as described previously (15). Briefly, cells—human embryonic kidney (HEK) 293T and 293A LC3-GFP cells as well as African green monkey simian virus 40 (SV40)-transformed kidney (COS7) cells—were grown at 37°C in 5% CO_2 in Dulbecco's modified Eagle medium (Invitrogen) supplemented with 10% fetal bovine serum (Labtech International). DNA transfections were performed by using Genejuice transfection reagent (Novagen) according to the manufacturer's instructions, and the cells were analyzed at 24 h posttransfection. Lipofectamine RNAiMAX (Invitrogen) was used for siRNA transfections according to the manufacturer's instructions for forward or reverse transfections, and the cells were analyzed after 24, 48, or 72 h, with the transfection being renewed every 24 h. For EGF and FGF2 stimulations, 293T cells were serum starved for 6 h, and ligand (plus 10 μg/ml heparin in the case of FGF2) was added to the cells at the indicated concentrations. Lysis was performed by the addition of 2× SDS sample buffer directly to the cells (50 $\mu l/cm^2$ of cells), followed by rigorous vortexing and heating to 95°C for 10 min. Lysates were run on 4 to 12% NuPAGE Bis-Tris SDS gels (Invitrogen), and Western blotting was performed by using Immobilon PVDF-FL (Millipore) membranes. Membranes were dried and incubated with primary antibodies overnight at 4°C, followed by washing and incubation with secondary antibodies for 1 h at room temperature. After additional washes, blots were visualized by Enhanced Chemiluminescence Plus reagent (GE Healthcare) or an Odyssey infrared imaging system (Li-COR).

Live-cell imaging, immunostaining, and confocal microscopy. Live-cell imaging with a Nikon A1R/TIRF microscope system (Nikon UK) was used to analyze receptor endocytosis and degradation. Cells transfected with GFP-tagged EGFR, with or without the cotransfection of Myc-Nbr1, were imaged by time-lapse epifluorescence microscopy employing a 60× objective and an Andor iXon 885 electron multiplier charge-coupled-device (EM-CCD) camera. Cells were imaged following stimulation with EGF, and EGFR-GFP fluorescence was analyzed to quantify endocytosis (number of intracellular endosomes positive for EGFR at each time point) and degradation (total cellular intensity at each time point). Five cells per group were analyzed, and nonstimulated cells were analyzed as a photobleaching control. Immunostaining and confocal microscopy were performed essentially as described previously (15). Briefly, cells grown on glass coverslips were fixed, permeabilized, blocked, and subjected to primary and fluorescently labeled secondary antibodies for 1 h per antibody with three washes in between before being mounted onto Mowiol. Coverslips were subsequently analyzed by laser scanning confocal microscopy using a Leica TCS SP2 confocal microscope system. All images were taken sequentially and as a single section at 200 Hz using the 63× objective lens. Final images were generated from the averages of eight consecutive scans. All presented images are representative of the majority of cells investigated.

Liposome preparation and circular dichroism. Liposomes were prepared as described previously (20). Briefly, phosphatidylcholine and the PIP of interest were mixed in a glass vial at 95:5 molar ratio. The lipid mixture was dried under an N_2 gas stream, redissolved in 1:1 $CHCl_3$-CH_3OH, and dried again under an N_2 stream followed by vacuum centrifugation for 1 h to remove residual chloroform. The lipids were subsequently resuspended in ultrapure H_2O and subjected to multiple rounds of freezing at −80°C and thawing in a 45°C sonicating water bath until the mixture became optically clear. Circular dichroism (CD) was performed as described previously (6). Briefly, spectra were acquired with a Jasco J715 spectropolarimeter using 0.5-mm cuvettes (Starna/Optiglass) with peptide concentrations of 1 mg/ml and liposome concentrations of 2 mg/ml where applicable. Spectra were recorded from 300 nm to 180 nm with a bandwidth of 2 nm, a data pitch of 0.2 nm, a scan speed of 100 nm/min, and a response time of 0.5. Four consecutively recorded spectra were averaged for each sample, and the relevant buffer baseline spectra were subtracted from each sample spectrum.

RESULTS

Nbr1 inhibits lysosomal degradation of RTKs. We previously reported that NBR1 is a specific late endosomal protein and that the regulation of FGFR trafficking and signaling by Spred2 depends on its interaction with NBR1 (15). These results suggested a novel role for NBR1 as a regulator of receptor trafficking, but it remained unclear whether the protein had any direct effect on RTK trafficking on its own. We therefore set out to investigate the trafficking role of NBR1 in more detail, focusing on its effect on EGFR and FGFR trafficking. We observed that ectopic Nbr1 expression inhibited the ligand-mediated degradation of endogenous EGFR (Fig. 2A and C). Similarly, the ligand-mediated degradation of endogenous FGFR2 was inhibited by ectopic Nbr1 expression (Fig. 2B and C). As a result, downstream ERK1/2 signaling was enhanced in response to both EGF and FGF2 (Fig. 2A and B). In neither case did Nbr1 have any effect on basal receptor levels as judged by immunoblotting (Fig. 2C). Moreover, the effect of ectopic Nbr1 expression on EGFR (Fig. 2D and F) or FGFR2 (Fig. 2E and F) was minimal in cells pretreated with the lysosomal inhibitor bafilomycin-A1 (BafA), supporting the notion that the observed difference in receptor levels is due to the inhibition of lysosomal degradation (Fig. 2F). These results demonstrate that Nbr1 acts to abrogate ligand-mediated RTK degradation.

We next investigated the effect of the depletion of endogenous NBR1 on the degradation of EGFR and FGFR2. In contrast to ectopic Nbr1 expression, the depletion of endogenous NBR1 in 293T cells by siRNA enhanced EGFR degradation (Fig. 3A and C). Similar results were obtained with HeLa cells, which express considerably higher endogenous EGFR levels (Fig. 3B and C). The reduction in receptor levels could be seen even in the absence of ligand treatment, suggesting that depleting endogenous NBR1 must be sufficient to force receptors toward the degradative endocytic route (Fig. 3C). However, a similar effect could not be detected for FGFR2 (data not shown). Since the prolonged knockdown of NBR1 results in cell death (15), it is very likely that the NBR1 depletion in these experiments was not complete. Thus, a possible explanation for this variation could be that FGFR2 and EGFR simply have different sensitivity thresholds toward a partial NBR1 depletion.

Nbr1 inhibits ligand-mediated receptor internalization from the cell surface. In order to generate a real-time analysis of RTK trafficking and degradation in live cells, we made use of the well-documented GFP-tagged EGFR construct (3, 23). We imaged the loss of EGFR from the plasma membrane and its appearance in cytosolic endosomes, followed by subsequent

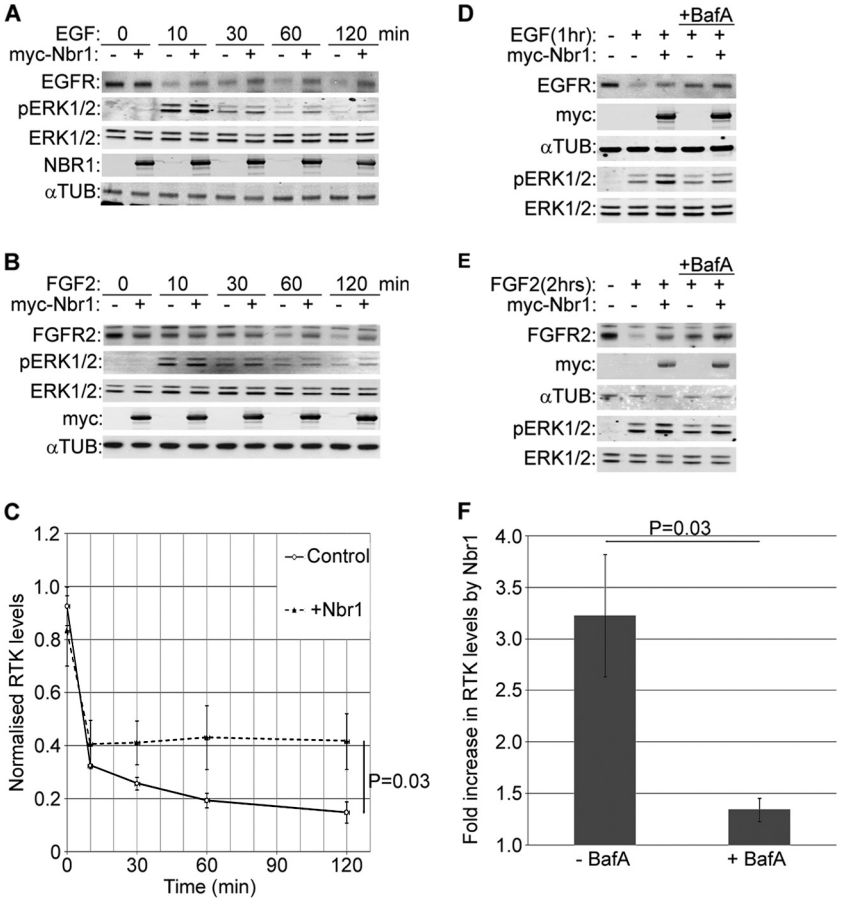

FIG. 2. Nbr1 abrogates ligand-mediated lysosomal degradation of RTKs and enhances downstream signaling. All error bars represent standard errors of the means (SEM). *P* values were calculated by a one-tailed paired *t* test ($n = 3$). (A) Overexpression of Nbr1 inhibits ligand-mediated EGFR degradation and enhances downstream ERK1/2 signaling. HEK293T cells transfected with Myc-Nbr1 or GFP as a control were serum starved and stimulated for the indicated time points with 50 ng/ml EGF. Cells were lysed and analyzed by Western blotting. (B) Overexpression of Nbr1 inhibits ligand-mediated FGFR2 degradation and enhances downstream ERK1/2 signaling. HEK293T cells transfected with Myc-Nbr1 or GFP as a control were serum starved and stimulated for the indicated time points with 20 ng/ml FGF2 plus 10 μg/ml heparin. Cells were lysed and analyzed by Western blotting. (C) Densitometry analysis of RTK degradation in the presence or absence of Myc-Nbr1 from panels A and B. (D) Nbr1 inhibition of ligand-mediated EGFR degradation is BafA sensitive. HEK293T cells transfected with Myc-Nbr1 or GFP as a control were starved and stimulated for the indicated times with 50 ng/ml EGF. Thirty minutes prior to stimulation, the specified cells were pretreated with 200 nM BafA. Cells were lysed and analyzed by Western blotting. (E) Nbr1 inhibition of ligand-mediated FGFR2 degradation is BafA sensitive. HEK293T cells transfected with Myc-Nbr1 or GFP as a control were starved and stimulated for the indicated times with 20 ng/ml FGF2 plus 10 μg/ml heparin. Thirty minutes prior to stimulation, the specified cells were pretreated with 200 nM BafA. Cells were lysed and analyzed by Western blotting. (F) Densitometry analysis of the effect of BafA treatment on Myc-Nbr1-mediated inhibition of RTK degradation from panels D and E. αTUB, α-tubulin.

degradation, live in HeLa cells. Following stimulation, EGFR-GFP clearly redistributed to cytosolic punctae (Fig. 4A). However, the expression of Nbr1 decreased the endocytic trafficking of activated EGFR (Fig. 4A). Quantification of the number of EGFR-positive spots at each time point following stimulation revealed that endocytosis was significantly delayed in cells expressing Nbr1 (Fig. 4B). These results suggest that a likely mechanism by which Nbr1 inhibits RTK degradation is via trapping the receptor on the cell surface. Furthermore, quantification of whole-cell fluorescence demonstrated that the degradation of EGFR following EGF stimulation was significantly attenuated in cells expressing ectopic Nbr1 (Fig. 4C). Thus, the results of these imaging-based assays concur with data from the above-described biochemical studies (Fig. 2C).

The C terminus of Nbr1 is essential but not sufficient for its function and localization. We next examined the contribution of different regions of Nbr1 to its inhibition of RTK degradation. Our previous study implicated the C terminus of NBR1 as being important for its function, as it was sufficient to mediate an association with SPRED2 (15). Therefore, we first compared the effect of full-length Nbr1 to that of a C-terminally deleted mutation lacking the last 133 amino acids on ligand-mediated RTK degradation. Unlike full-length Nbr1, the C-terminally deleted mutation did not inhibit EGFR degradation after EGF treatment (Fig. 5A and C), and similar results were obtained for FGFR2 (Fig. 5B and C). Accordingly, the enhancement of downstream ERK1/2 signaling was also lost when the C terminus of Nbr1 was deleted (Fig. 5A and B).

Next, we compared full-length Nbr1 with a C-terminal-only mutation (P856-Y988), which contains just the last 133 amino acids. We observed that similarly to the prolonged depletion of NBR1 by siRNA (15), the expression of the C-terminal-only

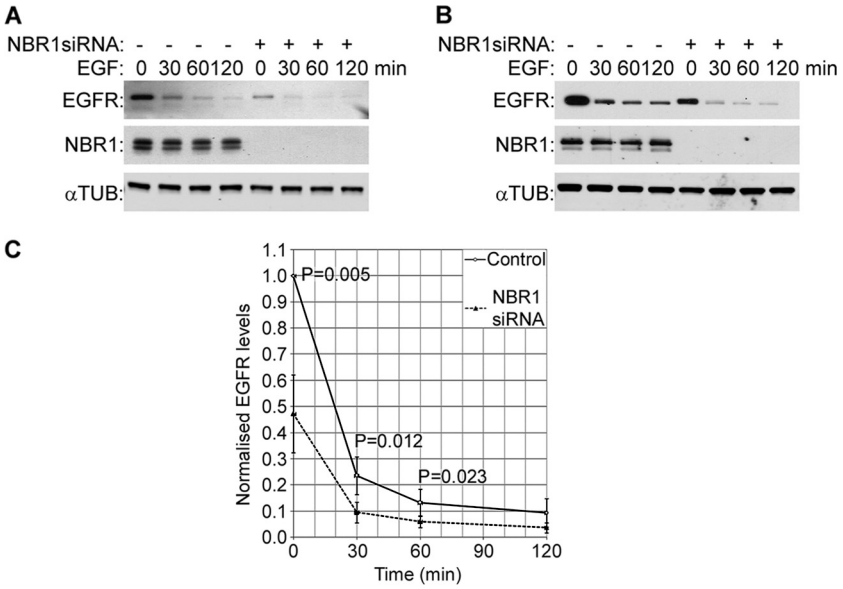

FIG. 3. Depletion of endogenous NBR1 enhances EGFR degradation. All error bars represent SEM. *P* values were calculated by a one-tailed paired *t* test ($n = 5$). (A) 293T cells were transfected with NBR1 or nonsilencing control siRNAs for 48 h, with the transfection being renewed after 24 h. Cells were serum starved and stimulated for the indicated times with 50 ng/ml EGF before being lysed and analyzed by Western blotting. (B) HeLa cells were transfected with NBR1 or nonsilencing control siRNAs for 48 h. Cells were starved and stimulated for the indicated times with 50 ng/ml EGF before being lysed and analyzed by Western blotting. (C) Densitometry analysis of EGFR levels in control or NBR1-depleted cells from panels A and B. Note that NBR1 depletion results in a reduction of EGFR levels even prior to stimulation.

mutation induced cell death by apoptosis (Fig. 5D), but this could be inhibited by a general caspase inhibitor, z-VAD-FMK (Fig. 5E). Unlike full-length Nbr1, the C-terminal-only Nbr1 mutation was not capable of inhibiting ligand-mediated EGFR (Fig. 5F and H) or FGFR2 (Fig. 5G and H) degradation in cells treated with z-VAD-FMK. The enhancement of downstream ERK1/2 signaling was also lost (Fig. 5F and G). Together, these results suggest that the C terminus of Nbr1 is essential but not sufficient for the inhibition of RTK degradation.

As Nbr1 specifically localizes to the limiting membrane of late endosomes (15), we asked whether this localization might be important for the effect on RTK trafficking. Using confocal microscopy, we investigated the late endocytic localization of different Nbr1 mutations. As expected, full-length Nbr1 exhibited a strong colocalization with the late endocytic marker LAMP2 (Fig. 6A). The deletion of the two N-terminal domains, the PB1 and ZZ domains, did not have an effect on protein localization (Fig. 6B). However, the loss of the C-terminal 133 amino acids (P856-Y988), which results in the loss of protein function (Fig. 5A, B, and C), had a dramatic impact on protein localization (Fig. 6C). This deletion resulted in the loss of colocalization with LAMP2, and the protein exhibited a diffuse cytosolic localization instead of a vesicular localization (Fig. 6C). Similarly, when a C-terminal-only (P856-Y988) Nbr1 mutation was investigated, it showed no colocalization with LAMP2 (Fig. 6D). However, this mutation was still localized to the limiting membrane of some intracellular vesicular structures (Fig. 6D). These vesicular structures were larger than full length (Fig. 6D) and stained positive for the early endosomal marker EEA1 (data not shown), which is suggestive of a potential defect in vesicle maturation/fission. These results indicate that the C terminus of Nbr1 is essential but not sufficient for its correct localization.

The C terminus of Nbr1 is constituted of UBA and JUBA. Having established the importance of the Nbr1 C terminus (P856-Y988) for protein localization and function, we sought to study this region in more detail. The C terminus of Nbr1 contains a well-conserved UBA domain (9, 36). However, a detailed study of the C terminus also revealed another region of high conservation that was located 10 amino acids N terminal to the UBA domain (Fig. 7A). Due to its proximity to the UBA domain, we called this region juxta-UBA (JUBA). JUBA is only 22 amino acids long and does not seem to be conserved in P62 (Fig. 7A). Secondary-structure prediction by JPRED-3 (5) suggests that it predominantly has an α-helical fold. Projection along the helical axis of the predicted α-helix of JUBA showed a highly amphipathic conformation, with charged or polar amino acids arranged on one side of the helix and hydrophobic amino acids on the other (Fig. 7A). Amphipathic α-helices are found in many proteins that peripherally associate with membrane bilayers. Examples include the epsin, amphiphysin, endophilin, Arf, and Arl proteins (16). These helices are characterized by being unfolded until they come into contact with a target lipid membrane. This induces α-helical folding, and the hydrophobic side gets inserted into the bilayer, while the polar/charged side remains outside and makes ionic contacts with the negatively charged headgroups of membrane lipids such as phosphatidylinositol-phosphates (PIPs) (16).

To find out whether JUBA is in fact one such α-helix, we used circular dichroism (CD) spectroscopy. CD spectroscopy is a powerful method to determine the secondary structure of peptides, as each secondary structure exhibits unique spectrum signatures: unfolded peptides give spectra with a single mini-

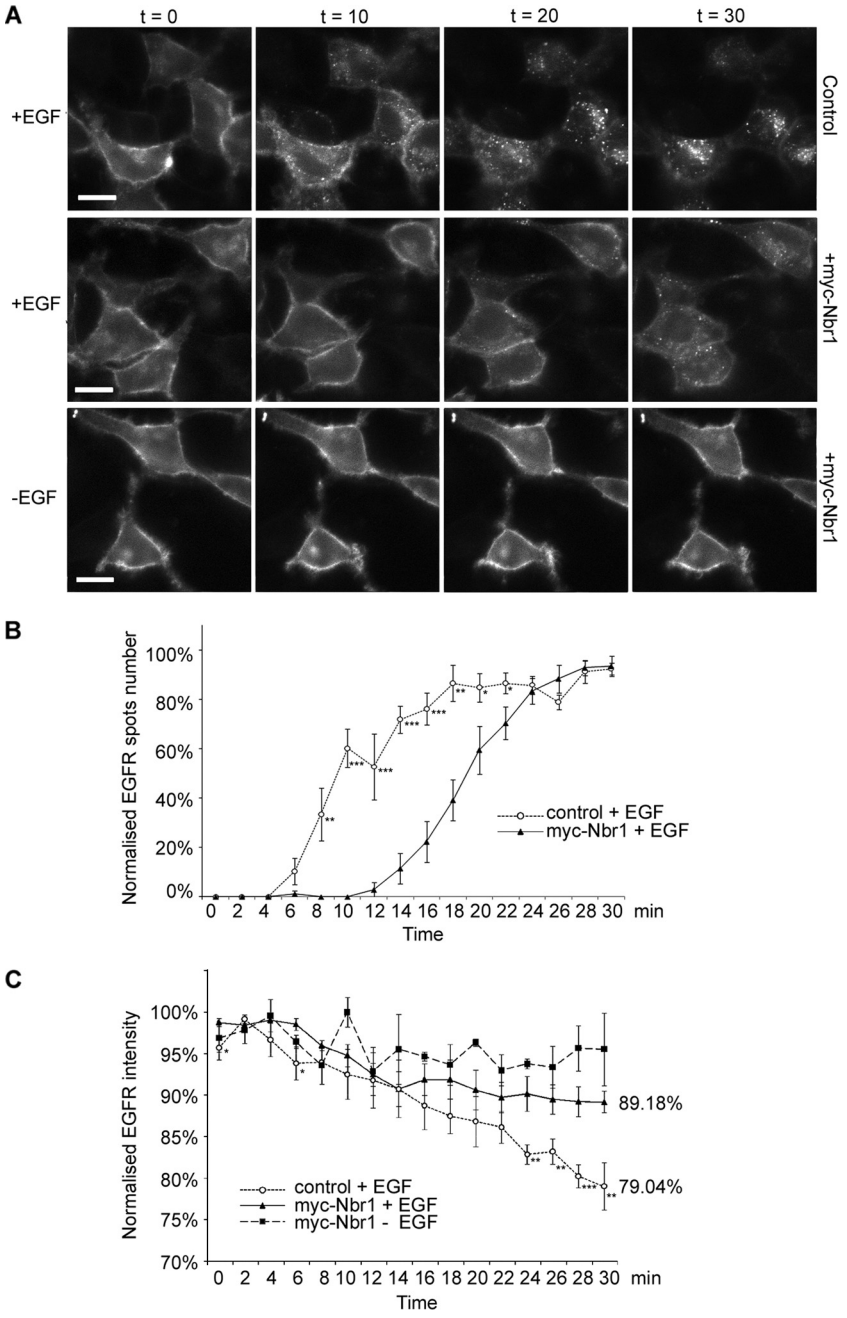

FIG. 4. Nbr1 traps EGFR on the cell surface and inhibits its degradation. All error bars represent SEM. *P* values were calculated by a nonpaired *t* test ($n = 5$ cells under each condition) (*, $P < 0.05$; **, $P < 0.01$; ***, $P < 0.001$). (A) HeLa cells were transfected with EGFR-GFP, with or without Myc-Nbr1, and subjected to live-cell imaging by epifluorescence microscopy for 30 min following the addition of EGF (50 ng/ml). A nonstimulated control was also included (bottom). Scale bars, 10 μm. (B) Quantification of the number of EGFR-GFP-internalizing spots per area. The overexpression of Myc-Nbr1 induces a delay of 8 min in EGFR internalization. (C) Normalized total EGFR-GFP fluorescence from whole-cell areas. The overexpression of Myc-Nbr1 abrogates the degradation of EGFR.

mum at around 200 nm, whereas α-helical peptides give a maximum at around 192 nm and two minima at around 208 nm and 222 nm (6). When we subjected a peptide corresponding to the predicted α-helix of JUBA (L907-S924) to CD spectroscopy, it gave an unfolded signature spectrum (Fig. 7B). The addition of phosphatidylcholine liposomes did not affect the folding (Fig. 7B). However, when liposomes additionally containing various PIPs were added to the peptide solution, they all induced an α-helical fold, as judged by the disappearance of the ~200-nm minimum as well as the appearance of the ~192-nm maximum and ~208- and ~222-nm minima (Fig. 7B). Finally, as a positive control the addition of trifluoroethanol (TFE), an α-helix-inducing agent (6), also resulted in the induction of an α-helical fold (Fig. 7B). These results show that JUBA folds into an α-helix in the presence of PIP-containing membranes. Since every tested PIP could similarly induce an

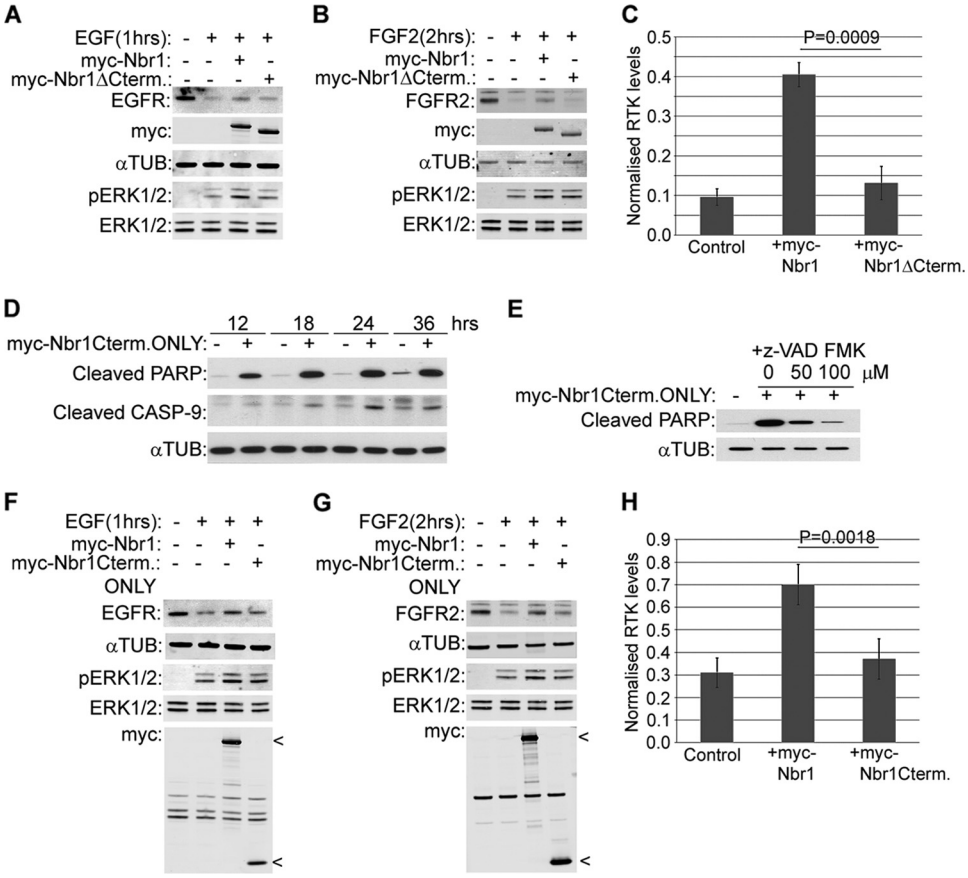

FIG. 5. The C terminus of Nbr1 is essential but not sufficient for its function. All error bars represent SEM. *P* values were calculated by a one-tailed paired *t* test ($n = 3$). (A and B) A C-terminally deleted mutation of Nbr1 lacking the last 133 amino acids does not inhibit ligand-induced RTK degradation. HEK293T cells were transfected with Myc-Nbr1, Myc-Nbr1ΔCterm, or GFP as a control. Cells were serum starved and stimulated with 50 ng/ml EGF (A) or 20 ng/ml FGF2 plus 10 μg/ml heparin (B) for the indicated times before being lysed and analyzed by Western blotting. (C) Densitometry analysis of RTK degradation by Myc-Nbr1 and Myc-Nbr1ΔCterm from panels A and B. (D) Expression of a C-terminal-only Nbr1 mutation containing the last 133 amino acids (P856-Y988) induces cell death by apoptosis. HEK293T cells were transfected for the indicated times with Myc-Nbr1Cterm only or GFP as a control. Cells were lysed and analyzed by Western blotting for the apoptotic markers cleaved PARP and cleaved CASP-9. (E) Apoptosis induced by a C-terminal-only Nbr1 mutation can be inhibited by a general caspase inhibitor. HEK293T cells transfected with Myc-Nbr1Cterm only or GFP as a control were treated with increasing concentrations of z-VAD-FMK. Cells were lysed and analyzed by Western blotting for the apoptotic marker cleaved PARP. (F and G) The C-terminal-only Nbr1 mutation (P856-Y988) does not inhibit ligand-induced RTK degradation. HEK293T cells were transfected with Myc-tagged full-length Nbr1 (Myc-Nbr1), Myc-Nbr1Cterm only, or GFP as a control. A total of 50 μM z-VAD-FMK was added to all cells in order to block cell loss by apoptosis. Cells were serum starved and stimulated with 50 ng/ml EGF (F) or 20 ng/ml FGF2 plus 10 μg/ml heparin (G) for the indicated times before being lysed and analyzed by Western blotting. (H) Densitometry analysis of RTK degradation by Myc-Nbr1 and Myc-Nbr1Cterm only from panels F and G.

α-helical fold (Fig. 7B), the results also suggest that JUBA on its own does not display specificity toward a particular PIP.

Having shown that JUBA forms a membrane-interacting α-helix, we next tested whether the C terminus of Nbr1 exhibits a lipid binding capacity *in vitro*. We used membrane strips dotted with different physiologically relevant membrane lipids in a technique commonly known as fat blotting. In this method, the membrane is blotted with a GST-tagged protein of interest, and bound proteins are subsequently detected by blotting with a GST antibody. While GST on its own did not associate with any of the lipids, the GST-tagged C terminus of Nbr1 (P856-Y988) could bind to all present PIPs as well as phosphatidic acid (PA) (Fig. 7C). As a positive control we used the pleckstrin homology domain of PLC-δ1 that specifically binds $PI45P_2$ (13), which gave the expected result (Fig. 7C). Similarly to PIPs, PA has a bivalent phosphate group, suggesting that JUBA might be interacting with bivalent phosphates of the lipid headgroups. To further confirm that the C terminus of Nbr1 does not display specificity toward a particular PIP, we performed fat blots using membranes dotted with increasing concentrations of each of seven PIPs. No significant preference was detected between different PIPs, while the pleckstrin homology domain of PLC-δ1 bound only $PI45P_2$ (Fig. 7C). As before, GST on its own did not show any lipid binding (Fig. 7C). The results confirm that at least *in vitro*, the C terminus of Nbr1 binds PIPs with broad specificity.

As we reported previously, Nbr1 associates with the limiting membrane of late endosomes (15). To determine whether the vesicular membrane association of Nbr1 *in vivo* depends on JUBA, we compared the localization of full-length Nbr1 and the C-terminal-only Nbr1 (P856-Y988) mutation with that of a JUBA-deleted mutation. Full-length Nbr1 was specifically lo-

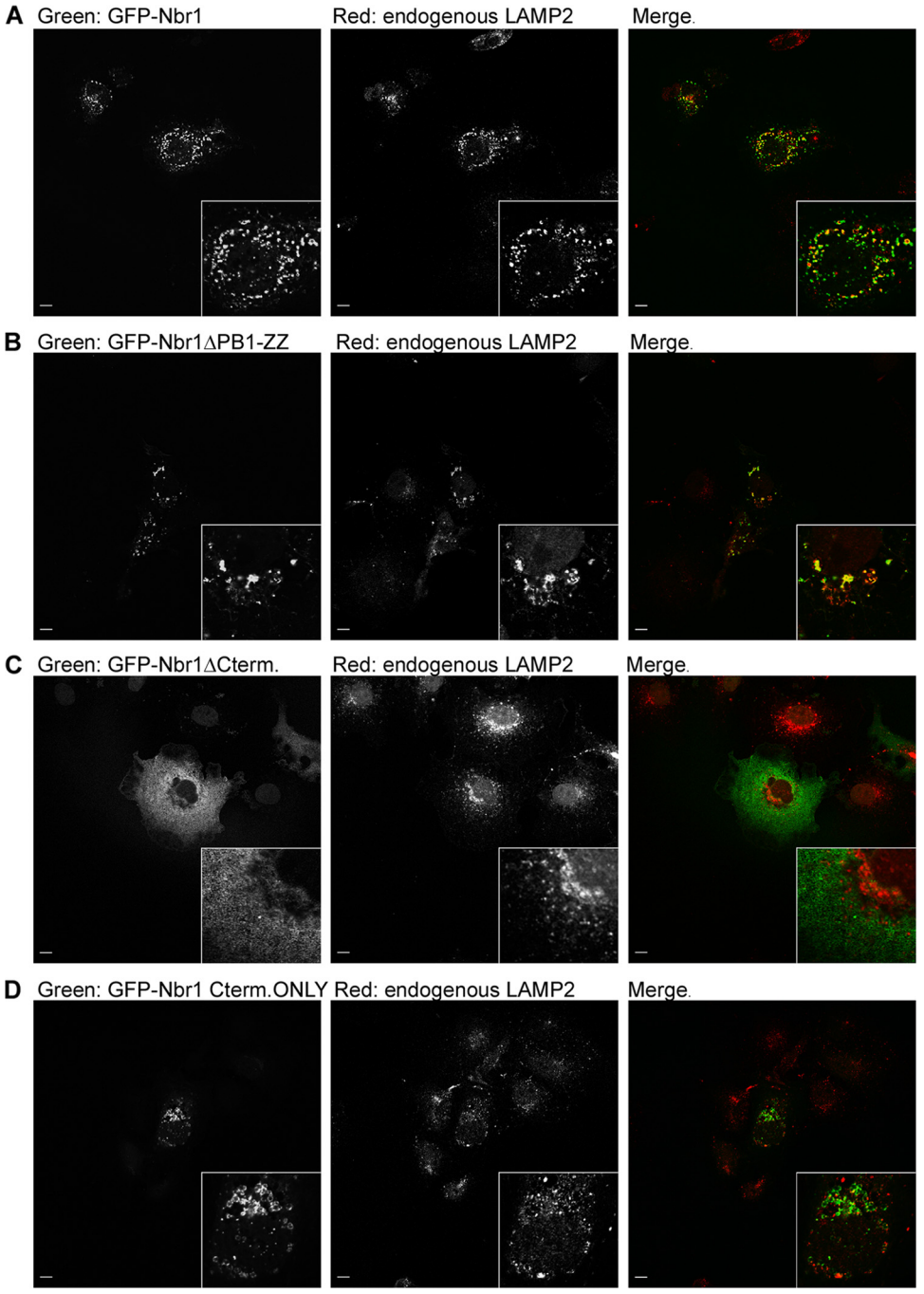

FIG. 6. The C terminus of Nbr1 is essential but not sufficient for its correct localization. Scale bars, 10 μm. (A) Full-length Nbr1 colocalizes with the late endocytic marker LAMP2. COS7 cells transfected with GFP-Nbr1 were fixed, immunostained for LAMP2, and analyzed by confocal microscopy. (B) PB1-ZZ-deleted Nbr1 colocalizes with the late endocytic marker LAMP2. COS7 cells transfected with GFP-Nbr1ΔPB1-ZZ were fixed, immunostained for LAMP2, and analyzed by confocal microscopy. (C) C-terminally deleted Nbr1 lacking the last 133 amino acids does not colocalize with the late endocytic marker LAMP2. COS7 cells transfected with GFP-Nbr1ΔCterm were fixed, immunostained for LAMP2, and analyzed by confocal microscopy. (D)The C-terminal-only Nbr1 mutation (P856-Y988) does not colocalize with the late endocytic marker LAMP2. COS7 cells transfected with GFP-Nbr1Cterm only were fixed, immunostained for LAMP2, and analyzed by confocal microscopy.

calized to the limiting membrane of vesicular structures *in vivo* (Fig. 7D). Similarly, the C-terminal-only mutation (P856-Y988) exhibited localization to the vesicular limiting membranes, although as mentioned above, the vesicles were relatively enlarged compared to that of full-length Nbr1 (Fig. 7D). However, a JUBA-deleted Nbr1 showed no localization to vesicular limiting membranes and instead exhibited an aggregate-like localization (Fig. 7D). These results reveal that JUBA is essential for the Nbr1 association with vesicular limiting membranes *in vivo*.

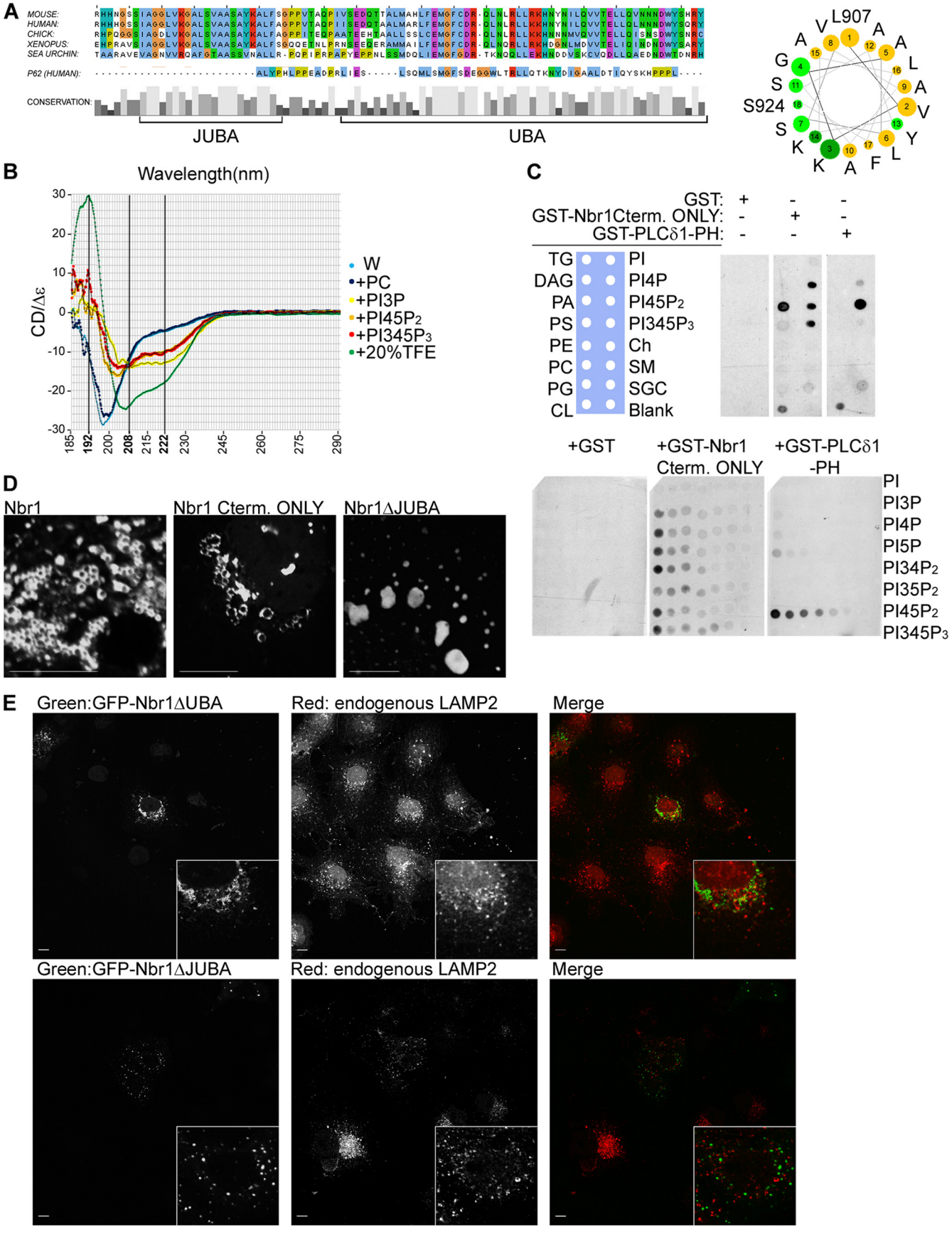
A
MOUSE:
HUMAN:
CHICK:
XENOPUS:
SEA URCHIN:
P62 (HUMAN):
CONSERVATION:
JUBA
UBA
L907
S924
B
Wavelength(nm)
CD/Δε
W
+PC
+PI3P
+PI45P2
+PI345P3
+20%TFE
C
GST:
GST-Nbr1Cterm. ONLY:
GST-PLCδ1-PH:
TG
DAG
PA
PS
PE
PC
PG
CL
PI
PI4P
PI45P2
PI345P3
Ch
SM
SGC
Blank
+GST
+GST-Nbr1 Cterm. ONLY
+GST-PLCδ1 -PH
PI
PI3P
PI4P
PI5P
PI34P2
PI35P2
PI45P2
PI345P3
D
Nbr1
Nbr1 Cterm. ONLY
Nbr1ΔJUBA
E
Green:GFP-Nbr1ΔUBA
Red: endogenous LAMP2
Merge
Green:GFP-Nbr1ΔJUBA
Red: endogenous LAMP2
Merge

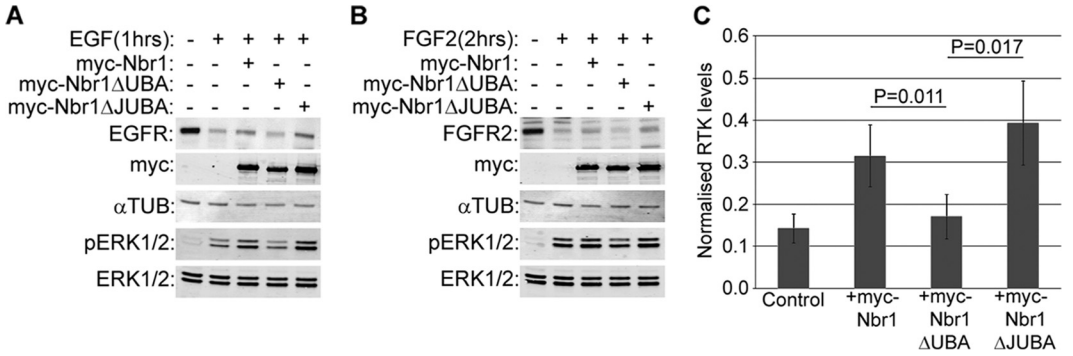

FIG. 8. UBA is necessary but JUBA is dispensable for Nbr1 function. All error bars represent SEM. *P* values were calculated by a one-tailed paired *t* test ($n = 4$). (A) Deletion of UBA but not JUBA abrogates Nbr1-mediated inhibition of EGFR degradation. HEK293T cells were transfected with Myc-Nbr1, Myc-Nbr1ΔUBA, Myc-Nbr1ΔJUBA, or GFP as a control. Cells were serum starved and stimulated with 50 ng/ml EGF for the indicated times before being lysed and analyzed by Western blotting. (B) Deletion of UBA but not JUBA abrogates Nbr1-mediated inhibition of FGFR2 degradation. HEK293T cells were transfected with Myc-Nbr1, Myc-Nbr1ΔUBA, Myc-Nbr1ΔJUBA, or GFP as a control. Cells were serum starved and stimulated with 20 ng/ml FGF2 plus 10 μg/ml heparin for the indicated times before being lysed and analyzed by Western blotting. (C) Densitometry analysis of RTK degradation by Myc-Nbr1, Myc-Nbr1ΔUBA, and Myc-Nbr1ΔJUBA from panels A and B.

Having established that the C terminus of Nbr1 consists of UBA and JUBA and that JUBA is an amphipathic membrane-interacting α-helix that targets Nbr1 to vesicular limiting membranes, we next sought to determine the contribution of each region to the late endosomal localization of Nbr1. The deletion of either UBA or JUBA resulted in the loss of Nbr1 late endosomal localization, suggesting that both domains are crucial for the correct localization of the protein (Fig. 7E). Interestingly, the effect of the loss of both regions together (Fig. 6C) is more dramatic than that of each region individually (Fig. 7E), suggesting that the two regions cooperate to localize Nbr1.

UBA but not JUBA is necessary for Nbr1 function. Having established the role of JUBA in Nbr1 localization, we next sought to assess its importance in the Nbr1-mediated inhibition of RTK degradation. While the deletion of the C-terminal UBA domain abrogated the effect of Nbr1 on the degradation of EGFR (Fig. 8A and C) and FGFR2 (Fig. 8B and C), the deletion of JUBA did not have any functional impact on the degradation of either receptor (Fig. 8A, B, and C). Thus, while both the UBA and JUBA regions are important for the late endocytic localization of Nbr1 (Fig. 7E), only UBA seems to be important for the Nbr1-mediated inhibition of RTK degradation.

Late endocytic localization of Nbr1 is LIR independent. Nbr1 contains two LIRs, which can bind to LC3 and target Nbr1 to autophagosomes (9). As the C-terminal-only (P856-Y988) Nbr1 mutation that lacks both LIRs (Fig. 1) cannot correctly localize to late endosomes (Fig. 6D), we asked whether the interaction with autophagosomes via LIRs is important for the late endosomal localization of Nbr1 since autophagosomes commonly fuse with endosomes on their route toward lysosomal degradation (29). The main Nbr1 LIR is located close to the C terminus of the protein (V739-E779) and contains a pivotal tyrosine (Y750), the mutation of which results in the loss of LC3 interactions (9). The second LIR (LIR2) is located further N terminally (A543-P634) and can compensate for the loss of the main LIR (9). When we tested

FIG. 7. The C terminus of Nbr1 contains UBA and JUBA, both of which are essential for its correct localization. Scale bars, 10 μm. (A, left) Cross-species multiple alignment of the C-terminal 93 amino acids of NBR1 reveals JUBA, a novel conserved stretch of amino acids next to the UBA domain, which is not present in P62. (Right) Projection along the helical axis of the predicted α-helix of JUBA (L907-S924) suggests that it would be amphipathic, with polar (light green) and charged (dark green) amino acids on one side and hydrophobic amino acids (yellow) on the other. (B) The JUBA peptide exhibits unfolded CD spectrum signatures in water or in the presence of PC and α-helical spectrum signatures in the presence of PIPs or the α-helix-inducing agent TFE. CD spectra of the JUBA peptide in water (W) and water plus phosphatidylcholine (PC) liposomes, plus phosphatidylinositol-3-phosphate (PIP3)-containing liposomes, plus phosphatidylinositol-4,5-phosphate ($PI45P_2$)-containing liposomes, plus phosphatidylinositol-3,4,5-phosphate($PI345P_3$)-containing liposomes, or plus 20% TFE. (C) The C terminus of Nbr1 binds to PIPs. (Top) The C terminus of Nbr1 associates with PIPs and PA. Membranes prespotted with 15 different biologically relevant lipids were incubated with the GST-tagged C terminus of Nbr1 (GST-Nbr1Cterm only), GST alone as a negative control, or the GST-tagged pleckstrin homology (PH) domain of PLC-δ1 (GST–PLC-δ1–PH) as a positive control. Membranes were analyzed by blotting with an anti-GST antibody. (Bottom) The C terminus of Nbr1 does not show specificity to any PIP. Membranes prespotted with increasing amounts of various PIPs were incubated with GST-Nbr1Cterm only, GST, or GST–PLC-δ1–PH as described above and blotted with an anti-GST antibody. (TG, triglyceride; DAG, diacylglycerol; PA, phosphatidic acid; PS, phosphatidylserine; PE, phosphatidylethanolamine; PC, phosphatidylcholine; PG, phosphatidylglycerol; CL, cardiolipin; PI, phosphatidylinositol; Ch, cholesterol; SM, sphingomyelin; SGC, 3-sulfogalactosylceramide). (D) Deletion of JUBA abrogates membrane associations *in vivo*. COS7 cells transfected with GFP-Nbr1, GFP-Nbr1Cterm only, or GFP-Nbr1ΔJUBA were fixed and analyzed by confocal microscopy. (E) Both JUBA and UBA are necessary for late endocytic localization of Nbr1. (Top) Deletion of the UBA domain abrogates Nbr1 colocalization with LAMP2. COS7 cells transfected with GFP-Nbr1ΔUBA were fixed, immunostained for LAMP2, and analyzed by confocal microscopy. (Bottom) Deletion of JUBA also abrogates Nbr1 colocalization with LAMP2. COS7 cells transfected with GFP-Nbr1ΔJUBA were fixed, immunostained for LAMP2, and analyzed by confocal microscopy.

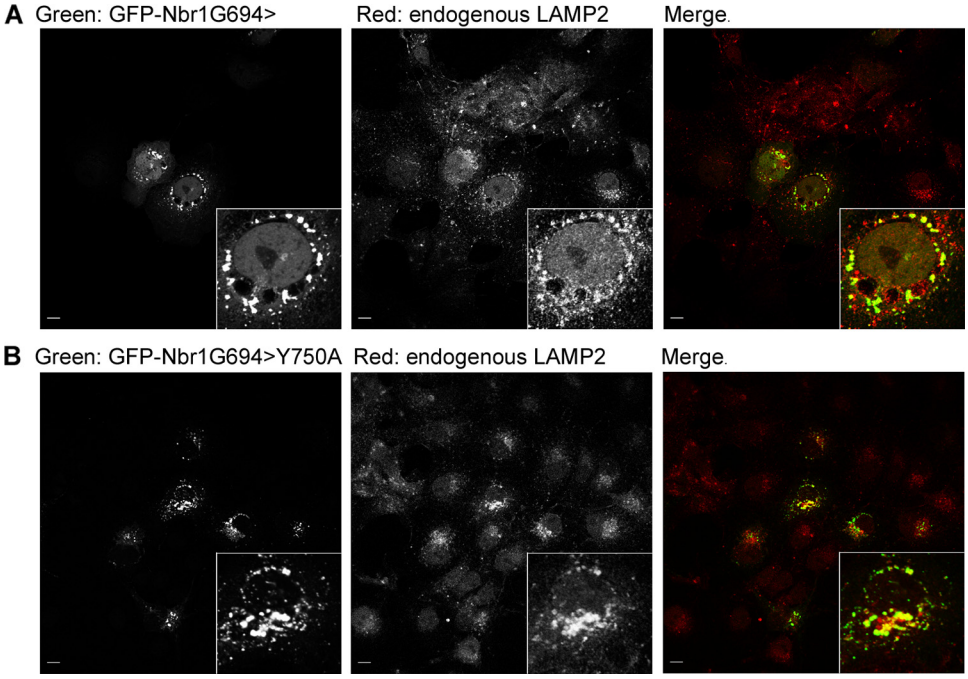

FIG. 9. Late endocytic localization of Nbr1 is independent of LIR. Scale bars, 10 μm. (A) A truncated Nbr1 mutation lacking LIR2 (Nbr1G694>) colocalizes with LAMP2. COS7 cells transfected with GFP-Nbr1G694> were fixed, immunostained for LAMP2, and analyzed by confocal microscopy. (B) This truncated mutation with an additional point mutation in the main LIR (Nbr1G694>Y750A) can still colocalize with LAMP2. COS7 cells transfected with GFP-Nbr1G694>Y750A were fixed, immunostained for LAMP2, and analyzed by confocal microscopy.

an N-terminal truncation mutation of Nbr1 expressing residues C terminal to G694, it could still colocalize with the late endocytic marker LAMP2 (Fig. 9A). As this mutation lacks LIR2 (Fig. 1), this result suggests that the loss of LIR2 alone does not have an effect on Nbr1 localization. However, like full-length Nbr1 (Fig. 10A), this mutation could still associate with autophagosomes (Fig. 10B). Therefore, we further mutated the pivotal tyrosine in the main LIR (Y750 to A) to assess whether the complete loss of LC3 binding affects the late endocytic localization of Nbr1. The association with autophagosomes was lost with this additional mutation (Fig. 10C), but colocalization with the late endocytic marker LAMP2 was not affected (Fig. 9B). These results reveal that the late endocytic localization of Nbr1 is independent of LC3 binding and autophagosomal association. Interestingly, we also observed that the C terminus of Nbr1 (P856-Y988), which is crucial for the late endocytic localization of the protein (Fig. 6C), is not needed for autophagosomal localization (Fig. 10D). Therefore, we conclude that the late endocytic and autophagic localizations of Nbr1 are independent of one another: the autophagic localization of Nbr1 requires the LIR but not the C terminus, while the late endocytic localization of Nbr1 requires the C terminus but not the LIRs.

DISCUSSION

The evidence presented in this study establishes Nbr1 as an inhibitor of ligand-mediated RTK degradation (Fig. 2 and 3). Live-cell imaging analysis suggests that the likely mechanism by which Nbr1 inhibits receptor degradation is via inhibiting receptor internalization from the cell surface (Fig. 4). The C-terminal 133 amino acids of Nbr1 are essential for its inhibition of RTK degradation (Fig. 5A, B, and C). We previously reported that the same region of Nbr1 also binds to Spred2 and that this binding is essential for the Spred2-mediated downregulation of ERK1/2 signaling by targeting the activated receptors to the lysosomal degradation pathway (15). As Nbr1 inhibits receptor degradation and consequently leads to an enhancement of downstream ERK1/2 signaling (Fig. 2A and B), it is possible that Spred2 binding to the critical C terminus of Nbr1 could be interfering with Nbr1 activity. Alternatively, Spred2 binding could be altering Nbr1 function from an inhibitor to an enhancer of RTK degradation. This is supported by the fact that while NBR1 does not have a negative impact on ERK1/2 signaling on its own, its coexpression with Spred2 results in a synergistic inhibition of ERK1/2 (15), which is suggestive of a cooperative rather than a simply antagonistic mechanism of functional interaction. Our results also reveal that further regions of functional significance other than the C terminus must exist within Nbr1, as a C-terminal-only mutation on its own is not sufficient to inhibit RTK degradation (Fig. 5F, G, and H).

The molecular interactions involved in the Nbr1-mediated inhibition of RTK internalization and degradation are not defined at the moment. A number of known binding partners of Nbr1, such as P62 (12), P14, transmembrane emp24-like trafficking protein 10 (Tmp21), and ubiquitin carboxyl-terminal hydrolase 8 (USP8/UBPY) (36), have roles in vesicular trafficking. USP8 is in particular very interesting in this regard, as its loss results in the inhibition of EGFR degradation (1, 24). USP8 deubiquitinates EGFR, and this is essential for ESCRT-dependent MVB sorting and the subsequent degradation of

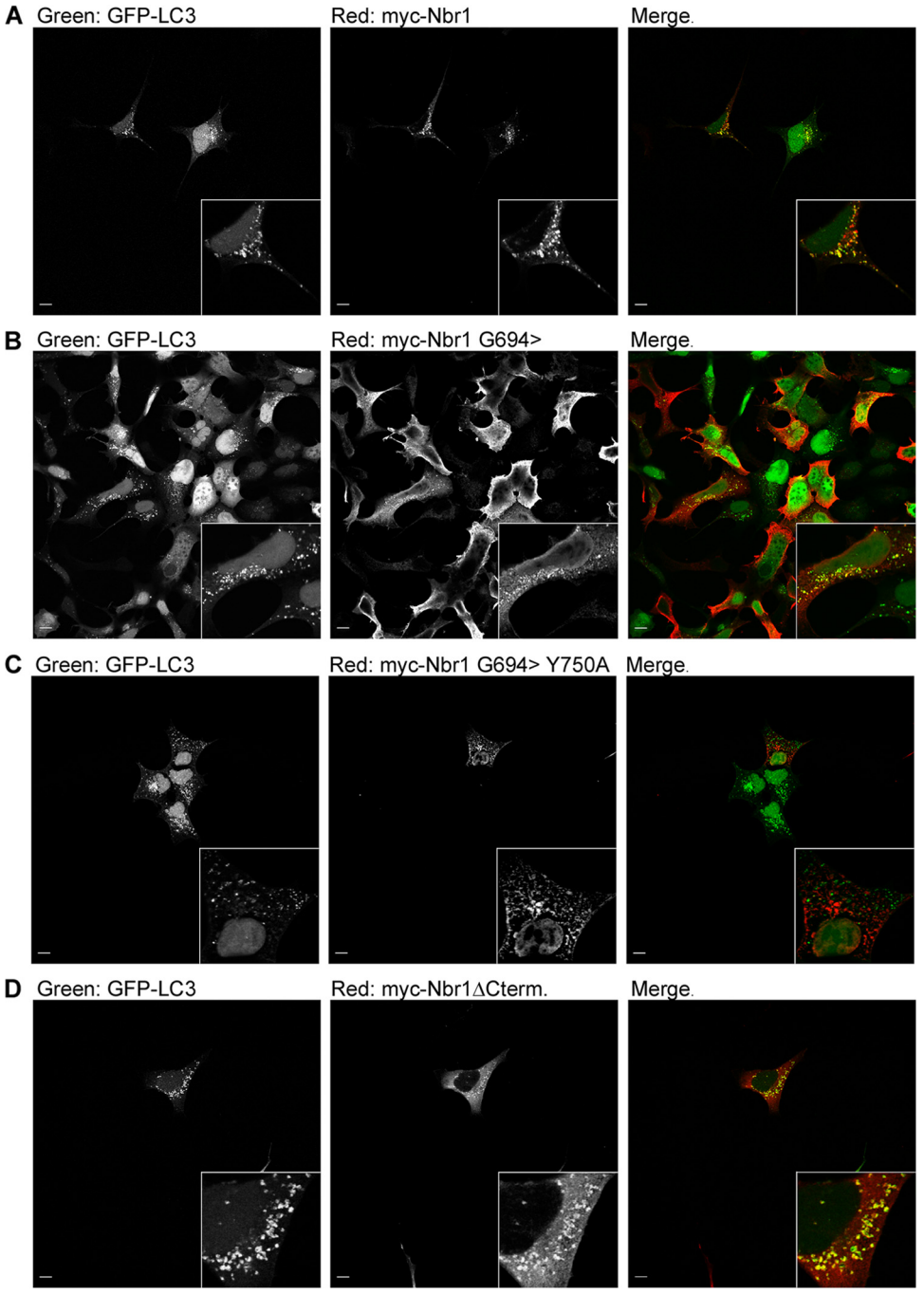

FIG. 10. Colocalization of Nbr1 with accumulated autophagosomes depends on LIR but not the C terminus. Scale bars, 10 μm. (A) Full-length Nbr1 can colocalize with autophagosomes. 293A cells stably expressing GFP-tagged LC3 were transfected with Myc-Nbr1. Cells were treated with 200 nM BafA for 4 h to accumulate autophagosomes before being fixed, immunostained for Myc, and analyzed by confocal microscopy. (B) The Nbr1G694> mutation lacking LIR2 can colocalize with autophagosomes. 293A cells stably expressing GFP-tagged LC3 were transfected with Myc-Nbr1G694>. Cells were treated with 200 nM BafA for 4 h to accumulate autophagosomes before being fixed, immunostained for Myc, and analyzed by confocal microscopy. (C) The Nbr1G694>Y750A mutation, which lacks the LC3 binding capacity, cannot colocalize with autophagosomes. 293A cells stably expressing GFP-tagged LC3 were transfected with Myc-Nbr1G694>Y750A. Cells were treated with 200 nM BafA for 4 h to accumulate autophagosomes before being fixed, immunostained for Myc, and analyzed by confocal microscopy. (D) The C-terminally deleted Nbr1 mutation lacking the last 133 amino acids (P856-Y988) can still colocalize with autophagosomes. 293A cells stably expressing GFP-tagged LC3 were transfected with Myc-Nbr1ΔCterm. Cells were treated with 200 nM BafA for 4 h to accumulate autophagosomes before being fixed, immunostained for Myc, and analyzed by confocal microscopy.

the receptor (1, 24). In addition, USP8 has a role in the regulation of ESCRT ubiquitin recognition machinery itself by deubiquitinating a number of its components (17). The fact that the phenotype of ectopic Nbr1 expression mimics that of the USP8 loss could be suggestive of a functional relationship. It remains to be determined whether a functional epistasis exists between the two proteins and, if so, how their interaction regulates endocytosis and receptor degradation.

We previously demonstrated that Nbr1 is a specific late endosomal protein (15). Here we reveal that the C terminus of Nbr1 is essential but not sufficient for its late endosomal localization (Fig. 6C and D). We also show that unlike its C terminus, the two LIR regions of Nbr1 are dispensable for late endocytic localization (Fig. 9). On the other hand, the autophagosomal localization of Nbr1 is dependent solely on the presence of LIRs and not the C terminus (Fig. 10). The fact that the late endocytic and autophagic localizations of Nbr1 are independent of each other indicates that the function of the protein in each context might be independent of one another as well. This is not surprising, as the association of Nbr1 with LC3 seems to result primarily in its removal from the cytoplasm and degradation via the autophagosomal pathway (9). In line with the above-described hypothesis, the inhibition of autophagy by the siRNA-mediated depletion of its key components did not affect the inhibition of RTK degradation by Nbr1 (F. K. Mardakheh and J. K. Heath, unpublished observations).

As mentioned above, the C terminus of Nbr1 contains a UBA domain, which can bind to polyubiquitin chains (9, 36). Here we show that the C terminus also contains a well-conserved membrane-interacting amphipathic α-helix, which we name JUBA. JUBA is crucial for the Nbr1 association with vesicular limiting membranes (Fig. 7D), and both UBA and JUBA are essential for the late endocytic localization of the protein (Fig. 7E). It was proposed previously that amphipathic α-helices might act as curvature sensors, being thermodynamically capable of inserting themselves into membranes with the right degree of curvature (16). In this light, JUBA could be providing further specificity with regard to Nbr1 localization by acting as a specific curvature sensor. Interestingly, despite numerous similarities at the level of domain architecture between Nbr1 and P62, JUBA seems to be a unique feature of Nbr1, as a similar region cannot be found in P62 (Fig. 7A). Thus, it is likely that the mechanisms by which these two proteins localize to late endosomes are different.

Finally, our results reveal that while JUBA is essential for the late endocytic localization of Nbr1 (Fig. 7E), it is dispensable for its effect on RTK trafficking (Fig. 8). The late endosomal localization *per se*, therefore, does not seem to be important for the function of Nbr1 in the context of RTK trafficking. In fact, the above-mentioned mislocalization of the C-terminal-only Nbr1 mutation to early endosomes (data not shown) suggests that it is probably trafficked through the endocytic machinery, and its late endocytic localization is therefore a steady-state phenomenon. The exact molecular mechanism by which Nbr1 associates with the endocytic machinery remains to be determined. The identification of novel Nbr1-interacting partners and determination of their mode of interaction should help shed light on this matter.

ACKNOWLEDGMENTS

We thank Susan Brewer for the bacterial expression and purification of the GST-tagged C-terminal-only Nbr1 mutation. We also thank Sharon Tooze for 293A LC3-GFP stable cells and Steve Dove for his help with vesicle preparation. Finally, we give special thanks to all our present and past laboratory members for useful discussions and feedback.

This work was funded by Cancer Research UK (J.K.H.) and the Biotechnology and Biosciences Research Council (J.Z.R.). G.A. is funded through a Medical Research Council Ph.D. studentship, and F.K.M. is funded through a Cancer Research UK Ph.D. studentship. The Nikon A1R/TIRF microscope used in this research was obtained through the Birmingham Science City Translational Medicine Clinical Research and Infrastructure Trials Platform, with support from Advantage West Midlands (AWM).

REFERENCES

1. **Alwan, H. A., and J. E. van Leeuwen.** 2006. UBPY-mediated epidermal growth factor receptor (EGFR) de-ubiquitination promotes EGFR degradation. J. Biol. Chem. **282:**1658–1669.
2. **Bjørkøy, G., T. Lamark, A. Brech, H. Outzen, M. Perander, A. Øvervatn, H. Stenmark, and T. Johansen.** 2005. p62/SQSTM1 forms protein aggregates degraded by autophagy and has a protective effect on huntingtin-induced cell death. J. Cell Biol. **171:**603–614.
3. **Carter, R. E., and A. Sorkin.** 1998. Endocytosis of functional epidermal growth factor receptor-green fluorescent protein chimera. Biol. Chem. **273:** 35000–35007.
4. **Chambers, J. A., and E. Solomon.** 1996. Isolation of the murine Nbr1 gene adjacent to the murine Brca1 gene. Genomics **38:**305–313.
5. **Cole, C., J. D. Barber, and G. J. Barton.** 2008. The Jpred 3 secondary structure prediction server. Nucleic Acids Res. **36:**W197–W201.
6. **Conner, M., M. R. Hicks, T. Dafforn, T. J. Knowles, C. Ludwig, S. Staddon, M. Overduin, U. L. Günther, J. Thome, M. Wheatley, D. R. Poyner, and A. C. Conner.** 2008. Functional and biophysical analysis of the C-terminus of the CGRP-receptor; a family B GPCR. Biochemistry **47:**8434–8444.
7. **Geetha, T., J. Jiang, and M. W. Wooten.** 2005. Lysine 63 polyubiquitination of the nerve growth factor receptor TrkA directs internalization and signaling. Mol. Cell **20:**301–312.
8. **Haugh, J. M., and T. Meyer.** 2002. Active EGF receptors have limited access to PtdIns(4,5)P(2) in endosomes: implications for phospholipase C and PI 3-kinase signaling. J. Cell Sci. **115:**303–310.
9. **Kirkin, V., T. Lamark, Y. S. Sou, G. Bjørkøy, J. L. Nunn, J. A. Bruun, E. Shvets, D. G. McEwan, T. H. Clausen, P. Wild, I. Bilusic, J. P. Theurillat, A. Øvervatn, T. Ishii, Z. Elazar, M. Komatsu, I. Dikic, and T. Johansen.** 2009. A role for NBR1 in autophagosomal degradation of ubiquitinated substrates. Mol. Cell **33:**505–516.
10. **Kranenburg, O., I. Verlaan, and W. H. Moolenaar.** 1999. Dynamin is required for the activation of mitogen-activated protein (MAP) kinase by MAP kinase kinase. J. Biol. Chem. **274:**35301–35304.
11. **Lampugnani, M. G., F. Orsenigo, M. C. Gagliani, C. Tacchetti, and E. Dejana.** 2006. Vascular endothelial cadherin controls VEGFR-2 internalization and signaling from intracellular compartments. J. Cell Biol. **174:**593–604.
12. **Lange, S., F. Xiang, A. Yakovenko, A. Vihola, P. Hackman, E. Rostkova, J. Kristensen, B. Brandmeier, G. Franzen, B. Hedberg, L. G. Gunnarsson, S. M. Hughes, S. Marchand, T. Sejersen, I. Richard, L. Edström, E. Ehler, B. Udd, and M. Gautel.** 2005. The kinase domain of titin controls muscle gene expression and protein turnover. Science **308:**1599–1603.
13. **Lomasney, J. W., H. F. Cheng, L. P. Wang, Y. Kuan, S. Liu, S. W. Fesik, and K. King.** 1996. Phosphatidylinositol 4,5-bisphosphate binding to the pleckstrin homology domain of phospholipase C-delta1 enhances enzyme activity. J. Biol. Chem. **271:**25316–25326.
14. **MacInnis, B. L., and R. B. Campenot.** 2002. Retrograde support of neuronal survival without retrograde transport of nerve growth factor. Science **295:** 1536–1539.
15. **Mardakheh, F. K., M. Yekezare, L. M. Machesky, and J. K. Heath.** 2009. Spred2 interaction with the late endosomal protein NBR1 down-regulates fibroblast growth factor receptor signaling. J. Cell Biol. **187:**265–277.
16. **McMahon, H. T., and J. L. Gallop.** 2005. Membrane curvature and mechanisms of dynamic cell membrane remodelling. Nature **438:**590–596.
17. **Mizuno, E., K. Kobayashi, A. Yamamoto, N. Kitamura, and M. Komada.** 2006. A deubiquitinating enzyme UBPY regulates the level of protein ubiquitination on endosomes. Traffic **7:**1017–1031.
18. **Mosesson, Y., G. B. Mills, and Y. Yarden.** 2008. Derailed endocytosis: an emerging feature of cancer. Nat. Rev. Cancer **8:**835–850.
19. **Nada, S., A. Hondo, A. Kasai, M. Koike, K. Saito, Y. Uchiyama, and M. Okada.** 2009. The novel lipid raft adaptor p18 controls endosome dynamics by anchoring the MEK-ERK pathway to late endosomes. EMBO J. **28:**477–489.

20. **Narayan, K., and M. A. Lemmon.** 2006. Determining selectivity of phosphoinositide-binding domains. Methods **39:**122–133.
21. **Pankiv, S., T. H. Clausen, T. Lamark, A. Brech, J. A. Bruun, H. Outzen, A. Øvervatn, G. Bjørkøy, and T. Johansen.** 2007. p62/SQSTM1 binds directly to Atg8/LC3 to facilitate degradation of ubiquitinated protein aggregates by autophagy. J. Biol. Chem. **282:**24131–24145.
22. **Piper, R. C., and D. J. Katzmann.** 2007. Biogenesis and function of multivesicular bodies. Annu. Rev. Cell Dev. Biol. **23:**519–547.
23. **Rappoport, J. Z., and S. M. Simon.** 2009. Endocytic trafficking of activated EGFR is AP-2 dependent and occurs through preformed clathrin spots. J. Cell Sci. **122:**1301–1305.
24. **Row, P. E., I. A. Prior, J. McCullough, M. J. Clague, and S. Urbé.** 2006. The ubiquitin isopeptidase UBPY regulates endosomal ubiquitin dynamics and is essential for receptor down-regulation. J. Biol. Chem. **281:**12618–12624.
25. **Schenck, A., L. Goto-Silva, C. Collinet, M. Rhinn, A. Giner, B. Habermann, M. Brand, and M. Zerial.** 2008. The endosomal protein Appl1 mediates Akt substrate specificity and cell survival in vertebrate development. Cell **133:**486–497.
26. **Schlessinger, J.** 2000. Cell signaling by receptor tyrosine kinases. Cell **103:**211–225.
27. **Scita, G., and P. P. Di Fiore.** 2010. The endocytic matrix. Nature **463:**464–473.
28. **Sigismund, S., E. Argenzio, D. Tosoni, E. Cavallaro, S. Polo, and P. P. Di Fiore.** 2008. Clathrin-mediated internalization is essential for sustained EGFR signaling but dispensable for degradation. Dev. Cell **15:**209–219.
29. **Simonsen, A., and S. A. Tooze.** 2009. Coordination of membrane events during autophagy by multiple class III PI3-kinase complexes. J. Cell Biol. **186:**773–782.
30. **Sorkin, A., and M. von Zastrow.** 2009. Endocytosis and signalling: intertwining molecular networks. Nat. Rev. Mol. Cell Biol. **10:**609–622.
31. **Sweet, S. M., F. K. Mardakheh, K. J. Ryan, A. J. Langton, J. K. Heath, and H. J. Cooper.** 2008. Targeted online liquid chromatography electron capture dissociation mass spectrometry for the localization of sites of in vivo phosphorylation in human Sprouty2. Anal. Chem. **80:**6650–6657.
32. **Teis, D., W. Wunderlich, and L. A. Huber.** 2002. Localization of the MP1-MAPK scaffold complex to endosomes is mediated by p14 and required for signal transduction. Dev. Cell **3:**803–814.
33. **Teis, D., N. Taub, R. Kurzbauer, D. Hilber, M. E. de Araujo, M. Erlacher, M. Offterdinger, A. Villunger, S. Geley, G. Bohn, C. Klein, M. W. Hess, and L. A. Huber.** 2006. p14-MP1-MEK1 signaling regulates endosomal traffic and cellular proliferation during tissue homeostasis. J. Cell Biol. **175:**861–868.
34. **Vieira, A. V., C. Lamaze, and S. L. Schmid.** 1996. Control of EGF receptor signaling by clathrin-mediated endocytosis. Science **274:**2086–2089.
35. **Vogelstein, B., and K. W. Kinzler.** 2004. Cancer genes and the pathways they control. Nat. Med. **10:**789–799.
36. **Waters, S., K. Marchbank, E. Solomon, C. Whitehouse, and M. Gautel.** 2009. Interactions with LC3 and polyubiquitin chains link nbr1 to autophagic protein turnover. FEBS Lett. **583:**1846–1852.
37. **Whitehouse, C., J. Chambers, K. Howe, M. Cobourne, P. Sharpe, and E. Solomon.** 2002. NBR1 interacts with fasciculation and elongation protein zeta-1 (FEZ1) and calcium and integrin binding protein (CIB) and shows developmentally restricted expression in the neural tube. Eur. J. Biochem. **269:**538–545.
38. **Whitehouse, C. A., S. Waters, K. Marchbank, A. Horner, N. W. McGowan, J. V. Jovanovic, G. M. Xavier, T. G. Kashima, M. T. Cobourne, G. O. Richards, P. T. Sharpe, T. M. Skerry, A. E. Grigoriadis, and E. Solomon.** 2010. Neighbor of Brca1 gene (Nbr1) functions as a negative regulator of postnatal osteoblastic bone formation and p38 MAPK activity. Proc. Natl. Acad. Sci. U. S. A. **107:**12913–12918.